



Development of Novel Antimicrobial Peptides

Nadin Shagaghi

Master of Science (Biotechnology) and Global Leadership Program

This thesis is presented for the degree of Doctor of Philosophy

July 2017

Department of Chemistry and Biotechnology

Faculty of Science, Engineering and Technology

Swinburne University of Technology

Melbourne, Australia

Abstract

Antimicrobial peptides (AMPs) are evolutionarily conserved main effector molecules of the innate immune system of many organisms. Due to their wide-range of activities and low potential to develop resistance against them, AMPs offer ideal templates to design novel peptide-based antimicrobial agents that can effectively control drug-resistance pathogens. The tryptophan (Trp)-rich peptides (TRPs) are a subset of AMPs that display potent antimicrobial activity, credited to the unique biochemical properties of Trp. A synthetic peptide, PuroA based on the unique Trp-rich domain (TRD) of a wheat endosperm, puroindoline A (PINA), showed antibacterial and antifungal activities. As many AMPs are not yet optimized for efficient *in vivo* activity, modifying the structural determinants of AMPs is a useful tool for optimizing their activity and cytotoxicity, as well boosting their potential for wide-range of applications. In the present work, PuroA was used as a template to design a number of TRPs with better potency and selectivity under physiological conditions. Some of PuroA variants were successfully designed; they displayed potent antimicrobial activities, maintained these activities under physiological salt concentration and resisted *in vitro* proteolytic degradation. Additionally, synthetic peptides based on the TRD of PINA and the related barley hordoindoline a (HINa) and the designed PuroA derivatives were found to be effective against *Bacillus subtilis* endospores and sessile and planktonic cells of *Pseudomonas aeruginosa*, *Listeria monocytogenes*, *Listeria innocua* and two clinical methicillin-resistant *S. aureus* (MRSA). Time-lapse fluorescence lifetime imaging microscopy (FLIM) and fluorescence microscopy were used to directly observe the localization and interaction kinetics of a fluorescently-tagged PuroA peptide on single *Candida albicans* cell in real time. It was found that loss of membrane integrity and/or pore formation at *C. albicans* membranes occur after translocating across the cell wall, cytoplasmic membrane and nuclear membrane, and binding to SYTO-labelled nucleic acids. Although, pore formation is secondary to rather than concurrent with PuroA entry to cells, it is the main mechanism of cell killing. It has been claimed that AMPs exert fundamental change(s) on the microbial cell that minimise the possible evolution of resistance compared to conventional antibiotics. The development of resistance to selected TRPs in *Staphylococcus aureus*, *Escherichia coli*, *Staphylococcus epidermidis* and *C. albicans* was tested. It was possible to experimentally evolve uninherited resistance to TRPs in *S. aureus*

and *E. coli* when they are consistently exposed to increased levels of the peptides. Preliminary analysis of the cytotoxicity profile of the TRPs against selected types of mammalian cells, including cancerous cells, suggested a potential use of two of the peptides as selective antitumor therapeutics. In conclusion, the designed TRPs have a significant potential of applications in pharmaceutical, food and/or agriculture industries.

Acknowledgements

I want to take the opportunity to sincerely thank the people who supported me throughout my research journey and shared with me unforgettable moments.

First and foremost, I would like to thank my principal supervisor, Prof Mrinal Bhave for all her constant guidance, support, encouragement and patience that helped making this project possible. I am exceedingly grateful for the knowledge, experience and time you have shared with me to overcome the challenging obstacles I have encountered during my research. To my co-supervisor, Prof Enzo Palombo, thank you for your constant support and encouragement. I am particularly grateful for all your feed-backs, advice, kind words. To my co-supervisor, Assoc. Prof Andrew Clayton, thank you for being always present, guiding me towards the most rewarding directions, and encouraging me to take the best decisions for my career.

I am extremely grateful to Swinburne University of Technology (SUT) for giving me the opportunity to undertake my doctoral degree, and for awarding me the Swinburne University Postgraduate Research Award (SUPRA) scholarship, which allowed me to study without financial constraints. I truly appreciate the support of the Faculty of Science, Engineering and Technology at Swinburne University of Technology through the funding and resources provided to me. Many thanks to Dr Rebecca Alfred, Dr James Wang, Dr Shanthi Joseph, Ngan Nguyen, Katharine Adcroft, Chris Key, Angela McKellar and Dr De Ming Zhu for their support and assistance during my research work. I owe particular thanks to Dr Rohan Shah for helping me with cytotoxicity assays.

I am very grateful to Prof Mibel Aguilar and Dr Tzong-Hsien Lee (Monash University) for their expert help and guidance with measuring the circular dichroism spectra of the peptides.

To Zaynab Derakhshani, Sanjida Topa, Tharushi Perera and Abdulaziz Alharthi, thank you for constant presence, the good time spent together and unforgettable memories. Thank you for being true friends. I would also like to thank my colleagues in laboratory and office, Gurvinder Kalra, Simon Grossemey, Qudsia Arooj, Tien Song

Hiep Pham, Muhammad Khattab, Zubaidah Ningsih, Dr Snehal Jadhav and Dr Avinash Karpe for their help, and for sharing the PhD journey with me.

My warmest thanks goes to my family. To Wael, Walid, Wisam, Nada, Widad, Yazan, Runya and Iman, I have been extremely fortunate in my life to have you all who have shown me unconditional love, support and encouragement. Thanks for always being there. To the two most important people in my life, Baba and Mama, thank you for encouraging me to follow my dreams, for accompanying me through every choice, success, and difficulty. Thanks for teaching me how to grow up, how to achieve my goals. Thanks for being my most important confidants, for being with me whenever I need, for listening to me and advising me. I know that regardless the distance and the time that flies, we will always be together.

*I dedicate this thesis with love to my dearest parents,
Mr. Mustafa Shagaghi and Mrs. Nagda Abdou...!*

Publications and awards arising from this work

Refereed journal articles

Shagaghi, N., Palombo, E. A., Clayton, A. H. A. & Bhave, M. 2016. Archetypal tryptophan-rich antimicrobial peptides: properties and applications. *World Journal of Microbiology and Biotechnology*, 32, 1-10.

Shagaghi, N., Alfred, R. L., Clayton, A. H. A., Palombo, E. A. & Bhave, M. 2016. Anti-biofilm and sporicidal activity of peptides based on wheat puroindoline and barley hordoindoline proteins. *Journal of Peptide Science*, 22, 492-500.

Shagaghi, N., Bhave, M, Palombo, EA & Clayton, AHA. 2017, Revealing the sequence of interactions of PuroA peptide with *Candida albicans* cells by live-cell imaging, *Scientific Reports*, vol. 7, no. 43542; doi: 10.1038/srep43542.

Conference presentations

Shagaghi, N., Clayton, A. H. A., Palombo, E. A., & Bhave, M. 2015. Sporicidal and anti-biofilm activity of PIN and PIN-like peptides. The 40th Lorne Conference on Protein Structure and Function, pp.68, 8-12 February, Lorne, Australia.

Shagaghi, N., Clayton, A. H. A., Palombo, E. A., & Bhave, M. 2016. Anticancer activity of rationally designed Trp-rich peptides based on PuroA peptide. IBS 2016, the 17th International Biotechnology Symposium and Exhibition, 24 – 27 October, 2016, Melbourne, Australia.

Shagaghi, N., Clayton, A. H. A., Palombo, E. A., & Bhave, M. 2016. Revealing a new interaction mechanism of antimicrobial peptides using live-cell imaging. The Swinburne Celebrates Research Conference, 22-23 June 2017, Melbourne, Australia.

Awards

Student best poster prize at the 40th Lorne Conference on Protein Structure and Function (8th to 12th of February 2015).

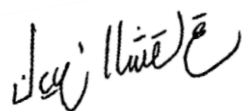
Shimadzu Prize as a highest achieving PhD student in Chemistry and Biotechnology in 2016.

Declaration

I, Nadin Shagaghi, declare that the PhD thesis entitled “**Development of Novel Antimicrobial Peptides**” is no more than 100,000 words in length, exclusive of tables, figures, appendices, references and footnotes. This thesis contains no material that has been submitted previously, in whole or in part, for the award of any other academic degree or diploma, and has not been previously published by another person. Except where indicated, this thesis is my own work.

Nadin Shagaghi

July 2017



Abbreviations

Standard chemical symbols, genetic notations, gene names and SI units are used without definition. Full gene names are given at their first mention.

Asn (or N)	Asparagine
Asp (or D)	Aspartic acid
Arg (or R)	Arginine
bp	Base pair
Cys (or C)	Cysteine
DMEM	Dulbecco's Modified Eagle's Medium
DNA	Deoxyribonucleic acid
DMSO	Dimethyl sulfoxide
EDTA	Ethylenediaminetetraacetic acid
eDNA	Extracellular DNA
FITC	Fluorescein isothiocyanate
<i>g</i>	Centrifugal force
Glu (or E)	Glutamic acid
Gln (or Q)	Glutamine
Gly (or G)	Glycine
GSP-1	Grain Softness Protein-1
<i>Hin</i>	<i>Hordoindoline</i> genes
<i>Hina</i>	<i>Hordoindoline-a</i>
<i>Hinb-1</i>	<i>Hordoindoline-b1</i>
<i>Hinb-2</i>	<i>Hordoindoline-b2</i>
HINA	Hordoindoline-a protein
HINB1	Hordoindoline-b1 protein
HINB2	Hordoindoline-b2 protein
His (or H)	Histidine
Ile (or I)	Isoleucine
kDa	KiloDalton
Leu (or L)	Leucine
Lys (or K)	Lysine
Met (or M)	Methionine

Abbreviations

mg	Milligram
mL	Millilitre
MTT	3-[4,5-dimethylthiazol-2-yl]-2, 5-diphenyltetrazolium bromide
MW	Molecular weight
NaCl	Sodium chloride
N-terminal	Amino terminal of a protein
OD	Optical density
Phe (or F)	Phenylalanine
<i>Pin</i>	<i>Puroindoline</i> genes
<i>Pina</i>	<i>Puroindoline-a</i>
<i>Pinb</i>	<i>Puroindoline-b</i>
PIN	Puroindoline proteins
PINA	Puroindoline-a protein (wild-type)
PINB	Puroindoline-b protein (wild-type)
<i>Pinb-2</i>	<i>Puroindoline-b2</i> genes
Pro (or P)	Proline
PI	Propidium iodide
QTL	Quantitative trait locus
RNA	Ribonucleic acid
RNase	Ribonuclease
SDS	Sodium dodecyl sulphate
Ser (or S)	Serine
SNP	Single nucleotide polymorphism
Thr (or T)	Threonine
TRIS	Tris(hydroxymethyl)aminomethane
Trp (or W)	Tryptophan
Tyr (or Y)	Tyrosine
UV	Ultra-violet
Val (or V)	Valine
°C	Degree Celsius

Table of contents

1.	General introduction and literature review	1
1.1	General introduction and thesis outline	2
1.1.1	General introduction	2
1.1.2	Thesis outline	2
1.2	Introduction to AMPs	3
1.2.1	Anionic antimicrobial peptides (AAMPs)	4
1.2.2	Cationic peptides with linear α -helical structures	4
1.2.3	Cationic or anionic peptides with β -sheet structures	4
1.2.4	Peptides formed by proteolytic digestion of larger proteins	5
1.2.5	Peptides with a predominance of specific amino acids	5
1.3	Factors that affect the antimicrobial activity and specificity of AMPs	5
1.3.1	Length	5
1.3.2	Primary sequence	6
1.3.3	Charge	7
1.3.4	Secondary structure	8
1.3.5	Hydrophobicity	9
1.3.6	Amphipathicity	10
1.3.7	Membrane composition	11
1.4	Archetypal Trp-rich peptides (TRPs)	11
1.4.1	Indolicidin	11
1.4.2	Tritrpticin	13
1.4.3	Lactoferricin	15
1.5	Rationally designed Trp-rich peptides	18
1.6	Wheat puroindoline proteins (PINs)	20
1.6.1	Biochemical properties of Puroindolines and effects on grain texture	20
1.6.2	Tertiary structure of PINs	23
1.6.3	<i>Pin</i> -related genes in related plant species	25
1.6.4	Proposed biological function of PINs in wheat	26
1.6.5	<i>In vitro</i> antimicrobial activities of PINs	26
1.6.6	<i>In vivo</i> antimicrobial activities of PINs	27

1.6.7	Antimicrobial activity of PIN-based peptides	29
1.6.8	The structure of PuroA peptide	30
1.7	Mechanisms of action of AMPs	31
1.7.1	Permeabilization mechanisms	36
1.7.1.1	Barrel stave pore model	36
1.7.1.2	Toroidal pore model	36
1.7.1.3	Carpet mechanism	36
1.7.2	Non-lytic membrane mechanisms	37
1.7.3	Non-lytic intracellular mechanisms	39
1.8	Mechanisms of action of TRPs and the significance of the tryptophan residues	44
1.9	Proposed mechanism of action for PINs and PIN-based peptides	47
1.10	Applications of AMPs	50
1.10.1	Clinical applications	50
1.10.1.1	Anticancer activity of AMPs	51
1.10.1.2	Trp-rich peptides with anticancer activity	53
1.10.2	Applications of AMPs in the food industry	57
1.10.3	Applications of AMPs in plant biology, aquaculture and animal husbandry	57
1.11	Resistance to Antimicrobial Peptides	59
1.12	Summary of the literature	63
1.13	Aims and strategy of the project	64
2.	Materials and methods	65
2.1	Equipment and materials	66
2.1.1	Equipment	66
2.1.2	Commercial kits and reagents	67
2.2	Prepared solutions and materials	67
2.2.1	Sterilisation	67
2.2.2	Buffers and solutions	67
2.2.3	Media for microbial growth	68
2.2.4	Media for cell culture	69

2.2.5	Microbial strains	69
2.2.6	Cell lines	70
2.2.7	Peptide solution	70
2.3	General methods	71
2.3.1	Peptide design	71
2.3.2	Physicochemical analytical tools	72
2.3.3	Antibacterial activity assay [Broth minimum inhibitory concentration (MIC)]	74
2.3.4	Anti- <i>Candida</i> activity assay [Broth minimum inhibitory concentration (MIC)]	75
2.4	Effect of salt on the antibacterial activity of peptides	76
2.5	Protease stability assay	76
2.6	Circular dichroism spectroscopy	76
2.7	Three dimensional structure prediction	77
2.8	<i>In vitro</i> DNA-binding assay	77
2.9	<i>E. coli</i> filamentation assay	78
2.10	Time-kill assay	79
2.11	Membrane permeability assay	79
2.12	Visualizing the effect of peptides on the morphology of the planktonic cell of MRSA using SEM	80
2.13	Inhibitory activity of peptides on biofilm formation	81
2.13.1	Preparation of bacterial cultures	81
2.13.2	Inhibition of initial cell attachment	81
2.13.3	Inhibition of preformed biofilm	81
2.13.4	Biofilm biomass assay (Crystal violet assay)	82
2.13.5	Biofilm metabolic activity assay (MTT assay)	83
2.13.6	Biofilm susceptibility testing by static chamber assay and confocal microscopy	83
2.13.7	Visualizing the activity of P1 on initial adhesion and biofilm formation of a clinical MRSA isolate using SEM	84
2.13.8	Inhibition of initial cell attachment on high density polyethylene surfaces (HDPE)	85
2.14	Sporicidal activity of peptides	86

2.14.1	Preparation of spore suspension	86
2.14.2	Sporicidal activity assay	86
2.14.3	Visualizing the effect of peptides on the morphology of spores of <i>B. subtilis</i> using SEM	86
2.14.4	Effect of peptides on the outgrowth of <i>B. subtilis</i> spores	87
2.14.5	Effect of peptides on the membrane integrity of <i>B. subtilis</i> spores	87
2.15	SEM visualization of the effect of PuroA on the morphology of <i>C. albicans</i> cells	88
2.16	Time-kill assay for PuroA and FITC-PuroA on <i>C. albicans</i> and <i>E. coli</i> cells	88
2.17	Cell cycle analysis	89
2.18	Cell cultures, chamber and reagents preparation for live cell imaging	89
2.19	Confocal laser-scanning microscopy for live cell imaging	90
2.20	Fluorescence lifetime imaging microscopy (FLIM)	91
2.21	Resistance selection (Serial transfer experiments)	93
2.22	Time-kill assay for resistant isolates	96
2.23	Fitness Measurements (cost of resistance)	96
2.24	Stability of resistance	97
2.25	Quantifying cross-resistance	97
2.26	Checkerboard assay (MIC of combining peptides)	97
2.27	Haemolytic activity assay	100
2.28	Cytotoxicity against mammalian Cells (cell proliferation and viability assay)	100
2.28.1	Thawing of cells	100
2.28.2	Subculturing of cells	101
2.28.3	Cryopreservation of cells	101
2.28.4	Cell viability assay	102
2.29	Visualizing the effect of peptides on the morphology of HeLa cells using scanning electron microscopy (SEM)	102
2.30	Statistical analysis	103

3.	Rational design of variant PuroA peptides and assessment of their biochemical properties and bioactivity effects	104
3.1	Abstract	105
3.2	Introduction	106
3.3	Results	108
3.3.1.	Peptide design and predicted physicochemical parameters	108
3.3.2	Antimicrobial activity	111
3.3.3	Antimicrobial activity in the presence of salts	113
3.3.4	Proteases Stability	113
3.3.5	Circular dichroism (CD) spectroscopy	117
3.3.6	Predication the three-dimensional structure	122
3.3.7	<i>In vitro</i> DNA-binding ability of peptides	123
3.3.8	Morphological effects of designed peptides on <i>E. coli</i> cells (<i>E. coli</i> filamentation assay)	126
3.4	Discussion	132
3.4.1	Importance of rationally design AMPs for clinical applications	132
3.4.2	Effect of length on antimicrobial activity and salt stability	133
3.4.3	Effect of net charge and C-terminal amidation on antimicrobial activity and salt stability	133
3.4.4	Effect of hydrophobicity on antimicrobial activity	135
3.4.5	The correlation between secondary structure of AMPs and their antimicrobial activity	135
3.4.6	The correlation between D-amino acids and antimicrobial activity and proteases stability of AMPs	136
3.4.7	Effect of cyclization on antimicrobial activity and stability of PuroA	137
3.4.8	Effect of dimerization on antimicrobial activity and stability of PuroA	138
3.4.9	Correlation between the antimicrobial activities of TRPs and their <i>in vitro</i> DNA binding and inducing of filamentation in <i>E. coli</i> cells	139

4.	Potential applications of PIN-based peptides: sporicidal and anti-biofilm activities	141
4.1	Abstract	142
4.2	Introduction	143
4.3	Results	146
4.3.1	Antibacterial activity of the PIN-based peptides [(minimum inhibitory concentration (MIC)]	146
4.3.2	Effect of PuroA on membrane integrity of <i>L. monocytogenes</i> and <i>P. aeruginosa</i>	149
4.3.3	Effect of PuroA and its derivatives on the morphology of MRSA cells	150
4.3.4	Inhibitory activity of the peptides on biofilm formation	151
4.3.4.1	Inhibitory activity of the peptides on biofilm formation of <i>P. aeruginosa</i> , <i>L. monocytogenes</i> and <i>L. innocua</i>	151
4.3.4.2	Biofilm susceptibility testing by static chamber assay	154
4.3.4.3	Inhibition of initial cell attachment on high density polyethylene surfaces (HDPE)	154
4.3.4.4	Effects of PuroA and its derivatives on biofilm of clinical MRSA isolate	155
4.3.5	Sporicidal activity of the peptides	158
4.3.6	Effect of the TRPs on the outgrowth of <i>B. subtilis</i> spores	164
4.3.7	Effect of peptides on membrane integrity of <i>B. subtilis</i> spores	165
4.4	Discussion	166
5.	Mechanism of action of PuroA peptide	170
5.1	Abstract	171
5.2	Introduction	172
5.3	Results	175
5.3.1	The effect of PuroA peptide on <i>C. albicans</i> and <i>E. coli</i> morphology	175
5.3.2	Time killing assay	179
5.3.3	Effect of PuroA on <i>C. Albicans</i> cell cycle	180

5.3.4	Time-lapse confocal microscopy	182
5.3.5	Time-lapse FLIM	185
5.4	Discussion	188
5.4.1	Anti- <i>Candida</i> mechanism of PuroA	188
5.4.2	Proposed bactericidal mechanism of PuroA	191
6.	Experimental evolution of resistance to TRPs	193
6.1	Abstract	194
6.2	Introduction	195
6.3	Results	197
6.3.1	Resistance to TRPs after selection	197
6.3.2	Time-kill assay	198
6.3.3	Cost of resistance	199
6.3.4	Stability of resistance	201
6.3.5	Cross-resistance studies	201
6.3.6	Determining the effects of peptide combinations on MIC and resistance development	202
5.4	Discussion	204
7.	Preliminary investigations of cell selectivity and anticancer potential of rationally designed TRPs	208
7.1	Abstract	209
7.2	Introduction	210
7.3	Results	212
7.3.1.	Haemolytic activity and cytotoxicity against mammalian cells	212
7.4	Discussion	222
8.	General discussion and conclusion	226
8.1	General discussion and conclusion	227
8.2	Future directions	233
	References	236
	Appendix	291

List of figures

1.1	Interdependent relationship between molecular determinants of biological activities of AMPs	7
1.2	Structure of PINA, PINB, PINB-2 and GSP-1 proteins in common wheat (<i>Triticum aestivum</i>).	21
1.3	Predicted tertiary structure of PINA using SWISS-MODEL	24
1.4	PINA structure prediction using I-TASSER	24
1.5	Alignment of predicted amino acid sequences of Hina, Hinb-1 and Hinb-2 from barley (<i>Hordeum vulgare</i>)	25
1.6	PuroA structure in the presence of SDS micelles	31
1.7	Various models of permeabilization and non-lytic membrane mechanisms of AMPs	38
1.8	Intracellular modes of action of AMPs	42
1.9	The aromatic ring structure of tryptophan (Trp) and its interaction with arginine (Arg)	45
1.10	General mechanism of action of Trp-rich antimicrobial peptides	47
1.11	Scanning electronmicrographs of <i>S. cerevisiae</i> cells treated with PIN-based peptides	49
1.12	Cationic antimicrobial peptide-resistance mechanisms in bacteria	60
2.1	Strategies used in two-colour live imaging experiments	90
2.2	Strategy used resistance selection experiments	94
2.3	Strategies used in studying evolution of resistance to TRPS and characterization of resistance isolates	95
2.4	Example of checkerboard assay set up in the 96-well microtiter plate of PuroA and W7 combination	99
3.1	Helical wheel projections of the design peptides	110
3.2	Circular dichroism spectra for PuroA and its variant peptides	121
3.3	Three-dimensional structure projections of PuroA and P1 peptides	122
3.4	Electrophoresis of plasmid DNA alone and when it is bound to PuroA, PuroA, Cyclic-PuroA and Di-PuroA peptides	124

3.5	Electrophoresis of plasmid DNA bound to P1, dP1, WW, dWW, W7, dW7, W8, R8, R7 and R6 peptides	125
3.6	Morphological changes induced in <i>E. coli</i> cells by designed peptides	127
3.7	Confocal microscopy of <i>E. coli</i> cells treated by peptides	128
3.8	Confocal microscopy of <i>E. coli</i> cells treated by peptides	129
3.9	Confocal microscopy of <i>E. coli</i> cells treated by peptides	130
3.10	Scanning electron micrographs of <i>E. coli</i> cells treated with peptides	131
4.1	Time-kill kinetics of PuroA and Pina-M at $1 \times$ MIC against bacteria	148
4.2	Time-kill kinetics of PuroA, P1 and W7 at $1 \times$ MIC against MRSA bacteria	148
4.3	Effect of PuroA on membrane integrity of <i>L. monocytogenes</i> , <i>P. aeruginosa</i> and MRSA M173525 isolate after 1 h incubation	149
4.4	Scanning electronmicrographs of MRSA M173525 planktonic cells treated with peptides at $1 \times$ MIC	150
4.5	Anti-biofilm activity of PuroA	154
4.6	The activity of P1 on initial adhesion and biofilm formation of the clinical MRSA M173525 isolate	156
4.7	Scanning electronmicrographs of the effect of P1 on initial adhesion of the clinical MRSA M173525 isolate at $1 \times$ MIC	157
4.8	SEM analysis of <i>B.subtilis</i> spores treated with PuroA peptide	160
4.9	SEM analysis of <i>B.subtilis</i> spores treated with P1 peptide	161
4.10	SEM analysis of <i>B.subtilis</i> spores treated with PuroB peptide	162
4.11	SEM analysis of <i>B.subtilis</i> spores treated with Hina peptide	163
4.12	Effect of the TRPs on the outgrowth of <i>B. subtilis</i> spores	164
4.13	Effect of peptides on membrane integrity of <i>B. subtilis</i> spores	165
5.1	Scanning electronmicrographs of <i>C. albicans</i> treated with PuroA	176
5.2	Scanning electronmicrographs of <i>E. coli</i> treated with PuroA	177

5.3	Morphological changes induced in <i>E. coli</i> cells by PuroA observed by light microscopy	178
5.4	Morphological changes induced in <i>E. coli</i> cells by PuroA using confocal microscopy	178
5.5	<i>C. albicans</i> killing kinetics by PuroA and FITC-PuroA peptides	179
5.6	<i>E. coli</i> killing kinetics by FITC-PuroA peptide	180
5.7	The effects of PuroA on the cell cycle progression of <i>C. albicans</i> cells	181
5.8	Fluorescence intensity histogram profiles of <i>C. albicans</i> cells after treatment with 125 µg/mL of PuroA using flow cytometer	181
5.9	Sequence of events during attack of a single <i>C. albicans</i> cell by FITC-PuroA at 8 µg/mL, time-lapse confocal microscopy images taken in real time	183
5.10	Plot of total FITC intensity (green line) and total PI intensity (red line) (right scale) and relative cell size (blue line) (left scale) vs time over 70 min	184
5.11	shows <i>E. coli</i> cell exposed to FTIC-PuroA peptide at 8 µg/mL	184
5.12	Time-lapse fluorescence lifetime images of FITC-PuroA interacting with a single <i>C. albicans</i> cell	186
5.13	Fractional fluorescence from free PuroA, pore forming PuroA and nucleic acids bound PuroA, as a function of time during attack of a single <i>C. albicans</i> cell	186
5.14	Fluorescence lifetime images of FITC-PuroA interacting with <i>E. coli</i> cells	187
5.15	Schematic showing the sequence of the three events (A, B and C) occurring upon interaction of PuroA peptides with <i>C. albicans</i> cell	188
6.1	Time killing kinetics of resistant isolates	199
6.2	Effect of resistance development on maximum growth rate (V_{MAX}) of bacteria	200

Contents

6.3	Checkerboard assay in the 96-well microtiter plate of PuroA and W7 combination against <i>S. aureus</i>	202
7.1	Example of haemolytic activity of peptides against sheep red blood cells (RBCs)	212
7.2	Light microscopy images of NIH-3T3 fibroblasts	216
7.3	Cell viability of mouse NIH-3T3 fibroblasts after peptide treatment	217
7.4	Cell viability of human cervical carcinoma HeLa cells after peptide treatment.	218
7.5	Light microscopy images of HeLa cells	220
7.6	Scanning electronmicrographs of HeLa cells after P1 and Di-PuroA treatment	221

List of tables

1.1	Example of peptides with specific amino acids predominance	5
1.2	Antimicrobial activities of indolicidin and its analogues	12
1.3	Antimicrobial activities of tritrypticin and its analogues	15
1.4	Antimicrobial activities of bovine lactoferricin and its analogues	17
1.5	Antimicrobial activities of rationally designed Trp-rich peptides	19
1.6	Selected <i>Pin</i> alleles in common wheat	22
1.7	Antimicrobial activity of the peptides based on the TRD of puroindolines and related proteins	30
1.8	Examples of biophysical techniques used recently to study the mechanism of action AMPs	33
1.9	Proposed Mechanism of action of AMPs	43
1.10	Examples of antimicrobial peptides with anticancer activities and their mechanisms of action	55
1.11	Applications of AMPs	58
1.12	Mechanisms of bacterial AMP resistance	61
2.1	Instruments and apparatus used	66
2.2	Commercial kits and reagents	67
2.3	Concentration and composition of solutions and buffers	68
2.4	Primary sequence, net charge, molecular weights, isoelectric points, hydrophobicity and Trp content of the designed TRPS	73
3.1	Primary sequence, net charge, molecular weights, isoelectric points, hydrophobicity and Trp content of the designed TRPS	109
3.2	Antimicrobial activities of peptides	112
3.3	Antibacterial activity of the peptides in the presence of NaCl	115
3.4	Antibacterial activity of the peptides treated with trypsin or proteinase K	116
4.1	Antibacterial activity of PIN-based peptides	147
4.2	Inhibition of initial cell attachment by the TRPs	152
4.3	Inhibition of preformed bacterial biofilms by PIN-based peptides at 1 h and 20h incubation	153

4.4	Inhibition of cell attachment to high density polyethylene surface by Pina-M peptide	155
4.5	Inhibition of initial cell attachment and preformed biofilms of MRSA by PuroA and it derivatives peptides	156
4.6	Sporicidal Activity of the Peptides	158
6.1	Selection response for resistance to selected TRPs	198
6.2	Growth behaviours of control and positive selection lines in unsupplemented medium	200
6.3	Response to compensatory adaptation selection for PuroA and indolicidin	201
6.4	Cross-resistance between peptides	202
6.5	Combination activities of PuroA with other TRPs	203
7.1	Haemolytic activity of the designed TRPs	213
7.2	Antibacterial activity, haemolytic activity and cell selectivity (therapeutic index) of the designed TRPs	214
7.3	Cytotoxicity activity of Trp-rich peptides against NIH 3T3 and HeLa	215

Chapter 1

General introduction and literature review

1.1 General introduction and thesis outline

1.1.1 General introduction

The continuing emergence and spread of drug-resistant pathogens has become of increasing worldwide concern. Although the precise correlation between emergence of resistance to antibiotics and their use can be highly variable, the irrational use of broad-spectrum and potent antibiotics has been recognized as a main reason for the emergence of multi-drug-resistant microbes (superbugs) at high rates. Thus, finding new bio-control agents that are able to combat drug-resistant pathogens is crucial. Since their discovery, antimicrobial peptides (AMPs) have been seen as novel antimicrobial therapeutics because of their wide range of activities, long evolutionary history and low potential of developing resistance against them. This project investigates the properties and applications of AMPs based on wheat antimicrobial proteins known as puroindolines (PINs).

1.1.2 Thesis outline

- Chapter 1 provides extensive background information on antimicrobial peptides, highlighting the research and developments in this field. It starts by introducing AMPs, discusses the biochemical determinants of their biological activities, focuses on Trp-rich antimicrobial peptides (TRPs) and describes the small family of wheat endosperm proteins called puroindolines (PINs) in detail as they form the basis of this study. It also discusses the mechanism of action of AMPs in general and TRPs in particular, describes the potential applications of AMPs and discusses the development of resistance against AMPs. The chapter concludes by summarising the research questions and aims of the present work.
- Chapter 2 describes the materials and methods used to investigate the research questions.
- Chapter 3 is the first results and discussion chapter, describes the design of several AMPs based on the tryptophan-rich domain (TRD) of puroindoline-a (PINA) and compares their antimicrobial activities, salt tolerance and protease stability to assess the biochemical signatures that are important for biological effect.
- Chapter 4 describes the activity of the designed peptides against bacterial endospores and biofilms.

- Chapter 5 investigates the membranolytic and intracellular mechanism of action of a selected peptide, PuroA.
- Chapter 6 investigates the potential of bacteria and yeast to develop resistance to PIN-based peptides.
- Chapter 7 describes a preliminary investigation of the cytotoxicity profile of the designed peptides against selected types of mammalian cells, including cancer cells.
- Chapter 8, the last chapter, summarizes the conclusions from this study, and suggests further research directions in this field.

1.2 Introduction to AMPs

AMPs are an integral part of the innate immune system of many organisms. They can act as endogenous antibiotics and kill pathogenic bacteria, fungi, viruses and protozoa directly, or indirectly by modulating the immune response in higher organisms (Zanetti 2004; Hancock & Sahl 2006). AMPs are multifunctional molecules that can influence many cellular processes. Beside their primary role in protecting the host against the invasion of pathogens, AMPs can be signalling molecules, immune modulators, mitogens, antitumor agents, contraceptive agents and drug delivery vectors and they are also playing a part in the wound healing process (Lai & Gallo 2009; Pushpanathan et al. 2013). Although a majority of AMPs are membrane-active and disrupt the integrity of the microbial membranes in many ways, it has been shown that some AMPs also target key cellular processes such as DNA and protein synthesis, enzymatic activity and cell wall synthesis (Yeaman and Yount, 2003, Brogden, 2005). Therefore, it was proposed that AMPs exert their activity through multiple mechanisms of action, giving them an advantage over existing antibiotics (which work on a specific cellular target) as development of microbial resistance against AMPs by gene mutations is less likely (Nguyen et al., 2011). Hence, AMPs are recognised as candidates with the most potential to substitute and/or complement the current antibiotics and effectively control drug-resistance pathogens.

At present, more than 2500 natural antimicrobial peptides have been registered into the antimicrobial peptide database (APD) (<http://aps.unmc.edu/AP/main.php>, last accessed February, 2017). AMPs are widely diverse in sequence and structure and

this diversity is essential for their broad spectrum antimicrobial activity. In general, AMPs are small in size (≤ 100 amino acids residues), and a majority are cationic due to the positively charged residues (arginine and/or lysine) while some are anionic. They also contain a significant proportion of hydrophobic residues (tryptophan, alanine or phenylalanine) and can arrange into amphipathic conformations. AMPs are commonly classified into five main subgroups for convenience, based on a combination of their net charge, secondary structures, origin and amino acid composition. These are summarised below.

1.2.1 Anionic antimicrobial peptides (AAMPs): The net charge of these peptides is typically -1 to -7, and the lengths are between 5 and 70 amino acids. AAMPs have broad antimicrobial activity against bacteria, fungi, viruses and/or insects (Harris et al. 2009, 2011). However, it is believed that they have other primary biological roles. AAMPs have been isolated from vertebrates, invertebrates and plants. Examples include bovine chromacin (YPGPQAKEDSEGSPSQGPASREK) (Strub et al. 1996), PsHCt1 (VTDGDADSAVPNLHENTEYNHYGSHGVYPDK) isolated from *Penaes stylirostris* (blue prawn) (Destoumieux-Garzón et al. 2001), and WjAMP-1 (QAGGQTCPPGGICCSQWGYCGTTADYCSPPNNCQSNCWASG) purified from leaves of *Wasabia japonica* (Kiba et al. 2003).

1.2.2 Cationic peptides with linear α -helical structures: These typically contain >40 amino acid residues, lack cysteine and are rich in basic amino acids such as arginine and lysine which give them a net positive charge (Wang et al. 2010a). Most are unstructured in aqueous solutions; however, they can adopt α -helical structures under certain conditions (Gennaro & Zanetti 2000). Human LL-37 (LLGDFFRKSKEKIGKEFKRIVQRIKDFLRNLPRTES) (Johansson et al. 1998) and buforin II (TRSSRAGLQFPVGRVHRLLRK) from the Asian toad, *Bufo garagrizans* (Yi et al. 1996) are classified under this group.

1.2.3 Cationic or anionic peptides with β -sheet structures: These peptides contain cysteine (Cys) residues that form disulphide bonds and stable β -sheets (Brogden 2005). The defensins are stabilized by three disulphide bonds and have a β -hairpin as their fundamental structural feature. Human HNP-1 (ACYCRIPACIAGERRYGTCTIYQGRLLWAFCC) (Selsted et al. 1985) and the antifungal defensin MsDef1 (RTCENL

ADKYRGPFCFSGCDTHCTTKENAVSGRCRDDFRCWCTKR) from alfalfa (*Medicago sativa*) seed (Spelbrink et al. 2004) belong to this group.

1.2.4 Peptides formed by proteolytic digestion of larger proteins: Some anionic or cationic peptides are fragments of larger proteins such as lactoferricin (Lfcin) from lactoferrin (Bellamy et al. 1992) (detailed in section 1.4.3) and casocidin-I (KTKL TEEKNRLNFLKKISQRYQKFALPQYLKTVYQHQQK) from human casein (Zucht et al. 1995). The proteins themselves have direct non-enzymatic antimicrobial activity, however, their primary function is usually immunity-related (Nguyen et al. 2011b).

1.2.5 Peptides with a predominance of specific amino acids: Some AMPs are rich in specific amino acids, mainly proline (Pro) (Otvos Jr 2002; Li et al. 2014), tryptophan (Trp), arginine (Arg) (Chan et al. 2006), and/or glycine (Gly) (Bulet et al. 1999) (examples given in Table 1.1). These peptides are generally linear due to the lack of cysteine (Cys) residues in their sequence; however, some can form extended coils (Broden 2005).

Table 1.1 Example of peptides with specific amino acids predominance

Peptide	Predominant amino acid(s)	Sequence	Reference
PR-39	Pro (49%), Arg (26%)	RRRPRPPYLPRPRPPPPFFPRLPP RIPPGFPPRFPPRFPP-NH ₂	(Agerberth et al. 1991)
Indolicidin	Trp (39%), Pro (23%)	ILPWKWPWWPWRR-NH ₂	(Selsted et al. 1992)
PuroA	Trp (38%)	FPVTWRWWKWWKG-NH ₂	(Jing et al. 2003)
shepherin I	Gly (67.8%), His (28.6%)	GYGGHGGHGGHGGHGGHGGHGGH GHGGGGHG	(Park et al. 2000)

1.3 Factors that affect the antimicrobial activity and specificity of AMPs

1.3.1 Length: The length of AMPs is a very important factor for their activity, as a minimum length of 7-8 amino acids is required to form an amphipathic structure with hydrophilic and hydrophobic faces (Bahar & Ren 2013). The length affects the mechanism of action as well; for instance, to penetrate the lipid bilayer of bacteria in a barrel-stave model, the AMP needs to be at least 22 amino acids to form an α -helical structure and 8 amino acids to form a β -sheet (Westerhoff et al. 1989). The peptide size can also affect its cytotoxicity level; e.g., a shorter 15-residue derivative of

melittin (GLPALISWIKRKRQQ), showed 5- to 7-fold less antibacterial activity and 300-fold less toxicity to rat erythrocytes compared to the full length melittin (Subbalakshmi et al. 1999). To study the effect of chain length on antimicrobial activity and haemolytic activity, Liu et al. (2007) synthesized a series of peptides containing simple sequence repeats, (RW) $_n$ -NH₂ (where $n = 1, 2, 3, 4, \text{ or } 5$). The antimicrobial and haemolytic activities of the peptides increased with chain length. The two shortest chains ($n=1$ or 2) were relatively inactive, while the three longer chains ($n = 3, 4, \text{ or } 5$) displayed almost at the same level of antibacterial activity, therefore, it was suggested that at (RW)₃, a threshold in biological response attained. Recently, Guzmán et al. (2013) found that Lys homopeptides with an odd number of residues, especially with 11 residues, showed broader inhibitory activity against Gram-positive bacteria than those with an even number of residues at concentrations of 10 μM . Whereas at higher peptide concentrations ($>20 \mu\text{M}$), the antibacterial activity of Lys homopeptides was directly related to the number of residues. Moreover, the cytotoxicity of Arg homopeptides were insignificant when the chains length were up to 11 residues at 100 μM ; however, there was an abrupt increase in cytotoxicity against eukaryotic cells when the peptide length reached 12 (Guzmán et al. 2013). This study has shown that differences in the number of residues can affect the potency and selectivity of AMPs.

1.3.2 Primary sequence: Generally, AMPs have very low sequence homologies, even among those belonging to similar families or isolated from the same source (plants, animals or insects). However, they have a high level of functional conservation and they form similar conformational patterns upon interaction with biological membranes (Teixeira et al. 2012). Analysis of the residue distribution in the N-terminal region of α -helical AMPs from different sources showed that, independently of the following residues, glycine (Gly) in position 1 is preponderant. This is mainly because it is a good N-capping residue for α -helices and can resist proteolytic cleavage by aminopeptidases (Tossi et al. 2000). In addition, in many AMPs, cationic amino acids such as Arg, Lys and hydrophobic aromatic residues, generally Trp, are highly overrepresented and often concentrated at a specific section of the peptide sequence. The positively charged residues are essential for the electrostatic interactions between the cationic AMPs and negatively charged pathogen membrane, while Trp has a key role in anchoring the peptide into the pathogens'

membranes (Chan et al. 2006). Therefore, many synthetic AMPs have been designed to contain repeats of amino acids such as Trp and Arg (Liu et al. 2007; Gopal et al. 2012). On the other hand, some amino acids such as aspartic acid (Asp) and glutamic acid (Glu) are rarely present.

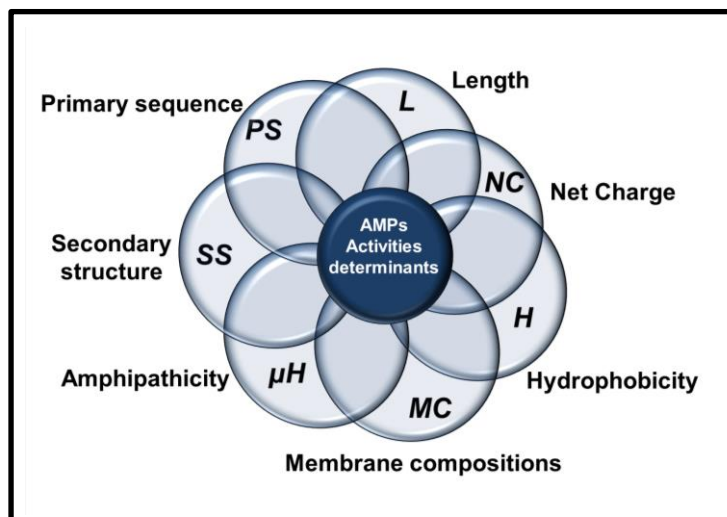


Figure 1.1 Interdependent relationship between molecular determinants of biological activities of AMPs.

All these parameters play a key role in determine the efficiency, spectrum of activity, mechanism of action and cytotoxic selectivity of AMPs.

1.3.3 Charge: The net charge is the sum of all ionisable group charges. Most cationic AMPs have a net positive charge ranging from + 2 to + 9 due to the presence of Arg and/or Lys (Hancock & Sahl 2006). The charge substantially affects the initial interaction of AMPs with cell membranes, as well as their antimicrobial activity and mechanism of action. Due to the difference in membrane composition and charge between prokaryotes and eukaryotes, the charge of peptides plays a critical role on their selective toxicity. Eukaryotic plasma membranes mainly contained zwitterionic and neutral membrane lipids such as phosphatidylcholine (PC) (Verkleij et al. 1973). In contrast, bacterial cytoplasmic membranes have an overall negative charge as they are rich in the acidic phospholipids, such as phosphatidylglycerol (PG), phosphatidylserine (PS), and cardiolipin (CL), and fungal cell walls have chitin chains and a layer of β -1,3-glucan (Ratledge & Wilkinson 1988), conferring a highly overall negative charge.

Giangaspero et al. (2001) designed peptides with different charge ranging from +1 to +11, but similar amphipathicity, degree of structure formation and mean hydrophobicity, to study the effect of charge on potency, spectrum of activity and selectivity. It was found that the analogues with net charge of +5 or +6 had potent and broad-range antimicrobial activity. Moreover, reducing the charge from +6 to +3 significantly decreased the potency toward bacteria and decreasing it further to +1 created an inactive analogue. However, increasing the charge up to +11 did not make any further improve in the antimicrobial activity, suggesting that it may have reached its limit of activity at +9 (Giangaspero et al. 2001). Although there is a direct correlation between peptide charge and potency (Dathe et al. 2001; Pasupuleti et al. 2008), it was observed that increasing the cationicity above +7 does not improve the activity further, because of the strong interaction between the peptides and phospholipid groups at the membrane. This strong interaction subsequently prevents the peptide structuring and translocation into the deeper layers of membranes (Tossi et al. 1994; Pasupuleti et al. 2012). However, pleurocidin (GWGSFFKKAHV GKHVGKAALTHYL-NH₂) with a notably greater cationicity, +8, compared to +5 of magainin 2 (GIGKFLHSAKKFGKAFVGEIMNS-NH₂), has greater antibacterial potency towards Gram-negative bacteria, and this potency was linked to its conformational flexibility and ability to penetrate the bacterial membrane much deeper than magainin 2 (Amos et al. 2016).

1.3.4 Secondary structure: Partitioning–folding coupling process refers to partitioning of polypeptide chains of AMPs into membranes, mainly accompanied by peptide secondary structure formation (Wieprecht et al. 1999; Seelig 2004). Many AMPs adapt either α -helical or β -sheet structures and the degree of structuring affects their activity and cytotoxicity. Helicity refers to the ability of AMPs to form spin structure (Bahar & Ren 2013). Secondary structure may be less important for the antimicrobial activity of AMPs, compared to the parameters of sequence or charge. However, it largely affects the toxicity to eukaryotic cells, as it was found that disruption of the α -helical structure of AMPs by incorporation of D-amino acids to create “diastereomers”, reduced the haemolytic effect and maintained the antimicrobial effect (Shai & Oren 1996; Avrahami et al. 2001; Huang et al. 2014a). Papo et al. (2002) replaced 35% of the L-amino acids of an α -helical 15 residue long peptide (LKLLKLLKLLKLL-NH₂) with D-amino acids at positions 3, 6, 8, 9, and

13 to disrupt the helical structure formation (LKLLKKLLKKLLKLL-NH₂). It was found that such a modification not only eradicated the haemolytic activity against human red blood cells (hRBCs) but it increased the solubility of the peptide in water, maintained full antimicrobial activity in serum and controlled the sensitivity to enzymatic degradation by trypsin and proteinase (Papo et al. 2002). On the other hand, significant α -helix disruption by introducing a high number of D-amino acids (4 and more) or completely removing the α -helical region, significantly decreased or completely eliminate the antibacterial activities of some AMPs (Huang et al. 2014a; Dong et al. 2016). Some amino acids such as Pro and Gly have lower helix-forming propensities compared to other amino acids (Pace & Scholtz 1998), therefore the helix propensity of each amino acid should be taken into consideration when designing α -helical AMPs (Bahar & Ren 2013).

1.3.5 Hydrophobicity: This refers to the percentage of hydrophobic residues in a peptide. About 50% of amino acids in the primary sequence of many naturally occurring AMPs are hydrophobic (Yeaman & Yount 2003). Hydrophobicity could greatly affect the antimicrobial activity, range of target pathogens and cytotoxic selectivity of AMPs, as it controls the partitioning of the peptide into the membrane hydrophobic core (Yount et al. 2006). Generally, there is an optimal hydrophobicity for each AMP; changing it outside a threshold can affect haemolytic and antimicrobial activities. There is a strong correlation between mammalian cytotoxicity and hydrophobicity; the toxicity of highly hydrophobic peptides increases in eukaryotic cells (Pasupuleti et al. 2008; Schmidtchen et al. 2009; Strandberg et al. 2015), which could be result from their poor solubility in aqueous solution (Dennison et al. 2005b). End-tagging of AMPs with hydrophobic amino acid stretches seems a noteworthy approach to design highly active and selective AMPs. Pasupuleti et al. (2009b) found that W-tagging of AMPs resulted in boosting of bactericidal effect against both Gram-negative and Gram-positive bacteria, as well as maintaining limited toxicity and stability against proteolytic degradation. In addition, a correlation has been found between hydrophobicity and self-association; peptides with higher core hydrophobicity display stronger self-association and aggregation tendencies compared to those with lower hydrophobicity (Yin et al. 2012). Joshi et al. (2015) also showed that increasing the hydrophobicity of ultra-short Trp- and Arg-rich peptides, X-W₃R₄ (X is aromatic organic moiety), by tagging the N-terminal with an organic tag induced

self-assembly of these peptides in water, increased their antibacterial activity and maintained high cell selectivity.

1.3.6 Amphipathicity: This refers to the distribution of hydrophobic and hydrophilic residues in AMPs. Upon interaction with target membranes, most AMPs fold into amphipathic structures; they commonly fold into amphipathic α -helix or β -sheets, whereas unfolded peptides are less common. In fact, the amphipathicity of AMPs is essential for their mechanism of action. The positively charged hydrophilic face drives the initial electrostatic attraction to the negatively charged components of the microbial membrane, and then the hydrophobic face inserts into the membrane through van der Waals interactions, producing loss of the membrane function and increasing its permeability (Hancock & Chapple 1999). Disrupting the amphipathic structure of AMPs can influence their mechanism of action and pore formation (Mihajlovic & Lazaridis 2012). Giangaspero et al. (2001) argued that folding into a helical structure without an amphipathic conformation can limit the efficiency and range of activity of AMPs and Fernández-Vidal et al. (2007) also claimed that amphipathicity has priority over hydrophobicity in designing synthetic AMPs for specific cells. Conversely, Zhu et al. (2014) designed a short α -helical imperfectly amphipathic peptide, PRW4 (RFRR LRWKTRWRLK KI-NH₂), by replacing the charged amino acid residues on the polar face of an amphipathic peptide RI16 (RFRRLLRKKTRKRLKKI-NH₂) with Trps. PRW4 with disruptive amphipathicity and hydrogen bonds formed by paired tryptophan residues showed stronger activity against Gram-negative and Gram-positive bacteria and a reduced haemolysis of hRBCs cells compared to RI16. Further, Hollmann et al. (2016) stated that increasing the amphipathicity resulted in a dramatic increase in the membrane affinity of hRBCs and peptides. Designing AMPs with radial amphiphilicity rather than typical facial amphiphilicity has been proposed as an alternative approach to overcome the undesirable effects of facially amphiphilic structures and to increase stability of peptides against proteases (Xiong et al. 2015).

1.3.7 Membrane composition: Specific phospholipids or membrane phases are essential for peptide translocation and may play as important a role as the peptide structure itself in controlling translocation efficiency through the cell membrane (reviewed in Phoenix et al. 2013). Further, the selectivity to microbial membranes over that of the host cell is believed to strongly depend on the chemical and structural properties of the lipids of the cell membrane (Michael Henderson & Lee 2013). The mechanism of action of AMPs can change depending on the negatively charged lipid content in membranes (Manzini et al. 2014) and on the initial peptide–membrane interaction (Praporski et al. 2015). In fact, significant differences in antibacterial activity of peptides with similar amino acid sequences, charge and/or hydrophobicity are due to the molecular mechanism of peptide-lipopolysaccharide (LPS) interactions that can either allow the peptides to traverse, or prevent them from traversing the LPS in the outer membrane of Gram-negative bacteria and targeting the inner membrane (Shang et al. 2016). Recently, it was proposed that antimicrobial activity and selectivity of antimicrobial proteins and peptides depends on membrane architecture, lipid composition, and fluidity (Sanders et al. 2016, 2017). Additionally, many factors such as the charge of lipids, or presence of receptors, can affect the activities of AMPs and their selectivity, and also need to be considered in designing AMPs.

1.4 Archetypal Trp-rich peptides (TRPs)

TRPs are a subset of AMPs that display broad and potent antimicrobial activity. The following section details the biochemical properties, antimicrobial activities and the mechanistic studies of some archetypal TRPs. A significant part of this section has been published by us (Shagaghi et al. 2016b).

1.4.1. Indolicidin: Isolated from bovine neutrophils, indolicidin (ILPWKWP WWPWRR-NH₂) was the first Trp-rich AMP discovered (Selsted et al. 1992) and has the highest Trp proportion (39%) among all naturally occurring AMPs. It is a 13 residue peptide, naturally amidated at the C-terminus (Selsted et al. 1992) and shows activity against a wide range of pathogens (Table 1.2).

Many efforts have been made to design indolicidin-based peptides with increased activity. The analogue CP11 was more effective against Gram-negative bacteria and

fungi (Table 1.2), and was less haemolytic (Falla & Hancock 1997). Further, its activity was enhanced by introducing two terminal Cys residues to form a U-shaped molecule that could be cyclized easily (CycloCP-11; IC₁LKKWPWWPWRRC₁K-NH₂) (Rozek et al. 2003). The antimicrobial activities of CycloCP-11 and linear CP11 were comparable, but CycloCP-11 remained active for longer in the presence of trypsin than the linear CP11 (Rozek et al. 2003). A short analogue, omiganan (Table 1.2), showed high activity against a number of clinically important microbial pathogens (Sader et al. 2004).

Table 1.2 Antimicrobial activities of indolicidin and its analogues

Peptide	Peptide sequence	Antimicrobial activities
Indolicidin	ILPWKWPWWPWRR-NH ₂	<i>Escherichia coli</i> , <i>Staphylococcus aureus</i> (Selsted et al. 1992), <i>Pseudomonas aeruginosa</i> , <i>Salmonella typhimurium</i> (Falla et al. 1996), <i>Campylobacter jejuni</i> , <i>Enterococcus faecalis</i> (Ebbensgaard et al. 2015), methicillin resistant <i>Staphylococcus aureus</i> (MRSA) (Dosler & Mataraci 2013), <i>Rhizoctonia cerealis</i> and <i>R. solani</i> (Phillips et al. 2011), human immunodeficiency virus (HIV) (Robinson et al. 1998), herpes simplex virus (HSV) (Yasin et al. 2000), <i>Giardia lamblia</i> (Aley et al. 1994)
CP11	ILKKWPWWPWR RK	<i>E. coli</i> , <i>S. aureus</i> , <i>P. aeruginosa</i> , <i>S. typhimurium</i> , <i>Staphylococcus epidermidis</i> , <i>Candida albicans</i> (Falla & Hancock 1997)
Omiganan	ILRWPWWPRRK-NH ₂	<i>E. coli</i> , <i>S. aureus</i> , <i>P. aeruginosa</i> , <i>E. faecalis</i> , <i>Streptococci</i> spp., <i>Corynebacterium</i> spp., <i>Klebsiella</i> spp., <i>Staphylococcus epidermidis</i> , <i>Enterococcus faecium</i> , <i>Acinetobacter bauannii</i> , <i>Bacillus</i> ssp., <i>C. albicans</i> (Sader et al. 2004)
R12-OH	LPWKWPWWPW R	Human immunodeficiency virus (HIV) (Robinson et al. 1998)
10R 11R	RRPWKWPWWPW RR RWRRWPWWPW RRK	<i>Erwinia carotovora</i> , Tobacco mosaic virus (TMV) (Bhargava et al. 2007)

Dimer and tetramer forms of indolicidin, created by linking at C-terminal ends via Lys residues, both displayed increased inhibitory activity against HIV-1 integrase (Krajewski et al. 2004). Shin (2013) investigated the effect of Lys-linked dimerization of indolicidin C-terminal hexapeptide (Ind-6; WWPWRR-NH₂) on prokaryotic selectivity by synthesizing its Lys-linked dimeric form (di-Ind-6; (WWPWRR)₂K-NH₂) of Ind-6. The dimeric peptide demonstrated 2- to 4-fold and 2- fold improved antimicrobial activity, compared to the monomeric Ind-6 and indolicidin, respectively. Further, di-Ind-6 was less haemolytic against human red hRBCs than indolicidin,

whereas Ind-6 did not show any haemolytic activity even at high peptide concentrations (up to 200 $\mu\text{g}/\text{mL}$) (Shin 2013). Chang et al. (2013) synthesized a peptidomimetic stereoisomer of indolicidin, consisting of alternating L and D enantiomers. This analogue showed high resistance to enzymatic degradation, showing its potential to be used as vaccine adjuvant, as it displayed a better enhancement in cell-mediated immune responses than native form of indolicidin in BALB/c mice (Chang et al. 2013).

In terms of mechanism of action, Subbalakshmi and Sitaram (1998) proposed that indolicidin exerts its activity by attacking multiple targets in bacteria. First it permeabilizes both the outer and the cytoplasmic membranes of *E. coli* without leading to lysis, then it affects DNA synthesis resulting in filamentation of bacteria cells and also partially affects RNA synthesis (Subbalakshmi & Sitaram 1998). Interestingly, Ghosh et al. (2014) clarified how indolicidin inhibits the DNA processes. Their microscopy and spectroscopic data showed that indolicidin binds to the major groove of duplex B-type DNA, wraps it around and stabilizes it so that it cannot unwind easily, resulting in inhibition of DNA replication and transcription (Ghosh et al. 2014). In contrast to early reports, in a recent study found that indolicidin exhibited no permeabilization of both membranes of *E. coli* (Rapsch et al. 2014). Further, indolicidin forms salt bridges with the phospholipids headgroups and, as it is inserted more deeply, it induces local thinning of the bilayer (Neale et al. 2014), supporting the findings of (Végh et al. 2011). Moreover, indolicidin did not promote pore formation at concentrations of 0.5 μM to 10 μM , and only adsorbed at the surface and partially inserted into the bilayer (Rokitskaya et al. 2011; Wang et al. 2015a).

1.4.2. Tritrpticin: It was initially isolated from porcine bone marrow and, as the name indicates, it has three uniquely consecutive Trp residues (Lawyer et al. 1996). Tritrpticin shows potent antibacterial, antifungal and antiprotozoal activities against many clinically and environmentally important pathogens (Table 1.3).

The peptide forms an unordered structure in Tris buffer but adopts a stable amphipathic conformation in sodium dodecyl sulphate (SDS) micelles without a regular secondary structure such as an α -helix or a β -sheet. It was suggested that the amphipathic conformation may give an energetic advantage, since in this structure the

Trp and Phe residues are all in vicinity and can rest in the interfacial area of the cytoplasmic membrane (Schibli et al. 1999). Arias et al. (2016) suggested that each Trp residue in tritrypticin plays a different role in membrane permeabilization. The sequence is nearly palindromic and its four Arg make it highly cationic at neutral pH. These positively charged residues are essential for its antimicrobial activity, as deleting of even one residue of the Arg doublets at both termini resulted in decreased antibacterial activity, while substitution by Lys did not affect the activity (Nagpal et al. 1999). However, substitution of Arg with Lys was later found to reduce the haemolytic activity and increase the selectivity for microbial cells (Schibli et al. 2006).

A number of analogues have been created to investigate the residues essential for its antimicrobial activity and the importance of the Trp cluster in the tritrypticin's core. The amidation of C-terminal resulted in a 2-fold increase in antibacterial activity (Strøm et al. 2000) (similar to the Falla et al., 1996 findings for indolicidin). Substitution of the two Pro residues with Nlys (Table 1.3) increased the antibacterial activity and decreased the toxicity to mammalian cells (Zhu et al. 2006). Moreover, replacing the three Trps by Phe or Tyr were also examined, as their side chains may promote deeper penetration into the membrane, or locate into the membrane interface, respectively (Schibli et al. 2006). The Phe substitution had no significant effect on activity against *E. coli* and *S. aureus*, whereas Tyr substitution led to a 5-fold decrease in this activity. These results disagree with previous study by Yang et al. (2002) wherein substituting the three Trps by Phe caused 2-4 fold increase in the antibacterial activity. Both analogues (Phe/Tyr) also had a considerably low haemolytic activity compared to tritrypticin, possibly due to their weaker binding to phospholipid bilayers (Schibli et al. 2006). Substitution of the three Trp with 5-hydroxytryptophan (5OHW), a naturally occurring non-ribosomal amino acid, did not largely affect the minimum inhibitory concentration (MIC) of the parent peptide against *E. coli* and *B. subtilis*. However, these changes significantly affected the peptide–lipid interactions and its mechanism of action (Arias 2015).

Table 1.3 Antimicrobial activities of tritripticin and its analogues

Peptide	Peptide sequence	Antimicrobial activities
Tritripticin	VRRFPWWPFLRR	<i>E. coli</i> , <i>P. aeruginosa</i> , <i>S. epidermidis</i> , <i>Klebsiella pneumoniae</i> , <i>Proteus mirabilis</i> , Group D <i>Streptococcus</i> , <i>C. albicans</i> (Lawyer et al. 1996), <i>S. aureus</i> (Wei et al. 2006), <i>Trichomonas vaginalis</i> (Infante et al. 2011)
TPK	VRRFNlysWWWNlys FLRR-NH ₂)	<i>E. coli</i> , <i>S. aureus</i> , <i>P. aeruginosa</i> , <i>S. typhimurium</i> , <i>S. epidermidis</i> , <i>Bacillus subtilis</i> (Zhu et al., 2006)
TP-Nhtrp	VRRFP \underline{W} \underline{W} PFLRR	<i>E. coli</i> , <i>S. aureus</i> , <i>P. aeruginosa</i> , <i>S. epidermidis</i> , (Ahn et al., 2013)
HW	VRRFP ^{5OH} \underline{W} ^{5OH} \underline{W} ^{5OH} \underline{W} P FLRR-NH ₂	<i>E. coli</i> , <i>B. subtilis</i> (Arias, 2015)

* Nlys = Lys peptoid residue, NH₂-(CH₂)₄-NH-CH₂-COOH), \underline{W} = Nhtrp (homotryptophan peptoid residue), ^{5OH}W = 5-hydroxytryptophan.

Tritripticin displayed the greater lytic activity in negatively charged membranes than indolicidin and lactoferricin B (Schibli et al. 2002) and it showed ion channel-like activity when incorporated into soybean phospholipids (Salay et al. 2004). The mechanism of action of tritripticin is believed to involve pore formation in bacterial membranes coupled to secondary intracellular targeting. Yang et al. (2006) stated that tritripticin kills bacteria via membrane depolarization, however, they could not exclude a secondary intracellular target after cell permeabilization. The strong interaction with negatively charged phospholipid monolayers and expansion of the monolayers with increasing peptide concentration support the toroidal pore mechanism of action (Bozelli Jr et al. 2012; Salay et al. 2012). Although intracellular targets are also believed to be a part of tritripticin action, its detailed mechanism is still not fully understood. Only one study showed the capability of tritripticin to interact with multiple classes of biomolecules (Sharma et al. 2013)

1.4.3. Lactoferricin: The glycoprotein lactoferrin (LF) is a large (80 kDa, 703-amino acid) iron-binding protein, belonging to the transferrin family (Masson et al. 1966). It has shown antimicrobial activity against Gram-positive and Gram-negative bacteria (Bellamy et al. 1992), fungi (Wakabayashi et al. 1996; Sengupta et al. 2012), viruses (Andersen et al. 2001; McCann et al. 2003), and parasites (Omata et al. 2001). It also showed anti-inflammatory (Kruzel et al. 2006) and anti-carcinogenic activity (Shimamura et al. 2004). Digested of LF by proteases at acidic pH (e.g., pepsin) yield peptides with high antimicrobial activity. Thus, mother's milk provides newborns with required nutrients as well as enhancing their defense (Chan et al. 2006).

The AMP lactoferricin (Lfcin) results from cleavage of the basic N-terminal region of LF by proteases such as gastric-pepsin (Bellamy et al. 1992). Lfcin peptides have been isolated from many species; however, bovine Lfcin (LfcinB) is possibly the most active (Gifford et al. 2005). LfcinB (25 residues) has a disulfide bond between its two Cys and wide-ranging activities against bacteria, fungi and viruses (Table 1.4), as well as antitumor (Mader et al. 2005; Richardson et al. 2009) and antihypertensive activities (Fernández-Musoles et al. 2014). A hexapeptide (LfcinB₄₋₉) with amidated C-terminal was identified as the active center of LfcinB and had a similar MIC against *E. coli* and *S. aureus* as that of LfcinB (Tomita et al. 1994). An 11 residue peptide (LfcinB₄₋₁₄) also retained the same antimicrobial activity as LfcinB, and had decreased haemolytic activity (Kang et al. 1996) whereas the 15 residue peptide LfcinB₁₋₁₅ showed less antibacterial activity than the full length LfcinB (Rekdal et al. 1999). A cyclized analogue of LfcinB₄₋₁₄, made by adding Cys residues at both termini, had increased antimicrobial activity (Nguyen et al. 2005). However, cyclization of the 25 residue LfcinB by click chemistry and sortase A techniques did not improve the antibacterial activity of the linear original peptide (Arias et al. 2014).

To identify the residues important for the antibacterial activity of LfcinB, an ‘Ala scan’ experiment was performed on the 15-residue peptide LfcinB 17-31 (FKCRRWQWRMKKLGA). The results indicated that the two Trps (Trp6 and Trp8) were most important with substitution of either by Ala completely abolishing the antibacterial activity (Strøm et al. 2000). Interestingly, replacement of the polar residues Cys3, Gln7 or Gly14 with Ala, a hydrophobic residue, increased the activity (Strøm et al. 2000). Increasing the number of hydrophobic amino acids seemed to contribute to the spectrum of activity, potency, haemolytic activity and cytotoxicity of Lfcin (Han et al. 2013a).

Table 1.4 Antimicrobial activities of bovine lactoferricin and its analogues

Peptide	Peptide sequence	Antimicrobial activities
LfcinB ₁₇₋₄₁	FKCRRWQWRMKKL GAPSTTCVRRAF	<i>E. coli</i> , <i>S. aureus</i> , <i>Salmonella enteritidis</i> , <i>K. pneumoniae</i> , <i>Proteus vulgaris</i> , <i>Yersinia enterocolitica</i> , <i>P. aeruginosa</i> , <i>C. jejuni</i> , <i>Streptococcus mutans</i> , <i>Corynebacterium diphtheriae</i> , <i>L. monocytogenes</i> (Bellamy et al. 1992), <i>C. albicans</i> (Bellamy et al. 1994), Human Cytomegalovirus (HCMV) (Andersen et al. 2001), herpes simplex virus (HSV) (Jenssen et al. 2004)
LFB ₁₇₋₃₁ or LfcinB ₁₇₋₃₁	FKCRRWQWRMKKL GA	<i>E. coli</i> , <i>S. aureus</i> (Strøm et al. 2000), <i>B. subtilis</i> , <i>S. cerevisiae</i> , <i>Penicillium digitatum</i> , <i>P. italicum</i> , <i>P. expansum</i> , <i>Alternaria sp.</i> , <i>Aspergillus nidulans</i> , <i>Botrytis cinerea</i> , <i>Fusarium oxysporum</i> , <i>Magnaporthe grisea</i> (Muñoz & Marcos 2006)
LfcinB ₂₀₋₂₅	RRWQWR	<i>E. coli</i> , <i>B. subtilis</i> , <i>S. cerevisiae</i> , <i>P. digitatum</i> , <i>P. italicum</i> , <i>P. expansum</i> , <i>Alternaria sp.</i> , <i>A. nidulans</i> , <i>B. cinerea</i> , <i>F. oxysporum</i> , <i>M. grisea</i> (Muñoz & Marcos 2006)
LfcinB ₄₋₉	RRWQWR-NH ₂	<i>E. coli</i> , <i>S. aureus</i> (Tomita et al., 1994)
LFB 2-Nal _{6,8}	FKCRR2NalQ2NalRM KKLGA	<i>E. coli</i> , <i>S. aureus</i> (Haug & Svendsen 2001)
LFB ₁₇₋₂₇	FKCRRWQWRMK	<i>E. coli</i> , <i>S. aureus</i> , <i>P. aeruginosa</i> (Strøm et al. 2002b)
Undeca 9	RRWYRWAWRMR- NH ₂	<i>E. coli</i> , <i>S. aureus</i> (Strøm et al. 2002b)
Octa 1	RRWYRWWR-NH ₂	<i>E. coli</i> , <i>S. aureus</i> , <i>P. aeruginosa</i> (Strøm et al. 2002a)
LfcinB ₄₋₁₄ Disu	CRRWQWRMKKLGC -NH ₂	<i>E. coli</i> , <i>S. aureus</i> (Nguyen et al. 2005)
LFB ₄₋₁₄	RRWQWRMKKLG	<i>E. coli</i> , <i>S. aureus</i> (Wei et al. 2006)
LF-6	KWRQWQSKWRRTN PFWWIRR	<i>E. coli</i> , <i>S. aureus</i> , <i>P. aeruginosa</i> , <i>S. epidermidis</i> , <i>S. typhimurium</i> (Han et al. 2013a)

*2Nal = β -(naphth-2-yl)alanine.

In terms of mechanism of action, it was suggested that Lfcin pulls the intact LF protein into the cytoplasm, as the whole LF protein enter cells spontaneously (He & Furmanski 1995; Chan et al. 2006). Although LfcinB can interact with negatively charged membranes, it does not cause bacterial lysis or major leakage from liposomes; it only causes depolarization of the cytoplasmic membrane of *E. coli* and fusion of negatively charged liposomes (Ulvatne et al. 2001). Therefore, it was proposed to have intracellular targets, interfering with the normal cell functioning which may explain the wide range of activity of Lfcin. Ulvatne et al. (2004) showed that LfcinB inhibited the macromolecular biosynthesis in both Gram-positive and Gram-negative bacteria. Liu et al. (2011) confirmed this mechanism of action when LfcinB did not destroy the integrity of the *E. coli* and *S. aureus* membranes, but only formed holes of various sizes on the cell surface and affected bacterial protein synthesis. *E. coli* proteome chips have also been used to identify the intracellular target of LfcinB. One

study proposed that LfcinB targets phosphoenolpyruvate carboxylase and pyruvate metabolism (Tu et al. 2011), while another found that it inhibits growth of bacteria by binding to two response regulators, BasR and CreB, of a two-component system (TCS, a defence system) and suppressing their phosphorylation (Ho et al. 2012).

1.5 Rationally designed Trp-rich peptides

The archetypical peptides discussed above were discovered and/or derived from natural origins. These discoveries have led to studies of other Trp-rich peptides based on rational design, an effective approach to improve their antimicrobial activity and selectivity (Fjell et al. 2012) and reduce the manufacturing costs. Besides Trp, other hydrophobic (His, Phe) and basic (Arg, Lys) residues have also been used in combinatorial library or rational design approaches (Table 1.5).

Synthetic peptides using a combinatorial library approach, Combi-1 and Combi-2 (Table 1.5), showed antibacterial and antifungal activities (Blondelle & Houghten 1996). The end-to-end cyclized analogue, cyclo-combi; RRWWRWF, was tenfold more active than the linear form against *E. coli* and *B. subtilis* (Dathe et al. 2004). The peptide PW2 (Table 1.5) was derived from screening phage display libraries against living sporozoites of the protozoan *Eimeria acervulina*, the cause of coccidiosis (an economically important disease in poultry production). PW2 shows anticoccidal activity and it is effective against a number of fungi but not against bacteria (da Silva et al. 2002).

PAF26 was identified from a hexapeptide combinatorial library and showed strong activity against phytopathogenic fungi such as *Penicillium digitatum* (the causal agent of postharvest green mould in citrus), *P. italicum*, and *Botrytis cinerea* (López-García et al. 2002). PAF26 and its derivatives from an octapeptide library, PAF38 (Ac-RRKKWFW-NH₂), PAF40 (Ac-HRKKWFW-NH₂), as well as BM0 (Ac-RFWWFRRR-NH₂), were found to be active against *P. digitatum*, *Saccharomyces cerevisiae* and *E. coli* (Muñoz et al. 2007). Pac-525 (Ac-KWRRWVRWI-NH₂) and its reverse Pac-525_{rev} (Ac-IWRVWRRWK-NH₂) demonstrated activity against both Gram-positive and Gram-negative bacteria, and had low haemolytic activity (Wei et al. 2006).

Liu et al. (2007) designed a peptide series containing a repeated pattern of Arg-Trp ((RW)_n, where $n = 1, 2, 3, 4, \text{ or } 5$) and varying in charge and hydrophobicity. Gopal et al. (2012) extended this work by designing a second set containing a Lys-Trp repeat pattern ((KW)_n where $n = 2, 3, 4 \text{ or } 5$). The RW series showed antibacterial and antifungal activities (Liu et al. 2007; Gopal et al. 2012) (Table 1.5). The KW series also showed fungicidal activity against *Fusarium* species; however, it was lower than that of the RW series (Gopal et al. 2012). Furthermore, (KW)₄ (KWKWKW-NH₂) showed improved bactericidal activity, including resistant strains such as *Salmonella typhimurium* (Gopal et al. 2013). Deslouches et al. (2013) designed an amphipathic WR peptide series of 6 to 18 residues by serial adding one Arg in the hydrophilic face and one Trp in the hydrophobic face. The highest antibacterial activity was achieved at 12 residues in length (WR12, Table 1.5). WR12 also retained this activity in saline solution containing 150 Mm NaCl and at different pH (Deslouches et al. 2013).

Table 1.5 Antimicrobial activities of rationally designed Trp-rich peptides

Peptide	Peptide sequence	Antimicrobial activities
Combi-1, Combi-2	Ac-RRWRF-NH ₂ Ac-FRWHR-NH ₂	<i>E. coli</i> , <i>S. aureus</i> , <i>Streptococcus sanguis</i> , <i>C. albicans</i> (Blondelle & Houghten 1996)
PW2	HPLKQYWWRPSI	<i>E. tenella</i> , <i>Eimeria acervulina</i> , <i>C. albicans</i> , <i>A. nidulans</i> (da Silva et al. 2002)
PAF26	Ac-RKKWFW-NH ₂	<i>Penicillium digitatum</i> , <i>P. italicum</i> , <i>P. expansum</i> , <i>B. cinerea</i> , <i>F. oxysporum</i> (López-García et al. 2002)
Pac-525	Ac-KWRRWVRWI-NH ₂	<i>E. coli</i> , <i>S. aureus</i> (Wei et al. 2006)
(RW) _n	RW-NH ₂ , RWRW-NH ₂ , RWRWRW-NH ₂ , RWRWRWRW-NH ₂	<i>E. coli</i> , <i>S. aureus</i> , <i>F. solani</i> , <i>F. oxysporum</i> (Liu et al. 2007; Gopal et al. 2012)
(KW) _n	KWKW-NH ₂ , KWKW-NH ₂ , KWK WKWKW-NH ₂ , KWKWKW-NH ₂	<i>F. solani</i> , <i>F. oxysporum</i> (Gopal et al. 2012)
WR12	RWWRWRRWRR	<i>Acinetobacter baumannii</i> , <i>Klebsiella pneumoniae</i> , <i>P. aeruginosa</i> , MRSA (Deslouches et al. 2013)
W2	(WRPGRW) ₂	<i>E. coli</i> , <i>S. aureus</i> , <i>B. subtilis</i> (Chou et al. 2016)

Moreover, the rationally designed amphiphilic Trp-rich peptide dendrimers, D186 (Staniszewska et al. 2014), and dendrimer 14 (Zielinska et al. 2015) showed potent activity against planktonic cells and biofilm of *C. albicans*. Additionally, Joshi et al. (2015) designed self-assembling Trp-Arg-rich ultra-short peptidomimetics, X-W₃R₄ (where, X is an aromatic organic moiety) that showed selective and potent antibacterial activity against multi-drug resistant (MDR) *S. aureus* strains. Recently, Chou et al. (2016) designed multiple-stranded β -hairpin peptides with Arg residues and a Trp zipper to stabilize the β -hairpin structure insisted of the disulphide bonds to reduce the

cost of production. W2 ((WRPGRW)₂), with a “S-shaped” motif to induce a globular structure formation, and a Trp zipper, showed improved antibacterial activity against Gram-positive and Gram-negative bacteria, cell selectivity and salt stability (Chou et al. 2016).

1.6 Wheat puroindoline proteins (PINs)

Puroindoline-a (PINA) and puroindoline-b (PINB) are small (148 residue, about 13 kDa), highly basic (pI 10.5), lipid-binding, Trp- and Cys-rich proteins present in the endosperm of wheat. The name puroindoline is derived from the Greek word for wheat, *puros*, and the indole ring in the side chain of Trp residues (Gautier et al. 1994). It has been established that they play a main role in controlling the hardness of the wheat kernels. PINs are mutated naturally and mutations in either or both *Pin* gene(s) affect grain hardness. There are strong suggestions for an *in vivo* defense role for PINs in wheat endosperm, the only organ wherein the *Pins* have been found to be expressed. Yet, the effects of the hardness-related mutations on the antimicrobial activities, the biochemical properties and mechanisms of action of PINs are little explored. The following sections will discuss PINs in details as they form the basis of this study.

1.6.1 Biochemical properties of puroindolines and effects on grain texture:

PINA and PINB are encoded by the 447 bp intronless genes, *Puroindoline a* (*Pina-D1*) and *Puroindoline b* (*Pinb-D1*), which are part of the *Hardness* (*Ha*) locus on the short arm of chromosome 5D (Greenwell & Schofield 1986; Gautier et al. 1994; Chantret et al. 2004). The PINs are 55% similar in amino acid sequence (Blochet et al. 1993) and both contain 10 Cys residues that are proposed to form 5 disulphide bonds. The two proteins have a noticeable unique feature in their primary structure which is the presence of a Trp rich domain (TRD) that also contains basic residues (Gautier et al. 1994). The TRD of PINA contains five Trp residues while in PINB contains only three (Fig. 1.2). PINA and PINB are synthesized as pre-pro-proteins with a 28/29 amino acid long N-terminal cleavable peptide; the potential processing site for PINA occurs after the 28th (Tyr) residue and for PINB occurs after the 29th (Asn) residue (Fig. 1.2). These regions comprise a signal peptide cleavage site after the 19th Ala residue in both proteins. It has been suggested that this signal peptide could play a role in the intracellular targeting and functions of PINs in wheat endosperm (Gautier et al. 1994; reviewed in Bhave & Morris 2008a).

absorption, rheology and flour characteristics compared to the durum parent cultivar (Heinze et al. 2016; Murray et al. 2016; Murray et al. 2017).

The soft grain phenotype is dominant and in the grain of soft common wheat (*Triticum aestivum* L.), both proteins must exist together in their functional wild-type (WT) forms (Giroux & Morris 1998; Hogg et al. 2004). Hard grain wheats result from deletions and/or various mutations in either or both *Pin* gene(s) (reviewed in Bhave & Morris 2008b; Pauly et al. 2013) (examples are given in Table 1.6). In addition, the *Gsp-1* genes are considered part of the *Ha* locus and tightly linked to *Pina* and *Pinb* genes on chromosome 5D. *Gsp-1* encodes a protein called the grain softness protein (GSP-1) which is around 40% homologous to the PIN proteins and its TRD truncated to only two Trp residues. Due to these similarities with PINs, GSP-1 has been suggested to affect the grain texture in wheat, however, its role in grain texture is ambiguous (reviewed in Bhave & Morris 2008a). In addition, it has been found that the *Ha* locus is not responsible for all the grain texture variations in common wheat. A second set of *Pinb-2* genes has been reported on chromosome 7A and associated with a minor hardness qualitative trait locus (QTL) (Wilkinson et al. 2008). At present, six groups of *Pinb-2* gene have been reported (*Pinb-2v1* to *Pinb-2v6*) and their putative proteins are approximately 57- 60% similar to PINB, with abbreviated TRD to two Trp residues only (Wilkinson et al. 2008; Chen et al. 2011; Ramalingam et al. 2012; Chen et al. 2013).

Table 1.6 Selected *Pin* alleles in common wheat

Phenotype	PIN protein	PIN allele	Change in protein sequence*	Reference
Soft	Wild-Type PINA	<i>Pina-D1a</i>	-	(Gautier et al. 1994)
Hard	PINA	<i>Pina-D1m</i>	Single SNP. Pro35Ser	(Chen et al. 2006)
Hard	PINA null	<i>Pina-D1r</i>	Gene deletion	(Ikeda et al. 2010)
Hard	PINA truncated	<i>Pina-D1t</i>	Single SNP. TRP41stop, premature stop codon	(Ramalingam et al. 2012)
Soft	Wild-Type PINB	<i>Pinb-D1a</i>	-	(Gautier et al. 1994)
Hard	PINB	<i>Pinb-D1b</i>	Single SNP. Gly46Ser	(Giroux & Morris 1997)
Hard	PINB	<i>Pinb-D1d</i>	Single SNP. Trp44Arg	(Lillemo & Morris 2000)
Hard	PINB truncated	<i>Pinb-D1ab</i>	Single SNP. Gln99stop, premature stop codon	(Tanaka et al. 2008)
Hard	PINB	<i>Pinb-D1ad</i>	Single SNP. Gln62stop, premature stop codon	(Ayala et al. 2016)

*SNP: Single nucleotide polymorphism

The role of *Pin* genes in determining grain hardness in wheat has been extensively reviewed (Bhave & Morris 2008a; Bhave & Morris 2008b) and studied by our group (Ramalingam et al. 2012). Although the complete mechanism by which these proteins affect grain texture is yet to be revealed, the functionality of puroindolines has been associated with their lipid-binding properties. The high affinity of PINs for lipid binding and their TRD seem to be directly involved in lipid binding (Blochet et al. 1993; Clifton et al. 2007a; Clifton et al. 2007b; reviewed in Bhave & Morris 2008b). It was found that the mutations in the *Pinb-D1b* (Gly46Ser) and *Pinb-D1d* (Trp44Arg) within the TRD of PINB considerably affect the interaction between PINs and anionic phospholipids (Clifton et al. 2007a; Clifton et al. 2007b). The decrease in selectivity towards the anionic phospholipids was observed for the mutant PINB (Clifton et al. 2007a) but also influences the interaction of PINA (Clifton et al. 2007b), suggesting mutations that can influence the lipid binding properties of one PIN protein can also affect the binding ability of the other. The biochemical basis behind the interdependence of PINA and PINB in controlling the grain texture is also unresolved. Our group assessed the protein-protein interactions (PPI) using a yeast two-hybrid system and this study suggested that involvement of residues outside the TRD and/or a little-known hydrophobic domain (HD) (Fig. 1.3) (Alfred et al. 2014).

1.6.2 Tertiary structure of PINs: PINA and PINB have similar structure with 30% α -helices, 30% β -sheets and 40% unordered structure at pH 7 based on infrared and Raman spectroscopy (Le Bihan et al. 1996). The location of the four α -helical structures of PINA and PINB are shown in Figure 1.2. PINs are Cys-rich proteins (containing 10 Cys residues), their TRD is enclosed by two Cys residues (Fig. 1.2), and the five predicted disulphide bonds allow PINA to fold in a compact 3D structure (Figure 1.3 and 1.4). The TRD is stabilized by disulphide bridges between the two unconnected Cys28 and Cys48 in PINA and Cys29 and Cys48 in PINB (Le Bihan et al. 1996).

*This image is unable to be reproduced online due to
Copyright
Please consult print copy held in the Swinburne
Library*

Figure 1.3 Predicted tertiary structure of PINA using SWISS-MODEL.

Source: Alfred et al. (2014). SWISS-MODEL (<http://swissmodel.expasy.org/>) showing the location of the TRD from Phe34 to Gly46, as an extended loop between α -helix 1 and 2 and the putative hydrophobic domain (HD) from Ile75 to Phe85 as a smaller loop between α -helix 3 and 4.

*This image is unable to be reproduced online due to Copyright
Please consult print copy held in the Swinburne Library*

Figure 1.4 PINA structure prediction using I-TASSER.

Source: Lesage et al. (2011). I-TASSER (<http://zhanglab.cmb.med.umich.edu/I-TASSER>) showing the 5 predicted disulphide bonds between Cys20/Cys55, Cys56/Cys104, Cys11/Cys66, Cys68/Cys110 and Cys28, Cys48 and the protruding TRD on the right.

1.6.3 Pin-related genes in related plant species: PIN homologs have also been identified in closely related *Triticeae* diploid species, such as barley (*Hordeum vulgare*, hordoidolines; HIN), oat (*Avena sativa*, avenoidolines) and rye (*Secale cereal*, secaloidolines) (Gautier et al. 2000). *Hordoidoline a* (*Hina*), *hordoidoline b-1* (*Hinb-1*), *hordoidoline b-2* (*Hinb-2*) and *grain softness protein* (*Gsp*) in barley are the homologs of wheat *Pin* and *Gsp-1* genes (Beecher et al. 2002). Barley kernel texture is of commercial interests in beer production (Brennan et al. 1996). HINs have been proposed to be associated with endosperm texture of barley (Beecher et al. 2002; Turuspekov et al. 2008), however, their clear contribution was established when a frame-shift (null) mutation in *Hinb-2* was found to result in increased grain hardness (Takahashi et al. 2010). The identities among the putative protein sequences of the *Pin*-related genes are very high, 85-100% for the PINA-related and 90-93% for the PINB-related proteins (reviewed in Bhave & Morris 2008a), proposing a shared function for this protein family.

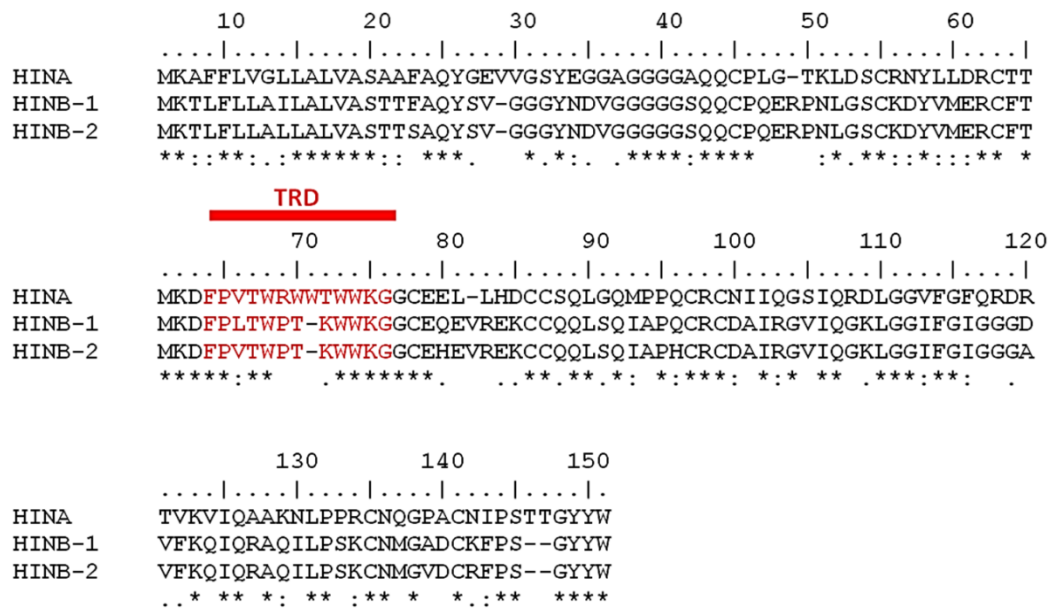


Figure 1.5 Alignment of predicted amino acid sequences of Hina, Hinb-1 and Hinb-2 from barley (*Hordeum vulgare*).

The TRD is shown in red. The source of the reported putative protein sequences is Caldwell et al. (2004). Alignment performed using Clustal Omega (<http://www.ebi.ac.uk/Tools/msa/clustalo>, last accessed February, 2017) and Bioedit software.

1.6.4 Proposed biological function of PINs in wheat: The primary biological role of PINs in wheat is not thought to be controlling the grain texture as grain hardness, although a commercially important property, it has no known benefit to the plant. The generally accepted hypothesis regarding the *in vivo* roles of PINs is protecting the wheat seed from phytopathogens as originally proposed by (Gautier et al. 1994). As with any other living system, plants produce antimicrobial peptides as a part of their innate immune system. This hypothesis is supported by the presence of the unique TRD in the PIN proteins (Blochet et al. 1993; Gautier et al. 1994), as Trp has been strongly associated with the microbicidal activity of many AMPs such as those discussed above (section 1.4). The biochemical properties of Trp in this context are detailed separately below (section 1.8).

1.6.5 *In vitro* antimicrobial activities of PINs: The first evidence of antimicrobial activity of PINs against phytopathogenic fungi was provided by Dubreil et al. (1998). PINA and PINB proteins purified from soft wheat seeds showed antifungal activity against *Alternaria brassicola*, *Ascochyta pisi*, *Fusarium culmorum* and *Verticillium dahlia*. However, PINB showed higher antifungal activity than PINA. Combining the PIN proteins with α -purothionin (α -PTH), an antimicrobial protein that also located in the starchy endosperm of wheat, led to a synergistic enhancement of their activity against *F. culmorum* (Dubreil et al. 1998). Purified PINA and PINB also showed antibacterial activity against *E. coli*, *S. aureus*, *Agrobacterium tumefaciens*, *Pseudomonas syringae phaseoli*, *Erwinia carotovora* and *Clavibacter michiganensis*. Combining the two proteins led to synergistic effects and as the both PIN proteins are always co-localized in the wheat kernel, this supports the defence role of these proteins against seed pathogens (Capparelli et al. 2005). It was also hypothesized that PINA and PINB may act in a different ways. PINA is a membrane acting protein, binding and producing trans-membrane pores whereas PINB interacts with intracellular components and inhibits normal cellular functions. Thus, PINA is proposed to be a ‘gate-opener’ for PINB to enter the cell (Capparelli et al. 2005; Chan et al. 2006).

As PINs occur in small quantities and only in the seed endosperm, obtaining them in adequate quantities and purity using low cost techniques can be challenging. A bacterial expression system was used to produce large quantities of recombinant pure PINs with relatively low cost. Recombinant PINA and PINB expressed in and purified

from *E. coli* cells have similar antibacterial activities to the native proteins (Capparelli et al. 2006). The recombinant PINs were able to kill intracellular *S. epidermidis* without exhibiting haemolytic activity or toxicity to mouse macrophage cells (Capparelli et al. 2007). Later, the same group used PINA and PINB for treating *Listeria monocytogenes*-infected mice and showed *in vivo* antibacterial and anti-inflammatory activities (Palumbo et al. 2010). In another study, Miao et al. (2012) constructed mutant forms of PINA containing two or three copies of TRD and expressed these in *E. coli*. The recombinant mutant PINA with two copies of TRD folded correctly and showed higher antimicrobial activities against *E. coli* and *S. aureus*, confirming the important role of TRD as the antimicrobial domain. Recently, our group successfully cloned and transiently over-expressed PINA and PINB in different subcellular compartments (chloroplast, apoplast, endoplasmic reticulum and cytosol) of *Nicotiana benthamiana* leaf cells, using the virus-based ‘magnICON[®]’ expression system (Niknejad et al. 2016). Various strategies were used to optimise PINA and PINB expression and purification. The recombinant PINs purified by His-tag affinity purification under native conditions or by the hydrophobic method retained their activities against *E. coli*, *S. aureus* and the filamentous fungi *Colletotrichum graminicola*, *Drechslera brizae*, *Rhizoctonia cerealis* and *Rhizoctonia solani* without exhibiting haemolytic activity to mammalian RBCs (Niknejad et al. 2016). Expression of PINs in adequate quantities with accurate tertiary structures is essential to further investigate their functionality and develop applications for agriculture or food safety or medical purposes.

1.6.6 *In vivo* antimicrobial activities of PINs: Transgenic studies involving introduction of wheat *Pina* and/or *Pinb* genes into plants that do not naturally encode these genes, such as rice, corn, durum wheat and all dicots including apple, showed the ability of PINs to impart biotic resistance to diseases in plants. In the first study, transgenic rice plants that constitutively expressed wild-type PINA and/or PINB showed increased tolerance to rice blast disease caused by *Magnaporthe grisea* with a 29-54% reduction in symptoms, and also increased tolerance to rice sheath blight caused by *Rhizoctonia solani*, with an 11 to 22% reduction in symptoms (Krishnamurthy et al. 2001). The incidences of both diseases in the transgenic rice expressing *Pinb-D1a* alone were higher than the lines that expressed *Pina-D1a* only. These results disagree with the observation of Dubreil et al. (1998) where PINB had

higher *in vitro* antifungal activity than PuroA, however, this may indicate species-specificity as *M. grisea* and *R. solani*, were not included in that study (Dubreil et al. 1998). This could also suggest that PINs act differently *in vivo* than *in vitro* due to their potential interactions with each other (Capparelli et al. 2005) and/or other plant proteins (Dubreil et al. 1998). PINB showed *in vitro* antifungal activity against *Venturia inaequalis*, the causal agent of apple scab (the most destructive disease causing serious economic losses in commercial orchards) (Chevreau et al. 2001). Therefore, apple (*Malus domestica*) genotypes ‘Ariane’ and ‘Galaxy’ were transformed with the *Pinb-D1a* gene, encoding PINB, led to 55% and 64% reduction in scab formation in their transgenic lines, respectively (Faize et al. 2004). The tetraploid durum wheat (AABB genome) varieties Luna and Venusia are highly sensitive to rust diseases which result in poor grain yield as with all durum, they lack *Pin* genes. These wheat cultivars were transformed with *Pina-D1a*, and the transgenic plants showed increased disease resistance to the leaf rust, caused by *Puccinia triticina* and consequently an increase in harvest yield (Luo et al. 2008). Introducing *Pina* and *Pinb* genes into corn leaves increased the plant’s tolerance to *Cochliobolus heterostrophus* which is the causal pathogen of corn southern leaf blight (SLB) (Zhang et al. 2011).

In addition, the overexpression of PINs in seeds (the endogenous location of PINA and PINB) were examined for the first time by assessing *Penicillium* sp. fungal growth inhibition (Kim et al. 2012). The overexpression of PINA and/or PINB was evaluated in two wheat varieties, Bobwhite and Hi-Line, and compared to near-isogenic lines (NILs) varying for mutations in PINA or PINB. Transgenic wheat seeds overexpressing PINA showed greater reduction in fungal infection and an increase of germination than PINB, mirroring Krishnamurthy et al. (2001) in transgenic rice.

These results collectively confirm that the PIN proteins are intrinsically antimicrobial in nature. Hence, the biochemical feature(s) of these proteins that may explain this property has been a subject of research interest and one such candidate domain is described below.

1.6.7 Antimicrobial activity of PIN-based peptides: The synthetic peptides, PuroA (FPVTWRWWKWWKG-NH₂) and PuroB (FPVTWPTKWWKG-NH₂) (Table 1.7), based on the TRDs of PINA and PINB, respectively, were tested for antibacterial activity against the Gram-positive and Gram-negative bacteria, *S. aureus* and *E. coli*, respectively (Jing et al. 2003). PuroA showed similar antibacterial activity against *S. aureus* to PINA and was more active against *E. coli*. However, PuroB showed poor antibacterial activity and did not inhibit bacterial growth even at the highest concentration tested (346 µg/ml) (Jing et al. 2003). This could suggest that the TRD of PuroB is not as effective as that of PuroA. The observed difference in the antibacterial activities of PuroA and PuroB peptides supports the proposed different role of the full-proteins (Capparelli et al. 2005) (discussed above), and suggests that TRD is the active domain of PINA for its membrane active property but not for the intracellular effects of PINB.

Our group designed thirteen peptides based on the TRD of PIN proteins encoded by wild type and mutant hardness alleles, and *Gsp-1* from chromosome 5D, as well as barley *hordoindoline-a* (*HinA*) and duplicated *hordoindoline-b* (*HinB*) loci. These synthetic peptides displayed strong activity against bacteria and phytopathogenic fungi (Table 1.7), and certain point mutations affected their activity at quantitative and/or qualitative levels (Phillips et al. 2011). In another study, our group designed two peptides, PINB- 2v1 and PINB-2v3, on the TRD of the PINB-2 protein. Both peptides displayed strong antibacterial activity and antifungal activity against the phytopathogenic fungi (Table 1.7) (Ramalingam et al. 2012). Comparing to PuroB, PINB- 2v1 and PINB-2v3 have considerably higher antimicrobial activity and this could suggesting that PINB-2 is a larger contributor to the defencing system of wheat seed than PINB. However, further tests are needed to confirm the role of PINB-2 protein in wheat. Selected PIN-based peptides were further tested against two common and severe rust diseases of wheat – stripe rust spores (*Puccinia striiformis* f. sp. *tritici*) and leaf rust spores (*P. triticina*). The peptides displayed inhibitory activity on the leaf and stripe rust spores and, consistent with previous observations (Phillips et al. 2011), PuroB had lower antimicrobial activity comparing to PuroA (Alfred et al. 2013a). These studies together reveal that antimicrobial activity is a feature shared by the TRD of the protein family of PINs, GSP-1 and hordoindolines, and support the hypothesis that the primary *in planta* role of this protein family is biotic defence. The

PIN-based peptides also showed thermal and high pH stability and they were stable after long-term storage (8 weeks) at ambient temperature (Alfred et al. 2013a). All these properties make PIN-based peptides excellent candidates as natural preservatives in the food industry (Capparelli et al. 2005; Alfred et al. 2013a).

Table 1.7 Antimicrobial activity of the peptides based on the TRD of puroindolines and related proteins

Peptide	Natural allele with this TRD	Peptide sequence	Antimicrobial activities
PuroA	<i>Pina-D1a</i>	FPVTWRWWKWWKG-NH ₂	<i>E. coli</i> , <i>S. aureus</i> , <i>Collectotrichum Graminicola</i> , <i>D. brizae</i> , <i>R. solani</i> , <i>R. cerealis</i> (Jing et al. 2003; Phillips et al. 2011)
Pina-M	<i>Pina-D1 m</i>	FSVTWRWWKWWKG-NH ₂	<i>E. coli</i> , <i>S. aureus</i> , <i>C. Graminicola</i> , <i>D. brizae</i> , <i>F. oxysporum</i> , <i>R. solani</i> , <i>R. cerealis</i> (Phillips et al. 2011)
PuroB	<i>Pinb-D1a</i>	FPVTWPTKWWKG-NH ₂	<i>R. solani</i> , <i>R. cerealis</i> (Phillips et al. 2011)
Pinb-B, D, Q	<i>Pinb-D1b</i> , <i>Pinb-D1d</i> , <i>Pinb-D1q</i>	FPVTWPTKWWKS-NH ₂ , FPVTWPTKWRKG-NH ₂ , FPVTWPTKWLKG-NH ₂	<i>R. solani</i> (Phillips et al. 2011)
PINb-2v1 PINb-2v3	<i>PINB-2v1</i> <i>PINB-2v3</i>	FSIARLLKWWKG-NH ₂ FPISTLLKWWKG-NH ₂	<i>C. graminicola</i> , <i>Fusarium oxysporum</i> , <i>R. solani</i> (Ramalingam 2012)
GSP-5D	<i>Gsp-1</i>	MPLSWFFPRTWGKR-NH ₂	<i>E. coli</i> , <i>S. aureus</i> , <i>C. Graminicola</i> , <i>R. solani</i> (Phillips et al. 2011)
Hina	<i>Hina</i>	FPVTWRWWTWWKG-NH ₂	<i>E. coli</i> , <i>S. aureus</i> , <i>C. Graminicola</i> , <i>D. brizae</i> , <i>F. oxysporum</i> , <i>R. solani</i> , <i>R. cerealis</i> (Phillips et al. 2011)
Hinb1	<i>Hinb-1</i>	FPLTWPTKWWKG- NH ₂	<i>D. brizae</i> , <i>R. solani</i> (Phillips et al. 2011)

1.6.8 The structure of PuroA peptide: The structure of PuroA peptide was determined using two-dimensional (2D) nuclear magnetic resonance (NMR) methods in presence of anionic SDS micelles (Jing et al. 2003). It showed no defined and stable secondary structure in aqueous solution; however, it adopted a well-defined structure in the presence of SDS micelles. Although the peptide did not adopt any distinct helical conformation (Fig. 1.6), it had a helical segment spanning from Trp8 to Trp10 preceded by a turn from Thr4 to Trp7. Overall, the charge distribution forms an amphipathic structure with the cationic side chains of Lys and Arg residues resting on the hydrophilic side. Interestingly, the Arg6 side chain rests directly between the two

aromatic indole rings of Trp5 and Trp7 and this is possibly due to the formation of energetically favourable cation– π interactions (Fig. 1.7) (Ma & Dougherty 1997).

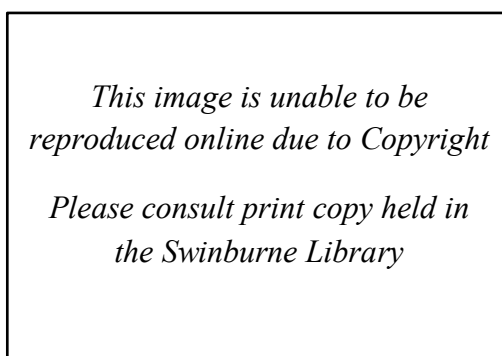


Figure 1.6 PuroA structure in the presence of SDS micelles.

Source: Jing et al. (2003). Trp residues are highlighted in blue, the cationic Lys and Arg residues are shown in pink.

1.7 Mechanisms of action of AMPs

AMPs often exert microbicidal effects, resulting from irreversible disruption in essential cellular structures and/or functions. The antimicrobial mechanisms of AMPs are very diverse and complex. Despite the wide diversities between their compositions, conformations and sources, all mechanisms of action involve the parallel and key steps of attraction, attachment, insertion into the target cells' membrane and permeability, followed by lytic or non-lytic mechanisms. It is generally believed that the initial attraction is mediated by electrostatic interaction between the cationic basic residues within many AMPs and the anionic components of the target cell's membrane (Huang 2000; Glukhov et al. 2005; Bastos et al. 2008; Jiang et al. 2008). In case of anionic AMPs, the initial action involves metal ions, by which these peptides gain access to target membranes (Harris et al. 2009). Unlike antibiotics, the initial interaction generally does not involve any specific receptor; however, some AMPs have a receptor-mediated mechanism such as nisin from *Lactococcus lactis* (Hsu et al. 2004) and microcin J25 from the faecal *Escherichia coli* AY25 strain (Destoumieux-Garzón et al. 2005). After binding to the membrane, most AMPs rearrange their conformation at the lipid–water interface and this conformational transition and formation of secondary structure is considered a key stage in the partition process, making it less energetically expensive (Kaiser & Kezdy 1983; Wimley & White 1996).

Many AMPs are membranolytic and kill the host organisms via lysis their membrane, whereas some AMPs are non-membranolytic and translocate through the lipid bilayer to then attack intracellular targets (Fig. 1.7 & 1.8) (Table 1.9). For example, buforin II forms transient toroidal pores through the bacterial membrane to translocate to the cytoplasm, wherein it binds to DNA and RNA and inhibit the cellular activities (Park et al. 1998; Kobayashi et al. 2004). Further, a few AMPs utilise multiple mechanisms; e.g., nisin can bind to lipid II in bacterial membrane, inhibit cell wall biosynthesis and form trans-membrane pores (Breukink et al. 1999; Wiedemann et al. 2001), and can also induce autolysis by activating relevant enzymes (Bierbaum & Sahl 1987). Moreover, the human LL-37 shows indirect activity via stimulating the human immune response and also direct activity by forming pores in the membranes of microorganisms (Nijnik & Hancock 2009; Lee et al. 2011). Therefore, AMPs have been called ‘dirty medications’ as they moderately hit microbe cells in multiple targets and disturb several biological functions, unlike antibiotics that powerfully act on a specific target. This feature makes AMPs able to control a broad range of pathogens without development of resistance (Peschel & Sahl 2006).

In the mechanistic investigations to elucidate how the peptides interact with biomimetic membranes, live cells and intracellular targets, a number of biophysical techniques have played a crucial role in providing the relevant experimental evidences. Table 1.8 summarizes some of recently used biophysical techniques in this field; some of these will be employed in the current investigation. Recent mechanistic studies have used imaging techniques that are able to capture fast mechanistic events and directly observe the real-time effect of AMPs on single cells. Live cell imaging provide a remarkably detailed picture of the timing, sequence, and subcellular location of specific events during the attack of AMPs on live cells. The use fluorescently labeled AMPs was a remarkable innovation for visualizing the dynamics of AMP–microbe interactions in recent years. The fluorescent AMPs have been used in combination with many time-resolved, live-cell imaging techniques such as fluorescence microscopy (either confocal or wide- field), fluorescence lifetime imaging microscopy (FLIM), fluorescence resonance energy transfer (FRET) microscopy and fluorescence correlation spectroscopy (FCS).

Table 1.8 Examples of biophysical techniques used recently to study the mechanism of action AMPs

Techniques	Applications	Advantages and limitations	AMPs	Bacterium or Biomimetic membranes*
Nuclear magnetic resonance (NMR) Spectroscopy	Secondary structure, orientation and lipid bilayer penetration	High accuracy, expensive, needs expertise	Indolicidin (Hsu et al. 2005; Ghosh et al. 2014)	SDS-d25 and DPC-d38 DNA
			Piscidin 1 (p1) and piscidin 3 (p3)(Perrin et al. 2014)	(DMPC)/(DMPG) and (POPE)/(POPG) DPC micelles
			Maculatin 1.1 (Sani et al. 2013)	<i>E. coli</i> PG and CL
			Protegrins (Kolossova et al. 2016), caerin 1.1 and aurein 1.2 (Laadhari et al. 2016)	DPC, <i>E. coli</i> and <i>B. subtilis</i>
Surface plasmon resonance (SPR) spectroscopy	Observation of the rate and amount of peptide adsorbing on and desorbing from lipid bilayer and intracellular compounds Peptide-lipid interaction kinetics and thermodynamics	High surface-sensitivity, real time interactions analysis	Melittin and magainin (Papo & Shai 2003)	SUV and PC/cholesterol
			RW-BP100 and R-BP100 (Torcato et al. 2013)	POPC and POPC/POPG
			Magainin 2 (Hall et al. 2014)	DMPC, DMPC/DMPG, DMPC/DMPG/cholesterol, DMPE/DMPG
Circular dichroism (CD) spectroscopy	Secondary structure orientation	Quick, inexpensive, less accurate than NMR	Indolicidin (Hsu et al. 2005)	SDS
			Magainin 2 and cecropin A (Avitabile et al. 2014)	<i>E. coli</i>
			Piscidin 1 (p1) and piscidin 3 (p3) (Perrin et al. 2014; Kocourková et al. 2017)	(DMPC)/(DMPG) and (POPE)/(POPG)
Quartz crystal microbalance (QCM)	Study of mass and structural changes in lipid bilayer that caused by peptides insertion in real time and <i>in situ</i>	Ultra-sensitive, limited materials can be studied using QCM	Fallaxidin 4.1a (Sherman et al. 2009)	(DMPC-d ₅₄) and (DMPG)
			Caerin 1.1, aurein 1.2 and oncocin (McCubbin et al. 2011)	DMPC

Table 1.8 continued				
Electrochemical impedance spectroscopy (EIS)	Study of changes in bilayer membranes thickness, ion permeability and homogeneity when interact with AMPs bilayer resistance and capacitance	Very sensitive, high precision measurements	LL-37 (Neville et al. 2007), FSKRGY and FSKRGY-L3 (Lin et al. 2012)	DOPC+DOPG and DOPC+lipid A, DOPC, DOPG and lipid A polymer-cushioned supported lipid bilayers (POPC + POPG and POPC + cholesterol bilayers) constructed on single crystal silicon
Atomic force microscopy (AFM)	Study of the structural changes in live cells and the location of specific binding sites	High-resolution images at nanometre level, long image acquisition, study small and flat samples only	Indolicidin (Végh et al. 2011)	PLL-PGA-DPPC and membrane of <i>Halobacterium salinarum</i>
			Bovine lactoferricin (LfcinB) (Liu et al. 2011)	<i>E. coli</i> and <i>S. aureus</i>
			RW-BP100 and R-BP100 (Torcato et al. 2013)	<i>E. coli</i> and <i>S. aureus</i>
			Magainin 2 (Hall et al. 2014)	DMPC and DMPC/DMPG
			Caerin 1.1 and melittin (Mularski et al. 2016)	<i>K. pneumoniae</i>
Fluorescence microscopy	Visualizing the membrane interaction and intracellular distribution of fluorescent-labelled-AMPs with/on biomimetic membranes and/or live cells Investigating the effect on membrane integrity	Inexpensive, wide-range of applications	CM15 (Fantner et al. 2010)	<i>E. coli</i>
			Histatin 5 and LL-37 (Den Hertog et al. 2005)	<i>C. albicans</i>
Confocal laser scanning microscopy	Study of morphological and kinetics evolution of live cells in real time	High-resolution images, performed directly in solution, low artefacts	Hexapeptide PAF26 (Muñoz et al. 2012)	<i>Neurospora crassa</i>
			LL-37 and CATH-2 (Ordonez et al., 2014)	<i>C. albicans</i>
			LL-37, P7 analogue (Li et al. 2015) CATH-2 (Schneider et al. 2016)	<i>E. coli</i>

Table 1.8 continued				
Fluorescence lifetime imaging microscopy (FLIM)	Imaging the interaction kinetics of AMPs with artificial membranes and live cells	Very sensitive, high precision, real time interactions, low-resolution images	Melittin K14 (Gee et al. 2013; Schneider et al. 2016)	DPPC, <i>E. coli</i>
Fluorescence correlation spectroscopy (FCS)	Determining the kinetics of killing of live cell in real time Study the size and nature of transmembrane pores induced by AMPs in synthetic membranes and/or live cells	Real time interactions, quick, accurate, measuring slow kinetics only (>1min)	Sushi 1 (Leptihn et al. 2009)	<i>E. coli</i>
			Mastoparan X (Kristensen et al. 2014)	POPC/POPG
Fluorescence (or Förster) resonance energy transfer (FRET) microscopy	Quantify membrane disruption in live cells Study of peptide self-association (dimerization) upon membrane insertion Determining the coil-to-helix transition upon peptide interaction with a lipid membrane Study of peptide translocation across the bilayer	High sensitive, depend on concentration of and distance between the donor and acceptor fluorophores, requires careful calibrations	Halocidin 18-mer (Hal 18) and magainin II (Kim & Cha 2006)	<i>E. coli</i>
			All-D F17-6K and magainin II (Glukhov et al. 2005)	POPE/DPPG/PC
			PMAP-23 (Orioni et al. 2009)	ePC and ePG
Time-resolved flow cytometry	Study the fast kinetics of permeabilization of live cells and quantitating the kinetics of cell killing	Reliable, quick, accurate	PepR (Freire et al. 2014)	<i>E. coli</i>
Proteome chip and micropatterned surface	Specifically identifying the intracellular targets	Simple, quick, wide-range of applications, expensive, low resolution	Lactoferricin B (Tu et al. 2011)	<i>E. coli</i>
			Indolicidin (Ghosh et al. 2014)	DNA

* **SDS**: Sodium dodecyl sulphate, **DPC-d38**: Dodecylphosphorylcholine-d₃₈, **DMPC**: dimyristoylphosphatidylcholine, **DMPG**: dimyristoyl phosphatidylglycerol, **POPE**: 1-palmitoyl-2-oleoyl-phosphatidylethanolamine, **POPG**: palmitoyloleoylphosphatidylglycerol, **DPC**: Dodecylphosphocholine, **POPC**: 1-palmitoyl-2-oleoyl-*sn*-glycero-3-phosphocholine, **CL**: cardiolipin, **PG**: phosphatidylglycerol, **SUV**: small unilamellar vesicles, **DMPC-d₅₄**: dimyristoylphosphatidylcholine, **DOPC**: 1,2-dioleoyl-*sn*-glycero-3-phosphocholine, **DOPG**: 1,2-dioleoyl-*sn*-glycero-3-[phospho-*rac*-(1-glycerol)], **DPPC**: dipalmitoylphosphatidylcholine, **POPC**: 1-palmitoyl-2-oleoyl-*sn*-glycero-3-phosphocholine, **PC**, phosphatidylcholine, **ePC**: egg phosphatidylcholine, **ePG**: phosphatidylglycerol, **PLL-PGA-DPPC**: poly(L-lysine)-poly(L-glutamic acid)-dipalmitoyl phosphatidylcholine.

1.7.1 Permeabilization mechanisms: Initially, at low peptide/lipid ratios, the peptides lie parallel onto the lipid bilayer (Yang et al. 2001). When the ratio increases, the peptides start to re-orientate perpendicularly, insert into the bilayer and form trans-membrane pores. A number of models have been proposed to describe this fundamental step (Fig. 1.7). Three such major models are summarised below:

1.7.1.1 Barrel stave pore model: The peptide spirals create a bundle of amphipathic α -helical or β -sheet peptides in the membrane with a central lumen, such as a stave or a barrel. The hydrophobic face of the peptide aligns with the lipid core of the bilayer while its hydrophilic lines the interior of the pore. This type of pore is induced by a few peptides such as alamethicin (Mathew & Balaram 1983; Yang et al. 2001), pardaxin (Hallock et al. 2002) and other peptaibols from the fungal genus *Trichoderma* (Leitgeb et al. 2007).

1.7.1.2 Toroidal pore model: Toroidal pore or wormhole was firstly proposed for magainin in the 1990s (Matsuzaki et al. 1996). After initial membrane binding, the aggregated peptides impose a positive curvature strain in the membrane by increasing the distance between the lipid head groups, also called membrane thinning. Then, when the peptides reach a critical concentration, they realign perpendicularly to the bilayer, resulting in cavitation of the membrane inwards, forming a pore. Protegrins and melittin can induce this type of pore (Yang et al. 2001; Brogden 2005).

1.7.1.3 Carpet mechanism: The carpet model was proposed by Pouny et al. (1992) for describing the interaction of dermaseptin peptide with phospholipid membranes, and is the possibly the most frequently utilized mechanism of action of AMPs (Wimley & Hristova 2011). Here, the peptides accumulate on the bilayer surface and orientate in a parallel manner ('in-plane'). They are attracted electrostatically to the anionic phospholipid head groups at many sites of the surface and cover it like a carpet. When the peptides reach a critical concentration, they re-orientate and form toroidal transient pores, resulting in extra peptides that can access the membrane. Eventually, the toroidal pores coalesce and form islands, causing global destabilization and micellization of the bilayer and ultimately fragmentation (Brogden 2005).

1.7.2 Non-lytic membrane mechanisms: Although membrane permeabilization seems fundamental to the antimicrobial effect of AMPs, permeabilization alone may not be enough to explain antimicrobial activity of some AMPs (Jenssen et al. 2006; Teixeira et al. 2012). All AMPs must interact with cell membrane, if only to gain access to their intracellular targets. In some cases, the effect on cell membrane topology is not severe enough to cause cell death. For example, the aggregate-channel model is a mechanism of ion diffusion through the lipid bilayer without formation of a stable channel. Peptides bind and insert into the membrane and then form unstructured aggregates over it. These aggregates associate with water molecules and form channels that allow ion diffusion. This model was proposed by Hancock and Chapple (1999), when some peptides such as the cyclic peptide bactenecin and the α -helical peptide were unable to depolarize the cytoplasmic membrane potential of *E. coli* at the MIC (Wu et al. 1999).

Another non-lytic membrane mechanism proposed for a number of AMPs is molecular electroporation (Fig. 1.7). Some peptides are able to generate an electric field across the membrane and trigger electrostatic potential sufficient for the pore formation. Molecular electroporation mechanism requires a considerably high charge density, which is achieved due to a high content of cationic amino acid residues in the peptide, to generate an electrostatic potential of at least 0.2 V over 0.1 ms (Miteva et al. 1999). This model has been proposed to describe the action of those AMPs that exert antimicrobial activity without apparent formation of transmembrane pores. The molecular electroporation model is particularly important as it provides new insight for the means by which AMPs increase membrane permeability without necessarily causing its disruption. This mechanical model has been proposed to explain the cell entry of annexin V (Karshikov et al. 1992) and oligoarginines cell-penetrating peptides (CPP) (Cahill 2010).

Sinking-raft model is also a worth mentioning non-lytic membrane mechanism. According to this model, amphipathic peptides form transient pores by binding to a particular lipid domain and sinking into the lipid bilayer, resulted in a mass imbalance which leads to peptide translocation through an increase in membrane curvature. Sinking-raft model is responsible for the formation of transient pores which are still lethal for the bacterial cells (Pokorny & Almeida 2004). This model has been proposed

for the peptides δ -Lysin (Pokorny & Almeida 2005) and polyphemusin (Haney et al. 2010).

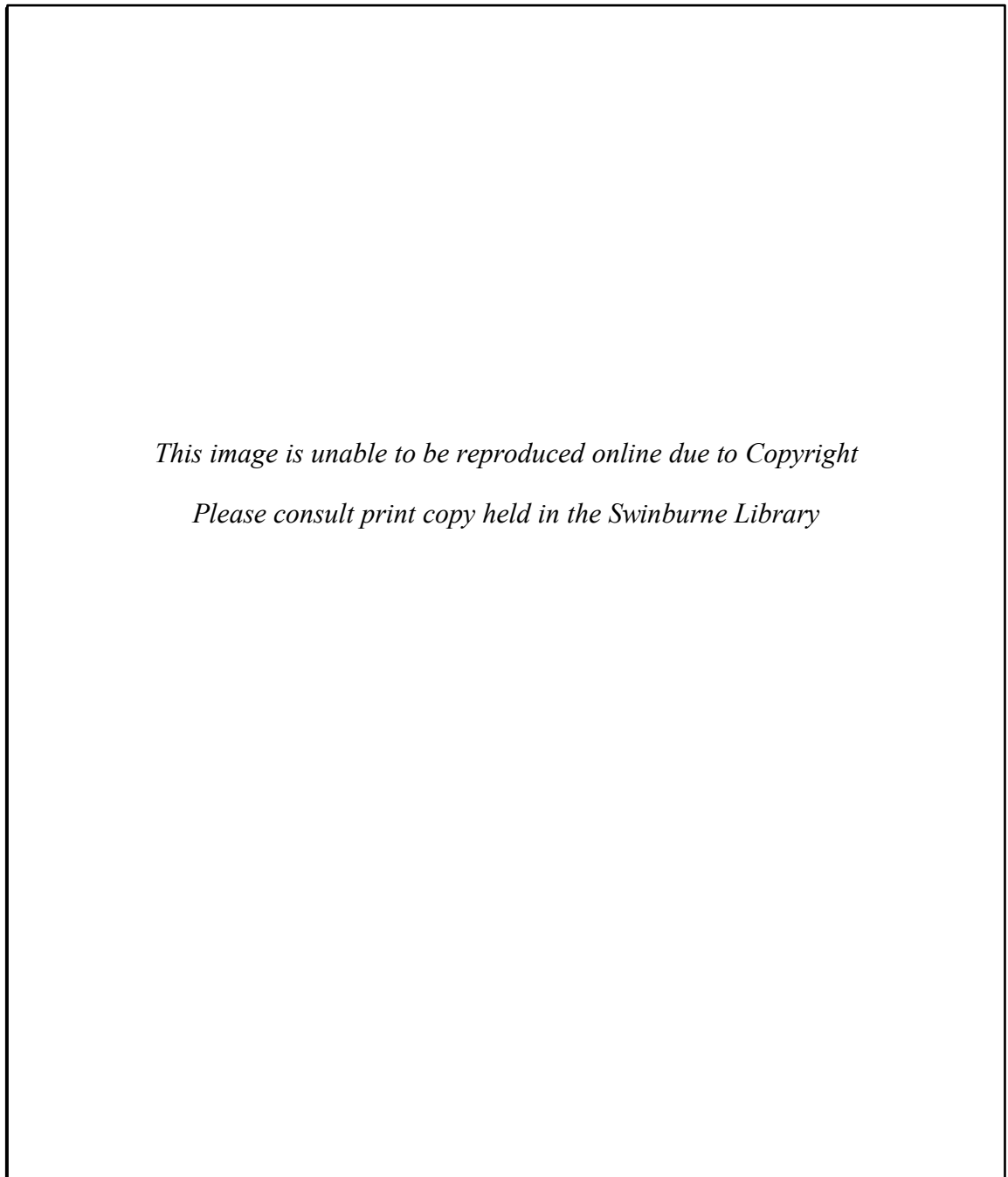


Figure 1.7 Various models of permeabilization and non-lytic membrane mechanisms of AMPs.

Source: Teixeira et al. (2012). Based upon AMPs properties, they can destabilize the membranes using several mechanisms.

1.7.3 Non-lytic intracellular mechanisms: Intracellular mechanism of action is another area of intensive focus regarding AMP mechanism of action has lately emerged, providing a new perspective to the mechanisms by which AMPs exert their antimicrobial effect. For non-lytic AMPs that act intracellularly, binding to nucleic acids, inhibiting the syntheses of nucleic acids, proteins or cell-wall, inhibiting enzymatic activities, altering the cytoplasmic membrane septum formation, or flocculation of intracellular contents are among the principal mechanisms of action proposed (Fig.1.8). Intracellular mechanism of action of AMPs has been extensively reviewed (reviewed in Brogden 2005; Hale & Hancock 2007; Guilhelmelli et al. 2013; Le et al. 2017). Examples of the well-documented studies on intracellular targets of AMPs are briefly summarized in Table 1.9.

An important evidence of a non-lytic intracellular mechanism of action is the temporal dissociation between target cell death and membrane permeabilization. For membranolytic AMPs, membrane permeabilization and cell killing are often rapid and concomitant events. On the other hand, non-lytic AMPs that act intracellularly, often display a lag period before observing dropping in the viable cell counts. For example, cecropin P1 caused an instantaneous lysis of *E. coli* cells, while PR-39 did not lyse the cells even after 130 min incubation. Instead, after a short lag period of 8 min, treated cells with PR-39 were killed with a mechanism that inhibits protein and DNA synthesis. The effect of PR-39 on macromolecular synthesis was measured using radioactive precursors for DNA and protein biosynthesis and monitoring isotope incorporation over time (Boman et al. 1993). Scanning electron microscopy confirmed that PR-39 did not lyse *Salmonella typhimurium*, however, the peptide-treated cells became extremely long (filamentous) after exposure to PR-39 for 15 min, suggesting that these cells were unable to undergo cell division (Shi et al. 1996).

Filamentation is a defect in cell division, wherein the cell continuing to grow without septum formation, it can be due to the inhibition of membrane proteins that are involved in septum formation, such as penicillin-binding protein 3 (PBP3). The β -lactam antibiotics piperacillin and furazlocillin induced cell filamentation through their selective binding to PBP3 (Botta & Park 1981). Cell filamentation could be also due to the blocking of DNA synthesis, e.g. the antibiotic nalidixic acid induces filament formation by interfering with DNA replication (Lutkenhaus 1990). Some

AMPs were found able to induce this profound morphological change in bacterial cells, giving an early indication for intracellular mechanism of action. For example, indolicidin induced filamentation of *E. coli* and this morphological change was proposed to be a result of DNA synthesis inhibition, as indolicidin did not inhibit protein synthesis in *E. coli* even at concentrations higher than MIC (Subbalakshmi & Sitaram 1998). Lactoferricin B (LfcinB), also induced profound filamentation of *E. coli* cells, this effect was correlated to the induction of an SOS-like response in the bacterial cells (Ulvatne et al. 2004). Moreover, the synthetic hexapeptides, WRWYCR and KWWCRW, induced filamentation in *E. coli* cells by interfering with DNA damage repair through trapping Holliday junctions (HJ), which are branched DNA intermediates that arise in several central DNA repair pathways and replication fork restarts (Gunderson & Segall 2006). Our group showed that PIN-based peptides could also induce filamentation in *E. coli*. It was suggested that these peptides inhibited DNA synthesis in the bacterial cells, as they were able to bind to plasmid DNA and shift the mobility of the DNA bands in agarose gel-retardation assay (Alfred et al. 2013b).

Gel retardation assay is generally used to test the binding capacity of AMPs to nucleic acids (DNA and/or RNA) *in vitro*, in which the effect of increasing peptide concentration on the migration of purified DNA or RNA in an agarose gel is measured. According to this assay, several cationic AMPs such as tachyplesin I (Yonezawa et al. 1992), buforin II (Park et al. 1998), indolicidin (Subbalakshmi & Sitaram 1998), LfcinB (Ulvatne et al. 2004), LL-37 and BMAP-27 (Mardirossian et al. 2014) have been shown strong affinity for nucleic acids. This fact is not unexpected given that the two molecules are oppositely charged. Therefore, gel retardation assay might reflect an unspecific electrostatic binding between the cationic AMPs and nucleic acids. To establish a link between DNA binding and intracellular mode of action of AMPs, *in vivo* macromolecular synthesis inhibition assays and cell cycle analysis of the peptide-treated cells using flow cytometry are often performed. For example, when PuroB (FPVTWPTKWWKG-NH₂) and its variants, PuroB3 (FRVTWRTKW WKG-NH₂) and PuroB5 (FKVTWTKWWKG-NH₂), showed different antibacterial activity and *in vitro* DNA binding affinity, macromolecular synthesis inhibition assays were performed. It was found that the peptides with highest antibacterial activities, PuroB3 and PuroB5, had strong DNA binding abilities *in vitro*, and they also caused

a substantial decrease in the amount of radioactive precursor incorporated into DNA, RNA and protein *in vivo*. Thus, it was suggested that these peptides inhibit the processes of DNA replication, transcribing the DNA strand into mRNA and the translation of the mRNA into protein (Haney et al. 2013). In addition, when APP peptide interacted with *C. albicans* genomic DNA and affected the DNA migration in gel retardation assay, the effect of APP on the cell cycle of *C. albicans* was analysed using flow cytometer. It was found that APP arrested cell cycle within the S-phase, suggesting that binding to DNA has a functional role (Li et al. 2016b).

Although inhibition of protein synthesis has been proposed to be the intracellular killing mechanism of several AMPs (Table 1.9), in some cases a detailed description of the inhibition mechanism has not been defined. The indolicidin variant, CP10A, inhibited incorporation of protein precursors in *S. aureus*, at 2-fold the MIC (Friedrich et al. 2001). A similar observation was obtained with the hybrid peptide of pleurocidin and dermaseptin, P-Der, it reduced the amount of radioactive precursor incorporated into protein in *E. coli* without damaging the cytoplasmic membrane at concentrations up to 5-fold its MIC (Patrzykat et al. 2002). Later, by using DNA microarray technology to monitor transcriptional alterations of *E. coli* in response to challenge with a sub-inhibitory concentration of Bac7 peptide, it was shown that this peptide induced expression of stress genes related to protein synthesis (Tomasinsig et al. 2004). More recently, by using photo-crosslinking technique between purified non-translating ribosomes and AMP-tagged with photo-reactive amino acid, it was found that Bac7₁₋₃₅ peptide binds to ribosomal proteins, and might thereby interfere with protein translation. The specific influence of this peptide on protein synthesis without significantly affecting RNA transcription and DNA synthesis was also evaluated by *in vivo* radioisotopes uptake assays (Mardirossian et al. 2014). Recently, Taniguchi et al. (2016a) used a cell-free rapid translation system (RTS), which is an *in vitro* protein synthesis assay based on *E. coli* lysate, for evaluating the inhibition of green fluorescent protein (GFP) synthesis by the octadecapeptide AmyI-1-18. It was found that this peptide inhibited GFP synthesis in a concentration-dependent manner. Further analysis of the transcription and translation inhibition steps using RT-PCR showed that the inhibition of GFP synthesis by AmyI-1-18 does not occur at the transcription step but at the translation step (Taniguchi et al. 2016a).

Some AMPs such as nisin (Wiedemann et al. 2001), plectasin (Schneider et al. 2010) and copsisin (Essig et al. 2014) have been found to inhibit cell wall biosynthesis by binding with the cell wall peptidoglycan precursor lipid II. A wide range of *in vitro* inhibition assays for cell wall synthesis were used to identify Lipid II as the cellular target of these peptides. Since peptidoglycan is not present in eukaryotic cells, peptides that inhibit its synthesis are interesting for therapeutic applications.

Pyrrhocoricin peptide was shown to act on bacterial proteins in a stereospecific manner. To identify biopolymers that bind to this peptide, biotin- and fluorescein-labelled forms of pyrrhocoricin were used with mass spectrometry, western blot, and fluorescence polarization techniques. It was found that pyrrhocoricin binds to the bacterial heat shock protein, DnaK (Otvos Jr et al. 2000). Further investigations using *in vitro* ATPase activity assay and other enzymatic assays showed that pyrrhocoricin inhibits the ATPase actions of DnaK and the refolding activity of this protein (Kragol et al. 2001). The binding of other AMPs, such as oncocin (Knappe et al. 2011), apidaecins (Czihal et al. 2012) and drosocin (Zahn et al. 2013) to DnaK was further characterized by crystallographic analyses to confirm the intracellular target for these peptides.

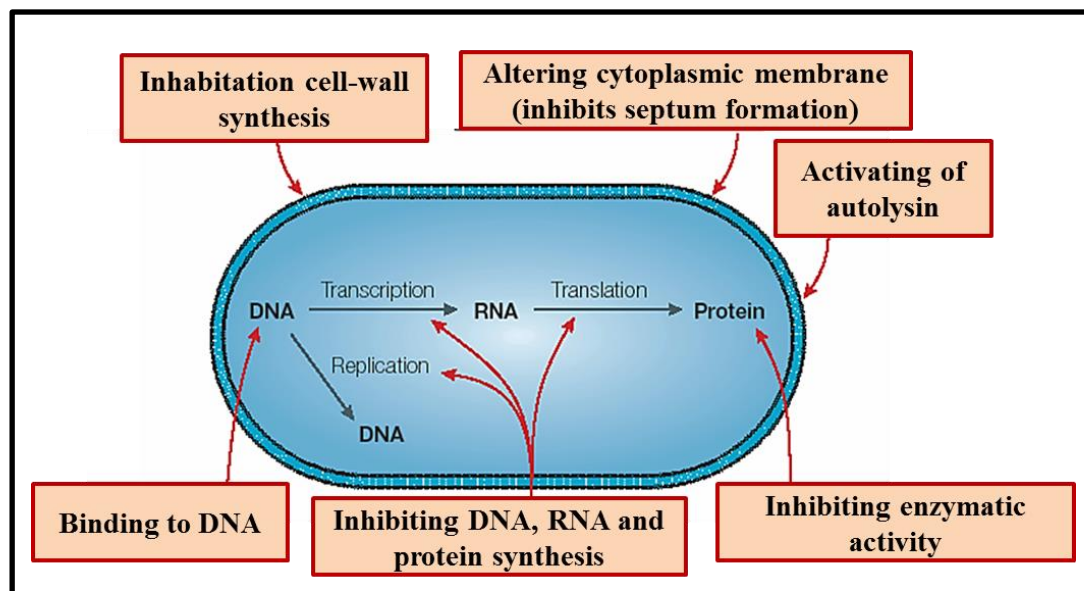


Figure 1.8 Intracellular modes of action of AMPs.

The mechanisms are not necessarily exclusive of each other. (Figure reproduced from Brogden 2005).

Table 1.9 Proposed Mechanism of action of AMPs

	Antimicrobial mechanism	Examples	References
Non –membranolytic	Flocculation of intracellular contents	Anionic peptides	(Brogden et al. 1996)
	Binding to nucleic acids	Buforin II, indolicidin, PuroA, APP	(Park et al. 1998; Marchand et al. 2006; Alfred et al. 2013b; Ghosh et al. 2014; Li et al. 2016b)
	Inhibition of nucleic acid synthesis	Pleurocidin, dermaseptil, lactoferricin B, PuroA	(Patrzykat et al. 2002; Ulvatne et al. 2004; Haney et al. 2013)
	Inhibition of DNA repair	The hexapeptide WRWYCR	(Su et al. 2010)
	Inhibition of enzymatic activity	Pyrrhocoricin, Bac 7, lactoferricin B	(Kragol et al. 2001; Scocchi et al. 2009; Tu et al. 2011)
	Inhibition of protein synthesis	CP10A, pleurocidin, dermaseptin, P-Der, lactoferricin B, PuroA	(Friedrich et al. 2001; Patrzykat et al. 2002; Ulvatne et al. 2004; Haney et al. 2013)
	Inhibition of cell-wall synthesis	Mesarcidin, plectasin, copsin	(Brötz et al. 1998; Schneider et al. 2010; Essig et al. 2014)
Membranolytic	Barrel-stave pore	Almethicin, BacSp222	(Bechinger 1999; Yang et al. 2001; Pieta et al. 2016)
	Toroidal pore	Magainin 2, melittin, tritrpticin, LL-37, CMA3	(Ludtke et al. 1996; Yang et al. 2001; Henzler Wildman et al. 2003; Salay et al. 2012; Lee et al. 2016a)
	Disordered Toroidal pore	Melittin, Magainin analog, BPC194	(Sengupta et al. 2008; Cirac et al. 2011)
	Huge Toroidal pore	Lacticin Q	(Yoneyama et al. 2009)
	Carpet mechanism	Cecropin, aurein 1.2, PuroA	(Gazit et al. 1995; Fernandez et al. 2012; Alfred et al. 2013b)
	Aggregate model	Magainins, CP26	(Matsuzaki 1998; Wu et al. 1999)
	Membrane thinning/thickening	PGLa, LL-37	(Lohner 2009)
	Charged lipid clustring	Magainin analogues	(Epand & Epand 2011)
	Tilted peptide mechanism	Aurein 1.2, Citropin 1.1	(Dennison et al. 2005a)
	Amyloid formation	Lactoferrin, LL-37, magainin 2	(Nilsson & Dobson 2003; Sood et al. 2008)

1.8 Mechanisms of action of TRPs and the significance of the tryptophan residues

A significant part of this section has been published (Shagghi et al. 2016b)

Tryptophan is aromatic, neutral, and the largest amino acid with the characteristic indole functional group (Fig 1.9). Trps have an important feature in that they can be set at different positions on the hydrophobicity scale of amino acids e.g., Trp is considered hydrophobic due to its uncharged side-chain; however, it does not reside in the hydrocarbon region of lipid bilayers and is thus placed towards the hydrophilic side of the scale (Trinquier & Sanejouand 1998). Both hydrophilic and hydrophobic attributes of Trp make it ideal for insertion into membranes (Strøm et al. 2000). Trp has a strong tendency to insert into membranes and partition near the membrane-water interface, positioning specifically near the lipid-carbonyl region (Schibli et al. 2002). Trp is found in high proportions in some AMPs (Tables 1.2, 1.3, 1.4 & 1.7) and its roles in AMPs have been studied extensively; however, the exact roles apart from its hydrophobic bulk are not clear and may vary somewhat depending on the peptide.

The large, bulky, paddle-like indole side-chain, about a third of the thickness of a phospholipid monolayer, interrupts the very favorable and cohesive hydrophobic interactions of the lipid acyl chains when this side chain buries deep. Therefore, the complex electrostatic nature of the interfacial region is proposed to be an ideal place to accommodate the equally complex Trps (Yau et al. 1998; Chan et al. 2006). Trps have intrinsic preference for a specific orientation when positioned at the interface of a phospholipid bilayer. Dipole-dipole interactions and steric constraints in the membrane hydrocarbon region decide the position and orientation of Trp residues, while H-bonding and cation- π interactions of indoles with lipid head-groups are less significant (Esbjörner et al. 2007). However, Haug and Svendsen (2001) argued that the size, shape and aromatic character of Trp are the most important features for the antibacterial activity of Trp-rich AMPs while the H-bonding ability and amphipathicity of the indole side chain are not essential. Replacing one and/or two Trp residues in the 15-residue LfcinB peptide (LfcinB 17-31, FKCRRWQWRMKKLGA) with natural and unnatural aromatic amino acids with aromatic hydrocarbon side chains, such as Phe and naphthylalanine isomers, gave the most active peptides against *E. coli* and *S. aureus*. Therefore, the authors proposed that

these aromatic residues were able to place themselves deeper, creating more efficient peptides for disrupting the bacterial cell membrane (Haug & Svendsen 2001).

The biochemical properties of Trp complement the cationic Arg residues in many Trp-Arg rich AMPs. Arginine is the most basic of all amino acids because of the guanidinium group at the end of its side chain. The positively charged Arg residues help in the first step of attracting the AMP to the target membranes and forming hydrogen bonds (H-bonds) with their negatively charged components (Schmidt et al. 2010). A guanidinium ion is not only able to form bidentate H-bonds with a phosphate group on a lipid head, but it can also form H-bonds with the lipid glycerol groups (Sun et al. 2014). Then comes the role of Trp, as it is the most suitable amino acid to continue the association of peptides with the membrane and insert them deeply into it. Microbial membrane insertion and permeabilization by AMPs is a crucial step in their antimicrobial activity.

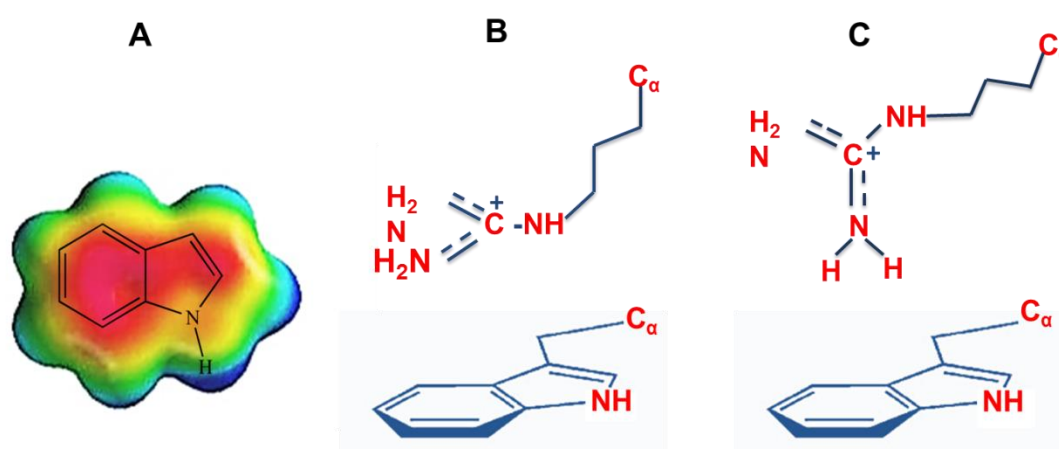


Figure 1.9 The aromatic ring structure of tryptophan (Trp) and its interaction with arginine (Arg).

A. Electrostatic surface of the Trp indole group (Figure reproduced from Chan et al. 2006). **B & C.** The parallel and the perpendicular cation- π interactions between Arg and Trp, respectively (Figure reproduced from Ma & Dougherty 1997).

Cation- π interactions in proteins are important for catalysis, substrate binding and ion channel activity (Ma & Dougherty 1997). This interaction between Arg and Trp can result in either a parallel or a perpendicular (T-shaped) orientation, however, the parallel conformation is preferred and energetically more favourable in aqueous solution (Minoux & Chipot 1999) (Fig. 1.9). Interestingly, in the parallel arrangement, the side chain of Arg can almost form H-bonds with water molecules as it is not engaged in any cation- π interactions (Aliste et al. 2003), whereas Lys cannot form H-bonds when it is involved in cation- π interactions with an aromatic residue (Mitchell et al. 1994; Aliste et al. 2003). This difference was suggested to be responsible for the higher activity of Arg-containing peptides compared to Lys-containing ones (Chan et al. 2006). The cation- π interaction between Arg and Trp makes the entry of Arg into the lipid bilayer energetically more favourable, as this interaction effectively shields the Arg residue from the hydrophobic environment inside the bilayer (Ma & Dougherty 1997; Jing et al. 2003).

Once in the cytoplasm, TRPs can inhibit the growth of the pathogen, or kill it, by diverse intracellular mechanisms (Fig. 1.8 & Fig. 1.10) (Table 1.9). It was suggested that all naturally occurring Trp-rich peptides (mentioned earlier in section 1.4) find intracellular targets after efficiently crossing the pathogen's membrane and/or permeabilizing the membrane without completely disrupting its integrity. Even for the most lytic peptide, tritrypticin, a secondary intracellular target could not be excluded (Yang et al. 2006; Sharma et al. 2013). Therefore, Trp might play an essential role, not only in lipid partitioning and peptide insertion, but also in peptides-nucleic acid and peptides-enzyme binding. For instance, substituting the Trp-Trp pair in the central PWWP motif of indolicidin with Ala-Ala, His-His, or Phe-Phe residues considerably altered its ability to bind and stabilize duplex DNA structures (Ghosh et al. 2014). However, the intracellular roles of Trp need to be further investigated.

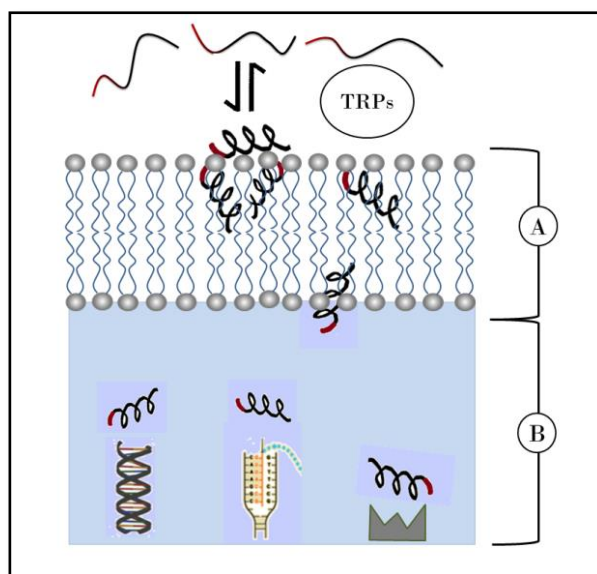


Figure 1.10 General mechanism of action of Trp-rich antimicrobial peptides.

A. The anchoring role of Trp. After interaction with the pathogen membrane through electrostatic interaction with anionic components of the membrane, the peptides undergo a restructuring to adopt a favourable secondary structure. Trps aid in residing the peptides in the interfacial region of bilayers and forming H-bonds with water and the lipids, to insert the deep into hydrocarbon core. **B.** The proposed intracellular role of Trp: binding to nucleic acids, inhibiting nucleic acid biosynthesis, and inhibiting protein synthesis and some enzymatic processes.

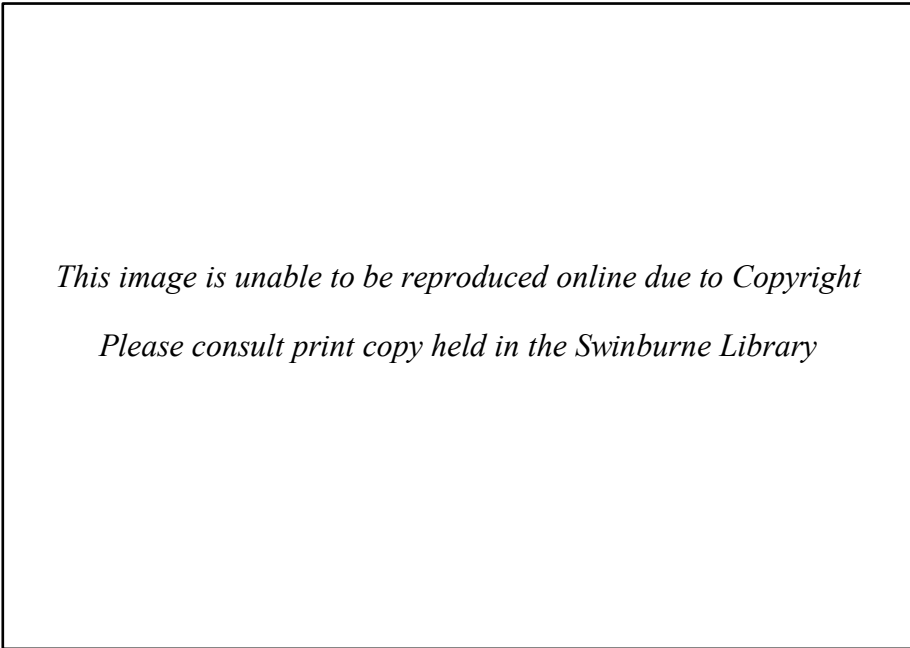
1.9 Proposed mechanism of action for PINs and PIN-based peptides.

PINs strongly bind and adsorb to phospholipid membranes (Kooijman et al. 1997; Le Guernevé et al. 1998; Rosicka-Kaczmarek et al. 2015). This strong interaction is probably due to the presence of the TRD which plays an important role in lipid binding and insertion into lipid membranes (Blochet et al. 1993). The Trp and the basic residues within the TRD are probably involved into two types of interaction with phospholipid membranes, a hydrophobic interaction between the lipid tails of phospholipids and Trp side chains, and an electrostatic interaction between the positively charged residues (Arg and Lys) of the TRD and the phosphate head-groups of the lipids (Kooijman et al. 1997). PINA and PINB interact differently with membrane lipids; PINA binds tightly to both phospholipids and glycolipids, whereas PINB interacts tightly with anionic phospholipids only and forms loose lipoprotein complexes with glycolipids (Dubreil et al. 1997). PINA showed slower adsorption and less anionic lipid insertion compared to PINB and this difference could be partially due to the higher helix content that PINA have in presence of lipid (Clifton et al. 2007a), compared to PINB (Clifton et al. 2007b). This difference is possibly due to

the variations in biochemical properties of the TRD in PINA and PINB. Interaction of PINA with *Saccharomyces cerevisiae* plasma membrane depended on Trp41 and Trp44, whereas PINB interaction depended on Lys residues (Evrard et al. 2008). Both PINs adsorbed strongly to the lipid head-group region and penetrated less into the lipid tail region of the model microbial anionic lipid layers. However, PINA competed very well with β -purothionin (β -Pth, co-localized protein in the wheat seed) and inhibited β -Pth penetration of the lipid layer by forming a blanket-like layer below the lipid surface, whereas PINB competed poorly and was prevented from binding strongly to the lipid in the presence of β -Pth (Sanders et al. 2013). Recently, the interaction between both wild type PINB and its mutant PINBs (Trp44 to Arg44) and model bacterial membranes with different lipid constituents was investigated using external reflection-Fourier transform infrared (ER-FTIR) spectroscopy, Brewster angle microscopy (BAM) and surface pressure measurements (Sanders et al. 2016). Results showed that this single residue mutation affected the lipid binding behaviour of the proteins, PINB was able to penetrate lipid layers of phosphatidylethanolamine (PE) and phosphatidylglycerol (PG) head groups more deeply compared to PINBs. Sanders et al. (2016) also suggested that the interaction of PINs with lipid membranes is not only driven by electrostatic forces, it is also influenced by domain formation of the membrane, controlled by the composition of head group and the unsaturated acyl tails in the lipid acyl region, as increasing the saturation of the lipid tails increased the penetration and adsorption of the wild type PINB.

As mentioned above, it was proposed that PINA is a membrane acting protein and could be a 'gate-opener' for PINB to enter the cell and interact with intracellular components (Capparelli et al. 2005). Studies with PuroA and PuroB peptides suggest a similar mechanism of action since PuroA could disrupt the integrity of lipid bilayers but PuroB could not, suggesting that the target of PuroB is not the bacterial membrane and it exerts its antibacterial effect intracellularly (Haney et al. 2013). Vogel's group showed that PuroA preferentially binds to negatively charged synthetic lipid vesicles and induces calcein leakage, suggesting it acts mainly on bacterial membranes and uses a lytic mechanism of action (Jing et al. 2003). PuroA was also found to be most likely resides at the solvent-lipid interface rather than deep in the hydrophobic region of the membranes (Jing et al. 2003). This observation is shared by the full-length PINA, which appears to locate just below the negatively charged DPPG lipid

monolayer in the lipid headgroup region but not deeper into the acyl chain region of the lipid layer (Clifton et al. 2011). However, in further work, Vogel's group suggested that the antibacterial activity of PuroA is more complex than originally assumed, as it bound to DNA, significantly inhibiting macromolecular synthesis at sub-inhibitory concentrations in *E. coli* and it also did not disrupt cytoplasmic membrane integrity in *E. coli*. Therefore, they proposed that the interaction of puroidoline peptides with bacterial membranes is only an initial step, followed by translocation into the bacterial cell, where they mainly exert their effects (Haney et al. 2013). Parallel, studies of our group (Alfred et al. 2013b) showed that *Saccharomyces cerevisiae* cells treated with PuroA appeared intact, with pore-like structures appearing in the membranes and leakage of extracellular material (Fig. 1.11). Further, and in agreement with Vogel's findings, the peptide was found to bind to DNA *in vitro* and selectively permeabilised negatively charged vesicles. Therefore, PuroA was suggested to exert its antimicrobial effects by disrupting the integrity of the cell membrane, followed by intracellular activity (Alfred et al. 2013b). The precise sequence and mechanism of action of these peptides is still under investigation, due to their potential significance in food, health and agriculture applications. One focus of the present work is further investigation these mechanisms.



*This image is unable to be reproduced online due to Copyright
Please consult print copy held in the Swinburne Library*

Figure 1.11 Scanning electronmicrographs of *S. cerevisiae* cells treated with PIN-based peptides.

Source: Alfred et al. (2013b). **A.** No peptide control; **B.** PuroA 64 µg/mL; **C.** PuroA 125 µg/mL; **D.** Pina-M 64 µg/mL.

1.10 Applications of AMPs

There have been several cases of successful use of AMPs in pharmaceutical, agriculture, the food industry, aquaculture and animal husbandry (Table 1.11), indicating a promising future for extensive applications of those peptides. However, there are several difficulties that need to be overcome to produce pure, stable, functional and cost effective AMPs in a large scale.

1.10.1 Clinical applications: Therapeutics use of AMPs offers many potential advantages over the current types of antimicrobials. Firstly, they are naturally occurring, therefore, may have unique ways of fighting pathogen. Secondly, they may have multiple targets, e.g., microbial membranes as well as intracellular targets. Hence, the possibility of development of resistance against AMPs seems low, compared to antibiotics that have a specific molecular target, such that any mutations therein potentially render the antibiotic less effective. Moreover, many AMPs have a wide spectrum of activities such as antibacterial, antiviral and/or antifungal.

Several AMPs have entered into clinical trials to date, while others are in the preclinical development stages (examples given in Table 1.11). A 1% w/w aqueous gel of the indolicidin analogue, omiganan (Table 1.2), was tested by applying at the catheter site and dressing changes (Rubinchik et al. 2009). Omiganan pentahydrochloride (MBI-226) has completed Phase III clinical trials for prevention of catheter-related local and bloodstream infections, a global healthcare problem, the results showing a reduction in microbial colonisations (www.clinicaltrials.gov; identifier NCT00027248). Additionally, it has completed phase II clinical trials for treatment of acne (www.clinicaltrials.gov; identifier NCT00211523) and of inflammatory papules and pustules associated with rosacea (www.clinicaltrials.gov; identifier NCT01784133). Further, IMX942 (a bovine indolicidin derivative) displays potential use with neutropenic patients, based on results of treating infected animals with antibiotic-resistant bacteria (Afacan et al. 2012). Hu et al. (2013) suggested that indolicidin has the potential to be used as a carrier for anionic materials, such as plasmid DNA for gene delivery.

Lactoferrin completed phase 2 clinical study for prevention of neonatal sepsis (NEOLACTO) (<https://clinicaltrials.gov>; identifier NCT01264536) and Phase III for prevention of diarrhea in children (<https://clinicaltrials.gov>; identifier NCT00560222). Currently, it is in phase II clinical trial for prevention the nosocomial infections in critically ill patients (<https://clinicaltrials.gov>; identifier NCT01996579). The LfcinB derivative, LTX-315 peptide, (detailed in section 1.10.1.2), showed potential as a new anticancer agent for intratumoral administration. This peptide has undergone a phase I study designed to determine its safety profile and recommended dose in patients with a transdermally accessible tumour (<https://clinicaltrials.gov>; identifier NCT01058616). LTX-315 is currently being tested in clinical phase I/IIa studies as a potential first-in-class oncolytic peptide-based local immunotherapy (www.clinicaltrials.gov; identifier NCT01986426).

Novel combinatorial use of AMPs with existing antimicrobials could further lead to synergistic effects, similar to the multidrug approach for treating HIV (De Clercq 2004), and may also reduce the possibility of development of resistant microbes. AMPs can be conjugated with themselves or with currently used antimicrobial agents, particularly for treating multi-resistant strains (Matsuzaki et al. 1998; Rosenfeld et al. 2006; Zhou & Peng 2013; Hu et al. 2015). Peptides with a tendency to permeabilize target microbial membranes and form pores can be used with conventional agents to overcome the surface resistance mechanisms in target pathogens. For instance, ranalexin and magainin II were shown to be synergistic with polymyxin E, doxycycline, clarithromycin, ceftriaxone, amoxicillin clavulanate, ceftazidime, meropenem, piperacillin and β -lactam antibiotics (Zhou & Peng 2013). Moreover, plectasin synergised with penicillins and aminoglycosides antibiotics against *S. aureus* (Zhang et al. 2014) and methicillin-resistant *Staphylococcus aureus* (MRSA) (Hu et al. 2015).

1.10.1.1 Anticancer activity of AMPs: Cancer is the third leading cause of mortality worldwide (Thun et al. 2010). The current treatment strategies focus on radiation therapy, chemotherapy and/or surgery, with all forms of therapy having a relatively low success rate and presenting a risk of reoccurrence and/or metastasis. The use of conventional chemotherapeutic agents is often associated with deleterious side-effects on healthy cells (Riedl et al. 2011). Resistance of cancer cells to

chemotherapy and radiation therapy is very common and an important medical challenge. The development of resistance could be a consequence of many cellular changes, including abnormal increase in expression of drug-detoxifying enzymes, the ability of cancerous cells to repair DNA damage, changed interactions between the anticancer drug and its target, or defects in apoptosis cellular mediated machinery (Gatti & Zunino 2005). Thus, the development of new classes of anticancer drugs without these concerns and drawbacks is an urgent need. In this context, certain AMPs are being considered as a potential resource.

Some cationic AMPs exhibit cytotoxicity to a variety of cancer cells including those that are multidrug resistant and, in some case, these anticancer peptides (ACPs) have shown high selectivity to cancer cells over non-cancerous cells (Papo & Shai 2005; Schweizer 2009; Slaninová et al. 2012; Harris et al. 2013). The progression of cancer has been correlated with changes in the cell membrane which are vital in the cell's response to surrounding signals. Differences in the cell membranes of malignant and healthy cells are thus believed to play a role in the selective killing of cancer cells by ACPs (Hoskin & Ramamoorthy 2008a). The main difference is that cancer cell membranes are typically negatively charged, unlike the zwitterionic membranes of normal cells, due to the increased expression of anionic molecules such as phosphatidylserine (PS) (Utsugi et al. 1991) and O-glycosylated mucins (Yoon et al. 1996). This characteristic is also shared by bacterial cells, therefore, it is believed that ACPs could induce necrosis in cancer cells by membranolytic mechanisms similar to the aforementioned permeabilization mechanisms of antimicrobial activity (Bhutia & Maiti 2008; Gaspar et al. 2013; Liu et al. 2015). Additionally, once the ACPs are inside the cells, another membranolytic effect that is likely to take a place is the permeation of the negatively charged mitochondrial membrane (mitochondrial membrane evolutionarily originating from bacterial membrane by endosymbiosis), accompanied with swelling of mitochondria, cytochrome *c* release and induction of apoptosis (Mai et al. 2001). Although the mode of action of ACPs does not appear to involve receptor-mediated routes (Schweizer 2009; Gaspar et al. 2013), some have been found to use non-membranolytic mechanisms. For example, some can interfere with DNA synthesis (Ourth 2011), inhibit angiogenesis (the formation of new blood vessels from the pre-existing vasculature) (Xu et al. 2008), bind to regulation receptors (Hetian et al. 2002; Yu et al. 2010), or mediate host immune responses (Wang et al.

2009; Ogawa et al. 2011). Nonetheless, the detailed mechanisms of the selectivity and toxicity of ACPs to cancer cells are not fully elucidated and it is believed that their activity is dependent upon characteristics of both the ACP and its target membrane (Harris et al. 2013).

1.10.1.2 Trp-rich peptides with anticancer activity: The Trp-rich peptide lactoferricin (Lfcin, mentioned earlier in section 1.4.3) has been found to exhibit cytotoxic activity towards several cancer cell lines (Yin et al. 2013). Anticancer activity of bovine Lfcin (LfcinB) was first reported when it showed cytotoxicity towards THP-1 human monocytic leukemia cells (Yoo et al. 1997a) and it also inhibited *in vivo* tumor metastasis and angiogenesis in mice (Yoo et al. 1997b). The apoptosis-inducing activity of LfcinB in THP-1 cells was mediated by the intracellular production of reactive oxygen species (ROS) and activation of $\text{Ca}^{2+}/\text{Mg}^{2+}$ - dependent endonucleases (Yoo et al. 1997a). Other studies showed that LfcinB can induce mitochondrial-dependent apoptosis in leukemia cells (Mader et al. 2005), breast carcinoma cells (Furlong et al. 2006) and B-lymphoma cells (Furlong et al. 2010). A direct lytic mechanism was also reported for LfcinB in Meth A fibrosarcoma (Eliassen et al. 2002) and neuroblastoma (Eliassen et al. 2006).

A number of peptides derived from LfcinB have shown potential to be new alternatives and/or adjuvants to current cancer therapies. LTX-315 (KKWWKKW-Dip-K-NH₂, Dip is unnatural amino acid, 3,3- diphenylalanine) was designed based on LfcinB and showed activity against a wide range of cancer cell lines, including drug-resistant ones, and lower toxicity toward normal cells (Camilio et al. 2014; Haug et al. 2016). Its activity is due to its direct lytic effect on the plasma membrane of cancer cells in addition to permeabilization of the mitochondrial membrane. Moreover, it can stimulate adaptive immune responses and induce immunogenic cell death and also induce an inflammatory response, resulting in complete cancer regression. Therefore, this peptide has been introduced in oncolytic peptide-based local immunotherapy (Haug et al. 2016), and is currently being tested in a clinical phase I/IIa study, as mentioned above. Khan et al. (2016) proposed that LfcinB may be used as a chemoprotective agent against 7, 12 dimethylbenz (a) anthracene (DMBA)-induced skin cancer, due to its antioxidant properties that could inhibit carcinogenesis and hepatocellular and renal damage in Swiss albino female mice. In addition, a short

LfcinB derivative, L5a CPP (RRWQW), showed potential for DNA delivery in gene therapy, when it delivered a plasmid encoding the enhanced green fluorescent protein (EGFP) into human lung cancer A549 cells and the protein was subsequently expressed (Liu et al. 2016). A number of human Lfcin derivatives are also promising candidates for anticancer therapy. Its derived di-peptides, DIM-LF11-318 (FWQRRIRRWRRFWQRRIRRWRR-NH₂) and R-DIM-LF11-337 (PFWRRRIRIRRRIRIRRRWFP-NH₂), killed cancer cells of melanoma, glioblastoma and rhabdomyosarcoma (Riedl et al. 2015). Moreover, the derivative LF11-322 (PFWRIRIRR-NH₂) showed *in vivo* antitumor activity in leukemia cells (Lu et al. 2016).

Table 1.10 Examples of antimicrobial peptides with anticancer activities and their mechanisms of action

Peptide	Source	Sequence	Mechanism	<i>In vitro/In vivo</i> studies	Reference
Alloferon-1 Alloferon-2	<i>Calliphora vicina</i> (blow fly)	HGVS \overline{S} HGQHGVHG GV \overline{S} HGQHGVHG	Immunomodulatory	DBA2 mice grafted with P388 murine leukemia cells	(Chernysh et al. 2002; Chernysh et al. 2012)
Aurein 1.2	Skin of <i>Litoria raniformis</i> (Australian Bell Frog)	GLFDI \overline{I} KKIAESF-NH ₂	Membranolytic	60 cancer cell lines tested in the US National Cancer Institute human cancer test programme T98G glioblastoma cells, breast cancer cells (MX-1 and MCF-7)	(Rozek et al. 2000b; Dennison et al. 2007; Han et al. 2013b)
BMAP-27 BMAP-28	<i>Bos taurus</i> (Bovine)	GRFKRFRKKFKKLFKLS \overline{P} IPLLHL GGLRSLGRKILRAWKKYG PIIVPIIRI	Membranolytic followed by apoptosis Mitochondria-dependent apoptosis inducer	Human hemopoietic tumor cells, human leukemia cells, U937(promonocytic) and K562 (erythroid) cells, breast cancer cells (MX-1 and MCF-7)	(Risso et al. 1998; Risso et al. 2002; Han et al. 2013b)
Buforin IIb	Stomach of <i>Bufo gargarizans</i> (Asian toad)	RAGLQFPVGRLLRRLRR LLR	Mitochondria-dependent apoptosis inducer Apoptosis inducer via Endoplasmic reticulum stress-mediation	60 cancer cell lines tested in the US National Cancer Institute as a part of the Developmental Therapeutics Program Breast cancer cells (MX-1 and MCF-7), human cervical carcinoma HeLa cells	(Lee et al. 2008a; Han et al. 2013b; Jang et al. 2015)
Cecropin A and B	Haemolymph of <i>Hyalophora cecropia</i> (Silk moth)	KWKL \overline{F} KKIEKVGQ \overline{N} IRDGI IKAGPAVAVVGQATQIAK KWKV \overline{F} KKIEKMGRNIRNG IVKAGPAIAVLGEAKAL	Membranolytic	Multidrug-resistant human breast and ovarian cancer cell lines CCRF-SB human lymphoblastic leukemia cells, lung cancer cells, Ags human stomach carcinoma cells	(Moore et al. 1994; Hui et al. 2002; Ye et al. 2004; Wu et al. 2009; Li et al. 2016c)
Citropin 1.1	Skin of <i>Litoria citropia</i> (Australian Blue Mountains tree frog)	GLFDVIKKVASVIGGL-NH ₂	Membranolytic	60 cancer cell lines tested in the US National Cancer Institute human cancer test programme human histiocytic lymphoma cell line U937.	(Doyle et al. 2003; Koszalka et al. 2011)
HNP-1	<i>Homo sapiens</i>	ACYCRIPACIAGERRYGTC IYQGRLWAFCC	Membranolytic Mitochondria-dependent apoptosis inducer Antiangiogenic	Renal cell carcinomas cell lines (A-498, Caki-2, 786-0, 769-P, ACHN), CT26 colon carcinoma, 4T1 breast carcinoma cells, human prostate adenocarcinoma PC-3 cells, human acute lymphoblastic leukemia (MOLT-4), oral squamous cell carcinoma cell lines (UT-SCC-43A and UT-SCC-43B)	(Müller et al. 2002; Xu et al. 2008; Wang et al. 2009; Gaspar et al. 2015; Musrati et al. 2016)

Lactoferricin	<i>Bos taurus</i> (Bovine)	FKCRRWQWRMCKLGPSTTCV RRAF	Membranolytic Mitochondria-dependent apoptosis inducer Antiangiogenic	leukemia cells, fibrosarcoma cells, breast, colon, mammary, colorectal adenocarcinoma and ovarian carcinoma, neuroblastoma cells, AGS human gastric cancer cell, H460 lung cancer cells	(Yoo et al. 1997a; Eliassen et al. 2002; Mader et al. 2005; Eliassen et al. 2006; Pan et al. 2013; Wang et al. 2015b)
LL-37	<i>Homo sapiens</i>	LLGDFFRKSKEKIGKEFKRIVQRI KDFLRNLPRTES	Membranolytic Mitochondria-dependent apoptosis inducer	Human oral squamous cell carcinoma SAS-H1 cells, A549 human lung carcinoma cells, Jurkat T leukemia cells, colon cancer cell line HCT116	(Okumura et al. 2004; Aarbiou et al. 2006; Mader et al. 2009; Kuroda et al. 2012)
Magainin 2	Skin of <i>Xenopus laevis</i> (African clawed frog)	GIGKFLHSAKKFGKAFVGEIMNS	Membranolytic Mitochondria-dependent apoptosis inducer	Hematopoietic cell lines, Ehrlich ascites tumor cells, human adenocarcinoma A549, bladder cancer lines (RT4, 647V, and 486P), human histiocytic lymphoma cell line U937, breast adenocarcinoma MDA- MB-231 cells, human mesothelioma M14K cells.	(Cruciani et al. 1991; Baker et al. 1993; Lehmann et al. 2006; Koszalka et al. 2011; Anghel et al. 2013)
Melittin	<i>Apis mellifera</i> (Honey bee venom)	GIGAVLKVLTTGLPALISWIKRK RQQ-NH2	Membranolytic Bcl-2 and caspase-3- dependent apoptosis inducer Antiangiogenic Metastasis inhibitor	Human hepatocellular carcinoma (BEL- 7402) cells, human osteosarcoma cells MG63, leukemic U937 cells, human neuroblastoma cancer cells, rat osteoblastic osteosarcoma UMR-106 cells	(Li et al. 2006; Chu et al. 2007; Moon et al. 2008; Drechsler & Andrä 2011; Qin et al. 2016)
Pardaxin	<i>Pardachirus mormoratus</i> (Moses sole fish)	GFFALIPKIISPLFKTLLSAVGSA LSSSGGQE	Membranolytic Caspase-dependent and ROS- mediated apoptosis inducer	human fibrosarcoma HT-1080 cells, murine fibrosarcoma MN-11 cells, murine bladder carcinoma (MBT-2) cells, human cervical carcinoma HeLa cells, canine perianal gland adenoma, oral squamous cell carcinoma (OSCC) cells	(Huang et al. 2011; Wu et al. 2012; Huang et al. 2013; Huang & Chen 2013; Pan et al. 2015; Han et al. 2016)
Tachyplestin	Hemocytes of <i>Tachypleus tridentatus</i> (Horseshoe crab)	KWC1FRVC2YRGIC2YRRC1R	Complement-mediated cell lysis activator Cancer cell differentiation inducer	TSU human prostate cancer cells, human hepatocarcinoma SMMC- 7721 cells, human gastric adenocarcinoma cell line BGC-823, U251 human glioma cells	(Chen et al. 2001; Li et al. 2003; Shi et al. 2006; Hoskin & Ramamoorthy 2008a; Ding et al. 2015)

1.10.2 Applications of AMPs in the food industry: Microbial growth is the main reason for food spoilage and poisoning. The massive use of preservatives has led to appearance of resistant forms of food pathogens (Keymanesh et al. 2009). Hence, there is a need for effective and nontoxic preservatives. As naturally originating compounds, AMPs have a strong potential in this regard. Bacteriocins are the preferred group of AMPs; as preservatives as they are effective against gram-positive bacteria such as *Listeria monocytogenes*, *Clostridium botulinum* and *Bacillus cereus* that cause of many food-borne diseases (Rydlo et al. 2006; Ghrairi et al. 2012). Nisin, a lantibiotic peptide, has been approved for use as a food preservative by the Joint FAO/WHO Expert Committee on Food Additives (www.fao.org; CAS Reg. No. 1414-45-5). It effectively prevents the activity of many food pathogens in foods such as dairy products and seafood (Delves-Broughton 2005). Additionally, lactoferrin and lactoferricin have shown several potential applications in the food industry (Weinberg 2003, 2007; Paul & Somkuti 2010; Quintieri et al. 2013).

1.10.3 Applications of AMPs in plant biology, aquaculture and animal husbandry: A new strategy for controlling plant disease has been proposed based on transgenic plants expressing AMP genes. For example, expression of MSI-99, a synthetic derivative of magainin II, in tomato, banana and tobacco led to significantly enhanced resistance to bacterial and fungal diseases (Keymanesh et al. 2009). Additionally, introducing the bovine lactoferrin gene into tobacco, wheat and tomato improved their resistance against fungal and bacterial pathogens (Lakshman et al. 2013).

In animal husbandry, transgenic goat mammary cells were able to synthesize and secrete bovine lactoferricin and all the milk samples collected inhibited several bacterial pathogens (Zhang et al. 2007). Further, a synthetic form of epinecidin-1 exhibited high antimicrobial activity against detrimental bacteria such as *Vibrio parahaemolyticus* and *Morganella morganii* in aquaculture (Yin et al. 2006). LfcinB was able to control virus infection in fish (Rodríguez Saint-Jean et al. 2012).

Table 1.11 Applications of AMPs

Peptide	Sequence	Application	Reference
Applications in health and medicine			
Omiganan (MX226/MBI-226)	ILRWPWWPWRRK-NH ₂	Prevention of catheter infections, topical antiseptic, severe acne and rosacea (Phase III/II)	NCT00027248 NCT00211523 NCT01784133
PAC-113	AKRHHGYKRKFH-NH ₂	Oral candidiasis (Phase IIb)	NCT00659971
Pexiganan acetate	GIGKFLKKAKKFGKAFVKILKK-NH ₂	Topical antibiotic for treatment diabetic ulcers (Phase III)	NCT00563433
OP-145	IGKEFKRIVERIKRFLRELVRPLR-NH ₂	Chronic middle ear infections (Phase I/II)	ISRCTN84220089
LTX-315	KKWWKKW-Dip-K-NH ₂	Anticancer agent for intratumoral administration	NCT01986426
human lactoferrin peptide (hLF1-11)	GRRRRSVQWCA-NH ₂	Treating bacteremia and fungal infections in immunocompromized hematopoietic stem cell transplant recipients (Phase I/II)	NCT00509938
Plectasin	GFGC1NGPWDEDDMQC2HNHC3KSIKGYKGGYC1A KGGFVC2KC3Y	Broad-spectrum antibiotic (preclinical)	(Haney & Hancock 2013)
Applications in animal health			
Bovine lactoferricin (LFB ₁₇₋₄₁)	FKCRRWQWRMKKLGAPSTTCVRRAF	Mastitis control in goat	(Zhang et al. 2007)
Applications in food industry			
Nisin	MSTKDFNLDLVSVSKKDSGASPRITSISLCTPGCKTG ALMGCNMKTATCHCSIHVSK	Food preservative	(Delves-Broughton 2005)
Applications in agriculture, aquaculture			
MSI-99	MLLAIAFLASVCVSSMGIGKFLKSAKKFGKAFVKIL NS	Antifungal and antibacterial in transgenic tobacco, tomato, grapevine, banana	(Chakrabarti et al. 2003)
CEMA	MKWKLFKKIGIGAVLKVLTGLPALKLTK	Antifungal in transgenic tobacco, antibacterial against pathogens in fish	(Keymanesh et al. 2009)

1.11 Resistance to Antimicrobial Peptides

Bacteria have different levels of intrinsic susceptibility to AMPs, and some are capable of developing countermeasures to limit the efficacy of AMPs. As a consequence of their slow exposure to AMPs, bacteria could evolve inducible (adaptive) resistance mechanisms including altered cell surface charge, extrusion of AMPs by active efflux pumps, production of proteases or AMPs-trapping proteins, and modification of intracellular targets and host cellular processes (Table 1.12). Alternatively, some bacteria have constitutive (passive) mechanisms of resistance that are expressed even in the absence of peptide exposure, such as altered membrane energetics, electrostatic shielding and niche-specific resistance (Yeaman & Yount 2003). However, all resistance mechanisms may have limitations and bacteria seem to not succeed in becoming fully insensitive to a broad range of AMPs (Kraus & Peschel 2006). Compared to present-day antibiotics, it seems to be a mystery how AMPs have been used successfully by nature for millions of years and yet have remain so efficient. AMPs cause cell death by using several independent or cooperative mechanisms in a “multi-hit process” (Yeaman & Yount 2003). Therefore, the extraordinary success of AMPs may be due to the fact that bacteria cannot completely change all their targets (detailed above in section 1.7).

*This image is unable to be reproduced online due to Copyright
Please consult print copy held in the Swinburne Library*

Figure 1.12 Cationic antimicrobial peptide-resistance mechanisms in bacteria.

Source: Bahar and Ren (2013). **A.** Gram-positive bacteria resist AMPs via modifying teichoic acid of LPS molecules and L-lysine of phospholipids. **B.** Gram-negative bacteria resist AMPs by modifying LPS molecules with aminoarabinose or acylation of Lipid A unit of LPS molecules. **C.** Bacteria produce positively charged proteins and integrate them in the membrane to reduce the net anionic charge of the membrane and subsequently reduce its affinity for cationic AMPs, as positive charges each other. **D.** Bacteria produce negatively charged proteins and secrete them into extracellular environment to bind and block AMPs. **E.** The intracellular AMPs are actively extruded from bacterial cells by efflux pumps. **F.** The intracellular AMPs are degraded by bacterial proteases.

Table 1.12 Mechanisms of bacterial AMP resistance

Resistance mechanism	AMPs	Organism	Reference
Proteolytic Degradation			
Gelatinase	LL-37	<i>Enterococcus faecalis</i>	(Schmidtchen et al. 2002)
Metalloproteinase	LL-37 Lactoferricin B LL-37	<i>Proteus mirabilis</i> <i>Escherichia coli</i> <i>Staphylococcus aureus</i>	(Schmidtchen et al. 2002) (Ulvatne et al. 2002) (Sieprawska-Lupa et al. 2004)
Aureolysin	LL-37	<i>Staphylococcus aureus</i>	(Sieprawska-Lupa et al. 2004)
SepA	dermcidin	<i>S. epidermidis</i>	(Lai et al. 2007)
SpeB	LL-37	<i>Streptococcus pyogenes</i>	(Schmidtchen et al. 2002; Johansson et al. 2008)
AMPs binding and inactivation			
M1 protein	LL-37	Group A <i>Streptococcus</i>	(Lauth et al. 2009)
SIC protein	LL-37	Group A <i>Streptococcus</i>	(Pence et al. 2010)
Cell Surface Modifications			
D-alanylation of teichoic acid and lipoteichoic acid in bacterial cell wall	HNP1-3, magainin II, protegrins, tachyplesin colistin, nisin, polymyxin B, indolicidin, Cecropin B, nisin and gallidermin colistin, nisin, polymyxin B, nisin, polymyxin B, colistin, cecropin B	<i>Staphylococcus aureus</i> <i>Listeria monocytogenes</i> <i>Streptococcus agalactiae</i> <i>Streptococcus pneumoniae</i> <i>Enterococcus faecalis</i> <i>Bacillus cereus</i>	(Peschel et al. 1999) (Abachin et al. 2002) (Poyart et al. 2003) (Kovács et al. 2006) (Fabretti et al. 2006) (Abi Khattar et al. 2009)
Lysinylation of phosphatidylglycerol	HNP1-3, protegrins 3, 5, tachyplesin 1 HBD-3, CAP18	<i>Staphylococcus aureus</i>	(Peschel et al. 2001) (Nishi et al. 2004)
Acylation of lipid A in lipopolysaccharide (LPS)	HBD-2 colistin, CP28, polymyxin B polymyxin B	<i>Haemophilus influenzae</i> <i>Klebsiella pneumoniae</i> <i>Vibrio cholerae</i>	(Starner et al. 2002) (Clements et al. 2007) (Matson et al. 2010)

Table 1.12 continued			
Dephosphorylation of lipid A in lipopolysaccharide (LPS)	polymyxin B	<i>Bacteroides thetaiotaomicron</i>	(Cullen et al. 2015)
Synthesis of lipooligosaccharide (LOS) capsule	LL-37 LL-37, polymyxin B	<i>Neisseria meningitidis</i> <i>Campylobacter jejuni</i>	(Jones et al. 2009) (Naito et al. 2010; Keo et al. 2011)
Lysinylation and Alanylation of phospholipids	HBD3, CAP18, melittin, NK-2 and arenicin-1 HNP-1, lysozyme protamine sulphate	<i>Staphylococcus aureus</i> <i>Mycobacterium tuberculosis</i> <i>Pseudomonas aeruginosa</i>	(Nishi et al. 2004; Andrä et al. 2011) (Maloney et al. 2009) (Klein et al. 2009)
Peptidoglycan O-acetylation and N-deacetylation	lysozyme	<i>Streptococcus suis</i> , <i>Bacillus anthracis</i>	(Fittipaldi et al. 2008; Laaberki et al. 2011)
Active AMPs e Efflux			
<i>Sap</i> (sensitivity to antimicrobial peptides) operon	Melittin, protamine, HBD-3	<i>Salmonella typhimurium</i> , <i>Haemophilus influenzae</i>	(Parra-Lopez et al. 1993; Mason et al. 2005)
<i>Mtr</i> efflux pump system	protegrin-1, LL-37 polymyxin B,	<i>Neisseria gonorrhoeae</i> <i>Neisseria meningitidis</i>	(Shafer et al. 1998) (Tzeng et al. 2005)
Regulatory pathway			
PhoP/PhoQ	polymyxin, azurocidin (CAP37), protamine CP28, polymyxin B LL-37, CNY100HL	<i>Salmonella enterica</i> <i>Pseudomonas aeruginosa</i> <i>Salmonella typhimurium</i>	(Gunn & Miller 1996) (Macfarlane et al. 2000) (Lofton et al. 2013)
PmrA/PmrB	Polymyxin, LL-37, CNY100HL Polymyxins, indolicidin, LL-37	<i>Salmonella typhimurium</i> <i>Pseudomonas aeruginosa</i>	(Gunn et al. 1998; Lofton et al. 2013) (McPhee et al. 2003)
VraDE/VraSR	Temporin L, ovispirin-1, dermaseptin K4-S4 ₁₋₁₆	<i>Staphylococcus aureus</i>	(Pietiäinen et al. 2009)
GraSR/VraFG	colistin	<i>Staphylococcus aureus</i>	(Falord et al. 2012)
Alteration of Host Processes			
Downregulation of AMP transcription and expression	LL-37, HBD-1	<i>Shigella dysenteriae</i>	(Islam et al. 2001)
Overexpression of host cathepsins	HBD-2, HBD-3	<i>Pseudomonas aeruginosa</i>	(Taggart et al. 2003)

1.12 Summary of the literature

Although AMPs are considered interesting novel antimicrobial chemotherapies (Section 1.2), many AMPs are not yet optimized for efficient *in vivo* activity. Natural peptides with broad spectrum activity, metabolic stability and low cytotoxicity are rare at present. AMPs with these attributes can be achieved by rational design based on variants in their physicochemical characteristics (Section 1.3). Modifying the structural determinants of AMPs is a useful tool for optimizing their activity and cytotoxicity, as well boosting their potential for wide-range of applications.

The tryptophan (Trp)-rich peptides (TRPs) are a subset of AMPs that display potent antimicrobial activity, credited to the unique biochemical properties of Trp (as discussed above in sections 1.4 & 1.8). The activities of naturally occurring Trp-rich cationic peptides such as indolicidin, tritrypticin, lactoferricin and their derivatives have been explored widely (Section 1.4). The wide-spectrum of activity of these TRPs triggered the study on the unique Trp-rich domain (TRD) of the wheat grain PIN proteins to examine their antimicrobial activity (Section 1.6). Most remarkably, among all natural TRPs, PINs are the only peptides with sequence variations in the TRD located within naturally mutated PIN proteins. The effect of these mutations on grain texture is well-established. While the primary *in vivo* role of PINs is believed to be to protect the wheat seed from phytopathogens, the effect of these mutations in the TRD on the antimicrobial activity of PINs is little explored. It will be important to investigate these aspects further, in particular against persistent pathogens.

AMPs often exert microbicidal effects due to disruption of vital cellular structures and/or functions. The mechanisms by which antimicrobial peptides act is a complex issue. As many AMPs use multiple killing mechanisms (Sections 1.7 and 1.8), it difficult to reveal all the molecular interactions that occur during AMP attack. It is essential to understand how PIN-based peptides act to properly exploit their use as antimicrobial agents. The precise mechanism of action of the synthetic peptide PuroA, based on the TRD of PINA (discussed in section 1.9) is not fully determined yet. Using advanced biophysical techniques and studying live cells in real time will be useful to reveal more detailed and precious mechanistic aspects of PuroA.

1.13 Aims and strategy of the project

The major aim of this project is to design antimicrobial peptides based on the Trp-rich domain of PINA that have effective, wide spectrum and selective antimicrobial activities.

The following objectives and strategies are designed to achieve the above major aim:

1. To identify the biochemical signatures of PIN-based peptides that are related to their antimicrobial activities, salt and protease stability.
 - By designing a number of variants based on PuroA peptide and testing their activities against selected pathogens, including *E. coli*, *S. aureus*, *P. aeruginosa* and *C. albicans*. In addition, their activities will be tested in the presence of salt and proteases.
2. To determine the potential applications of PIN-based peptides.
 - By determining their activities against persistent pathogens including biofilms of *P. aeruginosa*, *Listeria monocytogenes* and Methicillin-resistant *S. aureus* isolates and endospores of *Bacillus subtilis*.
3. To investigate the mechanisms of action of PuroA peptide.
 - By using fluorescence microscopy techniques including time-lapse fluorescence microscopy and fluorescence lifetime imaging microscopy (FLIM) to study the effect of a fluorescently-tagged PuroA peptide on live cells in real time.
4. To test the development of bacterial and fungal resistance to PIN-based peptides.
 - By determining if *E. coli*, *S. aureus* and *C. albicans* can develop resistance when grow in presence of increasing concentrations of the peptides.
5. To determine the cytotoxicity of the designed PIN-based peptides against mammalian cells.
 - By determining the peptides concentrations that lyse 50% of erythrocytes, or cause 50% growth inhibition in fibroblast NIH-3T3 cells and the human cervical carcinoma HeLa cell.

Chapter 2

Materials and methods

2.1 Equipment and materials

2.1.1 Equipment

The instruments and apparatus used to perform experiments are listed in Table 2.1

Table 2.1 Instruments and apparatus used

Equipment	Purpose	Manufacturer
Attune NxT Flow Cytometer	Cell cycle analysis	Invitrogen™; USA
C3040 digital camera	Capturing of gel images	Olympus, Tokyo, Japan
Electrophoresis power supply EOS 301	Agarose gel electrophoresis	GE Healthcare, Waukesha, USA
Minnie Gel Unit		
Finnpipettes (single-channel: 0.5 - 10, 10 - 100, 100 - 1000 µL and multi-channel: 10 - 100 µL)	Dispensing liquids	Thermo Scientific, Waltham, USA
FluoView FV1000 confocal microscope	Fluorescence imaging	Olympus, Tokyo, Japan
Field –emission SEM (FE SE) 40vp	Observing surface structure of cells	ZEISS SUPRA, Germany
Helios ε Spectrophotometer	Measuring OD ₆₀₀ Haemolytic assay	Thermo Scientific, USA
Lambert Instruments FLIM Attachment (LIFA) instrument	Fluorescence lifetime imaging	Lambert Instruments, Leutingwolde, Netherlands
Inverted microscope		Ti Eclipse, Nikon Inc, Japan
Light microscope	Visualising prokaryotic and eukaryotic cells	Olympus, Tokyo, Japan
Sorvall RC6	Centrifugation	Sorvall (part of Thermo Scientific, Waltham, USA)
Mini spin <i>plus</i>		Eppendorf, Hamburg, Germany
Milli-Q™ system	Filtering water	Millipore, Madison, USA
Microplate reader	MIC assays Growth rate assay Crystal violet assay MTT assay Cell culture assays	POLARstar Omega, Germany
NanoDrop spectrophotometer	Measuring DNA concentration	Thermo Scientific, Wilmington, DE, USA
Orbital shaker/incubator	Bacterial and fungi broth culture	Ratek, Victoria, Australia
Pioneer™ analytical balance	Weighing reagents	Ohaus Corporation, USA
SmartCHEM-LAB analyser	pH measurements	TPS, Brisbane, Australia
UV light transilluminator	Agarose gel visualisation	Integrated Sciences, Chatswood, Australia

2.1.2 Commercial kits and reagents

Table 2.2 Commercial kits and reagents

Kit/reagents	Purpose	Manufacturer
Wizard® PlusSV Plasmid Miniprep kit	Plasmid DNA purification	Promega, Madison, USA
LIVE/DEAD® BacLight™ Bacterial Viability Kit (contains 20 mM solution of propidium iodide and 20 mM of Syto 9 in DMSO)	Membrane permeability Assay	Molecular Probes®, USA
SYTO 85 Orange fluorescent nucleic acid, 5 mM Solution in DMSO	Staining cell nucleus	

2.2 Prepared solutions and materials

2.2.1 Sterilisation

The sterilisation of all solutions, media and buffers was carried out by autoclaving at 121°C for 20 min or filtering through a 0.22 µM syringe filter (Millipore, Madison, USA). All glassware and autoclavable plastics were also autoclaved at 121°C for 20 min.

2.2.2 Buffers and solutions

All the following buffers and solutions were prepared using sterile, ultrapure (18 MΩ) water which was quartz-distilled and deionised in a Milli-Q™ system (Millipore, Bedford, MA, USA), and according to Sambrook and Russell (2001).

Table 2.3 Concentration and composition of solutions and buffers

Solution/Buffer	Composition	Sterilization method
50× TAE (TRIS-acetate EDTA) buffer	2.0 M TRIS-base, 6.5 M EDTA disodium salt, pH 8.0	Autoclaved
6× DNA electrophoresis loading dye	30% (v/v) glycerol, 1 mg/mL xylene cyanol, 1 mg/mL bromophenol blue	Autoclaved
Ethidium bromide stain	0.5 µg/mL ethidium bromide in MilliQ water	-
Crystal violet stain	1% in MilliQ water	-
PBS (Phosphate-buffered saline)	140 mM NaCl, 2.5 mM KCl, 1.6 mM KH ₂ PO ₄ , 15 mM Na ₂ HPO ₄ , pH 7.4	Autoclaved
Tris-HCl buffer	140 mM NaCl, 2.5 mM KCl, 1.6 mM KH ₂ PO ₄ , 15mM Na ₂ HPO ₄ , pH 7.4	Autoclaved
Acetic acid solution	0.001% (v/v) in MilliQ water	Filter sterilized
0.85% saline	0.85% (w/v) NaCl	Autoclaved
Sodium chloride solution	2 M in MilliQ water	Autoclaved
Triton X-100	1% (w/v) in PBS pH 7.4	Autoclaved
100% DMSO	Analytical grade dimethyl sulfoxide (Merck, Germany)	
SDS (Sodium dodecyl sulfate)	40 Mm SDS detergent in MilliQ water	Autoclaved
Glutaraldehyde solution	2.5% in PBS, pH 7.4	Autoclaved
MTT solution	5 mg/mL and 1 mg/mL in PBS, pH 7.4	Filter sterilized
Poly-L-lysine	0.01% in MilliQ water (Sigma, USA)	Filter sterilized
Glucose solution	1% (w/v) in MilliQ water (Sigma, USA)	Filter sterilized
Tetracycline	10 mg/mL in MilliQ water (Sigma, USA)	Filter sterilized
Ampicillin	100 mg/mL in MilliQ water (Sigma, USA)	
Porcine trypsin	1 mg/mL in MilliQ water (Sigma, USA)	Filter sterilized
Proteinase K	1 mg/mL in MilliQ water (Sigma, USA)	Filter sterilized
Propidium iodide (PI)	1 mg/mL in MilliQ water (Sigma, USA)	Filter sterilized

2.2.3 Media for microbial growth

All the following microbial culturing media were prepared according to Sambrook & Russell (2001). All media were prepared in distilled water.

Luria-Bertani (LB) medium: 10 g/L tryptone, 5.0 g/L yeast extract, 5.0 g/L NaCl and 15 g/L bacteriological agar (Micromedia, added to plates only).

Nutrient agar (NA): 23 g/L nutrient agar (Oxoid).

Mueller-Hinton (MH) medium 21 g/L Mueller-Hinton broth (Oxoid) and 15 g/L bacteriological agar (Micromedia, added to plates only).

Potato Dextrose (PD) medium: 24 g/L Potato Dextrose broth (Difco) and 15 g/L bacteriological agar (Micromedia, added to plates only).

Brain heart (BH) medium: 37 g/L brain heart broth (Oxoid) and 15 g/L bacteriological agar (Micromedia, added to plates only)

Tryptic soya medium: 30 g/L tryptic soya broth (Acumedia) and 15 g/L bacteriological agar (Micromedia, added to plates only)

2.2.4 Media for cell culture

All cell culture media were prepared under aseptic conditions in a biological safety cabinet class II.

Complete Dulbecco's Modified Eagle Medium (DMEM): 90% (v/v) DMEM (Gibco, UK) and 10% (v/v) fetal bovine serum (FBS, Gibco, UK)

Cell freezing media: 10% (v/v) DMEM (Gibco, UK), 80% (v/v) fetal bovine serum (FBS, Gibco, UK) and 10% dimethyl sulfoxide (DMSO, Merck, Germany).

2.2.5 Microbial strains

Escherichia coli (ATCC 25922), *Staphylococcus aureus* (ATCC 25923), *Listeria monocytogenes* (ATCC 13932, stereotype 4B), *Bacillus subtilis* (ATCC 6051), *Pseudomonas aeruginosa* (ATCC 9027), and *Staphylococcus epidermidis* (ATCC14990) were all obtained from the culture collection at Swinburne University of Technology.

Listeria innocua (LI-451713/5) was obtained from food processing environments and kindly provided by Dr. Snehal Jadhav, Swinburne University of Technology.

Candida albicans (FRR 5580) yeast was obtained from CSIRO Food Fungal Culture Collection.

Methicillin-resistant *Staphylococcus aureus* (MRSA) isolates, M173525 and M180920 were kindly provided by Dr. P. B. Ward, Microbiology Department, Austin and Repatriation Medical Centre, Victoria, Australia.

Microbial stocks were prepared in 25% glycerol and stored at -80°C until needed. Prior to each experiment, the microbial culture was refreshed from stocks on suitable agar plate, and a fresh cell suspension was grown in broth overnight. For microtitre broth dilution assays, the not-cation-adjusted broth was used as recommended for the testing of cationic antimicrobial peptides (AMPs) (Wiegand et al. 2008).

2.2.6 Cell lines

The human cervical HeLa and mouse 3T3-L1 cell lines were kindly provided by Dr. Rohan Shah and Miss Katharine Adcroft, colleagues at Swinburne University of Technology.

The cells were maintained and subcultured as described in Section 2.28.

2.2.7 Peptide solution

Custom synthetic peptides were purchased from Biomatik Crop (Ontario, CA) and Mimotopes (Clayton, Australia) at $>95\%$ purity. Stock solutions of each peptide that was used in antimicrobial assays were prepared at 1 mg/mL in 0.01% glacial acetic (Wiegand et al., 2008) and stored at -20°C . Stock solutions of each peptide that was used in haemolytic and cell culture assays were prepared at 1 mg/mL in sterile MilliQ water. Solution of FITC-labelled PuroA was made immediately before the experiment in sterile PBS (pH 7.4) and it was vortexed for 30 s to avoid large FITC-PuroA aggregates.

Design of TRD-based peptides is described in Section 2.3.

2.3 General methods

2.3.1 Peptide design

Peptides were designed based on the Trp-rich domain (TRD) of the wild type PINA protein encoded by the wheat gene *Pina-D1a* (Gautier et al. 1994)(Genbank accession No. DQ363911) (Table 1). All peptides were commercially synthesized by solid phase methods using N-(9-fluorenyl) methoxycarbonyl (Fmoc) chemistry and analysed by reversed phase high performance liquid chromatography (RP-HPLC) and mass spectrometry to confirm their purity to be greater than to 95% at Biomatik Crop (Ontario, CA) or Mimotopes (Clayton, Australia). PuroA (FPVTWRWWKWWKG-NH₂) is a synthetic peptides based on the TRD of the wild type PINA and shows antimicrobial activity against a number of bacteria (Jing et al. 2003; Phillips et al. 2011), phytopathogenic fungi (Phillips et al. 2011) and fungi spores (Alfred et al. 2013a), as discussed in Chapter 1, Section 1.6. This peptide was used as a starting framework to design 13 Trp-rich peptides (TRPs) with different net charge, length and number of Trp residues. All the non-Trp residues in PuroA were substituted with the cationic amino acid Arg to generate R8. While to generate P1, all uncharged amino acids were substituted with both cationic amino acids Arg and Lys and additional Trp residue (Trp4) was inserted after Arg3. A number of short peptides, i.e., R6, R7, W7, W8 and WW, were designed based on the Arg-, Lys- and Trp-rich central region of PuroA. A cyclic analogue of PuroA with an additional head-to-tail bond in the peptide backbone, and a Lys linked dimeric C-terminal analogue (PuroA)_{2k}, were also designed. The C terminus of all peptides was amidated except in PuroA-OH peptide. Three peptides, P1, W7 and WW, were chosen to incorporate D-amino acids into their sequences and design three diastereomeric counterparts, dP1, dW7 and dWW, that consisted of 35-40% D-amino acids. The position of D-amino acids were selected to form short consecutive sections of 1–2 L-amino acids that cannot adapt α -helical structures (Papo et al. 2002).

For mechanistic studies (Chapter 5), PuroA was labelled with a green-fluorescent FITC probe at N-terminus to generate FITC- PuroA (FITC-FPVTWRWWKWWKG-NH₂).

2.3.2 Physicochemical analytical tools

The physical and chemical parameters of the designed peptides were analysed using a number of bioinformatics tools. Net charge of the peptides was calculated by adding up the number of positively-charged amino acids (Arg, Lys), as all designed peptide did not have negatively-charged amino acids, such as Asp and Glu (Nelson & Cox 2008). C-terminal amidation was not assigned with one positive charge when net positive charge was calculated in order to be consistent with the previous published information on PuroA and other PIN-based peptides (Alfred et al. 2013a). The isoelectric points (pI) and the molecular weight of the peptides were predicted using the ‘compute pI/MW Tool’ at the Expert Protein Analysis System (ExPASy) site (http://au.expasy.org/tools/pi_tool.html; last accessed October 2016). This tool calculates the peptide pI using pK values of amino acids as described in (Bjellqvist et al. 1993), which were defined by testing the migration of polypeptide between pH 4.5 to pH 7.3 in an immobilised pH gradient gel environment with 9.2M and 9.8M of urea at 15°C or 25°C. Charge density (ChD) was calculated by dividing the net charge with the chain length of peptide (Le et al. 2015). Mean values of hydrophobicity (*H*) were calculated using consensus value of hydrophobicity scale (Eisenberg et al. 1984). Hydrophobic ratio (HR) is the percentage of hydrophobic amino acid (Val, Phe, Thr, Trp) in the peptide chain. GRAVY is the grand average of hydropathy and calculated by dividing the sum of hydropathy values of all amino acids by the peptide length. The hydrophobic moment (μH), which represent the peptide amphipathicity (Eisenberg et al. 1982), and the helical wheel projection and were calculated online using Helical Wheel Projections (<http://rzlab.ucr.edu/scripts/wheel/wheel.cgi>; last accessed January 2017).

Table 2.4 Primary sequence, net charge, molecular weights, isoelectric points, hydrophobicity and Trp content of the designed TRPS.

Peptide ID	Sequences*	Length	Mw	No. of Trp	Charge	pI	ChD	<i>H</i>	HR	GRAVY	μ H
PuroA	FPVTWRWWKWWKG-NH ₂	13	1863	5	+3	11.17	0.23	-0.08	61.5	-0.962	5.21
Cyclic PuroA	FPVTWRWWKWWKG	13	1845	5	+3	11.17	0.23	-0.08	61.5	-0.962	5.21
Di-PuroA	(FPVTWRWWKWWKG) ₂ k-NH ₂	27	3836	10	+7	12.04	0.25	-0.11	59	-1.070	3.56
PuroA-OH	FPVTWRWWKWWKG	13	1863	5	+3	11.17	0.23	-0.08	61.5	-0.962	5.21
R8	RRRRWRWRRWRR-NH ₂	13	2198	5	+8	12.85	0.61	-0.94	38	-3.115	5.01
P1	RKRWRRWWKWWKR-NH ₂	14	2144	6	+7	12.48	0.5	-0.58	43	-2.700	7.88
dP1	R <u>R</u> R <u>W</u> W <u>R</u> W <u>W</u> K <u>W</u> W <u>K</u> R-NH ₂	14	2144	6	+7	12.48	0.5	ND	43	ND	ND
R6	RWWKWW-NH ₂	6	1047	4	+2	11.00	0.33	-0.23	66	-2.000	5.56
R7	RWWKWWK-NH ₂	7	1175	4	+3	11.17	0.42	-0.35	57	-2.271	6.01
W7	WRWWKWW-NH ₂	7	1233	5	+2	11.00	0.28	-0.14	71	-1.843	4.51
dW7	<u>W</u> <u>R</u> W <u>W</u> K <u>W</u> W-NH ₂	7	1233	5	+2	11.00	0.28	ND	71	ND	ND
W8	WRWWKWWK-NH ₂	8	1361	5	+3	11.17	0.37	-0.26	62.5	-2.100	4.71
WW	WWRWWKWW-NH ₂	8	1419	6	+2	11.00	0.25	-0.08	75	-1.725	6.32
dWW	W <u>W</u> <u>R</u> W <u>W</u> K <u>W</u> W-NH ₂	8	1419	6	+2	11.00	0.25	ND	75	ND	ND

*Underlined and bold amino acids are D-enantiomers. The C terminus is amidated except for PuroA-OH peptide. The isoelectric points (pI) of the peptides were predicted using the 'compute pI/MW Tool' at the Expert Protein Analysis System (ExPASy) site (http://au.expasy.org/tools/pi_tool.html; last accessed October 2016). Mean values of hydrophobicity (*H*) were calculated using consensus value of hydrophobicity scale (Eisenberg et al. 1984). Charge density (ChD) was calculated by dividing net charge with the chain length of peptide. Hydrophobic ratio (HR) is the percentage of hydrophobic amino acid (Val, Phe, Thr, Trp) in the peptide chain. GRAVY = the grand average of hydropathy and calculated by dividing the sum of hydropathy values of all amino acids by the peptide length. The hydrophobic moment (μ H) and the helical wheel projection were calculated using Helical Wheel Projections (<http://rzlab.ucr.edu/scripts/wheel/wheel.cgi>; last accessed January 2017). ND: not determined.

2.3.3 Antibacterial activity assay [Broth minimum inhibitory concentration (MIC)]

The antibacterial activity of the peptides was determined against the Gram-positive bacteria *Staphylococcus aureus* (ATCC 25923), *Listeria innocua* (LI-451713/5), *Listeria monocytogenes* (ATCC 13932, stereotype 4B) and *Bacillus subtilis* (ATCC 6051) and the Gram-negative bacteria *Escherichia coli* (ATCC 25922) and *Pseudomonas aeruginosa* (ATCC 9027). All bacterial cultures were obtained from the culture collection at Swinburne University of Technology (SUT), except for *L. innocua* which was obtained from food processing environments and kindly provided by Dr. Snehal Jadhav, SUT. Some of the peptides were also tested against two clinical Methicillin-resistant *Staphylococcus aureus* (MRSA) isolates, M173525 and M180920, that kindly provided by Dr. P. B. Ward (Microbiology Department, Austin and Repatriation Medical Centre, Victoria, Australia). The Minimum Inhibitory Concentration (MIC) was determined by the microtitre broth dilution method, as described in Phillips et al. (2011). Briefly, *S. aureus*, *B. subtilis*, *E. coli*, *P. aeruginosa* and MRSA were grown in Mueller-Hinton Broth (MHB; Oxoid) and *Listeria innocua* and *Listeria monocytogenes* were grown in Brain heart broth (BHB; Oxoid) at 37°C overnight with shaking (220 rpm). The cultures were adjusted to 0.5 McFarland turbidity standard (about 1×10^8 CFU/mL), then diluted 1:100 in MHB or BHB medium to 1×10^6 CFU/mL. Peptides in 25 μ L volumes were added to the wells of sterile, flat-bottomed, polypropylene 96-well microtitre plates (Corning, USA) and a two-fold serial dilution performed using 0.01% glacial acetic acid across each row, ranging from 250 μ g/mL to 0.5 μ g/mL. The wells were subsequently inoculated with 75 μ L of the bacterial suspension. Positive growth controls (inoculum and MHB or BHB with no peptide) and sterility controls (broth medium only) were also included in the plates and the plates were incubated overnight at 37°C. The MIC was defined as the lowest peptide concentration that completely inhibited bacterial growth (Wiegand et al. 2008), determined by both visual observation and measuring the absorbance at 595nm using a Microplate reader (POLARstar Omega, Germany). The assays were carried out in triplicates in each of two independent experiments.

2.3.4 Anti-*Candida* activity assay [Broth minimum inhibitory concentration (MIC)]

The anti-*Candida* activity of the peptides was determined against *Candida albicans* (FRR 5580), obtained from the culture collection at Swinburne University of Technology. Cultures of the yeast were grown in Potato Dextrose Broth (PDB; Difco-BD, USA) overnight at 30°C with shaking (200 rpm). The cultures were adjusted to 0.5 McFarland turbidity standard ($1-5 \times 10^6$ cells/mL), then diluted 1:200 with PDB to a final concentration of $0.5-2 \times 10^3$ cells/mL (Espinel-Ingroff & Cantón 2007). Peptides in 25 µL volumes were added to the wells of sterile, flat-bottomed, polypropylene 96-well microtitre plates (Corning, USA) and a two-fold serial dilution performed using 0.01% glacial acetic acid across each row, ranging from 250 µg/mL to 0.5 µg/mL. The wells were subsequently inoculated with 75 µL of the pathogens suspension. Positive growth controls (inoculum and PDB with no peptide) and sterility controls (PDB medium only) were also included in the plates and the plates were incubated overnight at 30°C. The MIC was defined as the lowest peptide concentration that completely inhibited yeast growth (Espinel-Ingroff & Cantón 2007), determined by both visual observation and measuring the absorbance at 595nm using a Microplate reader (Bio-Rad, USA). The assays were carried out in triplicates in each of two independent experiments.

The following sections in this Chapter explain specific methods which were used in a particular experimental Chapter as indicated below.

Methods specific to Chapter 3: Rational design of variant PuroA peptides and assessment of their biochemical properties and bioactivity effects

2.4 Effect of salt on the antibacterial activity of peptides

AMPs need to remain active under the physiological levels of salt to be used in clinical applications. NaCl is the predominant salt *in vivo* with a concentration of 120–150 mM (Nan & Shin 2011). To evaluate the salt sensitivity of the designed peptides below and at the physiological levels, we examined the MICs of the peptides against the Gram-positive *S. aureus* (ATCC 25923) and the Gram-negative *E. coli* (ATCC 25922) in the presence of different concentrations of NaCl (50, 100 and 150 mM) (Shin et al. 2002). The antibacterial assay was performed exactly as mentioned above in Section 2.3.3, except that the bacterial cultures were diluted 1:100 in MHB containing 0, 50, 100 and 150mM NaCl. The tests were carried out in triplicates in two independent experiments.

2.5 Protease stability assay

The effect of two well-studied proteases, porcine trypsin and proteinase K from *Tritirachium album*, on the activity of all the peptides was investigated as described by Carmona et al. (2013). Briefly, 1000 µg of the respective peptide was incubated with 50 µg of either porcine trypsin or proteinase K, ratio of 20:1(w/w) of peptide to protease, at 37 °C for 3 h in PBS (pH 7.4). After incubation, the enzyme activity was terminated by heat treatment (70 °C for 5 min), then the samples were centrifuged at 12000 × *g*. The antibacterial activity of the supernatant was tested as described above in Section 2.3.3 on *E. coli* and *S. aureus*. The tests were carried out in triplicates in two independent experiments.

2.6 Circular dichroism spectroscopy

Circular dichroism (CD) spectra were measured with a Jasco J-815 spectrophotometer (Japan Spectroscopic Company, Tokyo, Japan), as per Jing et al. (2003). Each spectrum (from 190 to 260 nm) was the average of three scans, obtained by using a quartz cuvette with a 1-mm path length at 25 °C. The measurements were performed in continuous scanning mode with scanning speed of 50 nm/min, at a step size of 0.1 nm, with a 1.0-nm bandwidth and a 4-s response time of the detector. Samples

contained 40 μM of peptide in 20 mM Tris-HCl buffer (pH 7.4) or in 20 mM SDS detergent. Spectra were baseline corrected by subtracting a blank spectrum containing all components except the peptide. After noise correction, ellipticities were converted to mean residue molar ellipticities $[\theta]$ expressed in units of degree square centimetre per decimole ($\text{deg cm}^2/\text{dmol}$).

2.7 Three dimensional structure prediction

The three dimensional (3D) structure of the long peptides (≤ 13 amino acids in length, Table 2.4) was predicted using iterative threading assembly refinement (I-TASSER) server (<http://zhanglab.ccmb.med.umich.edu/I-TASSER>; last accessed December 2016). The 3D structures were constructed from multiple threading alignments of amino acid sequences and iterative structural assembly simulations (Zhang 2008; Roy et al. 2010). The *ab initio* approach was used for structure prediction due to unavailability of an appropriate template, in this method the search returned proteins segments with close structural similarity to peptides.

2.8 *In vitro* DNA-binding assay

To examine the peptides capability to bind to purified DNA (which could give indication of their potential *in vivo* DNA binding ability), an agarose gel-retardation assay was performed as described by Alfred et al. (2013b). The plasmid pBlueScript SK+ (pBSK+) was purified from an overnight 5 mL culture of *E. coli* JM109 cells using the Wizard[®] Plus SV Minipreps DNA Purification System (Promega, Australia) according to the supplier's instructions. Briefly, a single colony of *E. coli* JM109 cells containing pBSK+ was grown overnight in LB broth containing 100 $\mu\text{g}/\text{mL}$ Ampicillin. The bacterial culture was centrifuged for 10 min at 10,000 rpm. The cell pellets were resuspended in 250 μL of Resuspension Solution and mixed with 250 μL Cell Lysis solution. Then, 10 μL of alkaline protease solution from the kit was added and the mixture was incubated for 5 min at room temperature. 350 μL Neutralisation Solution was added to this solution and the lysate was centrifuged at $14,500 \times g$ for 10 min. The supernatant was transferred to a column assembly that was provided with the kit and centrifuged at $14,500 \times g$ for 1 min. The column was washed twice with Wash Buffer, and the plasmid eluted from the column in 50 μL sterile MilliQ water. The purified plasmid concentration was determined using a NanoDrop spectrophotometer

(NanoDrop Products, Wilmington, USA). 100 ng of the plasmid was incubated at room temperature with increasing amounts of peptide (at final peptide concentrations of 8, 16, 32, 64, 125, 250 and 500 $\mu\text{g}/\text{mL}$) in a final volume of 15 μL , made up with sterile MilliQ water. After 1 h of incubation, 3 μL of 6 \times loading dye was added to the mixture and the whole mixture (18 μL) was loaded onto a 1% agarose gel in Tris-acetate-EDTA (TAE) buffer (pH 8). The samples were subjected to electrophoresis for 45 min at 100V. Subsequently, before imaging, the gels were stained by emersion in ethidium bromide (0.5 $\mu\text{g}/\text{mL}$) for 30 min. The gels were visualized on a UV transilluminator and imaged using C3040 digital camera (Olympus, Japan).

2.9 *E. coli* filamentation assay

The ability of designed peptides to induce filamentation in *E. coli* was assessed as described by Subbalakshmi and Sitaram (1998) and Alfred et al. (2013b). *E. coli* (ATCC 25922) was grown to logarithmic phase ($\text{OD}_{600} = 0.2$) Mueller-Hinton Broth (MHB; Oxoid) and then diluted to 1×10^8 CFU mL^{-1} . Twenty five microliters of peptide solution of a final concentration range of 2 - 250 $\mu\text{g}/\text{mL}$ was incubated with 75 μL of diluted bacterial culture for 3 h at 37°C. Bacterial cells mixed with 25 μL of sterile MilliQ water (no peptide) were used as negative control, and cells treated with PuroA were used as a positive control (Alfred et al. 2013b). The samples were stained with Crystal Violet for 1 min and observed using a light microscope (1000 \times magnification).

The change in bacterial morphology and the presence of any filamentous cells were also examined using an inverted confocal microscope (FluoView FV1000; Olympus, AU). After the 3 h incubation period (as described above), the cells were stained with SYTO 9 (green florescent cell-permeant nucleic acid dye) following the manufacturer's instructions and visualized under a 100 \times oil immersion objective.

Scanning electron microscope (SEM) was also used to examine the effect of the peptides on the morphology of *E. coli* cells. After the 3 h incubation period (as described above), the cells were collected by centrifugation at 1000 $\times g$ for 2 min, then washed twice by 0.1 M PBS (pH 7.4) and resuspended in 50 μL PBS. 20 μL aliquots of the cell suspensions were spotted onto clean glass slides and air-dried. The slides

were fixed in 2.5% glutaraldehyde in PBS for 2 h in a humid chamber (a Petri dish containing a filter paper soaked in sterile water), then washed with 0.1 M PBS for 10 min and dehydrated in an ethanol gradient (50%, 60%, 70%, 80%, 90% and 100%) (Chen et al. 2008). The slides were freeze-dried overnight and coated in a Dynavac CS300 unit with carbon and gold, followed by attachment of double-sided conducting carbon tape to the slide for better conductivity (Alfred et al. 2013b). The samples were observed using a ZEISS supra 10 VP field emission SEM (Carl Zeiss, NY, USA).

Methods specific to Chapter 4: Potential applications of PIN-based peptides: Sporicidal and anti-biofilm activities

2.10 Time-kill assay

Time-kill assays were performed as described in Liu et al. (2011). Bacterial suspensions of *Listeria monocytogenes* (ATCC 13932, stereotype 4B), *Listeria innocua* (LI-451713/5), *Bacillus subtilis* (ATCC 6051), *Pseudomonas aeruginosa* (ATCC 9027), and methicillin-resistant *Staphylococcus aureus* (MRSA) isolates M173525 and M180920 were prepared as described in Section 2.3.3. 75 μL aliquots of the bacterial suspension containing 1×10^6 CFU mL^{-1} were mixed with 25 μL of peptides to give a final concentration of $1 \times \text{MIC}$ (as determined in Section 2.3.3). The mixtures were incubated at 37 °C for 0, 1, 2, 3, 4, 5, 6, 8 and 24 h. Samples of 10 μL were withdrawn at these time intervals, centrifuged, and the cell pellet washed with sterile MilliQ water to remove any peptide residues. After that, the cell pellets were resuspended in 10 μL sterile MilliQ water, serially diluted and plated on Mueller-Hinton agar. The colony forming units (CFU) were counted after overnight incubation at 37 °C. Survival at each time point is given as the average number of CFU/mL of two independent experiments.

2.11 Membrane permeability assay

The LIVE/DEAD[®] BacLight[™] Bacterial Viability Kit and confocal laser-scanning microscopy were used to test the membrane permeabilisation activity of the peptides on bacterial cells as per Inácio et al. (2016) with some modifications. Briefly, cultures of *Listeria monocytogenes* (ATCC 13932, stereotype 4B), *Pseudomonas aeruginosa* (ATCC 9027) and methicillin-resistant *Staphylococcus aureus* (MRSA) M173525

isolate were cultivated overnight at 37°C in Mueller-Hinton Broth (MHB; Oxoid). The next day, the cells were adjusted to 1×10^8 CFU mL⁻¹ as described above (Section 2.3.3) and then collected by centrifugation and resuspended in PBS (pH 7.4). These cell cultures were incubated with PuroA peptide (at $1 \times$ MIC and $2 \times$ MIC as determined in Section 2.3.3) at 37 °C for 1 h. Subsequently, the cell were treated with the LIVE/DEAD® *BacLight*™ Bacterial Viability Kit (Molecular Probes®, USA), following the manufacturer's instructions. The samples were examined with a 100× oil immersion objective on an inverted confocal microscope (FluoView FV1000; Olympus, AU). For detection of SYTO 9 (green channel) and PI (red channel), excitation wavelengths of 488 and 568 nm were used, respectively. Images at both excitation wavelengths were captured and processed using Olympus FV10-ASW 1.7 software.

2.12 Visualizing the effect of peptides on the morphology of the planktonic cell of MRSA using SEM

SEM was used to examine the effect of peptides on the morphology of the planktonic cells of MRSA as described in (Lim et al. 2013). Cultures of MRSA M173525 were cultivated overnight at 37°C in MHB (Oxoid) with shaking (220 rpm), then the cell suspension was adjusted to 1×10^8 CFU mL⁻¹. 75 µL aliquots of the cell suspension were incubated with 25 µL aliquots of PuroA, P1, W7 and WW peptides (to final concentrations of $1 \times$ MIC, as determined in Section 2.3.3). The mixtures were incubated for 3 h at 37°C and then, the cells were collected by centrifugation at $1000 \times g$ for 2 min. The cells were then washed twice by 0.1 M PBS (pH 7.4), and resuspended in 50 µL PBS. 20 µL aliquots of the cell suspensions were spotted onto clean glass slides and air-dried. After that, the cells were treated and observed using SEM as described above in Section 2.9.

2.13 Inhibitory activity of peptides on biofilm formation

2.13.1 Preparation of bacterial cultures

Prior to use, stored bacteria at -80°C were thawed and *P. aeruginosa* (ATCC 9027) and MRSA M173525 isolate subcultured twice on Mueller–Hinton agar (MHA; Oxoid), whereas *L. innocua* (LI-451713/5) and *L. monocytogenes* (ATCC 13932, stereotype 4B) subcultured twice on Brain Heart Infusion (BHI, Oxoid) agar. Prior to each experiment, *P. aeruginosa*, *L. innocua* and *L. monocytogenes* were inoculated in 5 mL MHB (Oxoid), and MRSA isolate were inoculated in 5 mL Tryptic Soy broth medium (TSB; Acumedia) supplemented with 1% glucose and all bacteria incubated for 24 h at 37°C with shaking (220 rpm). After incubation, *P. aeruginosa*, *L. innocua* and *L. monocytogenes* were diluted in fresh MHB and MRSA in TSB-glucose supplemented with 1% glucose to 1×10^6 CFU mL^{-1} and these cultures were used in the experiments below.

2.13.2 Inhibition of initial cell attachment

The effect of peptides on biofilm formation was determined as described by Jadhav et al. (2013). 100 μL of peptide solutions, corresponding to $0.5 \times \text{MIC}$, $1 \times \text{MIC}$ and $2 \times \text{MIC}$ (as determined in Section 2.3.3), were added to individual wells of a sterile, flat-bottomed, polypropylene 96-well microtitre plates (Corning, USA). 100 μL of sterile MilliQ water was added as a negative control and 100 μL tetracycline (Sigma, USA) at $1 \times \text{MIC}$ ($3 \mu\text{g mL}^{-1}$ for *P. aeruginosa*, $2 \mu\text{g mL}^{-1}$ for *L. monocytogenes* and $64 \mu\text{g mL}^{-1}$ for *L. innocua*) was added as a positive control. 100 μL of bacteria suspensions (prepared as described above in section 2.13.1) were then added to the wells to make a final volume of 200 μL in each well. The plates were incubated at 37°C for 24 h to allow cell attachment. Biofilm formation was assessed using the crystal violet (CV) and the metabolic activity (MTT) assays (as described below). All the tests were carried out in triplicates in three independent experiments.

2.13.3 Inhibition of preformed biofilm

The effect of peptides on 6 h preformed biofilm was determined as described by Jadhav et al. (2013). Biofilms were allowed to form for 6 h before addition of peptides. Biofilm formation was achieved by adding 100 μL of inoculum (prepared as described above in section 2.14.1) into sterile, flat-bottomed, polypropylene 96-well microtitre

plates (Corning, USA). The plates were incubated for 6 h at 37°C to allow cell attachment and biofilm formation before addition of peptides. Following incubation, 100 µL of each peptide (at 0.5 × MIC, 1 × MIC and 2 × MIC, as determined in Section 2.3.3) were added to each well to a final volume of 200 µL. The same volumes of sterile MilliQ water or tetracycline (Sigma, USA) at 1 × MIC (3 µg mL⁻¹ for *P. aeruginosa*, 2 µg mL⁻¹ for *L. monocytogenes* and 64 µg mL⁻¹ for *L. innocua*) were added as a negative control and positive control, respectively. The plates were incubated for 1 h and 20 h at 37°C. Biofilm formation was assessed using the crystal violet (CV) assay and the metabolic activity (MTT) assay (as described below). All the tests were carried out in triplicates in three independent experiments.

2.13.4 Biofilm biomass assay (Crystal violet assay)

The crystal violet (CV) assay works as an indicator of attached biomass in a biofilm; however, it does not represent the metabolic status of the cells, as it stains both attached viable and non-viable cells (Kouidhi et al. 2010). Indirect assessment of cell attachment of *P. aeruginosa*, *L. monocytogenes*, *L. innocua* and MRSA was estimated using the modified CV assay (Djordjevic et al. 2002). After incubation for 24 h (initial cell attachment, Section 2.13.2) and for 1 h and 20 h (preformed biofilm, Section 2.13.3), the culture medium from each well was gently removed and any non-adherent bacteria removed by washing the plates five times with sterile MilliQ water. The plates were air-dried under sterile conditions and then oven-dried at 60°C for 1 h. The biofilm cells were stained with 100 µL of 1% CV (Sigma-Aldrich, UK), prepared in sterile MilliQ water, and incubated for 15 min at room temperature. Excess un-bound stain was then removed by washing the plates three times with sterile MilliQ water. 125 µL of 95% ethanol were then added to each well to destain the attached cells. 100 µL of destaining solution from each well were then transferred to a new plate, and the absorbance measured at 595 nm using a microplate reader (POLARstar Omega, Germany). The absorbance was used to determine the percentage inhibition of biomass formation for each concentration of the peptides using the following formula (Stepanović et al. 2007):

$$\left[\frac{(\text{OD}_{595} \text{ control well without peptide} - \text{OD}_{595} \text{ well with peptide})}{\text{OD}_{595} \text{ control well without peptide}} \right] \times 100.$$

2.13.5 Biofilm metabolic activity assay (MTT assay)

3-[4,5-dimethylthiazol-2-yl]-2, 5-diphenyltetrazolium bromide (MTT) is a salt which is reduced to a purple product in metabolically active cells. Hence the product works as a respiratory indicator of live cells only, and can be measured calorimetrically (Krom et al. 2007). The metabolic activity of biofilms was assessed using a modified MTT reduction assay as described by Schillaci et al. (2008). Briefly, the MTT salt (Sigma, USA) was dissolved in PBS (pH 7.4) to give a final concentration of 5 mg mL⁻¹. For the plates containing cells incubated with peptide, following the incubation periods at 24 h (initial cell attachment, Section 2.14.2) or 1 h and 20 h (preformed biofilm, Section 2.14.3), the culture medium was gently removed and the plates air-dried. 100 µL of PBS (pH 7.4) and 5 µL of MTT solution (5 mg mL⁻¹) were added into each well and incubated for 3 h at 37°C. The insoluble purple formazan (obtained by hydrolysis of MTT by the dehydrogenase enzyme in living biofilm-forming cells) was further dissolved in dimethyl sulphoxide (DMSO). The absorbance was then measured at 570 nm using a microplate reader (POLARstar Omega, Germany). Comparing the OD of the control wells without peptide with the OD of sample wells with peptides, the inhibition percentages for each concentration of the peptide were calculated by the following equation (Schillaci et al. 2008):

$$\left[\frac{(\text{OD}_{570} \text{ control well without peptide} - \text{OD}_{570} \text{ well with peptide})}{\text{OD}_{570} \text{ control well without peptide}} \right] \times 100.$$

2.13.6 Biofilm susceptibility testing by static chamber assay and confocal microscopy

PuroA showed the highest inhibitory activity among the tested peptides on *P. aeruginosa* and *L. monocytogenes* (as determined in Section 2.13.3), therefore its activity was visualised using confocal microscopy. To observe the anti-biofilm activity of PuroA on 6 h preformed biofilms, cultures of *P. aeruginosa* and *L. monocytogenes* were grown on coverglass cell culture chambers (Nunc™ Lab-Tek™ II, Thermo Scientific, USA) as described in Schillaci et al. (2008), with some modifications. Briefly, 500 µL of *P. aeruginosa* or *L. monocytogenes* cultures (prepared as described in Section 2.13.1) were inoculated into the wells of the chambers and incubated at 37°C for 6 h to allow the biofilm to establish. After

incubation, the chambers were washed gently with PBS (pH 7.4) to remove any non-adherent cells and 500 μ L of PuroA was added to the remaining biofilms at $1\times$ MIC and $2\times$ MIC (As determined in Section 2.3.3). The same volume of sterile MilliQ water was added as negative control. All chambers were incubated at 37 °C for 24 h, then washed gently with PBS and the attached biofilms stained with SYTO9 (green fluorescent stain for living cells) and propidium iodide (PI) (red fluorescent stain for dead cells) (Molecular Probes[®], USA) for 15 min.

PuroA and its derivatives, P1, W7 and WW, showed similar inhibitory activity on initial adhesion and biofilm formation of MRSA isolate M173525 as determined in Section 2.13.2. Therefore, one peptide, P1, was chosen to visualize this activity using confocal microscopy, as described in Anunthawan et al. (2015) with some modifications. Briefly, an aliquot of 500 μ L of the peptide was added to coverglass cell culture chambers (Nunc[™] Lab-Tek[™] II, Thermo Scientific). After, 500 μ L of MRSA M173525 culture (prepared as described in Section 2.14.1) was added to the same well. For negative control, 500 μ L of sterile MilliQ water was used instead of peptide. The chambers were incubated at 37 °C for 24 h. After incubation, they were washed gently with PBS and the remaining biofilms stained with SYTO9 and (PI) (Molecular Probes[®], USA) for 15 min.

All chambers were observed under a $100\times$ oil immersion objective on an inverted confocal microscope (FluoView FV1000; Olympus, AU) and excitation wavelengths of 488 and 568 nm used to detect SYTO 9 and PI, respectively. Images at both excitation wavelengths were captured and processed using Olympus FV10-ASW 1.7 software.

2.13.7 Visualizing the activity of P1 on initial adhesion and biofilm formation of a clinical MRSA isolate using SEM

SEM was used to closely visualize the effect of P1 peptide on the initial adhesion and biofilm formation of the clinical MRSA isolate M173525. An aliquot of 100 μ L of P1 peptide was added to glass slide in a humid chamber (a Petri dish containing a filter paper soaked in sterile water) and then, 100 μ L of overnight cultures of MRSA cells (prepared as described in Section 2.13.1) were added on top of peptide solution. For

negative control, 100 μ L of sterile MilliQ water was used instead of peptide. The humid chambers were incubated at 37°C for 24 h under sterile conditions. After incubation, the slides were gently washed with PBS (pH 7.4) to remove any non-adherent bacteria and the still-attached biofilms were fixed in 2.5% glutaraldehyde for 2 h. The slides then washed with 0.1 M PBS for 10 min and dehydrated in an ethanol gradient (50%, 60%, 70%, 80%, 90% and 100%). After that, the slides were treated and observed by SEM as described above in Section 2.9.

2.13.8 Inhibition of initial cell attachment on high density polyethylene surfaces (HDPE)

To test the biofilm inhibitory effects of Pina-M on initial cell attachment of *P. aeruginosa* and *L. monocytogenes* on an additional surface, coupons of high density polyethylene (HDPE) (20 \times 20 \times 1 mm) were used, as per Jadhav et al. (2013). The coupons were cleaned with a detergent, washed with sterile MilliQ water, then decontaminated with 70% ethanol and air dried for 1 h. The coupons were placed in petri plates and 1 mL of Pina-M peptide was placed on the coupons. Then, the same volume of *P. aeruginosa* or *L. monocytogenes* cultures (prepared as above in Section 2.13.1) were added to make a final peptide concentration of 1 \times MIC (as determined in Section 2.3.3). The coupons were incubated at 37 °C for 24 h to allow cell attachment. After incubation, the coupons were washed with sterile MilliQ water to remove any loosely attached cells, then immersed in 10 mL PBS (pH 7.4) and kept on a mechanical shaker for 5 min to remove the attached cells. After that, the cell suspensions were serially diluted and plated on Mueller-Hinton agar. The colony forming units (CFU) were counted after overnight incubation at 37 °C. A similar treatment was given to the negative control coupons (without peptides). The test was performed in triplicates in two independent experiments.

2.14 Sporicidal activity of peptides

2.14.1 Preparation of spore suspension

Spore suspensions of *B. subtilis* (ATCC 6051) were prepared based on Lawrence et al. (2009). Bacteria were grown on nutrient agar (NA) plates for 1 week to induce sporulation. The spores were washed from the plates using 2 mL sterile MilliQ water, which was then centrifuged at $4,500 \times g$ for 10 min. The spore pellet was washed twice with sterile MilliQ water to remove debris. The pellet was resuspended in 2 mL of sterile MilliQ water, heated for 20 min at 80°C to kill any vegetative cells, and the spore suspensions were stored at 4°C . Presence of spores was examined using a light microscope after spore staining. The spores were serially diluted and plated on NA to determine the number of viable spores.

2.14.2 Sporicidal activity assay

The sporicidal activity of TRPs based on PINA (PuroA and Pina-M) and HINA (Hina), as well as PuroA analogs (P1, W7 and WW) and indolicidin was tested as per Lawrence and Palombo (2009) with some modifications. In brief, 5 μL of spore suspension containing about 2×10^{11} CFU mL^{-1} (prepared as described in Section 2.14.1) were added to 50 μL of peptides to different final concentrations (500 $\mu\text{g mL}^{-1}$, 250 $\mu\text{g mL}^{-1}$, 125 $\mu\text{g mL}^{-1}$, 64 $\mu\text{g mL}^{-1}$, 32 $\mu\text{g mL}^{-1}$ and 16 $\mu\text{g mL}^{-1}$). Spore suspension with sterile MilliQ water was used as a negative control. In order to study the effect of the incubation time on the sporicidal activity of the peptides, the mixture was incubated for one day at 37°C , or at room temperature for one week. After incubation, to avoid the effects of remaining peptides on the growth of vegetative cells, spores were recovered by centrifugation at $4,500 \times g$ for 5 min, then washed with sterile 0.85% saline three times and resuspended in 1 mL of 0.85% saline. The spores were serially diluted and plated on NA to determine the number of colony-forming units.

2.14.3 Visualizing the effect of peptides on the morphology of spores of *B. subtilis* using SEM

SEM was used to examine the effect of peptides on the morphology of spores of *B. subtilis*. 5 μL of the spore suspension (prepared as described above in Section 2.14.1) were mixed with 50 μL of the peptides PuroA, P1, PuroB and Hina at a concentration of 250 $\mu\text{g mL}^{-1}$ and incubated at room temperature for one day and one week. 10 μL

aliquots of the spore suspensions were spotted onto clean glass slides and air-dried. After that, the samples were treated and observed by SEM as described above (Section 2.9).

2.14.4 Effect of peptides on the outgrowth of *B. subtilis* spores

The effect of peptides on the outgrowth of *B. subtilis* spores was observed using differential interference contrast (DIC) microscopy (Gut et al. 2008). Aliquots of 5 μL of viable spore suspension containing approximately 2×10^{11} CFU mL^{-1} (prepared as given in Section 2.14.1) were added 100 μL of Mueller–Hinton broth (MHB; Oxoid) supplemented with the peptides PuroA, P1, Pina-M and Hina to different final concentrations (500 $\mu\text{g mL}^{-1}$, 250 $\mu\text{g mL}^{-1}$, 125 $\mu\text{g mL}^{-1}$, 64 $\mu\text{g mL}^{-1}$, 32 $\mu\text{g mL}^{-1}$ and 16 $\mu\text{g mL}^{-1}$). The mixtures of spores and peptides were incubated at 37°C to allow the spores to germinate for 24 h. Negative controls containing spores alone in MHB without peptides were used. After 24 h, samples were mounted on glass slides in 20% glycerol and DIC microscopy images were acquired with an inverted confocal microscope (FluoView FV1000; Olympus, AU), using a 100 X oil immersion objective. All images were acquired and analysed with Olympus FV10-ASW 1.7 software.

2.14.5 Effect of peptides on the membrane integrity of *B. subtilis* spores

LIVE/DEAD[®] BacLight[™] Bacterial Viability Kit and confocal laser-scanning microscope were used to test the membrane permeabilisation activity of the peptides on *B. subtilis* spores (Young & Setlow 2003). 10 μL of spore suspension having about 2×10^{11} CFU mL^{-1} (prepared as described in Section 2.15.1) were added to 100 μL of PuroA and its derivatives (P1, W7 and WW) to different final concentrations (500 $\mu\text{g mL}^{-1}$, 250 $\mu\text{g mL}^{-1}$, 125 $\mu\text{g mL}^{-1}$, 64 $\mu\text{g mL}^{-1}$, 32 $\mu\text{g mL}^{-1}$ and 16 $\mu\text{g mL}^{-1}$) and incubated for 24 h at 37°C. The spores were treated with the LIVE/DEAD[®] BacLight[™] Bacterial Viability Kit (Molecular Probes[®], USA), following the manufacturer's instructions. The samples were examined using confocal microscope as described in Section 2.11.

Methods specific to Chapter 5: Mechanism of action of the PuroA peptide

2.15 SEM visualization of the effect of PuroA on the morphology of *C. albicans* cells

SEM was used to examine the effect of PuroA on the morphology of vegetative *C. albicans* cells as described in Chen et al. (2008). Cultures of *C. albicans* were cultivated overnight at 30°C in Potato Dextrose Broth (PDB; Difco), and then made to 1.5×10^7 cells/mL. 75 μ L aliquots of the cell suspension was incubated with 25 μ L aliquots of PuroA peptide (to a final peptide concentration of 64 μ g/mL, 125 μ g/mL and 250 μ g/mL). The mixtures were incubated for 1 h at 30°C, the cells collected by centrifugation at $1000 \times g$ for 5 min, then washed twice by 0.1 M PBS (pH 7.4), and resuspended in 100 μ L MilliQ water. 30 μ L aliquots of the above cell suspensions were spotted onto clean glass slides and air-dried. The cells were then treated and observed as described in Section 2.9.

2.16 Time-kill assay for PuroA and FITC-PuroA on *C. albicans* and *E. coli* cells

This assay was conducted to determine the timescale needed to induce biocidal effects on *C. albicans* and *E. coli* cells by PuroA or FITC-PuroA. For *C. albicans*, a cell suspensions at $0.5-2 \times 10^3$ cell/mL (determined as described in Section 2.3.4) was prepared. 25 μ L aliquots of PuroA or FITC-labelled PuroA (final concentration $1 \times \text{MIC}$ as determined in Section 2.3.4) were incubated with 75 μ L of yeast cell suspension for 0, 10, 20, 30, 40, 50, 60, 120, 180 and 240 min at 30°C. After these time periods, a 10 μ L aliquot was taken and serially diluted with sterile PBS and plated onto potato dextrose agar. After overnight incubation at 30°C, the viable cell numbers were determined. For *E. coli*, a cell suspensions at 1×10^6 CFU/mL (determined as described in Section 2.3.3) were prepared. 25 μ L aliquots of PuroA or FITC-labelled PuroA were incubated with 75 μ L of bacterial cell suspension to give a final concentration of $1 \times \text{MIC}$ (as determined in Section 2.3.3) at 37°C for 0, 1, 2, 3, 4, 5, 6, 8 and 24 h. After these time periods, a 10 μ L aliquot was taken and serially diluted with sterile PBS and plated onto Mueller-Hinton agar. After overnight incubation at 37°C, the viable cell numbers were determined. Survival at each time point is given as the average number of CFU/mL of three independent experiments.

2.17 Cell cycle analysis

Effect of PuroA on cell cycle of *C. albicans* was analysed as described by Li et al. (2016b) with some modification. In brief, *C. albicans* cells (1×10^6 cells, see Section 2.3.4) at log phase cultured in Potato Dextrose Broth (PDB; Difco), were harvested and incubated with 125 $\mu\text{g/mL}$ ($1 \times \text{MIC}$) of PuroA for 25 min only at 30°C. After 25 min incubation, the cells were centrifuged, washed with sterile PBS (pH 7.4) to remove any extracellular peptide residues, as it was found that incubation the cells with the peptide for longer than 25 min, most of the cells were already killed. The cells pellet was resuspended in a fresh PDB medium and incubated for 8 h at 30°C with agitation (200 rpm). After incubation, the cells were collected by centrifugation at $2000 \times g$ for 5 min at 4°C, washed twice with PBS (pH 7.4), resuspended and fixed in 70% ice cold ethanol for 3 h. The fixed cells were then harvested by centrifugation at $2000 \times g$ for 5 min at 4°C and resuspended in 500 μL PBS (pH 7.4) containing 20 μg RNase and allowed to react for 2 h at 37°C, to ensure only DNA, not RNA, will be stained. Subsequently, for DNA staining, 500 μL of propidium iodide (PI) were added to the suspension to make a final concentration of 50 $\mu\text{g/mL}$ and the samples were incubated for 1 h at 4°C in the dark. Cell cycle analysis was performed using Attune NxT Flow Cytometer (Invitrogen™; USA), and the results were analyzed using Attune NxT software.

2.18 Cell cultures, chamber and reagents preparation for live cell imaging

An aliquot of 100 μL of *E. coli* suspension (1×10^8 CFU/mL) or *C. albicans* suspension (1×10^6 cells) (prepared as described in Section 2.4.3 and 3.4.4, respectively) was deposited onto a chambered coverglass (Nunc™ Lab-Tek™ II, Thermo Scientific) that was previously coated with 0.01% poly-L-lysine (molecular weight > 150,000) for 20 min. The cells were allowed to adhere to the poly-L-lysine-coated coverglass to a target cell density of roughly 1 cell/60 μm^2 (Sochacki et al. 2011), and then any loosely-adhered cells were gently rinsed away with PBS (pH 7.4) (Gee et al. 2013). FITC-labelled PuroA was added (at $t = 0$) to give a final concentration of 8 $\mu\text{g/mL}$. The peptide was used at this concentration which is below the MIC values that were determined in Section 2.3.3 and 2.3.4 to delay the antimicrobial process and the interaction kinetics, so they could be measured in a timescale of minute. In some two-colour experiments, the nuclei of yeast cells were

stained with SYTO 85 Orange (Molecular Probes[®], USA), following the manufacturer's instructions, prior depositing onto the chamber (Fig. 2.1 A). In other two-colour experiments, to measure the propidium iodide (PI) influx and the membrane permeabilisation time, PI (Sigma, USA) was added with FITC-PuroA solution to give a final concentration of 20 μM and both (peptide and PI) were added to cell suspension at the same time (at $t = 0$) (Fig. 2.1 B).

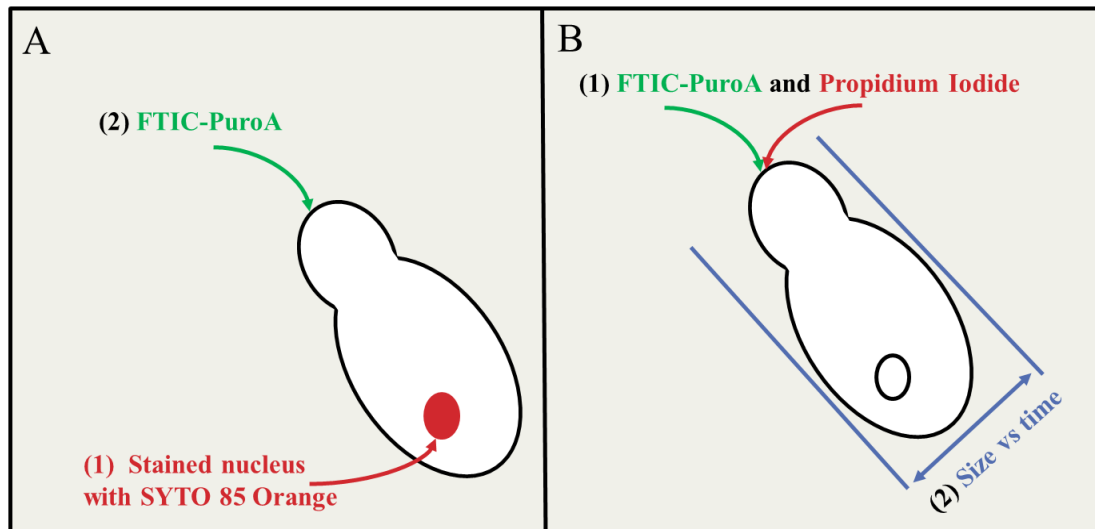


Figure 2.1 Strategies used in two-colour live imaging experiments.

(A) The nuclei of *C. albicans* cells were stained with SYTO 85 Orange before adding FITC-PuroA. (B) FITC-PuroA peptide and propidium iodide (PI) were added at the same time ($t = 0$).

2.19 Confocal laser-scanning microscopy for live cell imaging

To monitor the dynamic sequence of events during attack of a single *C. albicans* cell or *E. coli* cell by FITC-PuroA peptide at 8 $\mu\text{g}/\text{mL}$, a time-lapse confocal microscopy was used. Confocal images were acquired with an inverted confocal microscope (FluoView FV1000; Olympus, AU), using a 100 \times oil immersion objective. A 488-nm Argon laser was used for excitation of FITC-labelled PuroA and a 543-nm helium neon laser was used for excitation of both PI and SYTO 85 Orange. The bandpass emission filters U-MNIBA2 for the 488-nm laser green channel and U-MWIG2 for the 543-nm laser red channel, and no bandpass filter for differential interference contrast (DIC) and all filters were cycled with a BX filter wheel. The imaging sequence cycled among 488 nm fluorescence excitation, 561 nm fluorescence excitation, and DIC with each sequence repeated every 30 s. A 90 min-long movie

was obtained with an Olympus camera. The movie began immediately after adding solution containing FITC-PuroA or FITC-PuroA with PI (20 μ M, included when desired). All images were acquired and analyzed with Olympus FluoViewer software. ImageJ software (version 1.50b) was used for further analyzing the movies from time-lapse imaging and measuring the cell size.

2.20 Fluorescence lifetime imaging microscopy (FLIM)

All FLIM experiments were performed using a LIFA instrument (Lambert Instruments, Leutingwolde, The Netherlands) attached to an inverted microscope (Ti Eclipse, Nikon Inc., Japan). The samples were observed through a 100 \times NA 1.2 oil objective (Nikon Plan-Fluor, Nikon Inc, Japan). The fluorescence excitation source was a 474 nm LED with a sinusoidal modulation frequency of 35 MHz (Lambert Instruments, Leutingwolde, The Netherlands). The emission was passed through an acousto-optic tunable filter (Gooch and Housego) and imaged onto an image intensifier (Lambert Instruments, Leutingwolde, The Netherlands). Phase and modulation lifetimes were determined by taking a series of 12 phase images of differing phase shift (fluorescence lifetime image stack), utilizing the LI-FLIM software package (Version 1.2.3.11) supporting the LIFA instrument. Fluorescence lifetime image stacks were recorded after adding the peptide for up to 4 hours (typically 1-4 minute intervals). In some experiments, propidium iodide (Molecular Probes®, USA) was added to the cells and peptide solution to give a final concentration of 5 μ g/ml. Rhodamine 6G was used as a reference (lifetime R6G: 4.1 ns)(Gee et al. 2013). Fluorescence lifetime image stacks were recorded at 520nm, 580nm and 620nm.

Peptide-nucleic acid interactions in the nucleus of intact single yeast cells were measured by the quenching of the fluorescein lifetime from the FITC-PuroA peptide via fluorescence resonance energy transfer to a nucleic-acid bound SYTO 85 Orange acceptor. The lifetime of the FITC-PuroA fluorescence bound to the nucleus was measured and then compared to the lifetime of the FITC-PuroA bound to the nucleus of a cell counter-stained with SYTO 85 Orange.

Peptide-nucleic acid interactions in the cytosol of membrane-compromised single yeast cells were measured by quenching of the FITC-PuroA peptide lifetime upon addition of propidium iodide (PI). The lifetime of the FITC-PuroA peptide was measured without PI and then measured after addition of PI.

Peptide-peptide interactions were measured through lifetime self-quenching of the fluorescein dye on FITC-PuroA.

The FLIM data were converted to phasor space, where $x = m\cos Q$ and $y = m\sin Q$, where m is the modulation and Q is the phase (Clayton et al. 2004; Redford & Clegg 2005; Digman et al. 2008). Then the fluorescence was decomposed into fractional states, the fractional fluorescence from free peptide and peptide pore states (aggregate) were calculated. For a given phasor, $r(x,y)$, the fractional fluorescence from the peptide pore state, f_{pore} , is given by:

$$f_{pore} = \frac{r(x,y) - r(x,y)_{free}}{r(x,y)_{pore} - r(x,y)_{free}}$$

The fraction of peptides in non-pore states is given by

$$f_{free} = 1 - f_{pore}$$

And the ratio of peptide concentration in the free and pore states is given by

$$\frac{C_{pore}}{C_{free}} = \frac{f_{pore}}{f_{free}} \frac{\tau_{free}}{\tau_{pore}}$$

Methods specific to Chapter 6: Experimental evolution of resistance to selected Trp-rich peptides (TRPs)

2.21 Resistance selection (Serial transfer experiments)

The experimental evolution assay was carried out as per Habets and Brockhurst (2012). All bacterial experiments were performed in Mueller–Hinton broth (MHB; Oxoid) and incubated at 37°C with continuous shaking (220 rpm). Yeast experiments were performed in Potato Dextrose Broth (PDB) incubated overnight at 30°C with shaking (200 rpm). *Escherichia coli* (ATCC 25922) and *Staphylococcus aureus* (ATCC 25923) and *Staphylococcus epidermidis* (ATCC14990) were streaked on Mueller–Hinton agar. *Candida albicans* (FRR 5580) was streaked on Potato Dextrose Agar (PDA; Difco) to randomly isolate six independent colonies that were stored in 25% (v/v) glycerol at -80°C and were used to establish clonal lineages of isogenic strains. Eight 2 ml cultures were founded with approximately 1×10^6 CFU/mL of bacteria and $0.5\text{--}2 \times 10^3$ CFU/mL yeast isogenic cells of an overnight culture were propagated by serial transfer. Six replicate populations were supplemented with increasing concentrations of the peptide PuroA, P1, W7 and indolicidin, and two controls were propagated in the absence of the peptides. From a starting concentration of $0.5 \times \text{MIC}$ (as determined in Sections 2.3.3 and 2.3.4), every 24 h, 1% (20 μL) of each culture transferred to two tubes containing fresh medium to give a dilution of 100 (or allow approximately 6–7 doublings per growth cycle) with either the same concentration of peptide as used previously, or a twofold increased concentration. When growth was observed in the higher concentration, this culture was used for subsequent inoculation. After transfer, 25% glycerol was added to the cultures and stored in -80 °C. This procedure was repeated until populations grew in 1000 $\mu\text{g}/\text{mL}$ of peptide (Fig.2.2). Minimal inhibitory concentrations for ancestral (before selection) and evolved bacteria (after selection) were determined by microtitre broth dilution method as described in Sections 2.3.3 and 2.3.4.

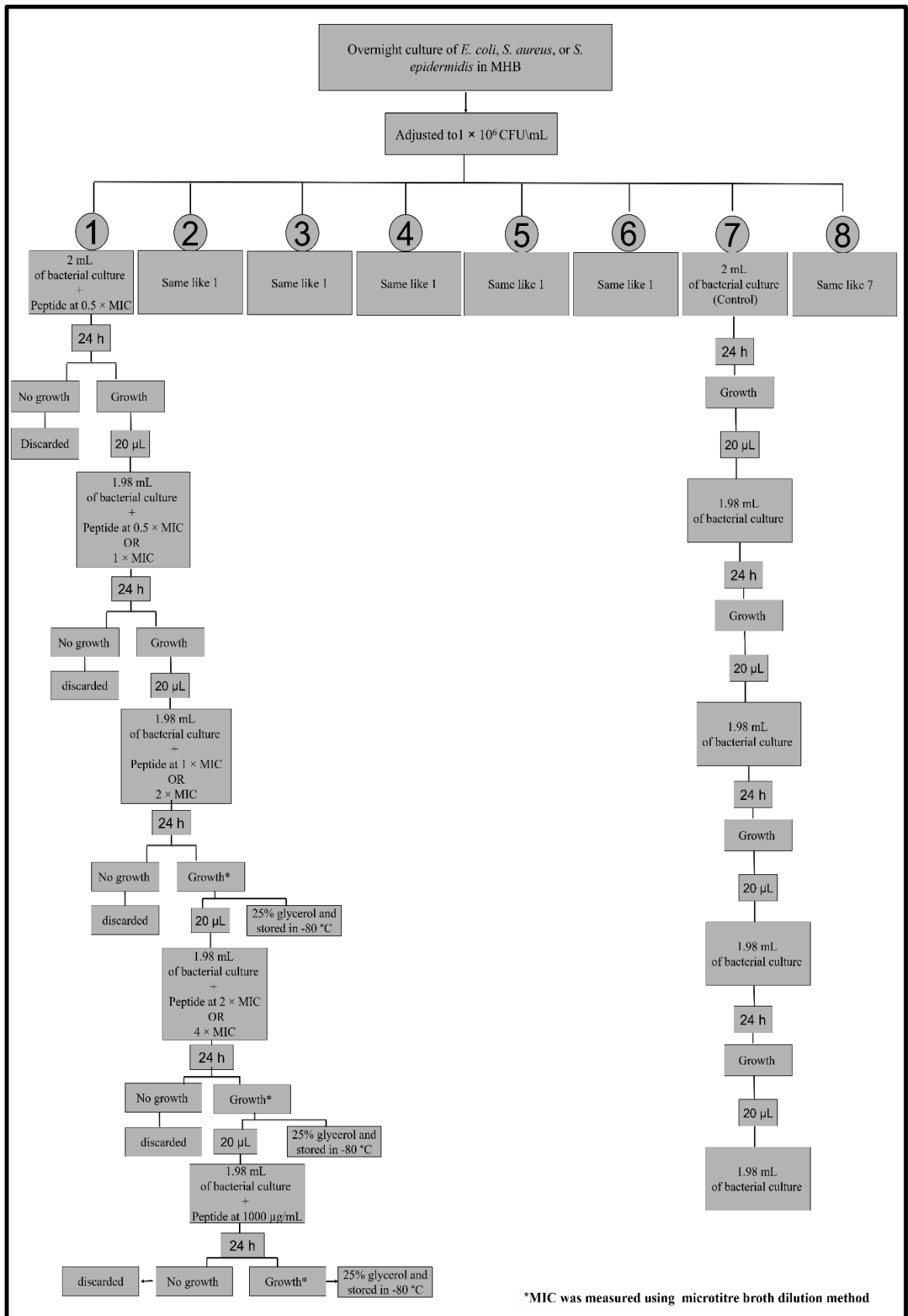


Figure 2.2 Strategy used resistance selection experiments.

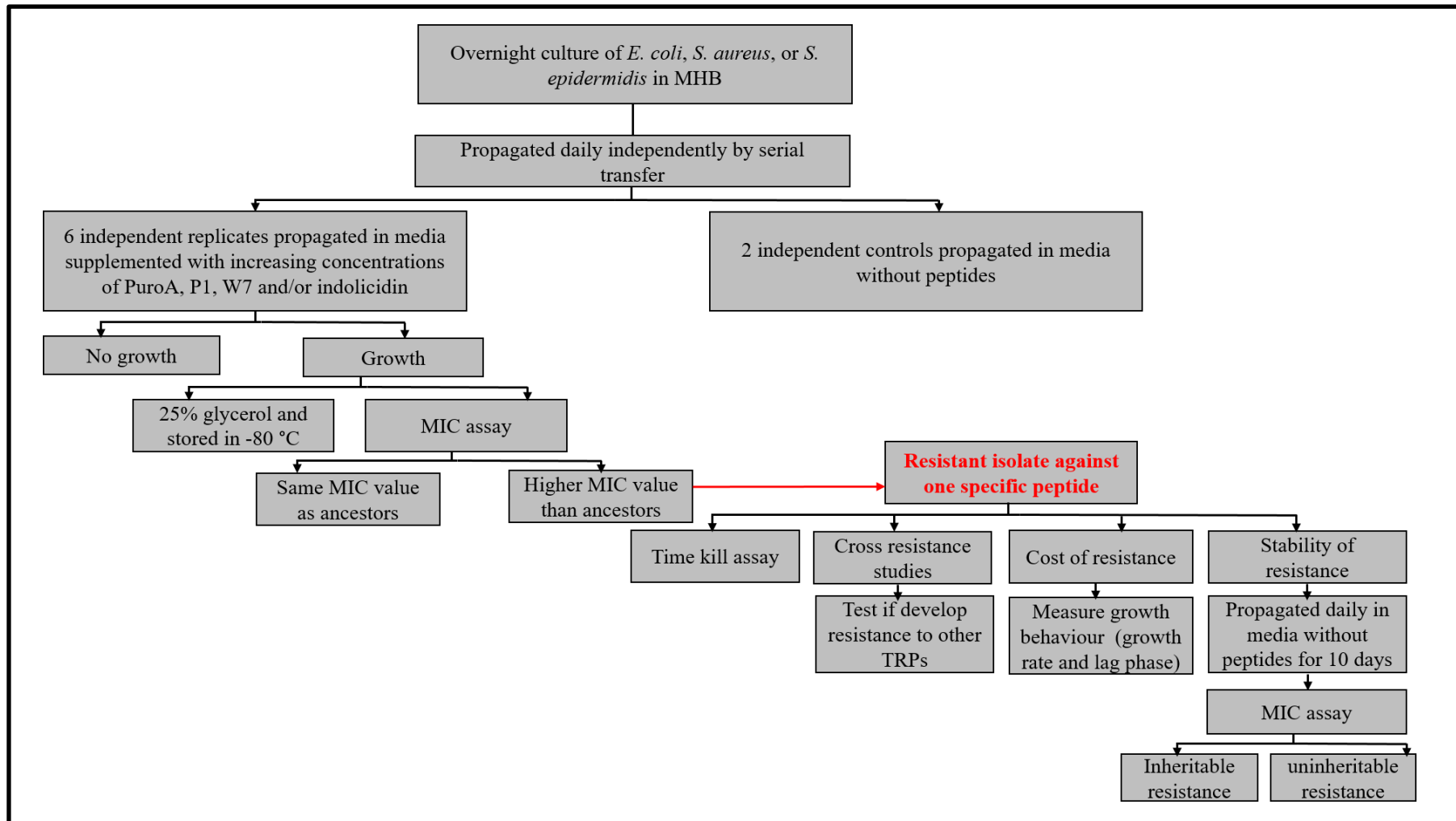


Figure 2.3 Strategies used in studying revolution of resistance to TRPs and characterization of resistance isolates.

2.22 Time-kill assay for resistant isolates

Bacterial suspensions of the wild type *S. aureus* (ATCC 25923) and *E. coli* (ATCC 25922) and the evolved isolates (isolated as above, Section 2.21), PuroA resistant *S. aureus*, indolicidin resistant *S. aureus* and PuroA resistant *E. coli*, were prepared as described in Section 2.3.3. 75 μL aliquots of the bacterial suspensions containing 1×10^6 CFU mL^{-1} incubated with 25 μL of PuroA or indolicidin peptide to give a final concentration of $1 \times \text{MIC}$ (as determined in Sections 2.3.3) at 37°C for 0, 1, 2, 3, 4, 5, 6, 8 and 24 h. Samples were withdrawn at these time intervals, centrifuged, and the cell pellet washed with sterile MilliQ water to remove any peptide residues. After that, the cell pellets were resuspended in 10 μL sterile MilliQ water, serially diluted and plated on Mueller-Hinton agar. The colony forming units (CFU) were counted after overnight incubation at 37°C . Survival at each time point is given as the average number of CFU/mL of two independent experiments.

2.23 Fitness Measurements (cost of resistance)

Development of resistance in bacteria is often associated with a fitness cost that is typically seen as a reduction in bacterial growth rate (Andersson & Hughes 2010). The growth behaviour of bacterial lines were measured as described in Lofton et al. (2013). Bacteria were grown overnight in Mueller–Hinton broth (MHB; Oxoid). The overnight cultures were then diluted to 1×10^6 CFU/mL in MHB. For each strain, 200 μL were added in quadruplicate to the wells of a sterile, round-bottomed polystyrene 96-well microtitre plate (Corning, USA). 200 μL of media were added as a blank in each experiment. Growth of the samples was monitored at 37°C with shaking for 18 h with a microplate reader (POLARstar Omega, Germany). OD_{600} measurements were taken every 5 min. Calculations were based on OD_{600} values between 0.02 and 0.2 (wherein the bacterial growth was exponential). The growth of parental strain and selected resistant isolate were measured in the same experiments and the experiments were performed in three separate times. Relative growth rate was calculated by dividing the generation time of the parental strain by the generation time of the resistant isolate from the same experiment. The generation time (G) was calculated using the following equation:

$$G = \frac{t}{3.3 \log b/B}$$

Where t is the time interval in hours or minutes, B is number of bacteria at the beginning of a time interval and b is number of bacteria at the end of the time interval.

The maximal growth rate (V_{MAX}) during exponential growth was also calculated from log-e transformed optical density values (Habets & Brockhurst 2012).

2.24 Stability of resistance

To test whether the developed resistance has a heritable nature, the frozen stocks of all evolved *S. aureus* and *E. coli* isolates and their ancestral clones were reconditioned from frozen stocks and subcultured on Mueller–Hinton agar (MHA). After growing overnight at 37°C, two independent colonies from each line were used to initiate two replicate populations. Populations were propagated in 10 mL MHB cultures by daily transfer of 1% of each population for 10 transfers in the absence of the peptide (Perron et al. 2006). Minimal inhibitory concentrations (MICs) and the growth rate were estimated for founding ancestral clone and evolved bacteria as described in Section 2.3.3 and 2.23, respectively.

2.25 Quantifying cross-resistance

Cross-resistance is the development of resistance to a substance (such as an antimicrobial agent) as a result of previous exposure and evolve resistance to a similar acting or related substance (Inoue et al. 1978). Evolved *S. aureus* and *E. coli* and their founding ancestral lines were examined for susceptibility to PuroA, P1, W7, Pina-M and indolicidin peptides. Cross-resistance against the TRPs used in this study was determined by measuring Minimum inhibitory concentration (MIC). MIC was measured by microtitre broth dilution methods (see Section 2.3.3). Each measurement was performed in three replicates for each line.

2.26 Checkerboard assay (MIC of combining peptides)

The combination effect of the peptides was determined against the Gram-positive *S. aureus* (ATCC 25923) and the Gram-negative bacteria *E. coli* (ATCC 25922) as per Berditsch et al. (2015). Bacterial suspensions were prepared as described in Section 2.3.3. 25 μ L of the two combined peptides (12.5 μ L each) were mixed with 75 μ L of

bacterial suspension containing 1×10^6 CFU/mL in the well of sterile, flat-bottomed, polypropylene 96-well microtitre plates (Corning, USA). For example, PuroA was 2-fold serially diluted down the columns of the plate from $64 \mu\text{g mL}^{-1}$ to $0.5 \mu\text{g mL}^{-1}$, and W7 was diluted in separate plates and then added to the test plate across the rows. The resulting checkerboard contained each combination of the two peptides in 8 doubly increasing concentrations with wells containing the highest concentration of each peptide at opposite corners (Fig. 2.4). Column with only one peptide and were prepared to confirm the MIC of each antimicrobial alone in the same plate. One column was used as a sterility control (SC, containing sterile MHB only) and one column used as a positive growth control without peptide (growth control, GC). The same set up was repeated for PuroA with Pina-M, P1 or indolicidin. The plates were incubated overnight at 37°C . The MIC is defined as the lowest concentration of peptides that completely inhibits bacterial growth (Wiegand et al. 2008), determined by both visual observation and measuring the absorbance at 595nm using a Microplate reader (POLARstar Omega, Germany). The synergistic interactions were expressed as the fractional inhibitory concentration index (FICI), which is calculated as the sum of MICs of the combination (MICc) divided by the MICs of the peptides alone (MICa) (Loewe 1953; Berditsch et al. 2015), using the following formula following:

$$\text{FICI} = \frac{\text{MICc of peptide 1}}{\text{MICa of peptide 1}} + \frac{\text{MICc of peptide 2}}{\text{MICa of peptide 2}}$$

The mean FICIs and standard deviations were calculated from the results from three experiments performed with each bacterial strain. A synergistic effect was defined at an FICI of ≤ 0.5 and a no interaction effect at an FICI between 0.56-1 and antagonistic effect at FICI > 4 (Odds 2003).

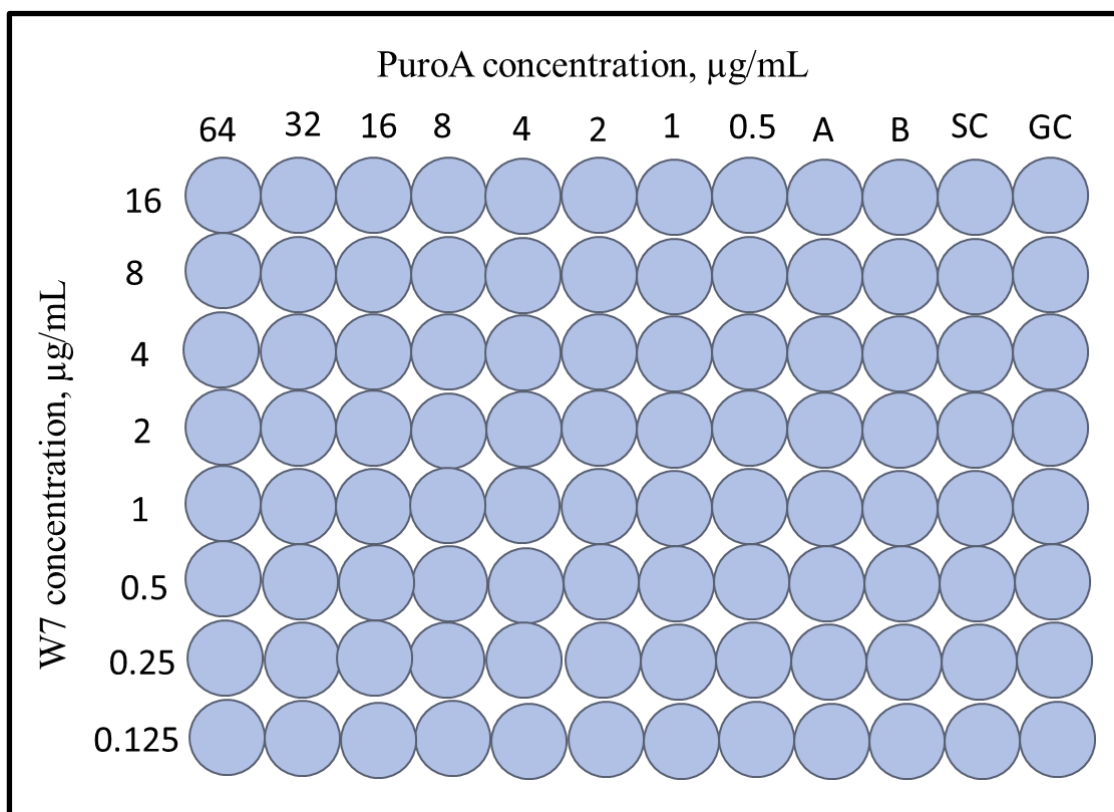


Figure 2.4 Example of checkerboard assay set up in the 96-well microtiter plate of PuroA and W7 combination.

Column A contains PuroA only at MIC against *S. aureus* or *E. coli* and B contains W7 only at MIC against *S. aureus* or *E. coli*. SC = sterility control (containing sterile MHB only) and GC = growth control without peptide.

Methods specific to Chapter 7: Preliminary investigations of cell selectivity and anticancer potential of rationally designed TRPs**2.27 Haemolytic activity assay**

The haemolytic activity of the all peptides was determined as described Dathe et al. (1996) and Phillips et al. (2011). Briefly, sheep red blood cells (RBCs) were collected from commercially obtained whole defibrinated blood (Amyl Media, Australia) by centrifugation at $1200 \times g$ for 10 min at 4°C . The RBCs pelleted were washed three times with PBS (pH 7.4) and resuspended in 2 mL of PBS ($1.9\text{-}2.5 \times 10^9$ cells/mL). The cells were diluted to 10% ($1.9\text{-}2.5 \times 10^8$ cells/mL) in PBS just before performing the assay. 25 μL of the RBC suspension were incubated with different final concentrations of peptides (16 to 500 $\mu\text{g}/\text{mL}$ in PBS) at 37°C for 1h with shaking (160 rpm). After incubation, the samples were centrifuged at $3200 \times g$ for 5 min and the absorbance of the supernatant was measured at 540nm in a UV-VIS Spectrophotometer (Thermo Scientific, USA). PBS (pH 7.4) and 1% Triton X-100 (Sigma, USA) were used as negative control (zero haemolysis) and positive control (100% haemolysis), respectively. Positive haemolytic activity was defined as the peptide concentration that lyses 50% of the RBCs (HD50). The tests were carried out in triplicate in each of two independent experiments. The percentage of haemolysis was determined using the following formula:

$$[(\text{OD}_{540} \text{ peptide} - \text{OD}_{540} \text{ PBS}) / (\text{OD}_{540} \text{ Triton} - \text{OD}_{540} \text{ PBS})] \times 100.$$

2.28 Cytotoxicity against mammalian Cells (cell proliferation and viability assay)**2.28.1 Thawing of cells**

The cryogenic vial containing the frozen cells was placed in a warm water bath at 37°C for < 1 min. The cell freezing medium (Section 2.2.4) usually contain 10% DMSO which is toxic at $\geq 4^{\circ}\text{C}$, thus the thawed cells were immediately diluted with pre-warmed media to 37°C to ensure a high percentage of the cells could survive the stressful thawing procedure. The cell suspension was centrifuged at $1000 \times g$ for 5 min at 4°C to collect the cells. The supernatant was discarded and the cell pellet

resuspended in 5 mL of fresh complete medium. After, the cell suspension was transferred to a disposable 25 cm² culture flasks (Sarstedt, Australia) and incubated in a humidified incubator (Heraeus Hera Cell incubator) at 37°C with 5% CO₂.

2.28.2 Subculturing of cells

The cells were regularly cultivated in disposable 25 cm² culture flasks (Sarstedt Australia) in complete DMEM (see Section 2.2.4). The cells were passaged when they reach 80-90% confluent (checked by light microscope). The culture medium was carefully removed from the culture flasks without disturbing the attached cells using a sterile pipette. The cells were then washed twice with 5 mL of sterile PBS (pH 7.4). 0.5 mL of 0.25% trypsin/ethylene diamine (EDTA) solution (Gibco, UK) were then added to the culture flask and the flask was incubated at 37°C for 3-4 min to allow the cells to detach. After incubation, 3.5 mL of fresh media was added to the culture flasks to resuspend the detached cells and neutralise the action of trypsin. The cell suspension was then removed from the flasks and centrifuged at 1000 × g for 5 min at 4°C. The supernatant was discarded and the cell pellet was resuspended in 5 mL of fresh complete media. Cells were counted using a haemocytometer to appropriately dilute the cell suspension. Cells were usually seeded at a density of 1.5 × 10⁵ cells per 25 cm² culture flasks and incubated at 37°C with 5% CO₂ atmosphere until next passage.

2.28.3 Cryopreservation of cells

To prepare cells for long term storage, a confluent monolayer of cells was detached from the culture flask using 0.25% trypsin/EDTA solution as described in Section 2.28.2. Cells were counted using a haemocytometer. The cell suspension was centrifuged at 1000 × g for 5 min at 4°C. The supernatant was discarded and the cell pellet was resuspended in cell freezing media (see Section 2.2.4). Aliquots of 1 × 10⁶ cells was placed in each cryogenic vial. The vials were placed on ice or in a refrigerator at 4°C till starting the freezing procedures. The cryogenic vials were then gradually frozen, placed first at -20°C for 2 h and then at -80°C for overnight and the next day were finally transferred to liquid nitrogen for long term storage.

2.28.4 Cell viability assay

The cytotoxicity effect of all the designed peptides on the human cervical carcinoma HeLa and the mouse fibroblastic NIH-3T3 cells were determined using the MTT assay, as reported in Scudiero et al. (1988) with minor modifications. As mentioned above, the cells were maintained in DMEM (Gibco, UK) with 10% Fetal Bovine Serum (FBS, Gibco, UK) in a humidified incubator (Heraeus Hera Cell incubator) at 37°C with 5% CO₂. The cells were seeded in sterile 96-well microtiter plates (Nunc™, USA) at a density of 1×10^4 cells/well and allowed to adhere for 24 h at 37°C with a 5% CO₂ atmosphere. The media were then gently removed and the adherent cells washed with PBS (pH 7.4). Fresh complete media containing serially diluted peptides (final concentration 4 to 250 µg/mL), were added to the cells and they were further incubated at the same conditions for 24 h. Wells having cells and complete media without peptides were used as negative controls. After incubation, the medium with the peptides was removed and the adherent cells were washed with PBS. Subsequently, 150 µL of 3-(4,5-dimethylthiazol-2-yl) -3,5-diphenyl tetrazolium bromide (MTT; Sigma-Aldrich) diluted to final concentration 0.33 mg/mL in DMEM, was added to each well and the plates incubated for a further 3 h at 37°C. The precipitated MTT formazan was dissolved using Dimethyl sulfoxide (DMSO). The absorbance at 570 nm was measured using a POLARstar microplate reader (Omega, BMG LabTech). Cell viability was determined relative to the untreated control using the following formula:

$$[\text{OD}_{570} \text{ peptide treated cells} / (\text{OD}_{570} \text{ untreated cells})] \times 100.$$

All the tests were carried out in triplicate in each of three independent experiments. Positive cytotoxic activity was defined as the peptide concentration that causes 50% growth inhibition in each cell lines (IC₅₀).

2.29 Visualizing the effect of peptides on the morphology of HeLa cells using scanning electron microscopy (SEM)

SEM was used to examine the effect of peptides on the morphology of HeLa cells. HeLa cells were seeded on a sterile glass coverslip at a density of 2×10^4 cells inside

a sterile 6-well microtiter plates (Nunc™, USA) and allowed to adhere for 24 h at 37°C with a 5% CO₂ atmosphere under sterile conditions. The cells were then washed with PBS (pH 7.4) and fresh media containing peptides (final concentration 64 and 125 µg/mL), were added and the coverslips were further incubated for 24 h at 37°C with 5% CO₂. Cells without peptides treatment were used as negative control. After incubation, the cells were washed with PBS (pH 7.4) and fixed with 2.5% glutaraldehyde in PBS for 1 h at 4°C. Then samples were then treated and observed by SEM as described above (Section 2.9).

2.30 Statistical analysis

All experiments were performed at least in triplicates and the data obtained were presented as mean values. Data of inhibitory activity of the peptides on biofilm formation was shown to be non-normally distributed using the Kolmogorov and Smirnov test, therefore the non-parametric Kruskal–Wallis test with a Dunn’s post hoc test were used to identify the differences between untreated control and treated samples with peptides. IBM SPSS Statistical version 23 for windows software was used for statistical analysis and differences with *P* values < 0.05 were considered statistically significant.

Chapter 3

Rational design of variant PuroA peptides and assessment of their biochemical properties and bioactivity effects

3.1 Abstract:

Antimicrobial peptides (AMPs) have been featured as promising candidates for the development of alternative antimicrobial agents. AMPs are ideal templates to design novel peptide-based antimicrobial therapeutics. For clinical applications, AMPs must have broad-spectrum activity, selective cytotoxicity toward microbes, and must be protease and salt-tolerant at physiological level. These characteristics can be achieved by rational design of peptides based on variants in their physicochemical characteristics which contribute to their biological activity. A synthetic peptide, PuroA, based on the unique tryptophan-rich domain of a wheat endosperm protein with antimicrobial properties, puroindoline A (PINA), was previously reported to display antibacterial and antifungal activities. In the present work, a number of peptides based on PuroA peptide were designed in order to investigate how the variations in their cationic charge, length, number of Trp residues, amphipathicity and hydrophobicity affected their activity against selected pathogenic bacteria and yeast cells, as well as their salt and protease tolerance. Additional structural modifications including cyclization and dimerization were also investigated. The 14-residue peptide, P1, with the highest amphipathicity, 6 Trp residues and net charge of +7, showed potent antimicrobial activity against the tested bacteria and yeast, and also high salt stability. The short derivatives with 7-8 residues, W7, W8 and WW that were based on the basic amino acids and Trp-rich region in the centre of PuroA peptide, were generally more active compared to the parent PuroA peptide against the tested pathogens and they showed greater salt tolerance properties. All peptide diastereomers with about 35-40% D-amino acids were resistant to proteolytic degradation. The current understanding of AMPs is inadequate to predict the potency and selectivity of novel peptide sequences. Our results improve the understanding of the peptide structure–activity correlations and will, therefore, help in advancing the design of AMPs towards systemic applications.

3.2 Introduction

AMPs are being recognised as the candidates with the most potential to effectively substitute the current antibiotics and control drug-resistance microbes. However, many naturally occurring AMPs are not optimized for efficient *in vivo* applications and require modification to improve their therapeutic potential. Over the past two decades, extensive AMP sequence modification studies have occurred, mainly aimed to enhance AMPs' broad spectrum antimicrobial activity and reduce cytotoxicity (Tossi et al. 2000; Chan et al. 2006; Pasupuleti et al. 2012). Interdependent molecular determinants such as length, charge, secondary structure, hydrophobicity and amphipathicity were found to significantly affect the efficiency, spectrum of activity and cytotoxic selectivity of AMPs (reviewed in Yeaman & Yount 2003; Matsuzaki 2009; Teixeira et al. 2012; Yin et al. 2012; Hollmann et al. 2016) (these crucial factors are extensively discussed in Chapter 1, Section 1.3). Therefore, modifications in these structural parameters have been a useful tool for optimizing the activity and cytotoxicity of AMPs. Besides engineering AMPs with improved antimicrobial properties, it is critical to engineer AMPs for enhanced protease and salt tolerance to increase their robustness especially for *in vivo* applications, as most AMPs are inactivated by enzyme and salt. With only a few studies to draw from, the correlation between peptide structure, biological activity, cytotoxicity, protease sensitivity and salt tolerance behaviour remains poorly understood.

AMPs are diverse and are generally classified into five main subgroups as detailed in Chapter 1, Section 1.2. Some AMPs are rich in specific amino acids, mainly tryptophan (Trp), arginine (Arg) (Chan et al. 2006), proline (Pro) (Agerberth et al. 1991), cysteine (Cys) (Selsted et al. 1985), or glycine (Gly) (Park et al. 2000). Trp-rich peptides (TRPs), such as indolicidin, tritrypticin, lactoferricin, and puroindolines, have been discovered in or are derived from natural origins. TRPs display potent antimicrobial activity against bacteria, fungi and/or viruses, and some are also active against protozoan pathogens and/or cancer cells (extensively reviewed in Chapter 1, Sections 1.4 and 1.6). This potent activity has been credited to the unique biochemical properties of tryptophan that allow the peptide to insert into biological membranes (Fimland et al. 2002; Schibli et al. 2002). The significant role of tryptophan residues in TRPs is detailed in Chapter 1, Section 1.8.

The potent antimicrobial activity of these TRPs prompted the study on the unique Trp-rich domain (TRD) of the wheat grain puroindoline (PIN) proteins (Blochet et al. 1993; Gautier et al. 1994). The biochemical properties and the antimicrobial activity of the PINs and the PIN-based peptides are detailed in Chapter 1, Section 1.6. Interestingly, among all natural TRPs, PINs are the only peptides with sequence variations in the TRD located within naturally mutated PIN proteins. The effects of these mutations on grain texture are well-established (Chapter 1, Section 1.6.1), but their collateral effects on antimicrobial activity is little explored. Our group designed a number of peptides based on the TRD of PINs encoded by wild type and mutant hardness alleles. These synthetic peptides displayed activity against bacteria and phytopathogenic fungi and certain point mutations affected their activity at quantitative and/or qualitative levels (Phillips et al. 2011)(Chapter 1, Section 1.6.6).

The synthetic peptides PuroA (FPVTWRWWKWWKG-NH₂) based on the TRD of the wild-type PINA showed antimicrobial activity against a number of bacteria (Jing et al. 2003; Phillips et al. 2011), phytopathogenic fungi (Phillips et al. 2011) and fungal spores (Alfred et al. 2013a). Therefore, in this work, PuroA was used as a starting template to design 13 peptides with different length, Trp content and charge. Consequently, changing those parameters resulted in change to the hydrophobicity, amphipathicity and the secondary structure of the designed peptides. Additional structural modifications such as incorporation of D-amino acids, head-to-tail cyclization and dimerization were also made. The designed peptides were evaluated for antimicrobial activities, and stability in the presence of proteases and salt. The methods applied are detailed in Sections 2.3 to 2.9. The results are presented below.

3.3 Results

3.3.1. Peptide design and predicted physicochemical parameters

Using the wild-type TRD of PINA, PuroA, as a starting framework, this work aimed to optimize the peptide design for more potent and selective biological activities under physiological conditions. For this purpose, the length, charge and Trp-content of the peptide were systematically changed (Table 3.1), to determine the optimal length, charge and Trp content for improved activities. Additional structural modifications including incorporation of D-amino acids, head-to-tail cyclization and dimerization were also investigated. Those modifications resulted in changes to other properties, including hydrophobicity and amphipathicity.

The theoretical calculated physicochemical properties of the peptides are summarized in Table 3.1. After modifications, the variants ranged from 6 to 27 residues in length, were all cationic, with a net charge of +2 or +8 and they contained 4 to 6 Trp residues. Of these 13 peptides, three peptides were composed of 35-40% D-amino acids. The percentage of hydrophobic residues in the peptides sequences were from 38% to 75%. The peptide hydrophobicity (H) ranged from -0.08 to -0.94 and their hydrophobic moment (μ_H), which represents their amphipathicity (Eisenberg et al. 1982), were between 3.56 to 7.88. The helical wheel (Edmundson wheel) was used to visually represent the amphipathic helix structure of the designed peptides, wherein the amino acids are plotted in a rotating manner with rotation angle between consecutive amino acids of 100° . Thus, the final plot reveals whether hydrophobic amino acids are concentrated on one side and the polar or hydrophilic amino acids are on the other side of the helix (Schiffer & Edmundson 1967). The predicted helical wheel structures of the peptides are shown in Figure 3.1.

Table 3.1 Primary sequence, net charge, molecular weights, isoelectric points, hydrophobicity and Trp content of the designed TRPS.

Peptide ID	Sequences*	Length	Mw	No. of Trp	Charge	pI	ChD	<i>H</i>	HR	GRAVY	μ H
PuroA	FPVTWRWWKWWKG-NH ₂	13	1863	5	+3	11.17	0.23	-0.08	61.5	-0.962	5.21
Cyclic PuroA	FPVTWRWWKWWKG	13	1845	5	+3	11.17	0.23	-0.08	61.5	-0.962	5.21
Di-PuroA	(FPVTWRWWKWWKG) ₂ -NH ₂	27	3836	10	+7	12.04	0.25	-0.11	59	-1.070	3.56
PuroA-OH	FPVTWRWWKWWKG	13	1863	5	+3	11.17	0.23	-0.08	61.5	-0.962	5.21
R8	RRRRWRWWRWRR-NH ₂	13	2198	5	+8	12.85	0.61	-0.94	38	-3.115	5.01
P1	RKRWRRWWKWWKR-NH ₂	14	2144	6	+7	12.48	0.5	-0.58	43	-2.700	7.88
dP1	R <u>R</u> W <u>R</u> W <u>W</u> K <u>W</u> W <u>K</u> R-NH ₂	14	2144	6	+7	12.48	0.5	ND	43	ND	ND
R6	RWWKWW-NH ₂	6	1047	4	+2	11.00	0.33	-0.23	66	-2.000	5.56
R7	RWWKWWK-NH ₂	7	1175	4	+3	11.17	0.42	-0.35	57	-2.271	6.01
W7	WRWWKWW-NH ₂	7	1233	5	+2	11.00	0.28	-0.14	71	-1.843	4.51
dW7	<u>W</u> <u>R</u> <u>W</u> <u>W</u> <u>K</u> WW-NH ₂	7	1233	5	+2	11.00	0.28	ND	71	ND	ND
W8	WRWWKWWK-NH ₂	8	1361	5	+3	11.17	0.37	-0.26	62.5	-2.100	4.71
WW	WWRWWKWW-NH ₂	8	1419	6	+2	11.00	0.25	-0.08	75	-1.725	6.32
dWW	<u>W</u> <u>W</u> <u>R</u> <u>W</u> <u>W</u> <u>K</u> WW-NH ₂	8	1419	6	+2	11.00	0.25	ND	75	ND	ND

*Underlined and bold amino acids are D-enantiomers. The C terminus is amidated except in PuroA-OH peptide. The isoelectric points (pI) of the peptides were predicted using the 'compute pI/MW Tool' at the Expert Protein Analysis System (ExPASy) site (http://au.expasy.org/tools/pi_tool.html). Mean values of hydrophobicity (*H*) were calculated using consensus value of hydrophobicity scale (Eisenberg et al. 1984). Charge density (ChD) was calculated by dividing net charge with the chain length of peptide. Hydrophobic ratio (HR) is the percentage of hydrophobic amino acid (Val, Phe, Thr, Trp) in the peptide chain. GRAVY = the grand average of hydropathy and calculated by dividing the sum of hydropathy values of all amino acids by the peptide length. The hydrophobic moment (μ H) and the helical wheel projection and were calculated online using Helical Wheel Projections (<http://rzlab.ucr.edu/scripts/wheel/wheel.cgi>). ND: not determined.

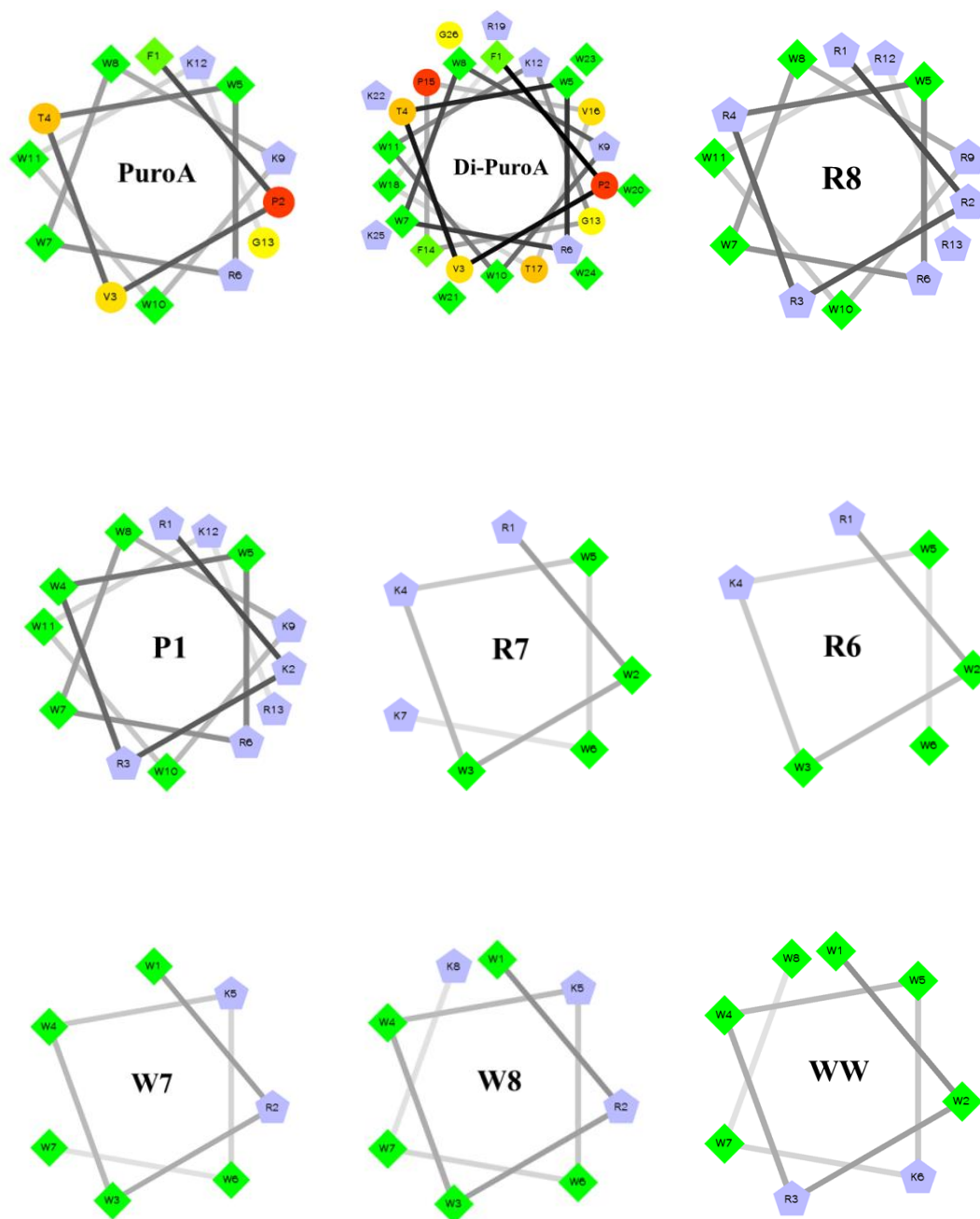


Figure 3.1 Helical wheel projections of the design peptides.

Residues in circles are hydrophilic, in diamonds are hydrophobic and pentagons are potentially positively residues. Hydrophobicity is colour coded: the most hydrophobic residue is green, and the green intensity is proportionally decreasing to the hydrophobicity, and residues with zero hydrophobicity are coded yellow. Hydrophilic residues are coded red; the most hydrophilic (uncharged) residues are pure red, and the red intensity proportionally decreasing to the hydrophilicity. The potentially charged residues are coded light blue.

3.3.2 Antimicrobial activity

The peptides were tested together for antimicrobial activity against *E. coli* (ATCC 25922), *S. aureus* (ATCC 25923), *P. aeruginosa* (ATCC 9027) and *C. albicans* (FRR 5580). The antimicrobial activity was determined using broth dilution minimum inhibitory concentration (MIC) assays in 96-well plates. The MICs were defined as the lowest peptide concentration to completely inhibit growth of the test organism (Wiegand et al. 2008). The results were assessed both by eye and by using a microplate reader to measure the turbidity (OD₅₉₅) of each well (data not shown). The results are summarized in Table 3.2.

Increasing the cationicity and reducing the hydrophobicity by substituting all the non-Trp residues with the cationic amino acid Arg in R8 reduced its antimicrobial activity but to a lesser extent than cyclization and dimerization (activity decreased by 4-fold against *E. coli* and *S. aureus* and 2-fold against *C. albicans*). P1 and dP1 peptides showed 2-fold increased activity against *P. aeruginosa* and one-fold against *C. albicans* while keeping the same activity as PuroA against *E. coli* and *S. aureus*. The effect of C-terminal amidation on the peptides' antimicrobial activity was also investigated. All peptides were amidated, except for PuroA-OH which displayed 2-fold less activity toward all tested organisms compared to its wild-type amidated counterpart.

The backbone cyclized variant (Cyclic PuroA) showed a substantial decrease in antimicrobial activity by at least 8-fold, compared to the wild-type linear peptide. Similarly, dimerization considerably decreased the ability of Di-PuroA to inhibit the growth of tested bacteria, but did not affect its antifungal activity.

Six of the short peptides (R7, W7, dW7, W8, WW, and dWW) were generally more active and displayed MIC values against *E. coli* and *S. aureus* $\leq 8\mu\text{g/mL}$. Among this group, R6 was the least active peptide with 2-fold decreased antibacterial activity against *E. coli*. In addition, the antimicrobial activity of the all L-amino acid peptides was similar to that of their counterpart diastereomers with 35-40% D-amino acids (Table 3.2).

Table 3.2 Antimicrobial activities of peptides

Peptide ID	Sequence*	MIC ($\mu\text{g mL}^{-1}$)			
		<i>E. coli</i>	<i>S. aureus</i>	<i>P. aeruginosa</i>	<i>C. albicans</i>
PuroA	FPVTWRWWKWWKG-NH ₂	16	16	64	125
Cyclic PuroA	FPVTWRWWKWWKG	250	125	>250	>250
Di-PuroA	(FPVTWRWWKWWKG) ₂ k-NH ₂	250	250	>250	125
PuroA-OH	FPVTWRWWKWWKG	32	64	125	250
R8	RRRRWRWWRWRR-NH ₂	64	64	64	250
P1	RKRWWRWWKWWKR-NH ₂	16	16	16	64
dP1	R <u>R</u> W <u>R</u> W <u>W</u> K <u>W</u> W <u>K</u> R-NH ₂	16	16	16	64
R6	RWWKWW-NH ₂	32	16	32	64
R7	RWWKWWK-NH ₂	8	16	32	64
W7	WRWWKWW-NH ₂	4	8	32	64
dW7	<u>W</u> <u>R</u> W <u>W</u> K <u>W</u> W-NH ₂	8	8	16	64
W8	WRWWKWWK-NH ₂	4	8	32	64
WW	WWRWWKWW-NH ₂	8	8	32	64
dWW	W <u>W</u> <u>R</u> W <u>W</u> K <u>W</u> W-NH ₂	8	8	32	64

* Underlined and bold amino acids are D-enantiomers. Results shown are the average of two independent experiments conducted in triplicates.

3.3.3 Antimicrobial activity in the presence of salts

For effective use of AMPs as anti-infective agents in clinical therapy, they need to remain active under the physiological levels of salt. Several AMPs seem to be salt sensitive and lost their antimicrobial activities under physiological salt conditions, such as human β -defensin (hBD-1) (Goldman et al. 1997), gramicidin S and indolicidin (Wu et al. 1999). As NaCl is the predominant salt *in vivo* with concentration of 120–150 mM (Nan & Shin 2011), the MICs of the peptides against *E. coli* and *S. aureus* were determined in the presence of different concentrations of NaCl (50, 100 and 150 mM) (Table 3.3).

When judged in terms of MIC values, PuroA only tolerated 50mM of NaCl and then showed 2-fold and 4-fold increase in the MICs toward both *E. coli* and *S. aureus* in the presence of 100 and 150 mM NaCl, respectively. Cyclic, dimeric and non-amidated forms of PuroA were not resistant to NaCl antagonism even at 50 mM NaCl. On the other hand, peptides P1, dP1 and R8 showed unchanged antibacterial activity at up to a 150 mM NaCl. Among the group of short peptides, only the antibacterial activities of R6 and R7 peptides were affected by the presence of the salt; all other short peptides showed greater salt resistance properties.

3.3.4 Protease stability

The *in vivo* proteolytic degradation of AMPs is one of the main barriers to their use as systematic therapeutics and has limited their clinical applications to topical uses (Hancock & Sahl 2006). To investigate the effects of peptide modifications on proteolytic susceptibility, the peptides were incubated with trypsin or proteinase K proteases for 3 h and then their antibacterial activity was assessed against *E. coli* and *S. aureus* using broth dilution MIC assays. Trypsin cleaves peptides on the C-terminal side of the positively charged lysine and arginine side chains. Proteinase K is an endopeptidase that preferentially cleaves the peptide bond adjacent to the carboxyl group of aliphatic and aromatic amino acid residues, such as glycine, valine, tryptophan and phenylalanine (Keil 1992).

All L-amino acid peptides were cleaved by enzymes and completely lost their antibacterial activity against the two tested bacteria. In contrast, all of the three diastereomers, dP1-PuroA, dW7 and dWW, exhibited strong resistance towards proteases degradation and they maintained full activities, i.e., they had the same MICs as the relevant untreated controls. (Table 3.4).

Table 3.3 Antibacterial activity of the peptides in the presence of NaCl

Peptide ID	MIC ($\mu\text{g mL}^{-1}$)*							
	Without Salt		With 50mM NaCl		With 100mM NaCl		With 150mM NaCl	
	<i>E. coli</i>	<i>S. aureus</i>	<i>E. coli</i>	<i>S. aureus</i>	<i>E. coli</i>	<i>S. aureus</i>	<i>E. coli</i>	<i>S. aureus</i>
PuroA	16	16	16	16	32	32	64	64
Cyclic PuroA	250	125	> 250	250	>250	250	>250	>250
Di-PuroA	250	250	> 250	> 250	>250	>250	>250	>250
PuroA-OH	32	64	64	125	>250	>250	>250	>250
R8	64	64	64	64	64	64	64	64
P1	16	16	16	16	16	16	16	16
dP1	16	16	16	16	16	16	16	16
R6	32	16	64	32	250	250	>250	>250
R7	8	16	32	32	250	250	>250	>250
W7	4	8	4	8	4	8	4	8
dW7	8	8	8	8	8	8	8	8
W8	4	8	4	8	4	8	4	8
WW	8	8	8	8	8	8	8	8
dWW	8	8	8	8	8	8	8	8

* Results shown are the average of two independent experiments conducted in triplicates.

Table 3.4 Antibacterial activity of the peptides treated with trypsin or proteinase K

Peptide ID	MIC ($\mu\text{g mL}^{-1}$)*					
	No protease		Trypsin		Proteinase K	
	<i>E. coli</i>	<i>S. aureus</i>	<i>E. coli</i>	<i>S. aureus</i>	<i>E. coli</i>	<i>S. aureus</i>
PuroA	16	16	>250	>250	>250	>250
Cyclic PuroA	250	125	>250	>250	>250	>250
Di-PuroA	250	250	> 250	> 250	>250	>250
PuroA-OH	32	64	>250	>250	>250	>250
R8	64	64	>250	>250	>250	>250
P1	16	16	>250	>250	>250	>250
dP1	16	16	16	16	16	16
R6	32	16	>250	>250	>250	>250
R7	8	16	>250	>250	>250	>250
W7	4	8	>250	>250	>250	>250
dW7	8	8	8	8	8	8
W8	4	8	>250	>250	>250	>250
WW	8	8	>250	>250	>250	>250
dWW	8	8	8	8	8	8

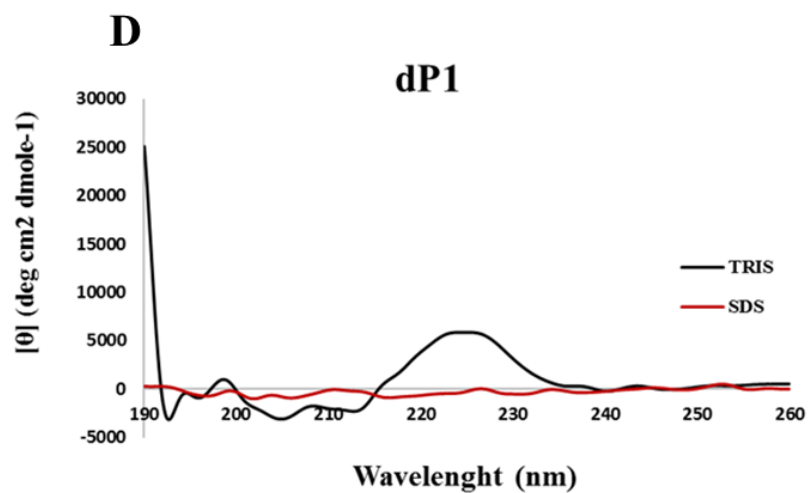
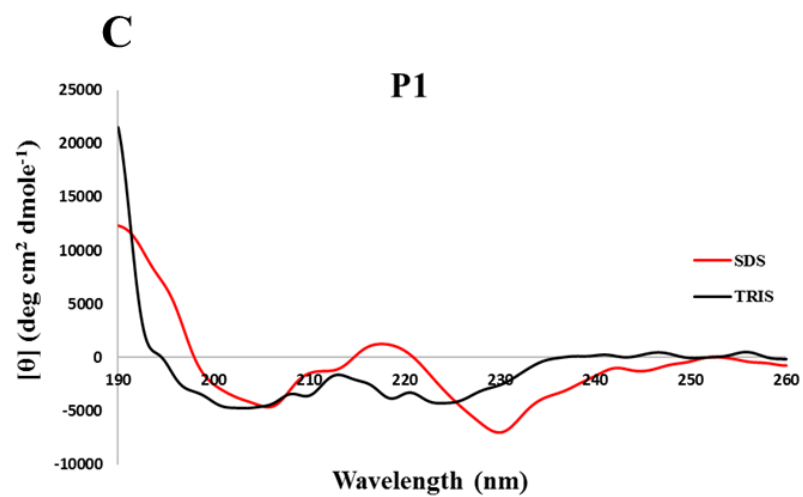
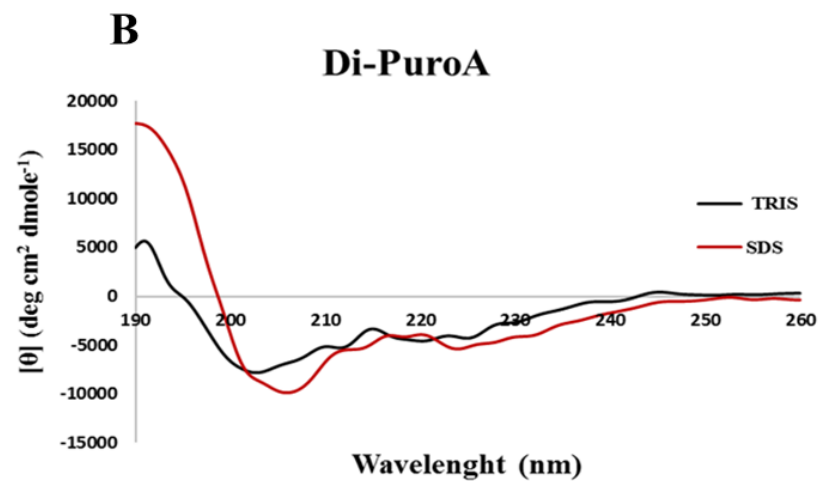
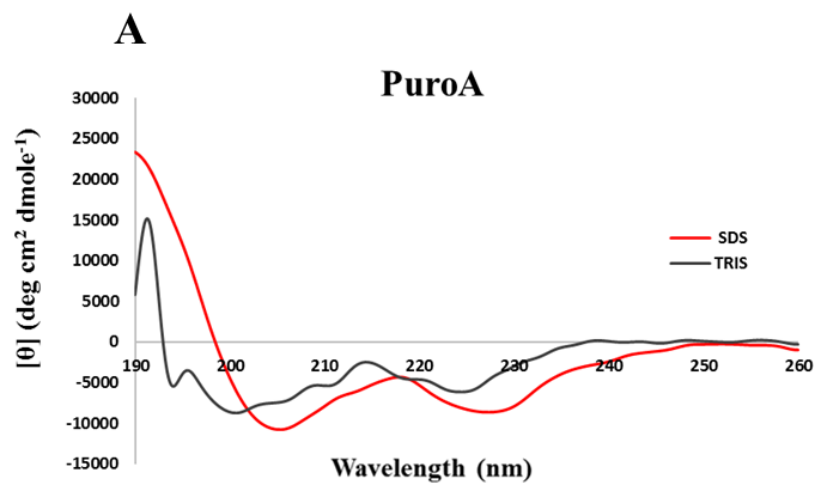
* Results shown are the average of two independent experiments conducted in triplicates.

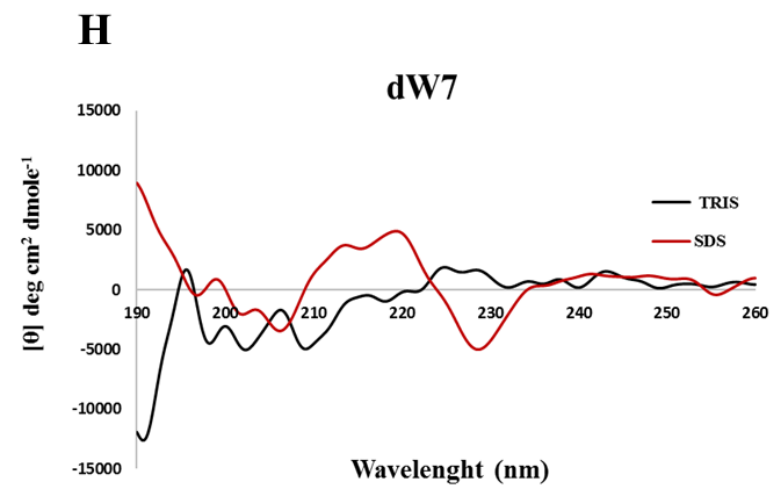
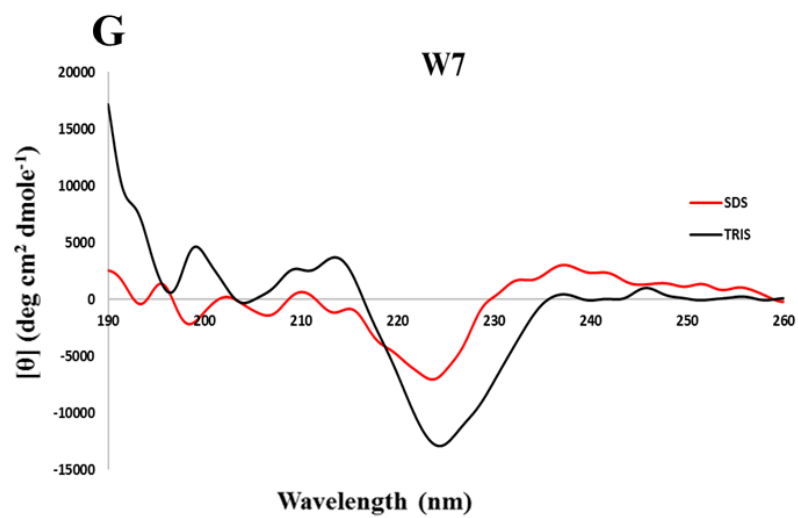
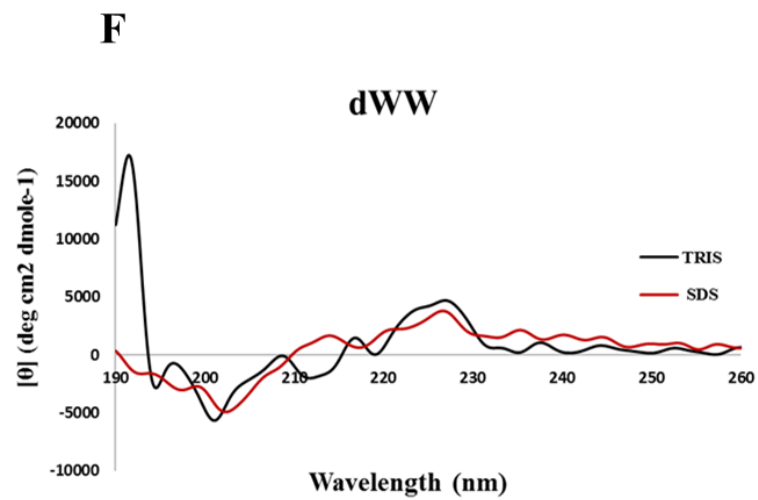
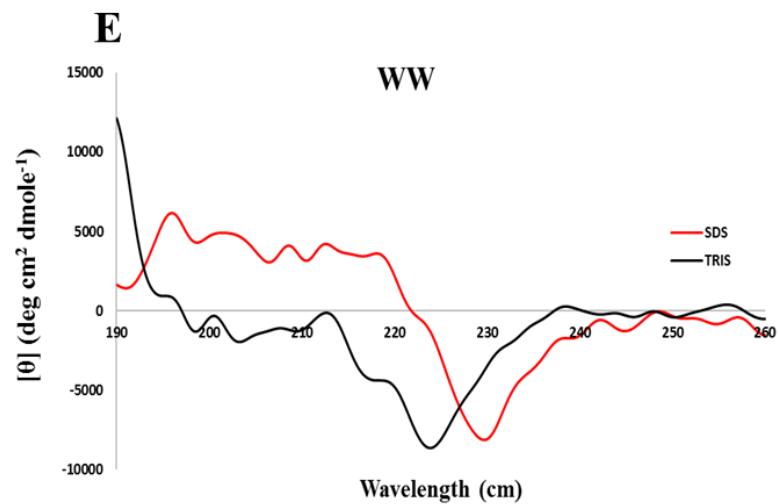
3.3.5 Circular dichroism (CD) spectroscopy

To determine the secondary structure of the peptides, their CD spectra were measured in two different environments, 20 mM Tris-HCL buffer (pH 7.4, mimicking aqueous environment) and 20 mM sodium dodecyl sulfate (SDS) detergent (mimicking negatively charged membrane environments).

In buffer, all of the peptides had strong negative peaks at ~200 nm. For example, the spectrum of PuroA, Di-PuroA and P1 in aqueous buffer showed a broad negative band at 201 nm with intensities of -8646 deg cm²/dmol, -7797 deg cm²/dmol and -4715 deg cm²/dmol, respectively (Fig. 3.2 A, B and C). The position of this band has been assigned to random coils or unordered conformation (Perczel & Hollosi 1996), but has also been observed for the poly-L-proline II helix in PR-39 and Bac5 peptides (Falla et al. 1996) and for β -turns (Perczel et al. 1991). For these three peptides, the negative band at 201 nm moved to 206 nm and was enhanced with a more pronounced effect in the presence of SDS. Below 200 nm, the positive 195 nm band was also enhanced in the presence of SDS, and this enhancement was more pronounced in both PuroA and Di-PuroA than in P1. In aqueous buffer, a second negative band appeared for all L-peptides at 225 nm separated by a maximum at ~215 nm. This negative band moved to ~230 nm for PuroA, P1 and R7 in the presence of SDS. The most noticeable change in dW7 spectra is the appearance of this 225 nm negative band in SDS buffer only. The second negative band at 225 nm has been assigned to the tryptophan side chain contribution, which depends on the orientation of this aromatic ring relative to the peptide backbone (Woody 1994). This band also overlaps with the distinctive broad minimum at 210-220 nm, usually displayed by β -stranded peptides (Wallace et al. 2003). A similar strong negative band at 225-230 nm was observed in the CD spectra described for Trp-rich peptides, such as indolicidin (Falla et al. 1996) and tritrypticin (Schibli et al. 1999). The CD spectrum of PuroA is consistent with the previous published one (Jing et al. 2003). For PuroA, P1 and Di-PuroA peptides, the enhancement of the maximum 195 nm and the minimum 206 nm suggests that there may be induction of a helical structure upon binding to SDS (Perczel & Hollosi 1996). However, the strong contribution of the five, six and ten tryptophan residues in PuroA, P1 and Di-PuroA peptides, respectively, prevented the secondary structure estimation by common deconvolution methods.

In the case of R8 and cyclic-PuroA, as well as the short L-amino acids peptides, W7, W8, WW and R7, it seems that they are less likely to adopt ordered secondary structures in the presence of detergent. In addition, substitution of certain L-amino acids in P1, WW and W7 with D-amino acids in their counterpart diastereomers significantly changed their CD spectra in both environments, buffer and detergent (Fig. 3.2 D, F and H). These observations confirmed that introducing D-amino acids into certain position of the peptide sequence to form short consecutive sections of 1–2 L-amino acids disrupted the helicity of the peptides (Papo et al. 2002).





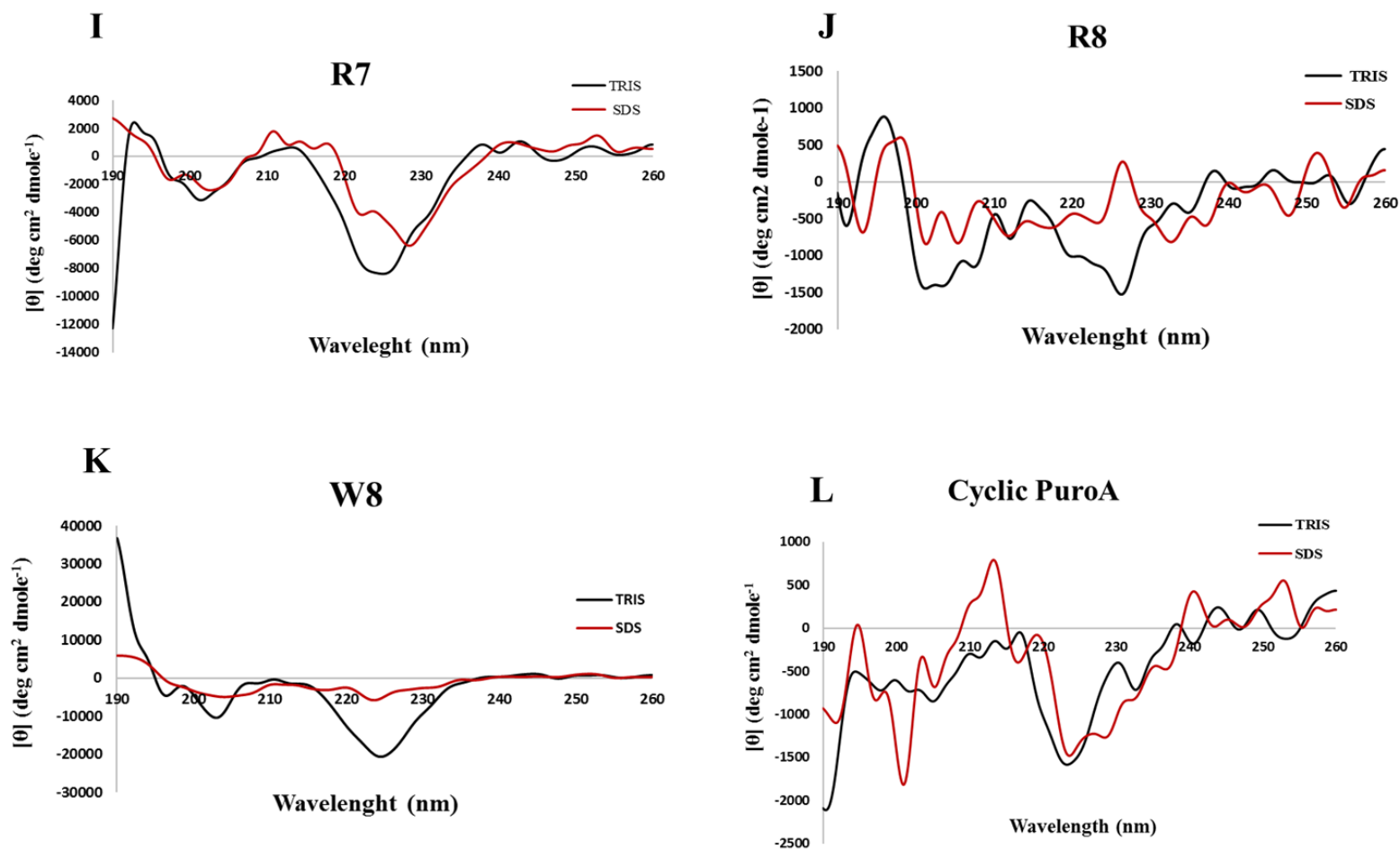


Figure 3.2 Circular dichroism spectra for PuroA and its variant peptides.

All spectra were recorded in 20 mM buffer (black lines) or in 20 mM SDS (red lines). θ : mean residue molar ellipticity.

3.3.6 Homology modelling of three-dimensional structure

The three-dimensional structure projections of the long peptides (≥ 13 amino acids in length), including PuroA, Di-PuroA, P1 and R8, were predicted using I-TASSER software (<http://zhanglab.ccmb.med.umich.edu/I-TASSER>, last accessed December, 2016). The three-dimensional structure of short peptides (≤ 8 amino acids in length) cannot be predicted with this software. In the hypothetical tertiary structures, PuroA was found to have a helical segment spanning from Trp5 to Trp8, while P1 and R8 have longer helical segments, from Arg1 to Lys12 and from Arg3 to Arg 12, respectively (Fig. 3.3). On the other hand, Di-PuroA contains two helical segments, from Trp5 to Gly13 and from Arg20 to Trp25.

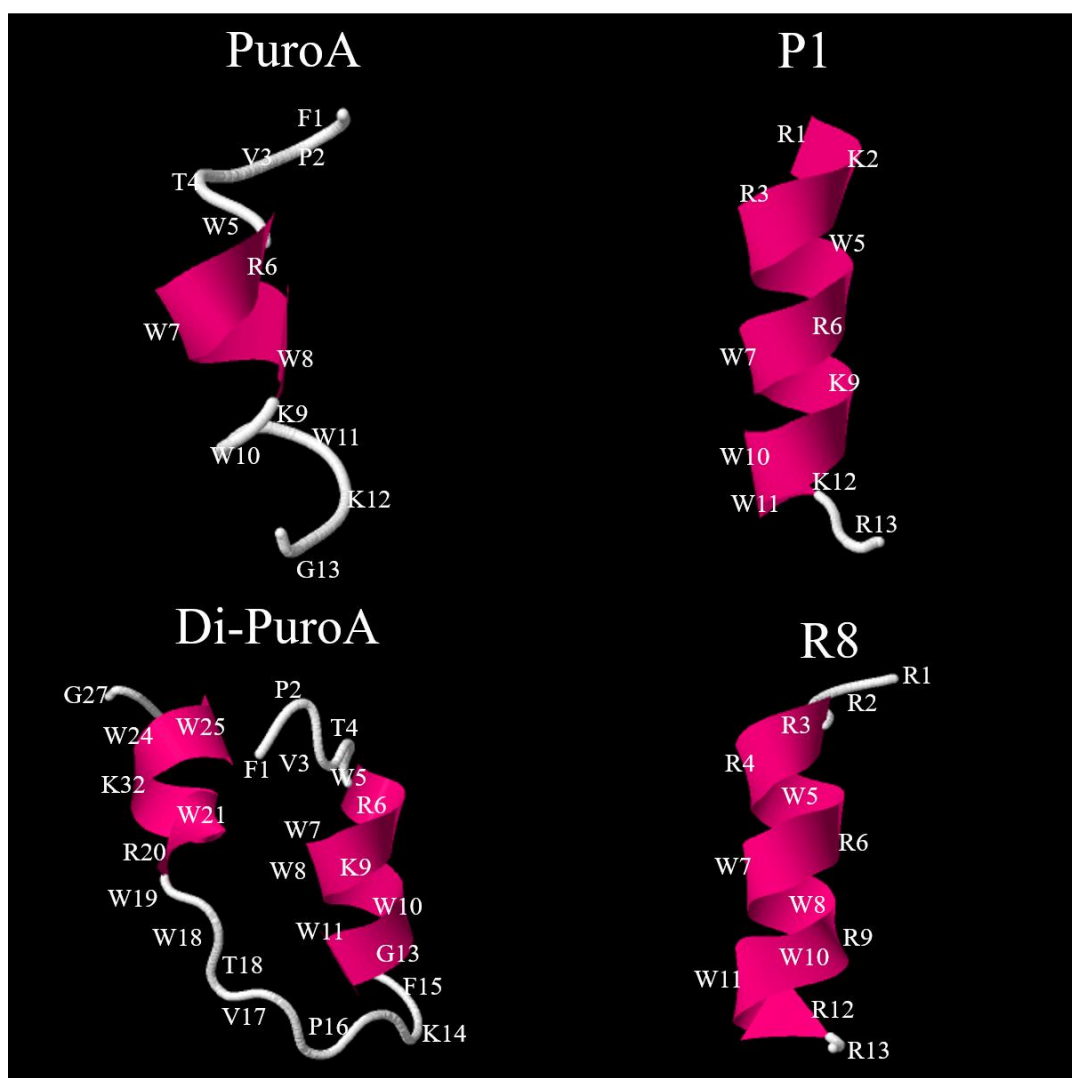


Figure 3.3 Three-dimensional structure projections of PuroA and P1 peptides. The structures were predicted by I-TASSER service (<http://zhanglab.ccmb.med.umich.edu/I-TASSER>, last accessed December, 2016).

3.3.7 *In vitro* DNA-binding ability of peptides

Binding to DNA and subsequently inhibiting the bacterial growth is a mode of action for some AMPs (Park et al. 1998; Marchand et al. 2006; Alfred et al. 2013b; Ghosh et al. 2014; Li et al. 2016b) (Chapter 1. Table 1.9). In order to investigate whether the peptides may have a possible intracellular mechanism of action, their ability to bind to DNA *in vitro* was indirectly investigated using a gel retardation assay. The peptides were serially diluted to a final peptide concentration range of 0 to 500 $\mu\text{g}/\text{mL}$, and then each dilution mixed with 100 ng of pBlueScript SK+ plasmid DNA (2958 bp) and electrophoresed in 1% agarose gels. The effect of different peptide concentrations on the migration of the plasmid DNA was monitored (Fig. 3.4, and 3.5).

PuroA and its non-amidated analogue completely inhibited the migration of plasmid DNA at concentrations of 32 $\mu\text{g}/\text{mL}$. Also, cyclized PuroA demonstrated similar activity and stopped DNA migration at 64 $\mu\text{g}/\text{mL}$, while the dimeric form displayed strong DNA binding ability with weak plasmid bands still present at 8 $\mu\text{g}/\text{mL}$ (Fig. 3.4). The DNA binding ability of cyclized and dimeric PuroA was not correlated to their antibacterial activity (Table 3.2). On the other hand, P1-PuroA and dP1-PuroA peptides showed the strongest ability to inhibit plasmid migration since no DNA bands were observed at the lowest concentration 8 $\mu\text{g}/\text{mL}$, correlating to their strong antimicrobial activity. Their short derivatives, WW and dWW, presented lower DNA binding activities than the parent peptides since they stopped DNA migration at 32 $\mu\text{g}/\text{mL}$. R6 and R7 demonstrated the weakest abilities to inhibit plasmid migration; complete migration inhibition was observed at 250 $\mu\text{g}/\text{mL}$ of peptide concentration (Fig. 3.5).

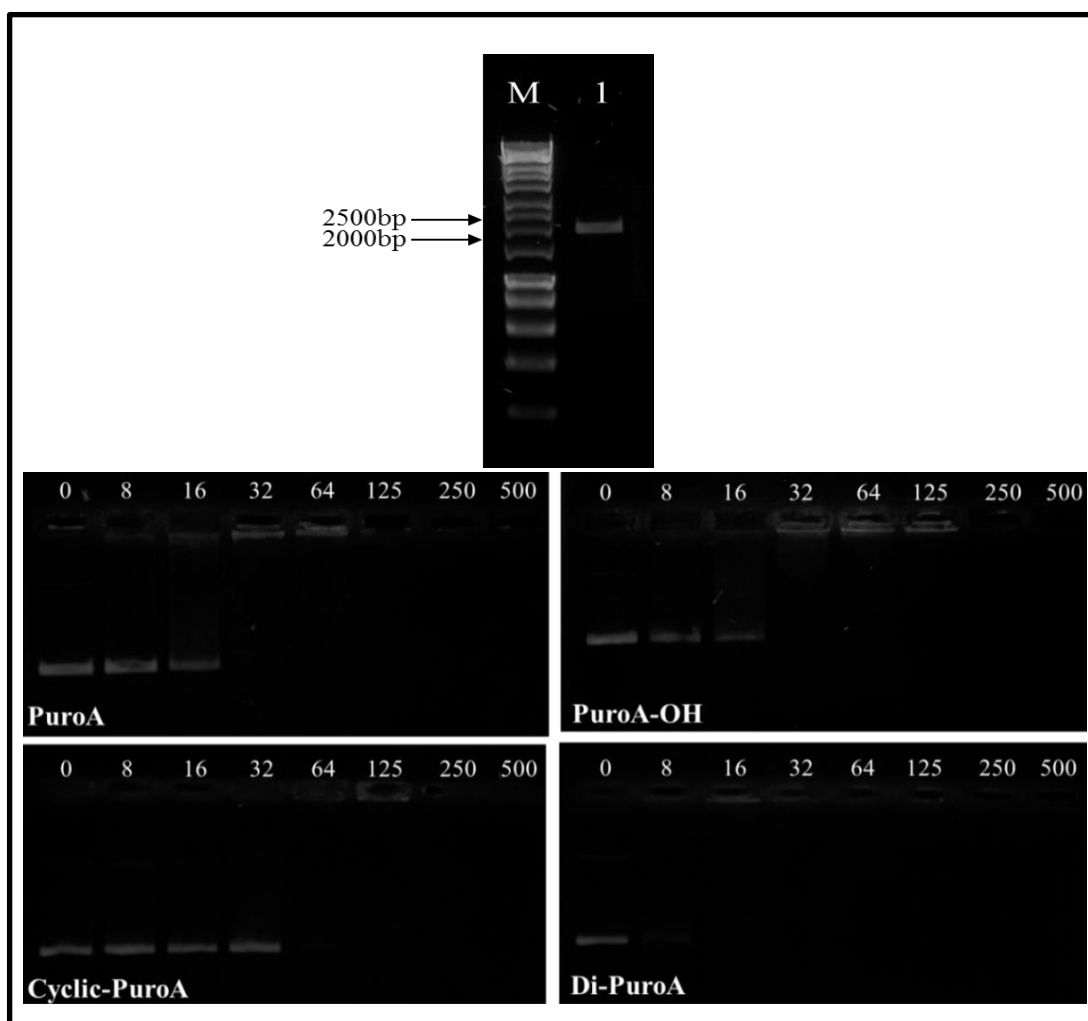


Figure 3.4 Electrophoresis of plasmid DNA alone and when it is bound to PuroA, PuroA, Cyclic-PuroA and Di-PuroA peptides.

100 ng of pBluescript SK+ plasmid bound to 0, 8, 16, 32, 64, 125, 250 or 500 $\mu\text{g/mL}$ of peptide were electrophoresed on 1% agarose gels for 30 min. Unbound pure pBluescript SK+ plasmid was also run as a negative control in lane 1. Marker (M): Hyperladder I.

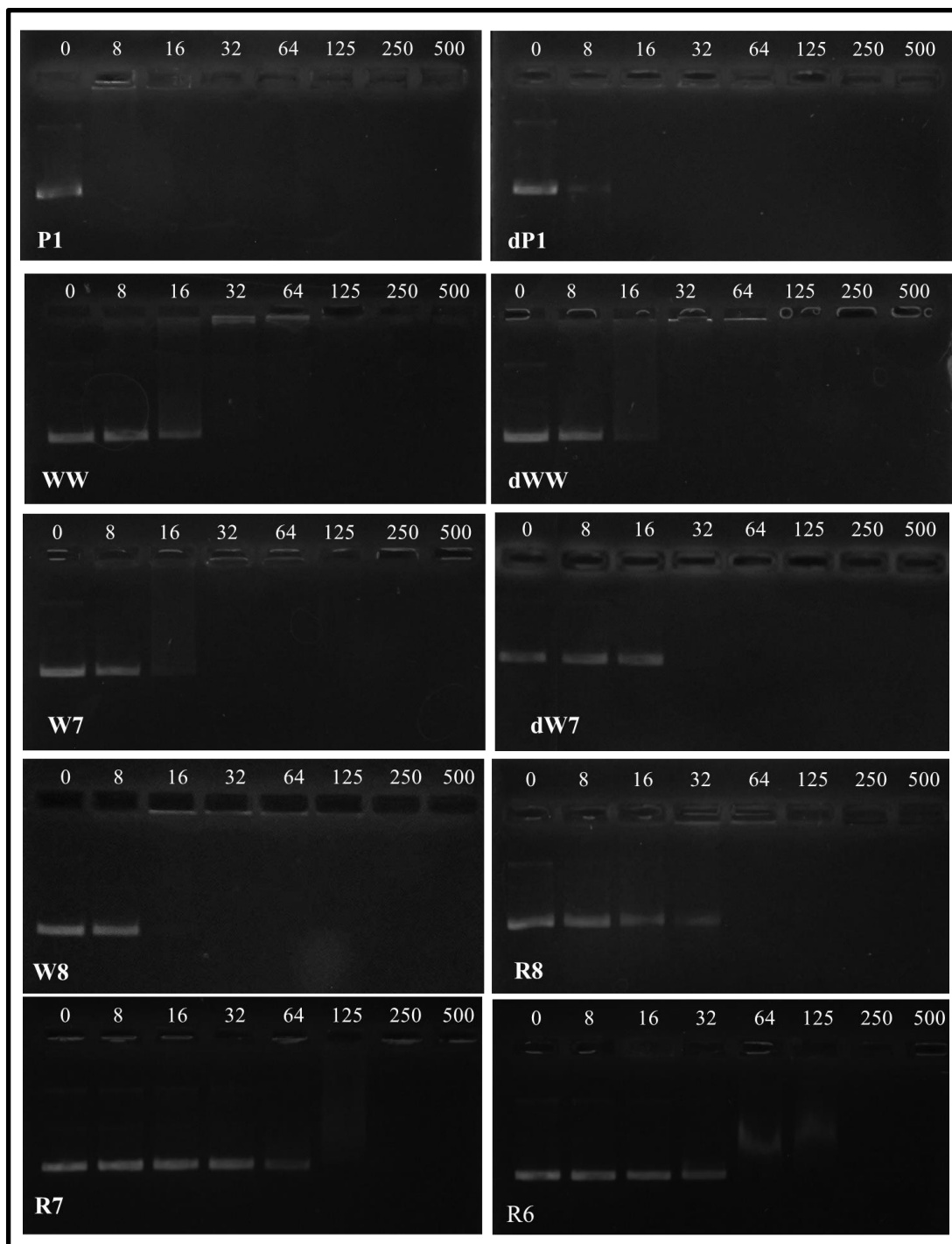


Figure 3.5 Electrophoresis of plasmid DNA bound to P1, dP1, WW, dWW, W7, dW7, W8, R8, R7 and R6 peptides.

100 ng of pBluescript SK+ plasmid bound to 0, 8, 16, 32, 64, 125, 250 or 500 µg/mL of peptide were electrophoresed on 1% agarose gels for 30 min.

3.3.8 Morphological effects of designed peptides on *E. coli* cells (*E. coli* filamentation assay)

Filamentation is a defect in the cell division where the cell continues to grow without septum formation (Donachie & Robinson 1987). Cell filamentation could be due to the blocking of DNA synthesis (Lutkenhaus 1990) or the inhibition of membrane proteins that are involved in the formation of the septum that separates the cell cytoplasm into two cells (Botta & Park 1981). Therefore, an *E. coli* filamentation assay was used to test if the peptides could affect DNA and/or protein synthesis.

A fixed number of *E. coli* cells (10^8 CFU/mL) was incubated with increasing concentration (from 0 to 250 μ g/mL) of the peptide under investigation and then after 3 h of exposure, the morphology of *E. coli* cells was observed by light microscopy. Control *E. coli* cells with no peptide treatment were used as a standard to show normal *E. coli* cell phenotype and length (Fig. 3.6). All the peptides, except dimeric PuroA, induced filamentation at their MIC for *E. coli* (given in Table 3.2). Notably, dimeric PuroA did not cause elongation of *E. coli* cells, however, it promoted their aggregation.

Additionally, after incubating *E. coli* cells with peptides at MIC for 3 h, the cells were stained with SYO 9 and inspected for filamentous growth using confocal microscopy and interleaved phase contrast microscopy. The cells length increased at least over 5-fold (Fig. 3.7, 3.8 and 3.9). The cell filamentation was also quantified by scanning electron microscopy to measure individual cell length. Representative images are shown in Fig. 3.11. The mean length of normal *E. coli* cells at log-phase was about 1-2 μ m. Addition of peptides and incubation for 3 h resulted in 7-fold to 14-fold increase in the cell length (7-16 μ m). The appearance of pores was observed on the surface of some filamentous cells (Fig. 3.10).

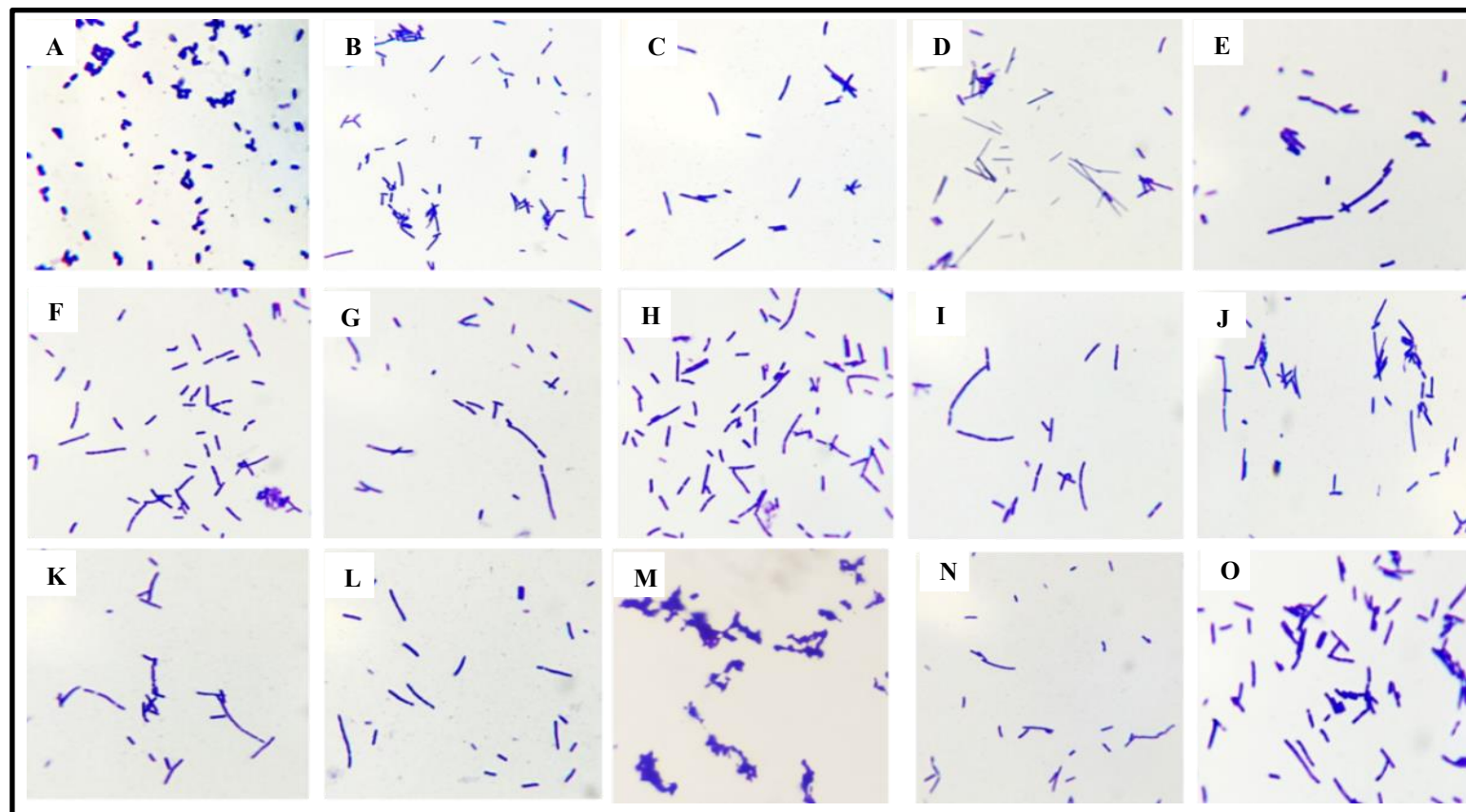


Figure 3.6 Morphological changes induced in *E. coli* cells by designed peptides.

The cells were observed using light microscopy at $\times 1000$ magnification under oil emersion after incubation with peptide for 3 h at 37 °C. Panels are: **A.** no peptide control; **B.** PuroA 16 $\mu\text{g}/\text{mL}$; **C.** Cyclic PuroA 250 $\mu\text{g}/\text{mL}$; **D.** PuroA-OH 32 $\mu\text{g}/\text{mL}$; **E.** R8 64 $\mu\text{g}/\text{mL}$; **F.** R6 32 $\mu\text{g}/\text{mL}$; **G.** R7 8 $\mu\text{g}/\text{mL}$; **H.** W7 4 $\mu\text{g}/\text{mL}$; **I.** dW7 8 $\mu\text{g}/\text{mL}$; **J.** W8 4 $\mu\text{g}/\text{mL}$; **K.** P1 16 $\mu\text{g}/\text{mL}$; **L.** dP1 16 $\mu\text{g}/\text{mL}$; **M.** Di-PuroA 250 $\mu\text{g}/\text{mL}$; **N.** WW 8 $\mu\text{g}/\text{mL}$ and **O.** dWW 8 $\mu\text{g}/\text{mL}$.

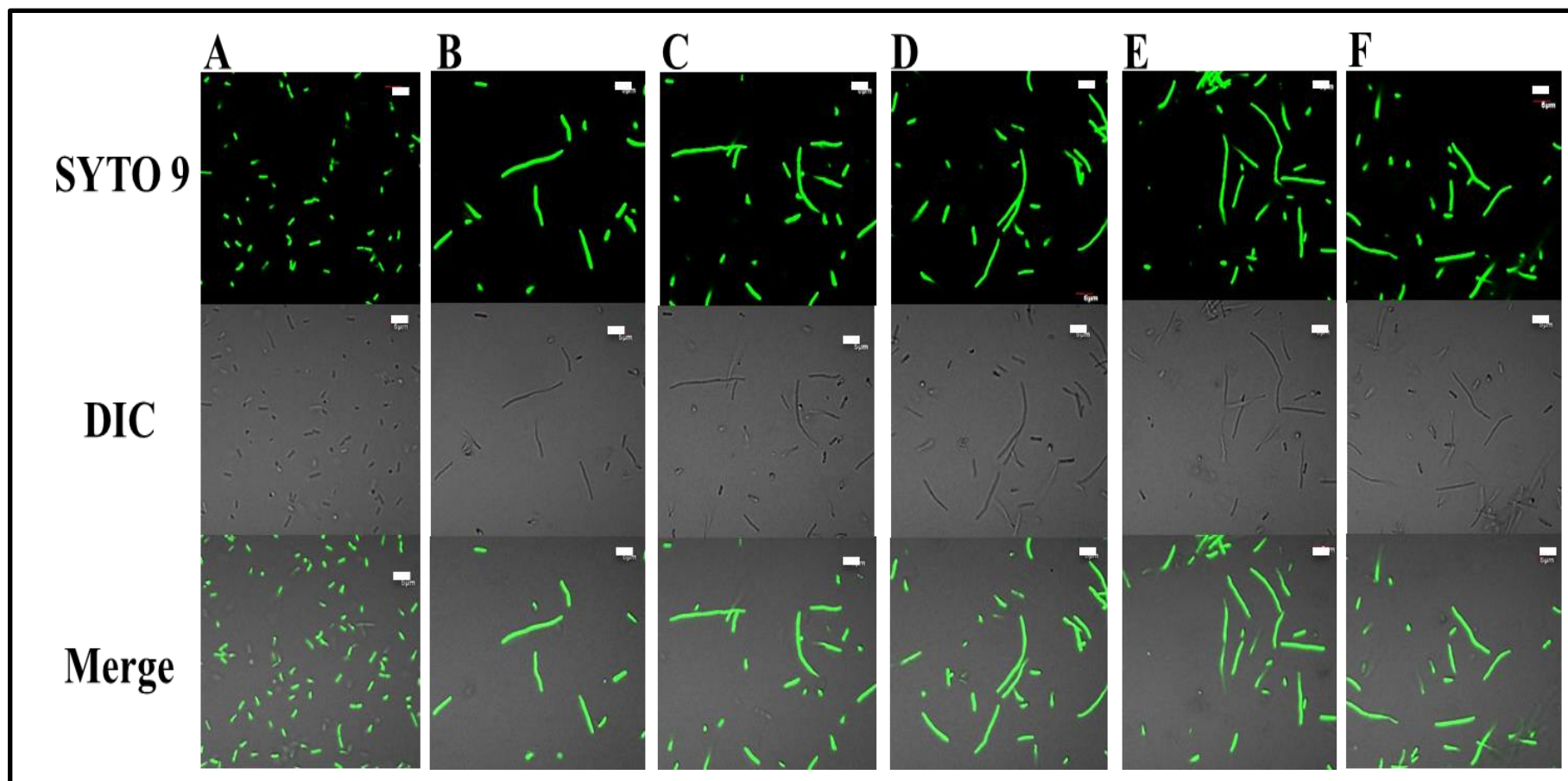


Figure 3.7 Confocal microscopy of *E. coli* cells treated by peptides.

The cells were observed at $\times 1000$ magnification under oil immersion after incubation with peptide for 3 h at 37 °C. **A.** no peptide control; **B.** PuroA 16 $\mu\text{g}/\text{mL}$; **C.** Cyclic PuroA 250 $\mu\text{g}/\text{mL}$; **D.** PuroA-OH 32 $\mu\text{g}/\text{mL}$; **E.** R8 64 $\mu\text{g}/\text{mL}$ and **F.** R6 32 $\mu\text{g}/\text{mL}$. Scale bar 5 μm . DIC: Differential interference contrast.

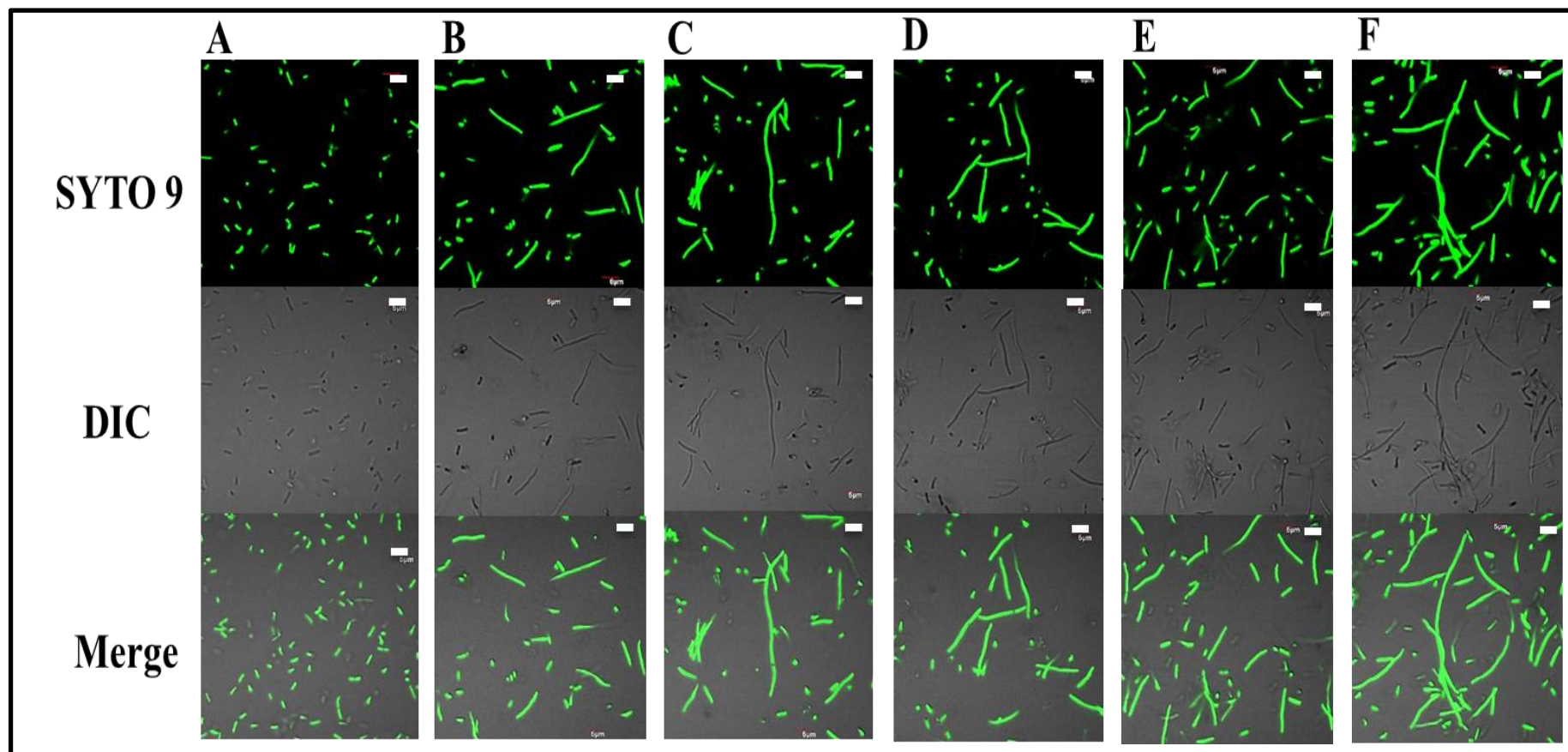


Figure 3.8 Confocal microscopy of *E. coli* cells treated by peptides.

The cells were observed at $\times 1000$ magnification under oil immersion after incubation with peptide for 3 h at 37 °C. **A.** no peptide control; **B.** R7 8 µg/mL; **C.** W7 4 µg/mL; **D.** dW7 8 µg/mL; **E.** W8 4 µg/mL and **F.** P1 16 µg/mL. Scale bar 5 µm. DIC: Differential interference contrast.

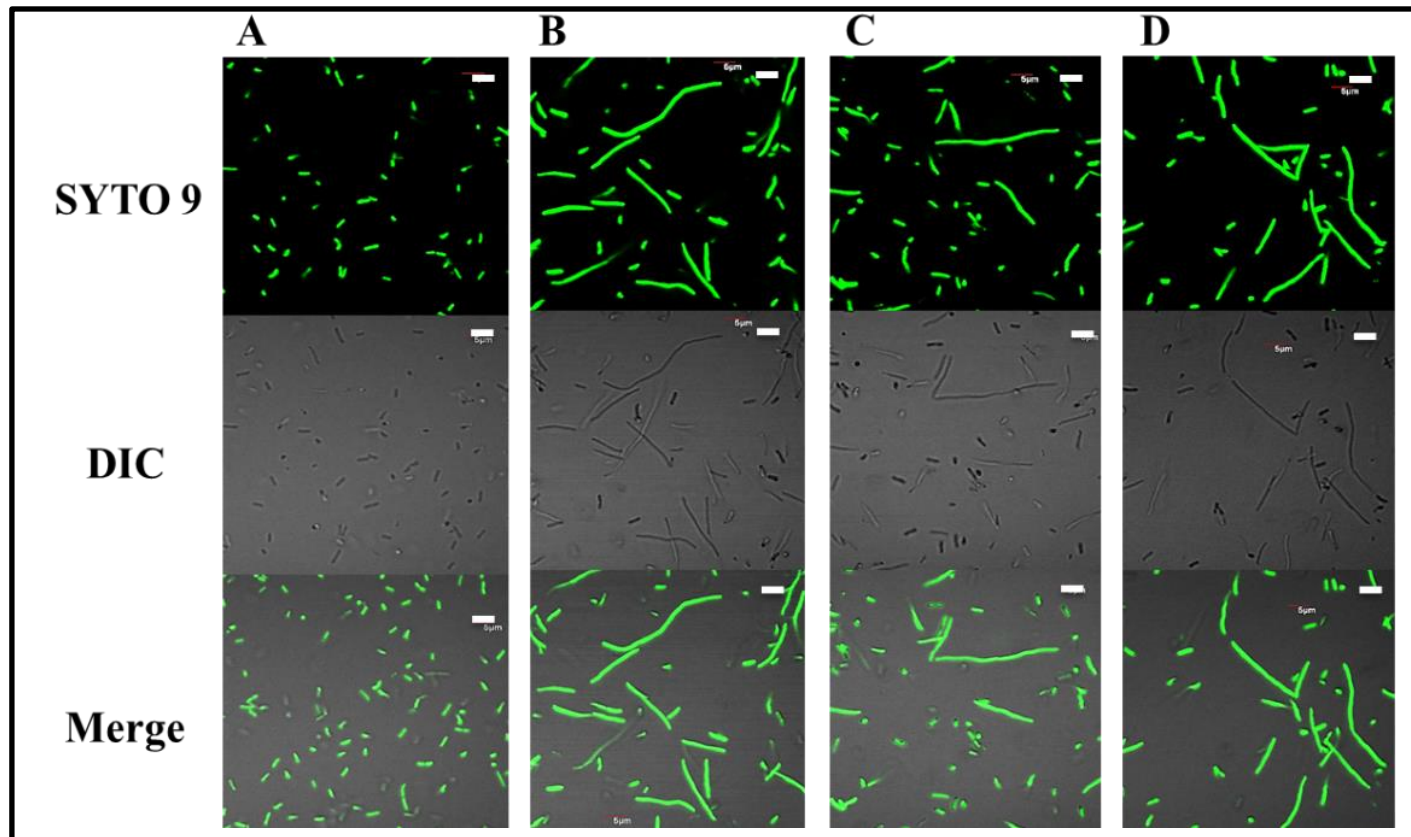


Figure 3.9 Confocal microscopy of *E. coli* cells treated by peptides.

The cells were observed at $\times 1000$ magnification under oil immersion after incubation with peptide for 3 h at 37 °C. **A.** no peptide control; **B.** dP1 16 $\mu\text{g}/\text{mL}$; **C.** WW 8 $\mu\text{g}/\text{mL}$ and **D.** dWW 8 $\mu\text{g}/\text{mL}$. Scale bar 5 μm . DIC: Differential interference contrast.

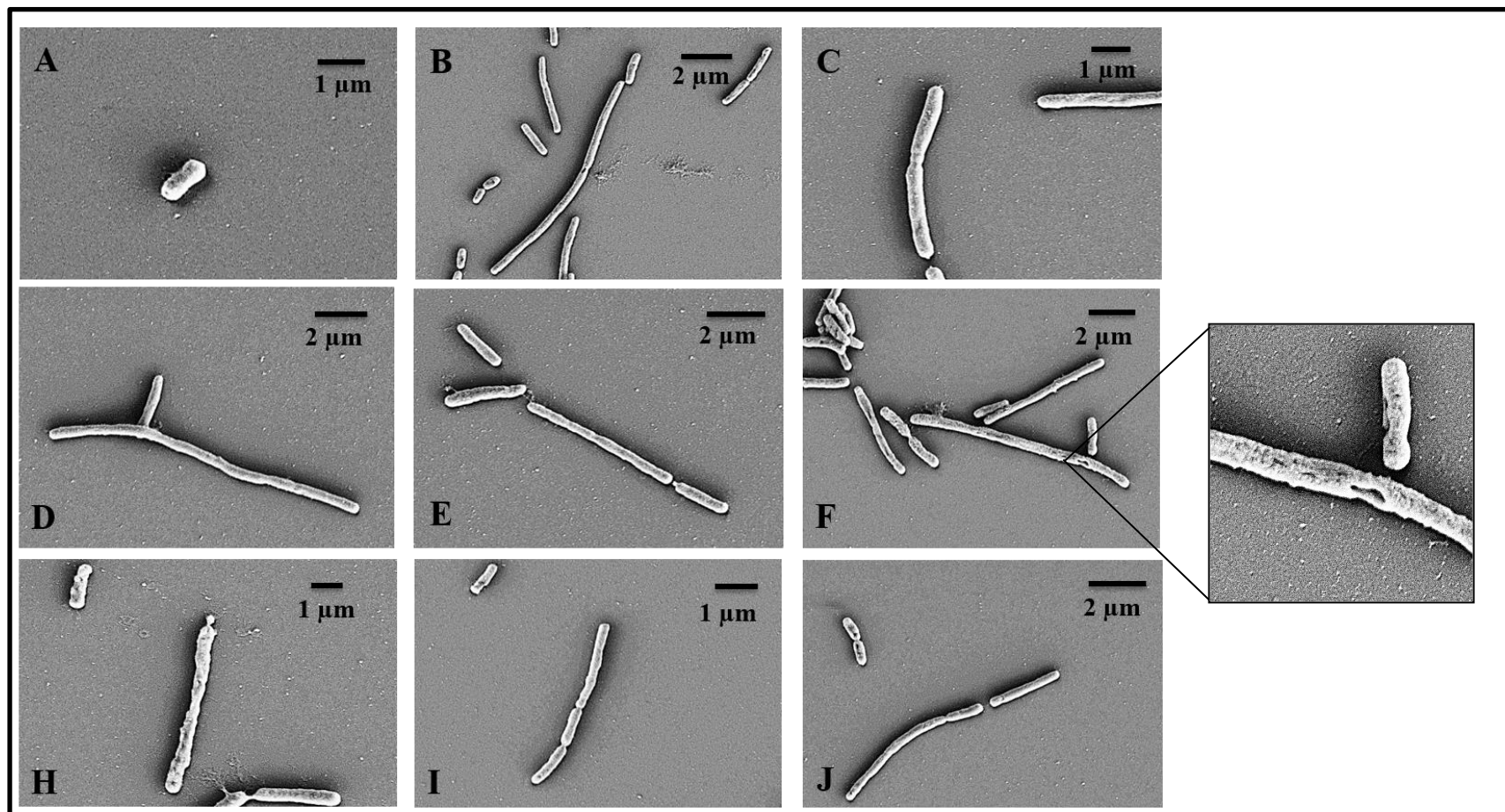


Figure 3.10 Scanning electron micrographs of *E. coli* cells treated with peptides.

A. no peptide control; B. PuroA 16 µg/mL; C. W7 8 µg/mL; D. P1 16 µg/mL; E. dP1 16 µg/mL; F. WW 8 µg/mL; H. R6 32 µg/mL; I. R7 8 µg/mL and J. W8 8 µg/mL.

3.4 Discussion

3.4.1 Importance of rationally design AMPs for clinical applications

Since their discovery, AMPs have been seen as novel promising antimicrobial therapeutics because of their wide-range of activities, long evolutionary history and low potential of developing resistance against them. The focus has been more on developing AMPs with superior activities; however, to be used as therapeutics, more attention should be paid to the behaviour of these interesting molecules in clinical environments. The main issues that need attention are their pharmacokinetic profile, degradation by proteolytic enzymes, *in vivo* microbicidal activity under physiological conditions, targeting and potential cytotoxicity on normal mammalian cells. As well as unclear mode of action, the absence of information about their antigenicity and immunogenicity and the high costs of synthesis are major obstacles for the widespread application of peptides in the near future.

Short AMPs with broad spectrum antimicrobial activity, metabolic stability and low cytotoxicity on normal mammalian cells are highly desired (Strøm et al. 2003). Naturally occurring peptides with all these attributes are very rare. Therefore, rational design of AMPs based on good understanding of peptide structure-function is a useful approach to obtain the desired peptides and this formed the basis of this study. Several TRPs isolated from, or designed based on proteins from natural sources showed a broad range of biocidal activities as discussed in Chapter 1, Sections 1.4 and 1.6. The biochemical properties of Trp complement the cationic Arg residues in many Trp-Arg rich AMPs (reviewed in Chan et al. 2006), see Chapter 1, Section 1.8. Several structure–activity relationship studies of Trp- and Arg- rich peptides, such as bovine lactoferricin (Tomita et al. 1994; Vogel et al. 2002) and indolicidin (Staubitz et al. 2001), have indicated that conserved RW motifs retain their antimicrobial activities. Based on these findings and by using PuroA as a template, this work aimed to design peptides to identify the factors that can lead to better efficiency and selectivity under physiological conditions. Towards this end, the peptides were designed based on some physicochemical constrains that have been outlined to contribute to the biological activities of AMPs, such as net charge, length, primary structure, hydrophobicity and amphipathicity (Yeaman & Yount 2003; Pasupuleti et al. 2012; Teixeira et al. 2012;

Lee et al. 2016b), see Chapter 1, Section 1.3. Additional design strategies, such as cyclization, dimerization and incorporating of D-amino acids were also used.

3.4.2 Effect of length on antimicrobial activity and salt stability

The length of AMPs is an important factor that can affect their activity, toxicity and mode of action, as discussed in Chapter 1, Section 1.3.1. On the other hand, the development of peptides as novel therapeutic agents has been limited by concerns relating to the relatively high cost of production of synthetic peptides, therefore, making shorter peptide candidates more desirable (Hilpert et al. 2005; Nguyen et al. 2010). To investigate the structure (length)-antimicrobial activity relationships and to identify the active center of PuroA, the basic amino acid and Trp-rich region was selected due to its proven role in the antimicrobial activity of PuroA. The short linear analogues of PuroA, i.e., R6, R7, W7, W8 and WW, showed higher antimicrobial activity against tested bacteria and yeast than the parent peptide and excellent salt stability behaviours (Table 3.2 and 3.3).

3.4.3 Effect of net charge and C-terminal amidation on antimicrobial activity and salt stability

Cationicity affects the initial interaction of AMPs with microbial membranes, their structural amphiphilicity and selective toxicity. To study the effect of cationicity on the biological activity of AMPs, the charge in peptide R8 was increased by substituting all the residues with the cationic amino acid Arg and only maintaining the bulky hydrophobic Trp residues. Trp and Arg complement the biochemical properties of each other in many Trp-Arg rich AMPs (discussed above) and Arg residues have a more dispersed positive charge on their side chain guanidinium group compared to the lysine, thus contributing to “snorkeling behavior” in Arg-rich AMPs (Strandberg et al. 2002), Arg was chosen over Lys to increase the net positive charge of the peptide. As expected, increasing the peptide charge overcame the salt’s charge-shielding effect; the shielding effect resulting from competing salt ions reduces the electrostatic attraction between positively charged AMPs and negatively charged microbial membranes (Li et al. 2013). However, increasing the cationicity to +8 in R8 peptides reduced its antibacterial and antifungal activity and that could be due to the strong interaction between the positively charged peptide and the negatively charged

phospholipid head groups, which prevents conformational change and structuring of the peptide and consequently affects the kinetics of membrane permeabilization and the translocation of the peptide (Tossi et al. 1994; Pasupuleti et al. 2012). On the other hand, P1 with net positive charge of +7, showed improved antimicrobial activity and salt stability. Compared to R8, the uncharged amino acids in P1 were replaced with Arg and Lys residues, not only Arg. These results confirming the previous observation that increasing the charge beyond +7 does not improve the antimicrobial activity (Pasupuleti et al. 2012). Based on the well-established direct correlation between peptide cationicity, and antimicrobial activity and salt stability, the high antimicrobial potency and salt stability of the short Trp-rich peptides which have a net positive charge of +2 or +3 was unexpected. At this point, it is unclear why these short peptides have excellent salt tolerance, although it seems that the amphipathic structure of these peptides and the cluster of the Trp-residues protect them from the salt inactivation effect. It was proposed that the “RRKK” motif in the C-terminus of human β -defensin-3 (HBD-3) peptides contributes to its salt-resistant behaviour (Li et al. 2013). However, this motif was not effective in overcoming salt intolerance in D0 peptide (SGKLCCRKK-NH₂), whereas increasing the Trp-content improved the antimicrobial and salt-tolerance behaviour of these decamers (Saravanan et al. 2014). Based these and other observations (Deslouches et al. 2005a; Deslouches et al. 2005b; Deslouches et al. 2013) and our results, adding Trp residue(s) to AMPs, could be a useful approach to design antimicrobial peptides effective at physiological salt concentration and subsequently increase the *in vitro* use of these peptides.

The positive charge of AMPs mainly derives from the cationic residues, Lys and Arg, and it can also come from a contribution of a C-terminal amide moiety. C-terminal amidation is the most common post-translational modification of defence peptides which suggested biological relevance. This structural moiety is associated with peptide resistance to enzymatic degradation (Andreu & Rivas 1998). It has been also suggested that the presence of this amide group enhances the antimicrobial activity of peptides, e.g., α -defensin 2 (Xie et al. 2005), tritrypticin (Schibli et al. 2006) and PMAP-23 (Kim et al. 2011). In order to gain further insight into this factor, this study investigated the effect of the C-terminal amide group on the activity of PuroA. Our

results clearly showed that this amidification increased the peptide antimicrobial activity but in terms of protease resistance and salt stability, it has a negligible effect.

3.4.4 Effect of hydrophobicity on antimicrobial activity

Hydrophobicity is considered to be independent of other structural physicochemical characteristic of AMPs (Pasupuleti et al. 2012). It has been shown that it greatly affects the antimicrobial activity of AMPs, their range of target pathogens and their cytotoxic selectivity (Yount et al. 2006; Pasupuleti et al. 2008; Pasupuleti et al. 2009a; Orådd et al. 2011; Strandberg et al. 2015). It is generally accepted that there is an optimal hydrophobicity for each AMP and changing it can affect the antimicrobial activity. However, our study showed that there is no clear correlation between hydrophobicity and peptide antimicrobial activity. For example, PuroA and WW have the same hydrophobicity but WW had higher antibacterial and antifungal activity. In addition, P1 and its shorter analogue, WW, have different hydrophobicity, P1 is much less hydrophobic as it contains more positively charged residues (Table 3.1), but they showed almost the same potent activity against bacteria and yeast (Table 3.2). Therefore, hydrophobicity does not seem an independent parameter affecting the peptide activity.

3.4.5 The correlation between secondary structure of AMPs and their antimicrobial activity

Partitioning of AMPs into membranes is mainly accompanied by secondary structure formation (Wieprecht et al. 1999; Seelig 2004). Many AMPs adopt either α -helical or β -sheet structures and the degree of structuring affects their activity and cytotoxicity, as discussed in Chapter 1, Section 1.3.4. PINA comprises four α -helices which are separated by loops and stabilised by five disulphide bonds (Le Bihan et al. 1996; Bhave & Morris 2008a). The TRD forms an extended loop between α -helix 1 and 2 (Chapter 1, Figures 1.2 and 1.3). As PuroA was synthesized based on this TRD, this peptide is expected to be unstructured in aqueous solution. In this study, the structure of the peptides was determined in (Tris-HCl) and in the presence of detergent (SDS) using CD spectroscopy (Section 3.3.5). PuroA, as expected, was unstructured in aqueous buffer, similar to all other designed TRPs as expected for linear peptides consisting of ≤ 14 residues. Upon binding to SDS, the peptides did not adopt any well-

defined α -helical or β -sheet secondary structures; only PuroA, Di-PuroA and P1 formed a more ordered structures. It is interesting that these three peptides showed considerably difference antimicrobial activities (Table 3.2), as well as the short the diastereomeric peptides, which are less likely to form any secondary structure, showed potent antimicrobial activities against the tested Gram-positive and Gram-negative bacteria, as well as yeast. Looking at the secondary structure of all the archetypal TRPs reviewed in Chapter 1, indolicidin, tritrpticin and lactoferricin (LfcinB), only LfcinB adopts an amphipathic β -sheet structure (Hwang et al. 1998), indolicidin (Rozek et al. 2000a) and tritrpticin (Schibli et al. 1999) adopt stable amphipathic structures in SDS micelle. In addition, Jing et al. (2003) used two-dimensional (2D) nuclear magnetic resonance (NMR) to show that PuroA also forms a well-defined amphipathic conformation when it binds to SDS micelles. These observations and our results lead us to agree with Rozek et al. (2000a) who suggested that AMPs do not need to conform to a recognized secondary structure to exert their antimicrobial activities; adopting an amphipathic configuration seems to be more important.

3.4.6 The correlation between D-amino acids and antimicrobial activity and proteases stability of AMPs

Despite the successful use of some antimicrobial peptides for treating specific infections having been demonstrated in mouse models (Woong et al. 2007; Noto et al. 2008; Wu et al. 2014), clinical use of AMPs has thus far been limited to topical applications (Hancock & Sahl 2006); a number of concerns has risen regarding the systematic and dynamic application of AMPs and their *in vivo* activity might be different from that displayed in *in vitro* assays. In systemic use, proteolytic degradation, rapid clearance and unfavourable pharmacokinetics are significant obstacles. To date, several design strategies have been used to decrease the susceptibility of AMPs to serum proteases and increase their half-life, for example, cyclization (Rozek et al. 2003), introduction of unnatural amino acids such as D-amino acids (Papo et al. 2002; Matsuzaki 2009; Carmona et al. 2013), derivatives with unnatural side chains (Haug et al. 2008; Gentilucci et al. 2010), and β -amino acids (Raguse et al. 2002). In this study, about 35-40% of the sequence of the diastereomers consisted of D-amino acids and their positions were designed to have short consecutive stretches of 1–3 L-amino acids. It is well studied that the incorporation of

D-amino into peptides sequences can affect the helicity, the hydrophobicity and the cell selectivity of peptides (Shai & Oren 1996; Chen et al. 2005; Prenner et al. 2005; Huang et al. 2014b). Our findings showed that, irrespective of sequence, helicity and hydrophobicity change, the antimicrobial activity of the all L-amino acid peptides was similar to that of their corresponding diastereomers. However, all L-isomers were fully inactivated by trypsin and proteinase K while the diastereomers retained their full antimicrobial activity in the presence of these two proteases up to 3 h. Interestingly, these results suggest that once a potent peptide is designed, D-amino acids can be introduced into specific positions in the peptide sequence to produce a new active peptide with the same potency and spectrum of activity while being less susceptible to enzymatic degradation.

3.4.7 Effect of cyclization on antimicrobial activity and stability of PuroA

The design strategy of cyclization of the AMPs backbone is reported to have led to potent antimicrobial analogs of indolicidin (Rozek et al. 2003), bovine lactoferricin (LfcinB₄₋₁₄), tritripticin (Nguyen et al. 2011a), melittin (Unger et al. 2001), histatin (Brewer & Lajoie 2002) and other short TRPs (Nguyen et al. 2010). Moreover, circularization improved their haemolytic activity and proteolytic stability. In fact, there are a number of naturally occurring cyclic AMPs, e.g., microcin J25 (Rosengren et al. 2003), rhesus theta-defensin (Selsted 2004) and daptomycin.

In this study, a cyclic analogue of PuroA with an additional head-to-tail bond in the peptide backbone was designed. Interestingly, the biological activity studies showed that this analogue had decreased activity against both bacteria and fungi compared to the linear PuroA. Unger et al. (2001) and Nguyen et al. (2011a) reported similar reduction of antibacterial activity by cyclization of magainin 2 and tritripticin, however, they used a different cyclization strategy, through a disulfide bond between Cys residues. In addition, cyclization did not give PuroA any protection against proteolytic degradation; this result contradicts previous studies that suggest cyclization is an effective modification to eliminate any susceptibility to exoproteases (Rozek et al. 2003; Dathe et al. 2004; Nguyen et al. 2010). The role of linearity and cyclization in biological function and mode of action of AMPs is not easy to rationalize and needs to be studied further.

3.4.8 Effect of dimerization on antimicrobial activity and stability of PuroA

The aggregation/oligomerization of AMPs molecules, either before or at binding to the cell membrane, is important for pore formation, and, consequently, for the peptide's mechanism of action (Sengupta et al. 2008; Melo et al. 2009). Additionally, it is believed that the cellular selectivity of AMPs is affected by peptide self-association (oligomerization) in aqueous environments (Chen et al. 2007; Long Zhu & Shin 2009). Thus, many dimeric peptides have been designed (Welling et al. 2007; Lee et al. 2008b; Dewan et al. 2009; Zhu & Shin 2009; Liu et al. 2017). In some cases, dimerization led to improved pharmacotechnical characteristics, antimicrobial activity, solubility and high salt and protease resistance, e.g., magainin (Dempsey et al. 2003), indolicidin (Krajewski et al. 2004) and other synthetic peptides (Santos-Filho et al. 2015). Therefore, dimerization seems a promising strategy to develop novel AMPs. However, in some cases, dimerization has led to reduced antimicrobial activity and/or an increase in cytotoxicity (Yang et al. 2009; Lorenzón et al. 2012; Lorenzón et al. 2013). Therefore, in this study, to evaluate the effect of dimerization on the biological activity of PuroA, a C-terminal dimeric analogue of the peptide (PuroA)₂k was synthesized. Dimerization did not improve the antimicrobial activity of the monomeric PuroA, nor its salt or proteases resistance. Although the dimeric peptide showed strong *in vivo* DNA binding ability, it did not induce filamentation in *E. coli* cells; however, it promoted the aggregation of the cells (Fig. 3.6). Lorenzón et al. (2013) reported a similar effect of the dimeric aurein 1.2 peptide which induced aggregation of *C. albicans* cells. It has been shown that AMPs selectively interact with lipopolysaccharides in Gram-negative bacteria (Bucki & Janmey 2006). Therefore, inducing aggregation in *E. coli* cells and having reduced antibacterial activity could be due to the interaction with a component of the cell wall which could prevent the dimeric peptides from reaching the bacterial membranes. Although the antibacterial activity decreased with dimerization, the ability of dimeric peptides to induce aggregation on bacterial cells makes them attractive candidates to inhibit the adhesion of bacteria to biological and medical surfaces.

3.4.9 Correlation between the antimicrobial activities of TRPs and their in vitro DNA binding and inducing of filamentation in E. coli cells

In this work, preliminary investigation of the effect of the designed TRPs on DNA-binding and/or DNA synthesis was undertaken. Two methods were used, *in vitro* DNA-binding essay (gel retardation assay) which shows the effect of different peptides concentrations on the migration of DNA in agarose gels (Section 3.3.6), and *E. coli* filamentation assay which demonstrates the ability of peptides to inhibit DNA synthesis *in vivo* (Section 3.3.7). However, cell filamentation could also result from the inhibition of membrane proteins that are involved in septum formation (Botta & Park 1981). The designed peptide showed different affinity for the plasmid DNA *in vitro*, however, there was no correlation between their antimicrobial activities and the DNA binding affinity. For example, dimeric PuroA (Di-PuroA), P1 and dP1 showed the strongest affinity for the plasmid DNA (Figures 3.4 and 3.5), though in terms of activity, Di-PuroA is much less active compared to P1 and dP1 against bacteria and yeast. It may be that the number of Trp is related to DNA binding, as these three peptides have ≥ 6 Trp residues. Hsu et al. (2005) proposed that TRPs insert into DNA with Trp residues stacking between the bases of deoxyribose sugars. Moreover, substituting the Trp–Trp pair at the central PWWP motif of indolicidin with Ala–Ala, His–His, or Phe–Phe considerably changed the ability of the peptide to bind and stabilize duplex DNA (Ghosh et al. 2014). In addition, there was no correlation between the DNA binding affinity of peptides and their net charge, as R8 peptide with net positive charge of +8 showed less affinity to the plasmid DNA than W8 with net charge of +3 only (Figure 3.5). Although it is believed that positively charged amino acids are probably responsible for the electrostatic binding with phosphate groups of the duplex DNA (Hsu et al. 2005). It was also shown that substituting Trp 3 or 4 in indolicidin with the positivity charged Lys resulted in a peptide analogue with more stronger DNA binding ability than indolicidin (Nan et al. 2009).

All the designed TRPs in the present study, except dimeric PuroA, induced filamentation in *E. coli* cells at their MIC, regardless of the differences in their physicochemical characteristics. This observation could suggest a role of Trp residues in inducing this morphological change, in particular, other TRPs such as indolicidin, (Subbalakshmi & Sitaram 1998) and LfcinB (Ulvatne et al. 2004) also induced

filamentation of *E. coli*. Although dimeric PuroA showed very strong affinity to DNA *in vitro*, this peptide did not cause elongation in *E. coli* cells, and only promoted the aggregation of cells (discussed above in section 3.4.2).

In conclusion, the variants P1, W7, W8, and WW which displayed potent antimicrobial activities and maintained these activities under physiological salt conditions were successfully designed. The diastereomers, dP1, dW7 and dWW, also resisted *in vitro* proteolytic degradation and retained the same potent antimicrobial activities. The present results not only provide a template for future novel design and engineering of short TRPs for improved antimicrobial activity, salt tolerance, and biocompatibility properties, but they also reveal that the biological activities depend on a number of interrelated factors, such as charge, length and hydrophobicity.

Chapter 4

Potential applications of PIN-based peptides: sporicidal and anti-biofilm activities

4.1 Abstract

Bacterial endospores and biofilms are highly resistant cells and cell communities, respectively, with significant implications in medical and food industries. The puroindolines (PIN) are small, basic proteins which are primary determinants of wheat grain texture, with proposed roles in seed defence from pathogens. Synthetic peptides based on the unique tryptophan-rich domain (TRD) of PINs and the related barley hordoindolines (HIN) display antimicrobial properties. In this study, a number of synthetic peptides were tested for effects on planktonic cells and biofilms of common human pathogens, including *Pseudomonas aeruginosa*, *Listeria monocytogenes*, the non-pathogenic *Listeria innocua* and two clinical methicillin-resistant *S. aureus* (MRSA) isolates. The peptides tested included: PuroA (FPVTWRWWK WWKG-NH₂), PuroB (FPVTWPTKWWKG-NH₂) and Pina-M (FSVTWRWWKW WKG-NH₂) based on the TRD of PIN proteins encoded by the wild type alleles *Pina-D1a* and *Pinb-D1a*, and the hardness alleles *Pina-D1m*, respectively; Hina (FPVTWRWWTWWKG-NH₂) based on the TRD of PIN orthologs in barley, *Hina*; and, PuroA derivatives, P1 (RKRWWRWWKWWKR-NH₂), WW (WWRWWK WW-NH₂) and W7 (WRWWKWW-NH₂). PuroA and Pina-M at 2 × MIC prevented initial biomass attachment by 85-90% and inhibited >90% of preformed biofilms of *P. aeruginosa*, *L. monocytogenes* and *L. innocua*. Hina, with reduced cationicity due to the substitution of Lys-9 with uncharged Thr, showed inhibitory activity on *Listeria* biofilms only. PuroA derivatives showed higher activity on initial biomass attachment than preformed biofilms of *P. aeruginosa*, *L. monocytogenes* and *L. innocua*, whereas, they showed similar inhibitory activity (>90%) on initial biomass attachment and preformed biofilm of MRSA. The peptides were also tested against vegetative cells and endospores of *Bacillus subtilis*. Our results give the first demonstration that the peptides killed *B. subtilis* even in sporulated state, reducing the number of viable spores by at least 4 log units. The treated spores appeared withered and severely damaged under scanning electron microscopy. The results establish the potential of these peptides in controlling persistent pathogens of relevance to food industries and human health.

4.2 Introduction

Antimicrobial peptides (AMPs), often termed as ‘nature’s antibiotics’, are an evolutionarily conserved component of the innate immune system of many organisms. AMPs showed broad-spectrum activity against diverse bacteria, fungi, viruses, protozoa or even cancer cells (Jenssen et al. 2006; Hoskin & Ramamoorthy 2008b). These multifunctional molecules are highly diverse and include several subgroups, as detailed in Chapter 1, Section 1.2. Naturally occurring Trp-rich AMPs (TRPs) such as indolicidin, tritrypticin and lactoferricin showed strong antimicrobial activities as discussed in Chapter 1, section 1.4. The grains of wheat contain two small, Cys- and Trp-rich proteins called puroindoline-a (PINA) and puroindoline-b (PINB), encoded by the genes *Pina-D1* and *Pinb-D1*, respectively (Gautier et al. 1994). The PIN proteins purified from wheat flour or bacterial expression systems have been shown to exhibit antimicrobial properties (Capparelli et al. 2005) and transgenically-transferred *Pin* genes also confer biotic defense (Kim et al. 2012). The unique tryptophan-rich domain (TRD) of PINs has been associated with these properties (Blochet et al. 1993; Gautier et al. 1994). The synthetic peptides PuroA (FPVTWRWWKWWKG-NH₂) and PuroB (FPVTWPTKWWKG-NH₂) based on the TRD of PINA and PINB, respectively, showed *in vitro* antimicrobial activity against a number of bacteria (Jing et al. 2003; Phillips et al. 2011), phytopathogenic fungi (Phillips et al. 2011) and fungal spores (Alfred et al. 2013a). The barley hordoindolines HINA, HINB1 and HINB2, encoded by *hordoindoline a (Hina)*, *hordoindoline b-1 (Hinb-1)* and *hordoindoline b-2 (Hinb-2)*, respectively, are the homologs of wheat *Pin* (Beecher et al. 2002; Li et al. 2011). The antimicrobial activity of HINs is little explored as yet, except for one study by our group which has shown the high antimicrobial activity of the peptide Hina (FPVTWRWWTWWKG-NH₂) but limited activities of Hinb1 (FPLTWPTKWWKG-NH₂) and Hinb1a (FPLTCPTKWWKG-NH₂) (Phillips et al. 2011). The antimicrobial activity of the wheat puroindoline proteins and their homologs are extensively discussed in Chapter 1, Section 1.6.

Bacterial biofilms are structured multicellular microbial communities attached to a surface, producing extracellular matrix composed of numerous polysaccharides, proteins and extracellular DNA (eDNA) (Branda et al. 2005). Biofilm formation is a

survival factor, as bacteria embedded in a biofilm are protected from antibiotics, food preservatives or other stresses such as acidic conditions, heat and high salinity (Hall-Stoodley et al. 2004; Shi & Zhu 2009). Bacterial cells in biofilms are more tolerant to the effects of antimicrobial agents than planktonic cells by 10¹⁰ times (Mah & O'Toole 2001; Olsen 2015). About 80% of human bacterial infections and 60% of nosocomial infections are biofilm-associated and these refractory biofilm-associated infections are difficult to be treated and contributing greatly to treatment costs and patient morbidity (Lewis 2001; Darouiche 2004; Römling & Balsalobre 2012). *Pseudomonas aeruginosa*, a Gram-negative bacterium, is amongst the major causes of infections in hospitalized patients. It is an opportunistic human pathogen that is the main cause of fatal lung infections in patients with cystic fibrosis (CF), and also the cause of nosocomial, catheter and urinary tract infections and sepsis in burn wounds, chronic wounds and immunocompromised patients (reviewed in Hancock & Speert 2000). Its ability to form biofilms is a key factor in chronic infections (Drenkard & Ausubel 2002), as these sessile communities are less susceptible to antibiotics such as gentamicin and ceftazidime than their non-attached planktonic counterparts (Ishida et al. 1998). *Listeria monocytogenes* is a Gram-negative pathogen that occurs commonly in uncooked meat products, vegetables and soft cheeses (reviewed in Jadhav et al. 2012) and can cause listeriosis which is a foodborne disease with a higher mortality rate, especially in the elderly, neonates, pregnant women and immune-compromised patients (reviewed in Kathariou 2002). It has been shown to form biofilm on materials commonly used in food industry, leading to recurrent contamination of food products (Beresford et al. 2001). *Staphylococcus aureus* is an opportunistic human pathogen that can cause moderate to severe infections. Methicillin-resistant *S. aureus* (MRSA) strains, which are now resistant to most conventional antibiotics, such as aminoglycosides, macrolides and lincosamides (Haaber et al. 2012), have arisen as a cause of potentially lethal infections. Besides multidrug resistance, MRSA has the ability to form biofilms on abiotic surfaces, such as indwelling medical devices (Darouiche 2004; Otto 2008), therefore, MRSA nosocomial infections have become a significant cause of morbidity, increased length of hospital stay and cost of treatment (Morell & Balkin 2010; Watkins et al. 2012). In addition, this pathogen has an increasing prevalence in the general population and become associated with

community-acquired infections as well, especially in CF patients (Goodrich et al. 2009; Okesola 2011; Pompilio et al. 2013).

Another defence mechanism utilised by certain bacteria, e.g., *Bacillus* or *Clostridium*, when they encounter nutritionally unfavourable conditions, is the production of a dormant structure called an endospore. Bacterial spores have caused many serious problems in medical environments (Wilcox & Fawley 2000) and the food industry (Bottone 2010). Endospores of *Bacillus* species are extremely resistant to multiple stress treatments, including toxic chemicals, radiation and heat (reviewed in Setlow 2006). Using high concentrations of chemicals or extended periods of heat treatment to eradicate bacterial endospores can be impractical in the food and health industries. Therefore, spore of these and related species have caused serious problems in food and medical fields (Martínez Viedma et al. 2011).

Thus, bacterial endospores and biofilms both are of significant concern in the healthcare sector and food industries and innovative strategies for their control are urgently required. The unique properties of AMPs and the low potential of developing resistance against them compared to conventional antibiotics make them promising as substitutes or complements to current antibiotics and efficiently control drug-resistant microbes.

In the present study, the potential applications of PIN-based peptides in controlling persistent pathogens in food and health contexts were explored. The activity of the synthetic peptides PuroA, and Pina-M based on the TRD of PINA, and Hina based on the TRD of HINA, as well as the selected PuroA derivatives P1, WW and W7 that showed highest antimicrobial activities against tested pathogens in Chapter 3, was tested on the cultures and biofilms of the pathogenic *P. aeruginosa*, *L. monocytogenes*, the non-pathogenic *L. innocua* (commonly used as a model) and two clinical MRSA isolates. Additionally, the peptides were investigated for their effects on the viability of *B. subtilis* spores. The methods applied are explained in Sections 2.10 to 2.14. The results are presented below. A major part of this work has been published (Shagaghi et al. 2016a).

4.3 Results

4.3.1 Antibacterial activity of the PIN-based peptides [(minimum inhibitory concentration (MIC)]

Peptides modelled on the TRD of PINA, PINB and HINA, as well as PuroA derivatives, were tested for their antibacterial activity against *P. aeruginosa*, *L. monocytogenes*, *L. innocua* and *B. subtilis*. Due to its Trp-rich nature, indolicidin was included for comparisons. Pina-M with mutant PINA sequence (Pro-35 to Ser) had higher inhibitory effect on all tested bacteria than PuroA, PuroB and Hina peptides (Table 1). However, PuroA and Pina-M had almost the same bactericidal activity and killed most of the *P. aeruginosa* and *L. innocua* cells after 3 h incubation and 90% of *B. subtilis* cells after 6 h (Fig. 4.1).

Hina, based on the natural HINA TRD, showed similar activity to PuroA and Pina-M against *B. subtilis*, *L. innocua* and *L. monocytogenes*, but was not active against *P. aeruginosa*. Indolicidin displayed almost the same antibacterial activity as PuroA and its MIC value was found to be consistent with that reported against *P. aeruginosa* (Falla et al. 1996), whereas was 2-fold higher than the reported values against *L. monocytogenes* (Friedrich et al. 2000; Ebbensgaard et al. 2015). However, two different strains of *L. monocytogenes* were used in these studies. PuroB peptide showed negligible antibacterial activity compared to other tested peptides. PuroA derivatives were more active by at least 2-fold than the archetypal PuroA against *P. aeruginosa*, *L. innocua* and *B. subtilis*.

In addition, PuroA and its derivatives were tested against two MRSA clinical isolates, and the results (MIC values) are summarized in Table 4.1. Overall, the activity showed by the three newly synthesized PuroA derivatives was higher than the parent peptide. In terms of the bactericidal dynamic of the peptides, the results of time-killing assays showed that P1 peptide exerted the fastest bactericidal effect on MRSA cells among the three peptides, killed 99% of the cells after 3 hr. However, the bactericidal effect of PuroA and W7 peptides was not complete; at 24 h, a re-growth was observed although with colony counts lower than untreated controls (Figure 4.2).

Table 4.1 Antibacterial activity of PIN-based peptides

Peptide	Sequence	<i>Pin</i> allele (Genbank) or reference	MIC ($\mu\text{g mL}^{-1}$)* against bacteria					
			<i>B. subtilis</i>	<i>P. aeruginosa</i>	<i>L. monocytogenes</i>	<i>L. innocua</i>	MRSA M173525	MRSA M180920
PuroA	FPVTWRWWKWWKG-NH ₂	<i>Pina-D1a</i> (DQ363911)	8 (\pm 0)	64 (\pm 0)	8 (\pm 0)	8 (\pm 0)	16 (\pm 0)	16 (\pm 0)
P1	RKRWWRWWKWWKR-NH ₂	N/A	8 (\pm 0)	16 (\pm 0)	8 (\pm 0)	4 (\pm 0)	16 (\pm 0)	8 (\pm 0)
W7	WRWWKWW-NH ₂	N/A	2 (\pm 0)	32 (\pm 0)	8 (\pm 0)	4 (\pm 0)	8 (\pm 0)	8 (\pm 0)
WW	WWRWWKWW-NH ₂	N/A	2 (\pm 0)	32 (\pm 0)	8 (\pm 0)	4 (\pm 0)	4 (\pm 0)	4 (\pm 0)
Pina-M	FSVTWRWWKWWKG-NH ₂	<i>Pina-D1m</i> (EF620907)	2 (\pm 0)	32 (\pm 0)	8 (\pm 0)	6 (\pm 2)	N/D	N/D
PuroB	FPVTWPTKWWKG-NH ₂	<i>Pinb-D1a</i> (DQ363913)	64 (\pm 0)	>250	>250	>250	N/D	N/D
Hina	FPVTWRWWTWWKG-NH ₂	<i>Hina</i> (AY644140)	4 (\pm 0)	>250	16 (\pm 0)	8 (\pm 0)	N/D	N/D
Indolicidin	ILPWKWPWWPWR-NH ₂	(Selsted et al. 1992)	8 (\pm 0)	64 (\pm 0)	16 (\pm 0)	8 (\pm 0)	N/D	N/D

*Mean of triplicate assays. N/A: not applicable, rationally designed PuroA derivatives from Chapter 3. N/T: not tested.

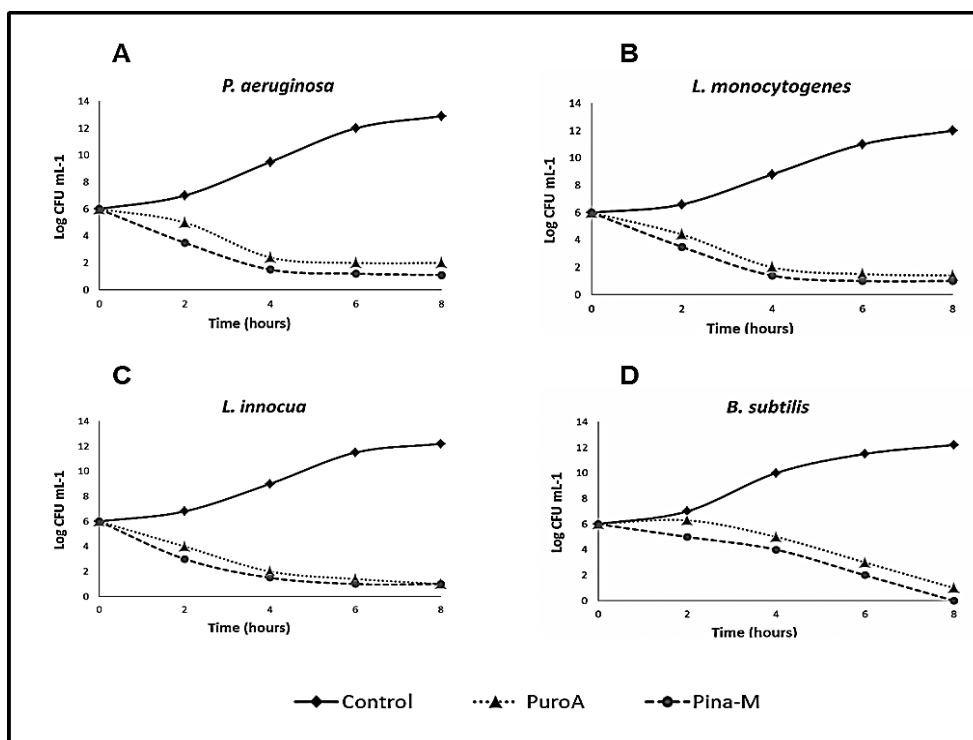


Figure 4.1 Time-kill kinetics of PuroA and Pina-M at 1 × MIC against bacteria. *P. aeruginosa* (A); *L. monocytogenes* (B); *L. innocua* (C); *B. subtilis* (D). All tests were conducted three times ($P < 0.05$).

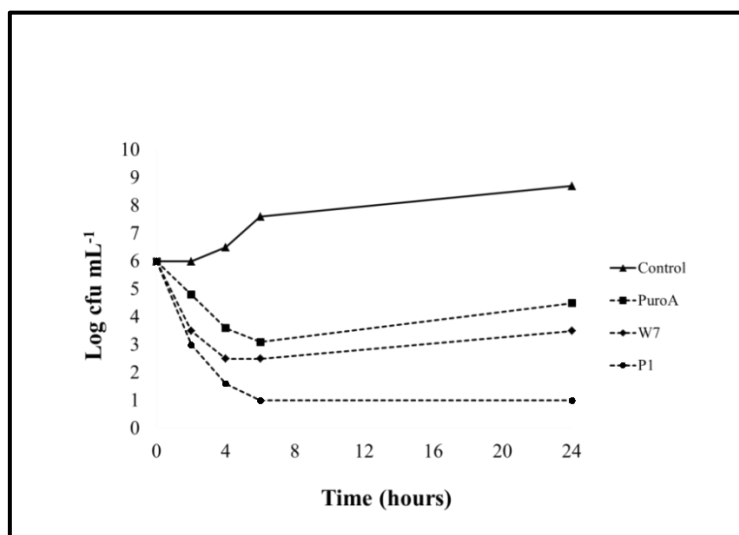


Figure 4.2 Time-kill kinetics of PuroA, P1 and W7 at 1 × MIC against MRSA bacteria. All tests were conducted three times ($P < 0.05$).

4.3.2 Effect of PuroA on membrane integrity of *L. monocytogenes* and *P. aeruginosa*

The membrane integrity of bacteria after treatment with PuroA peptide was assessed using the LIVE/DEAD BacLight Bacterial Viability Kit. After treating *L. innocua* and *L. monocytogenes* with PuroA (at $1 \times \text{MIC}$ and $2 \times \text{MIC}$) for 1 h, all cells appeared red (corresponding to PI). Additionally, the size and number of cells was much less than in the controls (Fig. 4.3), indicating that many had lysed. On the other hand, after treating *P. aeruginosa* and MRSA M173525 isolate with $1 \times \text{MIC}$ PuroA for 1 h, most of the cells appeared green (corresponding to SYTO 9), and while increasing the concentration to $2 \times \text{MIC}$ resulted in red cells, suggesting that a higher concentration of PuroA is required to disrupt the integrity of *P. aeruginosa* and MRSA membranes.

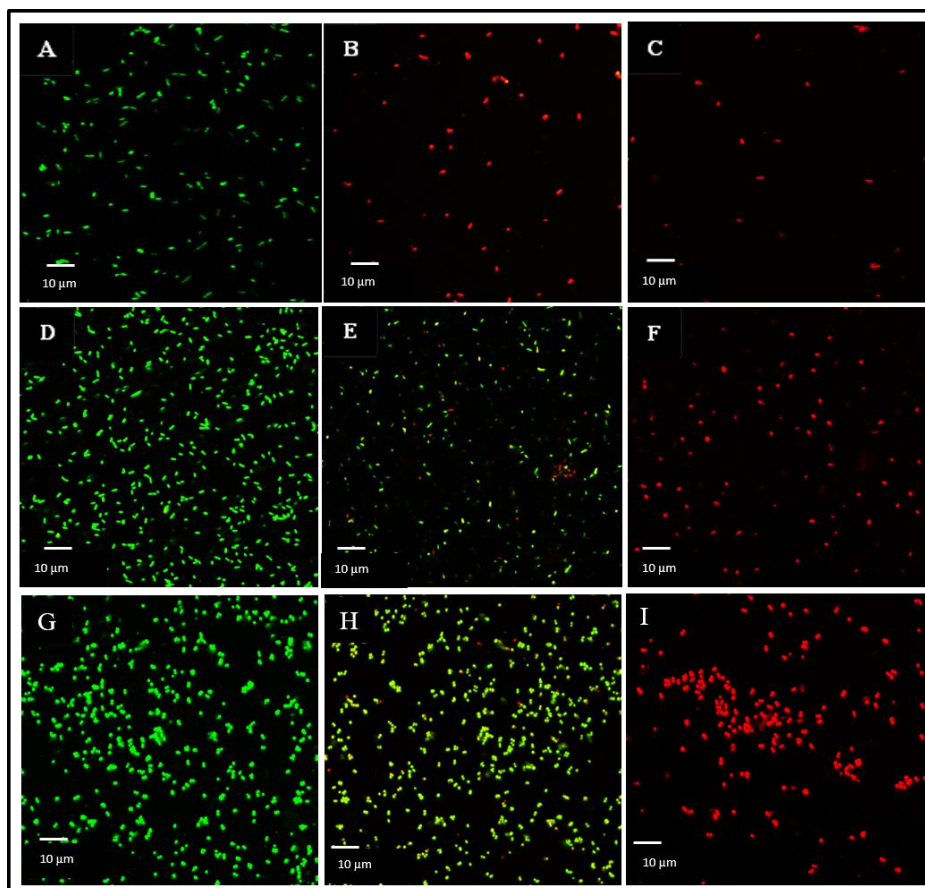


Figure 4.3 Effect of PuroA on membrane integrity of *L. monocytogenes*, *P. aeruginosa* and MRSA M173525 isolate after 1 h incubation.

A: *L. monocytogenes* control (no peptide); **B:** *L. monocytogenes* treated with PuroA at $1 \times \text{MIC}$; **C:** *L. monocytogenes* treated with PuroA at $2 \times \text{MIC}$; **D:** *P. aeruginosa* control (no peptide); **E:** *P. aeruginosa* treated with PuroA at $1 \times \text{MIC}$; **F:** *P. aeruginosa* treated with PuroA at $2 \times \text{MIC}$; **G:** MRSA control (no peptide); **H:** MRSA with PuroA at $1 \times \text{MIC}$; **I:** MRSA treated with PuroA at $2 \times \text{MIC}$. Cells appearing green indicate SYTO9 uptake; those appearing red indicate PI uptake. Images captured using confocal laser scanning microscopy. Scale bar 10 μm .

4.3.3 Effect of PuroA and its derivatives on the morphology of MRSA cells

SEM was utilized to visualize the effects of peptides on the morphology of MRSA planktonic cells. Exposing the cells to $1 \times \text{MIC}$ of peptides resulted in visible damage and pores were observed on the surface of some peptide-treated cells. Additionally, in some cells, there was extracellular material leaking from the cells, whereas control cells which were not exposed to peptide showed a regular cell shape with intact cell surface (Fig. 4.4).

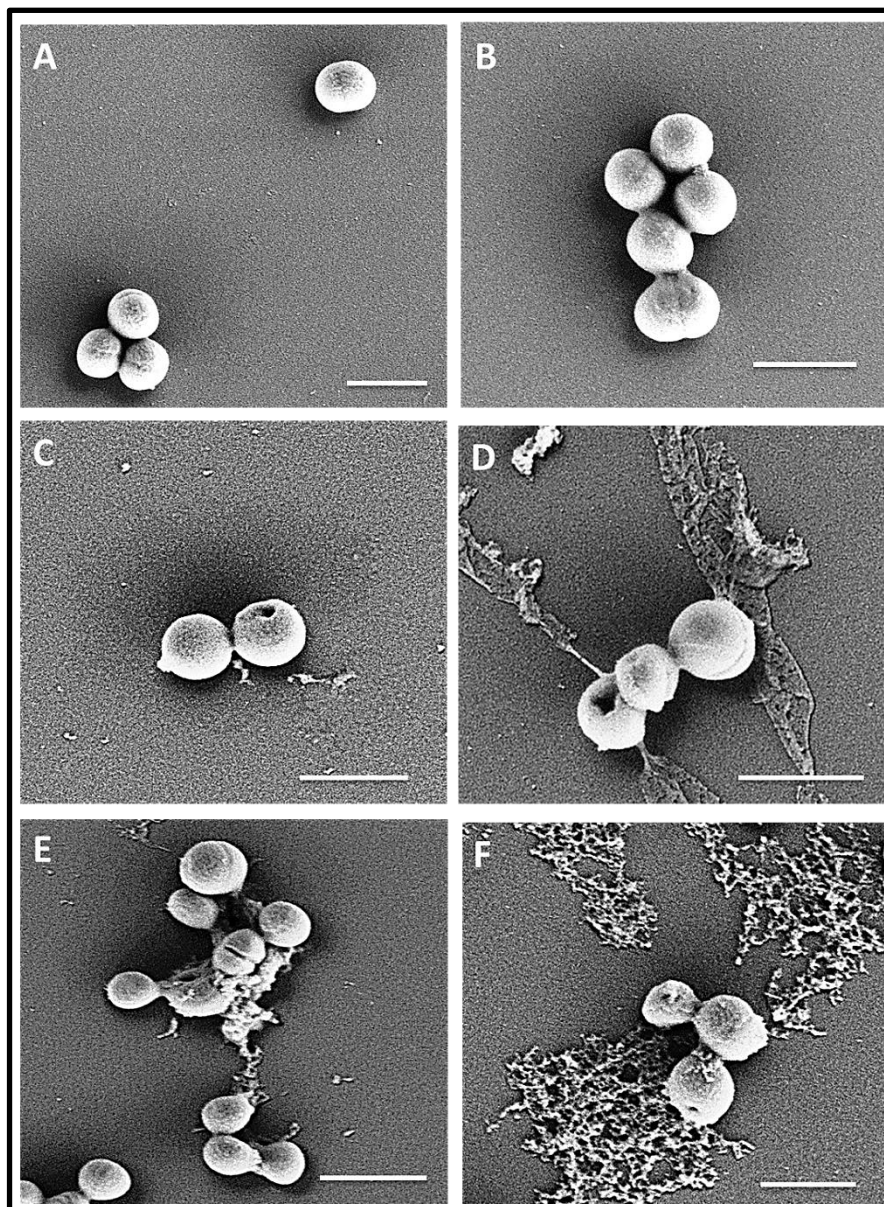


Figure 4.4 Scanning electronmicrographs of MRSA M173525 planktonic cells treated with peptides at $1 \times \text{MIC}$.

A & B. No-peptide control; **C.** P1 at $16 \mu\text{g/mL}$; **D.** PuroA at $16 \mu\text{g/mL}$; **E.** WW at $4 \mu\text{g/mL}$; **F.** WW7 at $8 \mu\text{g/mL}$. Magnifications $40,000\times$, scale bar $1 \mu\text{m}$.

4.3.4 Inhibitory activity of the peptides on biofilm formation

4.3.4.1 Inhibitory activity of the peptides on biofilm formation of *P. aeruginosa*, *L. monocytogenes* and *L. innocua*:

To determine whether the peptides could be used as potential anti-biofilm agents to prophylactically prevent colonization, we evaluated their effects at sub-inhibitory concentrations ($0.5 \times \text{MIC}$), inhibitory concentrations ($1 \times \text{MIC}$) and super-inhibitory concentrations ($2 \times \text{MIC}$) on both the initial cell adhesion by planktonic cells and 6 h preformed biofilms of *P. aeruginosa*, *L. monocytogenes* and *L. innocua* on polystyrene (MIC values obtained earlier, Table 4.1). This was carried out using two separate assays, crystal violet (CV) and methylthiazolyldiphenyl-tetrazolium (MTT) assays. CV assays indicated that the PIN peptides and PuroA derivatives inhibited the initial cell attachment by planktonic cells; e.g., Pina-M at $1 \times \text{MIC}$ reduced the biomass attachment by about 65% for *P. aeruginosa* and by more than 70% for *L. innocua* and *L. monocytogenes* (Table 4.2). The effect was dosage dependent; however, complete cell attachment inhibition could not be achieved even at $2 \times \text{MIC}$. Interestingly, the percentage inhibition of initial cell attachment did not vary considerably from $0.5 \times \text{MIC}$ to $2 \times \text{MIC}$ (Table 4.2). The peptides also showed time-dependant inhibition of preformed biofilms; e.g., Pina-M at $2 \times \text{MIC}$ inhibited only 47% of performed biofilm of *P. aeruginosa* after 1 h incubation, which increased to 74% after 20 h (Tables 4.3). The MTT assays confirmed significant anti-biofilm effects on both initial cell attachment and preformed biofilms. As assessed by MTT assays, PuroA at $2 \times \text{MIC}$ prevented the initial biomass attachment by 88%, 79% and 90% for *P. aeruginosa*, *L. monocytogenes* and *L. innocua*, respectively (Table 4.2), and 92% of preformed biofilms of all three bacteria after 20 h incubation (Tables 4.3). The observations indicate that the peptides penetrated the biofilms efficiently and killed the cells. However, the short derivatives of PuroA, W7 and WW, were less effective in eradication of preformed biofilms than the long peptides; as assessed by MTT assay. W7 peptide at $2 \times \text{MIC}$ showed 53% and 70% inhibition of preformed biofilms of *P. aeruginosa* and *L. monocytogenes*, respectively, after 20 h incubation whereas PuroA showed more than 90% eradication of preformed biofilms of both pathogens after the same incubation time.

Table 4.2 Inhibition of initial cell attachment by the TRPs

Peptide	Peptide concentration	Percentage of inhibition of initial cell attachment (%)					
		<i>P. aeruginosa</i> (ATCC 9027)		<i>L. innocua</i> (LI-451713/5)		<i>L. monocytogenes</i> (ATCC 13932)	
		CV	MTT	CV	MTT	CV	MTT
PuroA	0.5 × MIC	57 ± 5.6	59 ± 0.89	57 ± 5.0	80 ± 2.9	43 ± 4.2	55 ± 4.9
	1 × MIC	64 ± 4.1	75 ± 1.1	62 ± 3.6	85 ± 0.78	67 ± 6.5	74 ± 3.8
	2 × MIC	65 ± 4.4	88 ± 0.75	63 ± 7.5	90 ± 1.9	69 ± 5.9	79 ± 4.7
P1	0.5 × MIC	62 ± 2	83 ± 3.5	69 ± 6.3	80 ± 1.0	64 ± 2.6	72 ± 1.8
	1 × MIC	75 ± 0.5	90 ± 1.2	75 ± 5	89 ± 2.5	70 ± 4.5	79 ± 3.1
	2 × MIC	80 ± 3.4	91 ± 1.5	84 ± 2.5	92 ± 0.5	78 ± 4.1	88 ± 1.5
WW	0.5 × MIC	55 ± 3.0	70 ± 1.6	72 ± 7.0	77 ± 3.5	61 ± 3	71 ± 4.6
	1 × MIC	85 ± 2.7	92 ± 1.0	75 ± 9.2	85 ± 3.1	75 ± 2.5	79 ± 3.1
	2 × MIC	88 ± 3.1	93 ± 2.2	88 ± 4.5	90 ± 2.7	78 ± 6.4	86 ± 3.5
W7	0.5 × MIC	63 ± 6.2	80 ± 2.0	60 ± 7.4	72 ± 4.5	61 ± 3	70 ± 2.0
	1 × MIC	80 ± 3.5	89 ± 1.0	77 ± 2.0	81 ± 3.0	75 ± 2.5	79 ± 3.2
	2 × MIC	85 ± 1.4	90 ± 0.5	83 ± 3.5	87 ± 1.5	78 ± 6.4	86 ± 2.5
Pina-M	0.5 × MIC	64 ± 3.1	65 ± 1.5	63 ± 5.2	59 ± 0.99	50 ± 9.8	59 ± 2.1
	1 × MIC	67 ± 1.9	77 ± 1.3	66 ± 4.3	87 ± 1.6	57 ± 7.9	79 ± 0.6
	2 × MIC	65 ± 6.1	87 ± 2.1	74 ± 5.4	88 ± 2.4	72 ± 6.0	85 ± 1.7
Hina	0.5 × MIC	N/T	N/T	60 ± 6.3	81 ± 1.2	57 ± 2.9	57 ± 2.0
	1 × MIC	N/T	N/T	65 ± 6.6	86 ± 0.69	63 ± 3.1	75 ± 1.4
	2 × MIC	N/T	N/T	68 ± 4.7	89 ± 2.2	80 ± 7.4	81 ± 5.6
Indolicidin	0.5 × MIC	45 ± 0.99	60 ± 1.7	59 ± 6.4	50 ± 3.2	44 ± 5.5	54 ± 0.88
	1 × MIC	50 ± 1.6	74 ± 3.1	65 ± 3.8	83 ± 1.7	56 ± 2.9	69 ± 4.6
	2 × MIC	51 ± 2.5	84 ± 5.3	67 ± 3.2	86 ± 0.86	71 ± 3.6	76 ± 5.0

N/T: Not tested, as Hina did not showed inhibitory activity against planktonic cells of *P. aeruginosa* within the tested concentration (up to 250 µg/mL) as shown in table 4.1. Significant inhibitions ($p < 0.05$) were achieved with each peptide at each concentration in comparison to untreated control.

Table 4.3 Inhibition of preformed bacterial biofilms by PIN-based peptides at 1 h and 20h incubation

Peptide	Peptide concentration	% Inhibition of preformed biofilm											
		<i>P. aeruginosa</i> (ATCC 9027)				<i>L. innocua</i> (LI-451713/5)				<i>L. monocytogenes</i> (ATCC 13932)			
		1 h incubation		20h incubation		1 h incubation		20h incubation		1 h incubation		20h incubation	
		CV	MTT	CV	MTT	CV	MTT	CV	MTT	CV	MTT	CV	MTT
PuroA	0.5 × MIC	33 ± 2.1	33 ± 1.4	32.5 ± 9.2	57 ± 4.9	26 ± 5.8	31 ± 3.1	19 ± 6.0	41 ± 2.9	37 ± 6.5	45 ± 0.89	39 ± 7.0	48 ± 5.7
	1 × MIC	38 ± 5.6	49 ± 5.5	59 ± 7.5	71 ± 4.0	35 ± 7.1	53 ± 2.9	30 ± 7.6	55 ± 0.88	46 ± 6.4	53 ± 3.4	72 ± 2.9	81 ± 2.5
	2 × MIC	41 ± 9.7	83 ± 3.4	77 ± 7.7	92 ± 1.6	44 ± 6.4	91 ± 3.0	41 ± 5.3	92 ± 0.76	65 ± 3.9	79 ± 2.9	79 ± 4.3	91 ± 0.9
P1	0.5 × MIC	43 ± 4.0	50 ± 2.5	40 ± 8.5	51 ± 3.6	55 ± 5.0	64 ± 6.8	48 ± 6.7	55 ± 4.5	46 ± 7.0	45 ± 1.9	45 ± 6.5	48 ± 5.0
	1 × MIC	48 ± 2.9	59 ± 4.0	49 ± 6.7	63 ± 2.5	64 ± 6.7	69 ± 2.9	54 ± 7.0	70 ± 2.9	60 ± 4.8	59 ± 3.5	60 ± 3.9	61 ± 2.5
	2 × MIC	52 ± 6.0	63 ± 3.4	61 ± 5.0	75 ± 1.7	83 ± 6.5	81 ± 2.5	74 ± 4.7	82 ± 3.5	73 ± 5.5	70 ± 2.5	77 ± 1.7	80 ± 4.9
WW	0.5 × MIC	29 ± 7.3	42 ± 3.8	39 ± 6.4	58 ± 4.2	54 ± 3.9	63 ± 5.1	47 ± 6.4	54 ± 3.6	49 ± 2.5	43 ± 5.3	44 ± 5.0	47 ± 5.7
	1 × MIC	35 ± 5.9	50 ± 1.5	55 ± 7.8	67 ± 3.4	65 ± 6.7	72 ± 4.6	61 ± 5.5	74 ± 2.4	52 ± 6.6	55 ± 3.0	65 ± 7.5	68 ± 2.8
	2 × MIC	43 ± 9.3	55 ± 5.5	63 ± 5.8	73 ± 3.0	72 ± 7.5	78 ± 1.9	78 ± 6.9	82 ± 4.0	62 ± 4.1	67 ± 4.9	76 ± 3.4	75 ± 4.9
W7	0.5 × MIC	12 ± 8.9	15 ± 6.4	29 ± 7.3	40 ± 2.0	35 ± 3.2	42 ± 6.0	35 ± 7.2	48 ± 3.7	38 ± 8.5	35 ± 6.8	39 ± 6.0	40 ± 3.0
	1 × MIC	15 ± 6.5	20 ± 4.5	37 ± 5.0	45 ± 7.0	40 ± 6.7	53 ± 2.9	50 ± 2.8	59 ± 8.5	44 ± 6.7	49 ± 3.7	52 ± 2.5	51 ± 5.8
	2 × MIC	33 ± 4.9	35 ± 6.0	42 ± 8.2	53 ± 6.4	59 ± 3.0	60 ± 5.7	69 ± 4.5	76 ± 2.5	62 ± 3.6	55 ± 2.5	66 ± 8.0	70 ± 2.9
Pina-M	0.5 × MIC	34 ± 6.7	35 ± 0.9	44 ± 6.9	62 ± 2.1	23 ± 3.8	30 ± 1.7	29 ± 4.1	32 ± 3.9	47 ± 2.7	49 ± 3.3	36 ± 6.6	40 ± 8.0
	1 × MIC	40 ± 8.2	53 ± 1.1	57 ± 5.8	72 ± 2.8	38 ± 3.8	53 ± 0.9	40 ± 5.9	75 ± 3.0	52 ± 8.2	56 ± 0.91	58 ± 2.1	75 ± 1.9
	2 × MIC	47 ± 7.1	89 ± 1.9	74 ± 3.1	90 ± 1.1	48 ± 6.9	88 ± 4.7	65 ± 0.9	94 ± 1.1	71 ± 5.5	82 ± 4.0	84 ± 3.5	89 ± 1.0
Hina	0.5 × MIC	N/T	N/T	N/T	N/T	20 ± 1.9	21 ± 1.5	26 ± 7.0	37 ± 1.9	19 ± 7.0	22 ± 5.2	35 ± 6.5	41 ± 2.0
	1 × MIC	N/T	N/T	N/T	N/T	25 ± 6.2	48 ± 1.1	33 ± 8.3	50 ± 3.5	28 ± 6.8	40 ± 3.0	59 ± 7.9	65 ± 1.0
	2 × MIC	N/T	N/T	N/T	N/T	46 ± 7.8	86 ± 2.3	40 ± 2.9	90 ± 2.0	59 ± 8.1	73 ± 1.6	71 ± 5.4	90 ± 2.2
Indolicidin	0.5 × MIC	30 ± 6.5	26 ± 3.1	30 ± 8.7	56 ± 5.0	21 ± 0.8	30 ± 3.5	25 ± 5.7	38 ± 5.9	18 ± 6.2	20 ± 2.7	34 ± 8.9	39 ± 3.2
	1 × MIC	33 ± 3.8	35 ± 2.7	55 ± 8.4	69 ± 1.3	28 ± 6.4	47 ± 3.2	32 ± 5.0	49 ± 2.4	28 ± 6.9	31 ± 6.1	51 ± 7.4	55 ± 3.0
	2 × MIC	36 ± 4.5	82 ± 4.1	59 ± 5.4	89 ± 2.0	38 ± 2.9	85 ± 1.8	54 ± 9.9	91 ± 2.0	59 ± 7.1	65 ± 0.79	64 ± 9.1	88 ± 2.5

N/T: Not tested, as Hina did not showed inhibitory activity against planktonic cells of *P. aeruginosa* within the tested concentration (up to 250 µg/mL) as shown in table 4.1. Significant inhibitions ($p < 0.05$) were achieved with each peptide at each concentration in comparison to untreated control.

4.3.4.2 Biofilm susceptibility testing by static chamber assay

The anti-biofilm activity of PuroA was confirmed by confocal microscopy of *P. aeruginosa* and *L. monocytogenes* biofilm grown on the surface of the bottom glass slide of a static chamber and stained with SYTO9 and PI. As shown in Figure 4.5, the biofilm biomass of both bacteria was remarkably reduced in the presence of the peptide, confirming that 6 h preformed biofilm of *P. aeruginosa* and *L. monocytogenes* were not resistant to PuroA peptide.

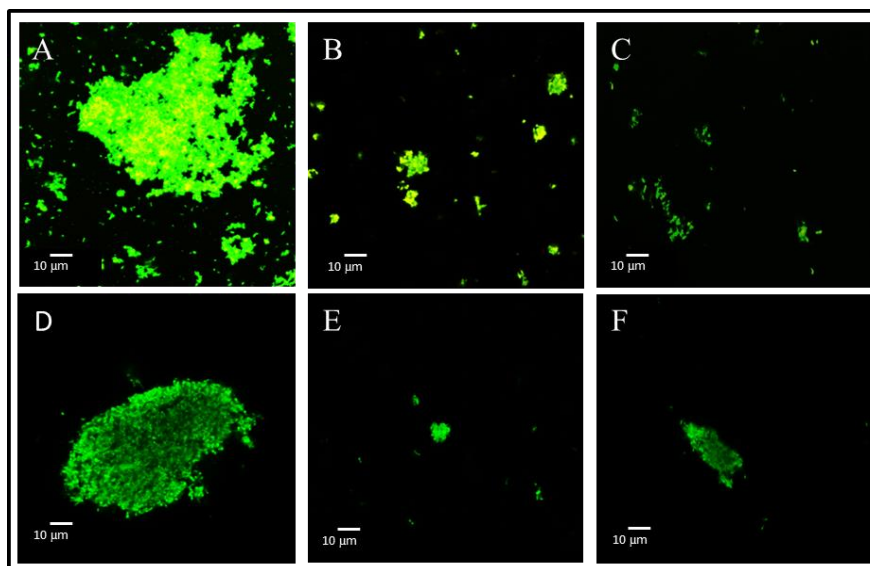


Figure 4.5 Anti-biofilm activity of PuroA .

(A) 6 h-old *P. aeruginosa* biofilm; (B) after treatment with PuroA at $1 \times \text{MIC}$; (C) after treatment with PuroA at $2 \times \text{MIC}$; (D) 6 h-old *L. monocytogenes* biofilm; (E) after treatment with PuroA at $1 \times \text{MIC}$; (F) after treatment with PuroA at $2 \times \text{MIC}$. Bar = 10 μm .

4.3.4.3 Inhibition of initial cell attachment on high density polyethylene surfaces (HDPE)

Since the peptides showed significant inhibition of initial cell attachment on polypropylene surface for all tested bacteria, further studies were undertaken to investigate its effect on an additional abiotic surface (HDPE). An initial inoculum of 10^6 CFU mL^{-1} resulted in an average of $4.12 \log \text{ CFU mL}^{-1}$ (*L. monocytogenes*) and $4.26 \log \text{ CFU mL}^{-1}$ (*P. aeruginosa*) adhered cells after 24 h incubation. The inhibition of attachment at the MIC of Pina-M exhibited as a logarithmic (log) reduction in the initial number of cells attached to HDPE and the final number of attached cells after treatment with the peptide. The results indicate that the log reduction was comparable

between the two bacteria. However, the inhibitory effect of Pina-M was more prominent on *P. aeruginosa* (Table 4.4).

Table 4.4 Inhibition of cell attachment to high density polyethylene surface by Pina-M peptide

Organism	log-reduction
<i>P. aeruginosa</i>	2.86 ± 0.12
<i>L. monocytogenes</i>	2.54 ± 0.09

4.3.4.4 Effects of PuroA and its derivatives on biofilm of clinical MRSA isolate

The inhibitory activity of PuroA and its most active derivatives (selected based on the results of Chapter 3) on both the initial cell attachment and 6 h preformed biofilms of MRSA on polystyrene was assessed using CV and MTT assays at $0.5 \times \text{MIC}$, $1 \times \text{MIC}$, and $2 \times \text{MIC}$. To do this, we selected MRSA M173525 isolate. Overall, the adhesiveness of MRSA cells was considerably affected by the peptides, regardless of the concentration used (Table 4.5). The percentage inhibition of initial cell attachment did not vary considerably from $0.5 \times \text{MIC}$ to $2 \times \text{MIC}$ (Table 4.5). PuroA at $0.5 \times \text{MIC}$ reduced the biomass attachment by about 72% and penetrated the biofilms efficiently and killed 92 % of the cells as assessed by MTT assay. At $2 \times \text{MIC}$, the biomass attachment and cell viability reduced by 79% and 95%, respectively. With regards to the ability to eradicate preformed immature 6 h biofilms, all peptides showed an overall comparable activity and significantly reduced the biomass and the viability of biofilms formed, regardless of concentration tested.

The ability of P1 peptide to inhibit initial cell attachment and biofilm formation of MRSA M173525 isolate was confirmed by confocal microscopy. Biofilm was grown on the surface of the bottom glass slide of a static chamber in the presence and absence of the peptide and then attached biofilm stained with SYTO9 and PI (Fig. 4.6).

Table 4.5 Inhibition of initial cell attachment and preformed biofilms of MRSA by PuroA and its derivatives peptides

Peptide	Peptide concentration	Percentage of inhibition of initial MRSA cells attachment		% Inhibition of preformed 6 h MRSA biofilm at 1 h incubation	
		CV	MTT	CV	MTT
PuroA	0.5 × MIC	70 ± 5.6	92 ± 1.5	68 ± 9.2	90 ± 2.5
	1 × MIC	75 ± 4.0	95 ± 1.1	75 ± 7.5	92 ± 4.0
	2 × MIC	79 ± 4.5	95 ± 0.5	77 ± 7.0	95 ± 2.6
P1	0.5 × MIC	72 ± 3.1	92 ± 3.0	70 ± 6.9	93 ± 5.0
	1 × MIC	75 ± 1.9	95 ± 2.3	74 ± 5.8	95 ± 3.8
	2 × MIC	78 ± 6.1	95 ± 2.5	78 ± 3.1	95 ± 4.0
W7	0.5 × MIC	69 ± 3.6	90 ± 2.9	67 ± 6.0	88 ± 2.5
	1 × MIC	75 ± 5.0	95 ± 4.0	75.5 ± 3.0	90 ± 4.7
	2 × MIC	76 ± 4.8	96 ± 1.5	75 ± 5.5	94 ± 0.5
WW	0.5 × MIC	71.5 ± 3.5	90 ± 2.0	69 ± 7.8	91 ± 3.0
	1 × MIC	73 ± 6.2	95 ± 3.1	71 ± 4.5	92 ± 3.5
	2 × MIC	79 ± 7.5	96 ± 0.5	74 ± 2.0	95 ± 1.7

Significant inhibitions ($p < 0.05$) were achieved with each peptide at each concentration in comparison to untreated control.

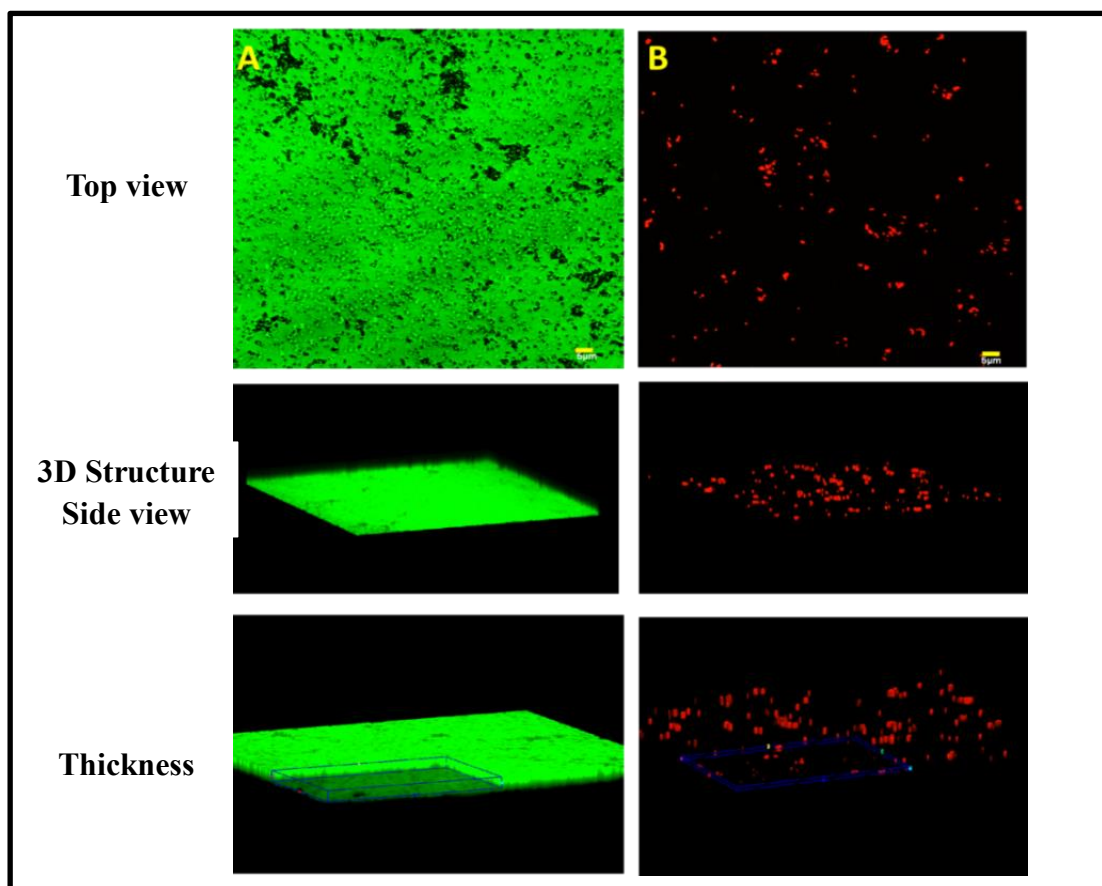


Figure 4.6 The activity of P1 on initial adhesion and biofilm formation of the clinical MRSA M173525 isolate.

The biofilms were visualized by confocal laser scanning microscopy with the Live/Dead viability stain (SYTO9/PI); the viable cells exhibit green fluorescence, whereas dead cells exhibit red fluorescence. **A.** No-peptide control; **B.** P1 at 16 µg/mL. Magnifications 1,000×, scale bar 5 µm.

The ability of P1 peptide to inhibit initial cell adhesion of MRSA M173525 isolate was also visualised using SEM. The peptide remarkably reduced the cell attachment to the surface of the glass slide and any attached cells looked damaged with pores on their surface (Fig. 4.7).

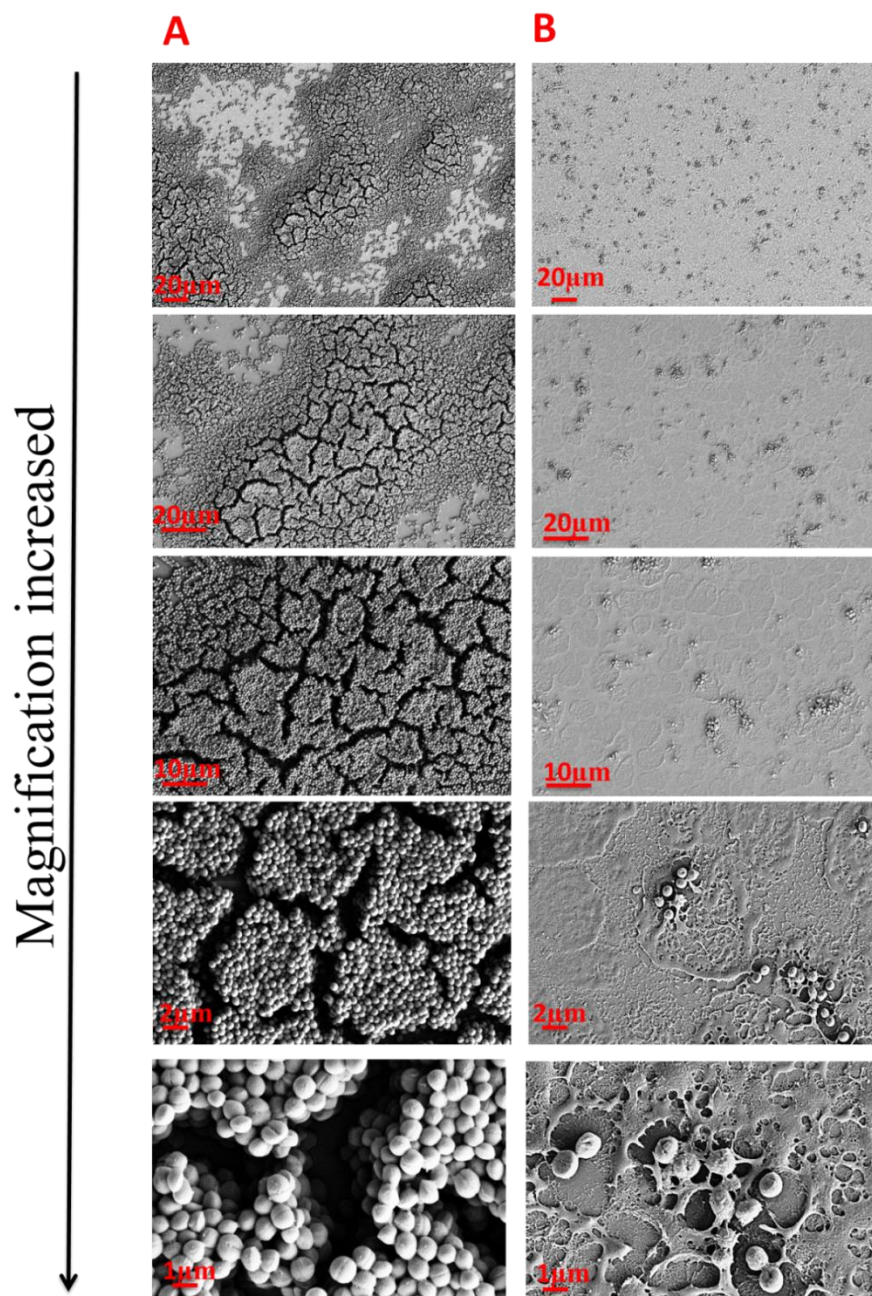


Figure 4.7 Scanning electronmicrographs of the effect of P1 on initial adhesion of the clinical MRSA M173525 isolate at $1 \times \text{MIC}$.

A. No-peptide control; B. P1 at $16 \mu\text{g/mL}$.

4.3.5 Sporicidal activity of the peptides:

TRPs based of PINA and HINA, as well as PuroA analogs and indolicidin, were investigated for their abilities to decrease the viability of *B. subtilis* spores. PuroA, Hina, Pina-M, P1 and indolicidin exhibited a similar level of sporicidal activity; reducing the number of viable spores by approximately 2 to 3 log units after 1 day of exposure. However, the sporicidal activity was reduced by 75% in case of PuroB. W7 and WW showed less sporicidal activity than PuroA peptide, particularly at concentrations of $\leq 64 \mu\text{g/ml}$. The activity positively correlated with peptide concentration and exposure time; higher concentrations (up to $500 \mu\text{g mL}^{-1}$) and longer exposure (up to a week) reduced the number of viable spores by about 4 log units (Table 4.6).

Table 4.6 Sporicidal Activity of the Peptides

Peptide ID	Peptide concentration	1 day	1 week
		Log Reduction *	Log Reduction *
PuroA	500 $\mu\text{g/ml}$	1.95 \pm 0.35	3.9 \pm 0.21
	250 $\mu\text{g/ml}$	1.60 \pm 0.14	3.1 \pm 0.42
	125 $\mu\text{g/ml}$	1.45 \pm 0.21	2.45 \pm 0.07
	64 $\mu\text{g/ml}$	0	2.2 \pm 0.28
	32 $\mu\text{g/ml}$	0	1.6 \pm 0.14
	16 $\mu\text{g/ml}$	0	1.2 \pm 0.21
P1	500 $\mu\text{g/ml}$	3.8 \pm 0.29	4.0 \pm 0.29
	250 $\mu\text{g/ml}$	3.4 \pm 0.29	3.5 \pm 0.29
	125 $\mu\text{g/ml}$	2.7 \pm 0.29	2.7 \pm 0.29
	64 $\mu\text{g/ml}$	2.2 \pm 0.29	2.3 \pm 0.29
	32 $\mu\text{g/ml}$	1.5 \pm 0.29	2.1 \pm 0.29
	16 $\mu\text{g/ml}$	0.5 \pm 0.29	1.7 \pm 0.29
W7	500 $\mu\text{g/ml}$	3.0 \pm 0.29	3.1 \pm 0.29
	250 $\mu\text{g/ml}$	2.5 \pm 0.29	2.5 \pm 0.29
	125 $\mu\text{g/ml}$	1.5 \pm 0.29	1.8 \pm 0.29
	64 $\mu\text{g/ml}$	0	1.15 \pm 0.29
	32 $\mu\text{g/ml}$	0	0.7 \pm 0.29
	16 $\mu\text{g/ml}$	0	0
WW	500 $\mu\text{g/ml}$	2.5 \pm 0.29	2.6 \pm 0.29
	250 $\mu\text{g/ml}$	2.2 \pm 0.29	2.2 \pm 0.29
	125 $\mu\text{g/ml}$	1.8 \pm 0.29	1.9 \pm 0.29
	64 $\mu\text{g/ml}$	1.0 \pm 0.29	1.4 \pm 0.29
	32 $\mu\text{g/ml}$	0.5 \pm 0.29	1.1 \pm 0.29
	16 $\mu\text{g/ml}$	0	0.9 \pm 0.29

Table 4.6 continued

Peptide ID	Peptide concentration	1 day	1 week
		Log Reduction *	Log Reduction *
Pina-M	500 μ g/ml	3.5 \pm 0.29	3.9 \pm 0.29
	250 μ g/ml	2.7 \pm 0.24	3.2 \pm 0.35
	125 μ g/ml	2.5 \pm 0.35	2.7 \pm 0.42
	64 μ g/ml	2.3 \pm 0.28	2.5 \pm 0.14
	32 μ g/ml	1.2 \pm 0.21	1.6 \pm 0.25
	16 μ g/ml	0.2 \pm 0.01	0.3 \pm 0.28
PuroB	500 μ g/ml	0.55 \pm 0.21	1.7 \pm 0.07
	250 μ g/ml	0.35 \pm 0.14	1.4 \pm 0.16
	125 μ g/ml	0.05 \pm 0.02	1.1 \pm 0.20
	64 μ g/ml	0	0.8 \pm 0.21
	32 μ g/ml	0	0.5 \pm 0.23
	16 μ g/ml	0	0.4 \pm 0.17
PuroA + PuroB	500 μ g/ml of each peptide	3.31 \pm 0.11	3.48 \pm 0.16
	250 μ g/ml of each peptide	2.65 \pm 0.21	3.10 \pm 0.28
	125 μ g/ml of each peptide	1.75 \pm 0.21	1.85 \pm 0.21
	64 μ g/ml of each peptide	1.05 \pm 0.35	1.7 \pm 0.21
	32 μ g/ml of each peptide	0.05 \pm 0.02	1.00 \pm 0.28
	16 μ g/ml of each peptide	0.03 \pm 0.01	0.75 \pm 0.21
Hina	500 μ g/ml	2.1 \pm 0.56	3.8 \pm 0.29
	250 μ g/ml	1.7 \pm 0.24	2.95 \pm 0.35
	125 μ g/ml	1.55 \pm 0.35	2.2 \pm 0.42
	64 μ g/ml	0.7 \pm 0.28	1.8 \pm 0.14
	32 μ g/ml	0.25 \pm 0.21	1.35 \pm 0.25
	16 μ g/ml	0.02 \pm 0.01	0.9 \pm 0.28
Indolicidin	500 μ g/ml	3.3 \pm 0.35	3.6 \pm 0.21
	250 μ g/ml	2.8 \pm 0.14	3.0 \pm 0.42
	125 μ g/ml	2.4 \pm 0.21	2.6 \pm 0.07
	64 μ g/ml	2.2 \pm 0.28	2.35 \pm 0.28
	32 μ g/ml	1.25 \pm 0.28	1.4 \pm 0.14
	16 μ g/ml	0.25 \pm 0.28	0.4 \pm 0.21
	Negative control	0	0

* Averages and standard deviations of three independent experiments.

SEM was utilized to visualize the effects of peptides on spore morphology. Exposure to 250 μ g/mL of peptides resulted in visible damage, treated spores appearing shrivelled and deflated with some leakage of intracellular material. Interestingly, there was no difference in the appearance of spores treated for 24 h or 1 week. Further, spores treated with 0.01% glacial acetic acid were indistinguishable from untreated controls, indicating that the solvent alone had little effect on spore viability and the altered appearance of peptide-treated spores was attributable to the peptides.

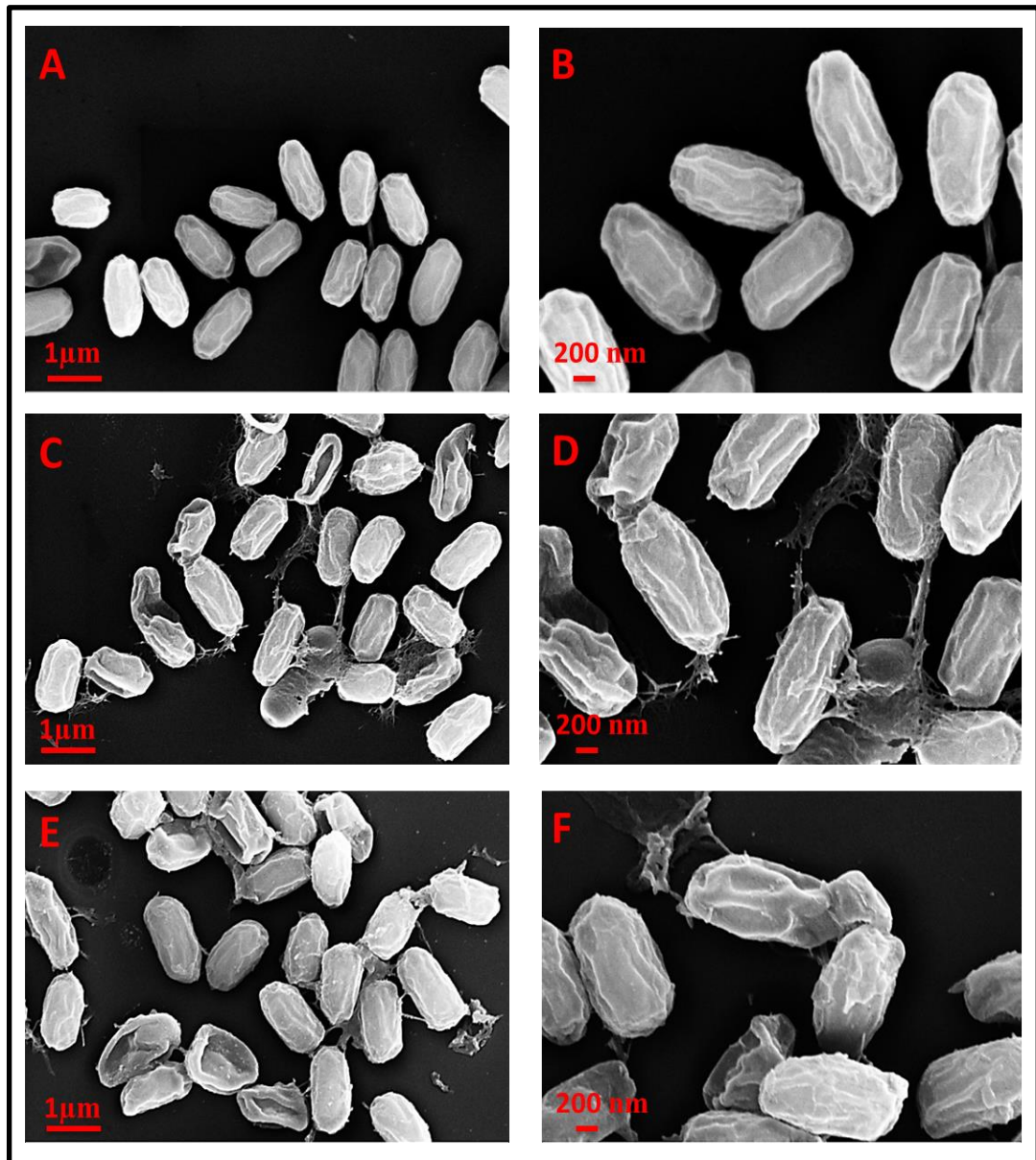


Figure 4.8 SEM analysis of *B. subtilis* spores treated with PuroA peptide. A and B untreated *B. subtilis* spores; C and D treated spores with PuroA for one day; E and F treated spores with PuroA for one week. Magnifications are 2000× in A, C and E, and are 4000× in B, D and F.

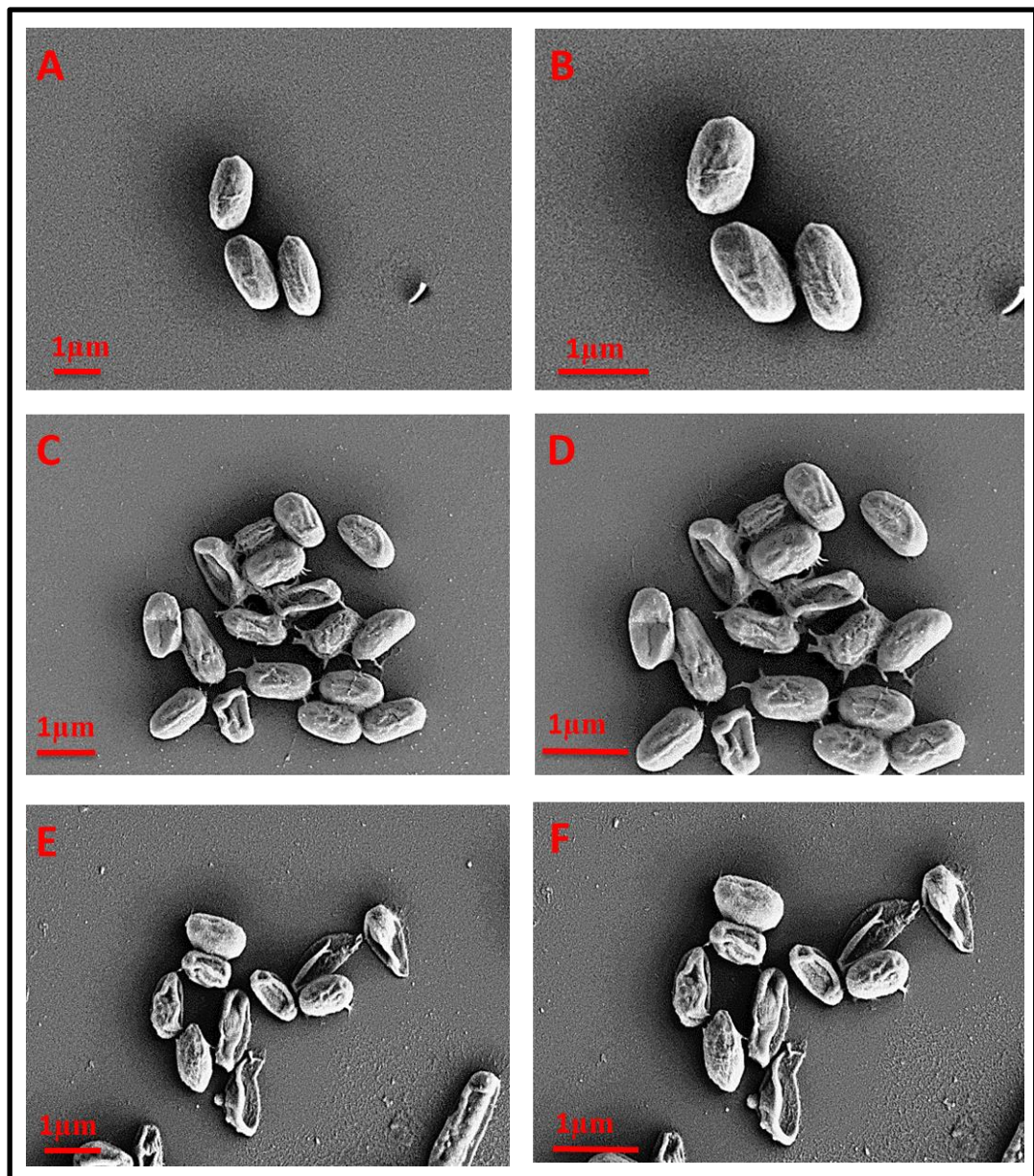


Figure 4.9 SEM analysis of *B.subtilis* spores treated with P1 peptide.

A and B untreated *B.subtilis* spores; C and D treated spores with P1 for one day; E and F treated spores with P1 for one week. Magnifications are 3000× in A, C and E, and are 4000× in B, D and F.

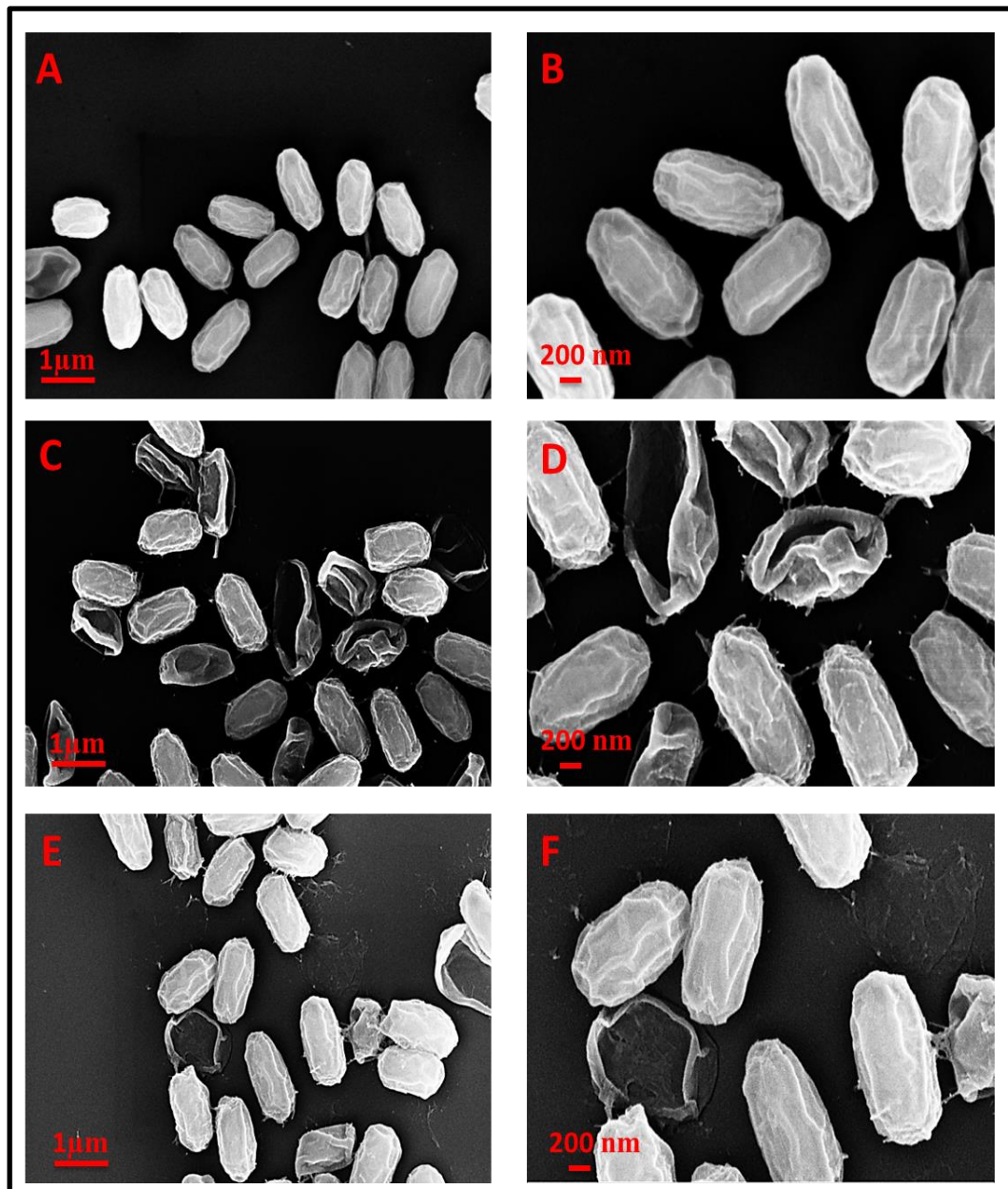


Figure 4.10 SEM analysis of *B. subtilis* spores treated with PuroB peptide.

A and B untreated *B. subtilis* spores; C and D treated spores with PuroB for one day; E and F treated spores with PuroB for one week. Magnifications are 2000 \times in A, C and E, and are 4000 \times in B, D and F.

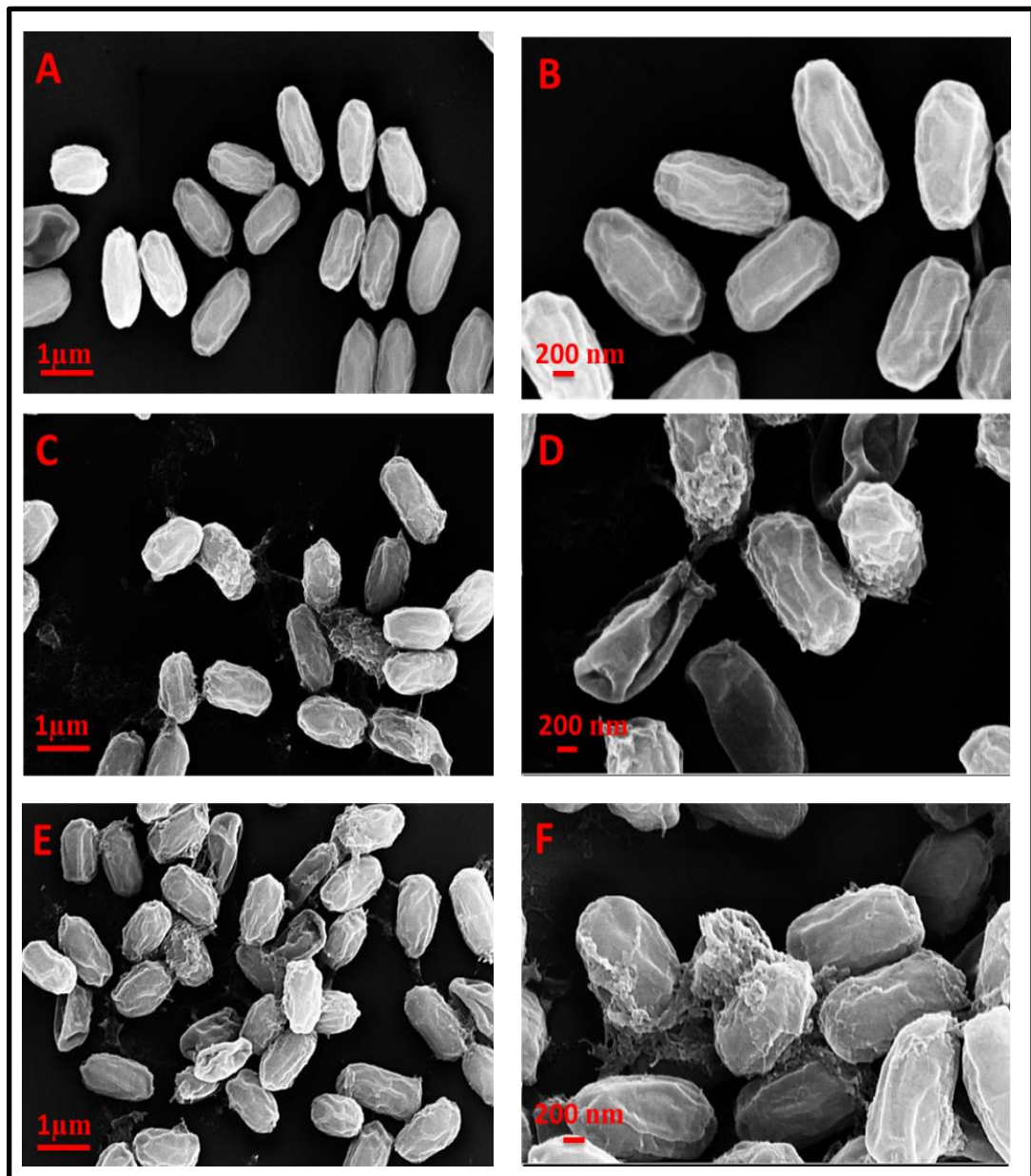


Figure 4.11 SEM analysis of *B.subtilis* spores treated with Hina peptide. A and B untreated *B.subtilis* spores; C and D treated spores with Hina for one day; E and F treated spores with Hina for one week. Magnifications are 2000× in A, C and E, and are 4000× in B, D and F.

4.3.6 Effect of the TRPs on the outgrowth of *B. subtilis* spores

To obtain additional insights into the effects of peptides on spores, the extended growth of spore cultures in MHB was monitored in the presence or the absence of selected peptides which showed high sporicidal activity (Table 4.6). Examination of these cultures after 24 h by DIC microscopy revealed no vegetative bacilli were present within cultures supplemented with $\geq 125 \mu\text{g/ml}$ peptides; the peptides prevented *B.subtilis* spores development into vegetative bacilli. Whereas characteristic chains of vegetative bacilli were present in cultures supplemented with $\leq 125 \mu\text{g/ml}$ peptides and in no peptide control (Fig. 4.12).

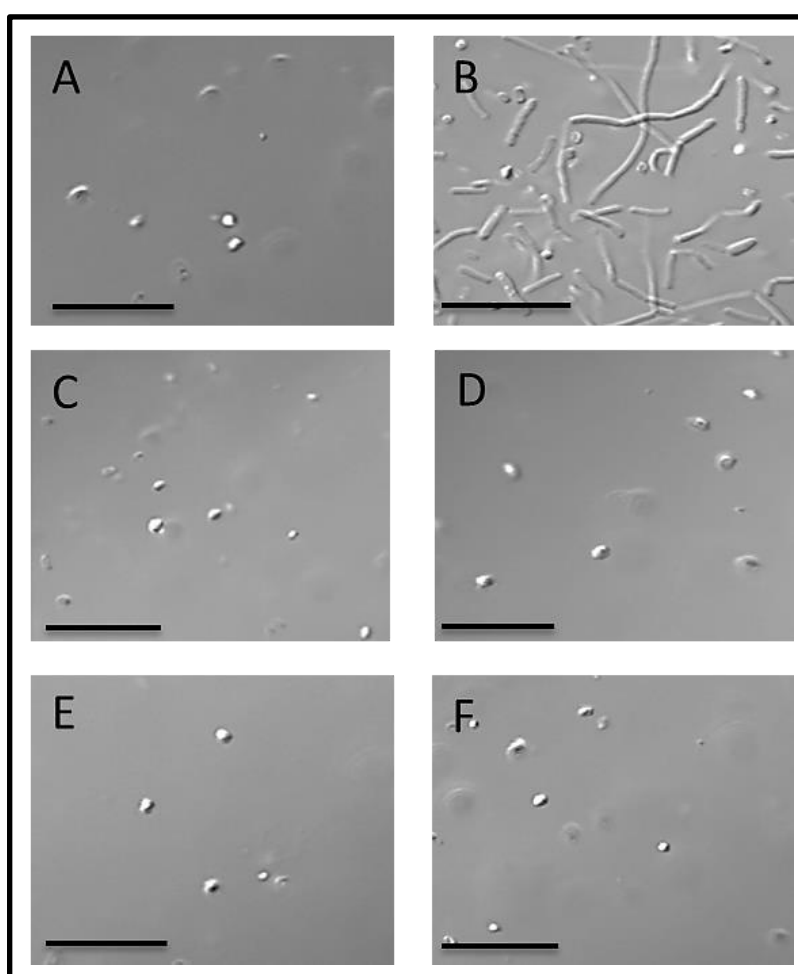


Figure 4.12 Effect of the TRPs on the outgrowth of *B. subtilis* spores.

At time zero and 24 h, samples were removed and visualized by DIC microscopy. **A.** Untreated spores at zero time; **B.** Untreated spores after 24 h incubation in MHB; **C.** Treated spores with $125 \mu\text{g/mL}$ of PuroA after 24 h treatment; **D.** Treated spores with $125 \mu\text{g/mL}$ of P1 after 24 h treatment; **E.** Treated spores with $125 \mu\text{g/mL}$ of Pina-M after 24 h treatment; **F.** Treated spores with $125 \mu\text{g/mL}$ of Hina after 24 h treatment. All samples visualised at $1000\times$ magnification. Bars, $10 \mu\text{m}$.

4.3.7 Effect of peptides on membrane integrity of *B. subtilis* spores. The increase in membrane permeability of the bacteria spores after treatment with peptides was assessed using the LIVE/DEAD *BacLight* Bacterial Viability Kit and fluorescence confocal microscopy. This experiment revealed that incubating *B. subtilis* spores with $\geq 125 \mu\text{g/ml}$ of PuroA and P1 peptides induced a disruption of membrane integrity as revealed by a large PI uptake by spores. Whereas the shorter peptides, WW and W7, could not disrupt the integrity of spore membranes and, therefore, the PI uptake was much less compared to the longer peptides as shown in Figure 4.13.

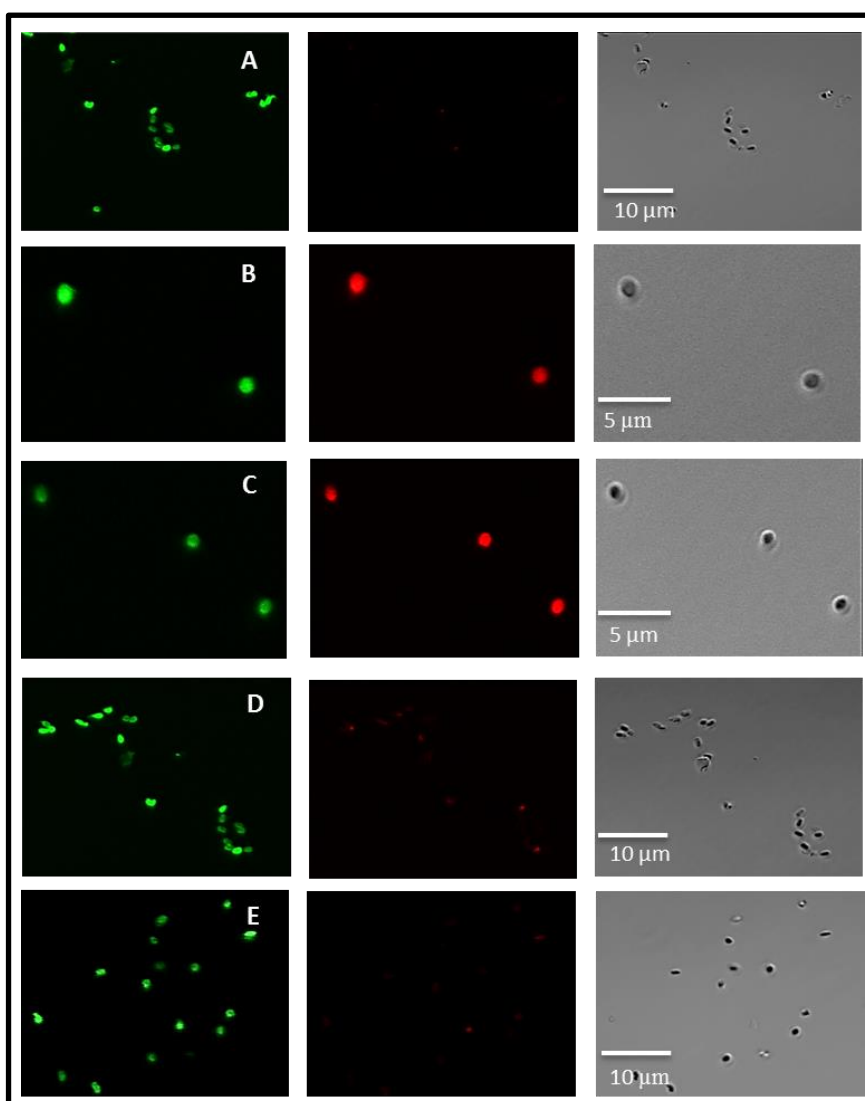


Figure 4.13 Effect of peptides on membrane integrity of *B. subtilis* spores. **A.** Untreated spores; **B.** Treated spores with $125 \mu\text{g/mL}$ of PuroA after 24 h treatment; **C.** Treated spores with $125 \mu\text{g/mL}$ of P1 after 24 h treatment; **D.** Treated spores with $125 \mu\text{g/mL}$ of W7 after 24 h treatment; **E.** Treated spores with $125 \mu\text{g/mL}$ of WW after 24 h treatment.

4.4 Discussion

Cationic Trp-rich AMPs (TRPs) have attracted attention in the last decades due to their rapid action, prospective potency, and broad spectrum of activities against bacteria, fungi, viruses and/or parasites. The antimicrobial activity of the cationic TRPs derived from natural sources, such as indolicidin from bovine neutrophils, tritrypticin from porcine bone marrow and lactoferricin from bovine milk, have been explored widely, as discussed in Chapter 1, Section 1.4. However, the antimicrobial activity of PINs and HINs is little explored as yet. Synthetic peptides designed based on the TRDs of wheat PINA, PINB proteins and barley HINA protein were tested for antibacterial activity against clinically and industrially important Gram-negative and Gram-positive bacteria; *P. aeruginosa*, *L. innocua*, *L. monocytogenes* and *B. subtilis*. A number of PuroA analogs were also tested against these pathogens and two clinical MRSA isolates. Pina-M with mutant PINA at the TRD (Pro-35 to Ser) (Chen et al. 2006), detailed in Chapter 1, Section 1.6, had higher inhibitory effect on all tested bacteria compared to PuroA, PuroB and Hina, supporting the suggestion that the replacement of the cyclic side-chain of Pro with a smaller one could allow the adjacent aromatic Phe to penetrate the lipid membrane deeper. Similar to Trp, Phe is favoured for membrane partitioning (Wimley & White 1996). Hina had no antibacterial activity against *P. aeruginosa*. The likely reason for this may be the substitution of the basic residue Lys (Lys42 of PINA) with an uncharged Thr in Hina, as decreasing the positive charge can significantly affect the antimicrobial activity of an AMP (Nagpal et al. 1999; Giangaspero et al. 2001; Pasupuleti et al. 2008). The PuroA analog, P1 with six Trp residues and replacement of the uncharged amino acids with the basic residues Arg and Lys, showed higher antibacterial activity against *P. aeruginosa* by 4-fold and *L. innocua* by 2-fold. In addition, the short PuroA variants, W7 with five Trp residues and WW with six Trp residues, derived from the Trp-, Arg- and Lys-rich center of PuroA, showed higher antibacterial activity against all tested pathogens than the parent PuroA. These results emphasize the importance of Trp residues and basic amino acids in the antibacterial activity of AMPs. Our results also support the previous studies that have showed that the conserved (RW) motifs retains antimicrobial activity of the parent peptide. For example, the 6-mer peptide, RRWQWR-NH₂, showed the same antibacterial activity as the 25 residue bovine lactoferricin (LfcinB, FKXRRWQWRMKKLGAPSITXVRRAF) (Tomita et al. 1994). Also, the 8-mer,

WPWWPWRR-NH₂ showed similar activity as indolicidin, LPWKWPWWPWRR-NH₂, against *Micrococcus luteus* (Staubitz et al. 2001).

The mode of action of AMPs involves disrupting the physical integrity of bacterial membranes and/or targeting key intracellular components or processes (Hancock & Sahl 2006). The mechanism of action of PuroA is extensively studied later in Chapter 5, however, in the current Chapter, the effect of PuroA on the membranes of the tested pathogens was examined. PuroA appeared to have damaged the integrity of cell membranes, induced membrane permeabilization and PI influx in *L. innocua* and *L. monocytogenes* at 1 × MIC and in *P. aeruginosa* and MRSA at 2 × MIC. After 1 h of incubation, at 1 × MIC, PuroA did not permeabilize the membranes of *P. aeruginosa* and MRSA. Disturbing the membrane integrity might need a longer exposure (more than 1 h) at lower peptide concentrations, whereas higher concentration made the process of pore formation and membrane disruption happen sooner, as the peptide-treated MRSA cells for 3 h appeared to have pronounced pore-like structures in the membrane under SEM. These observations indicate that the membrane-disrupting property of PuroA depends on the membrane composition of the targeted cells, peptide concentrations and exposure time.

Bacterial endospores are highly resistant cells whose destruction requires exposure to high levels of chemicals or heat (Russell 1990; Setlow 2006; Leggett et al. 2012), which can be impractical in food and pharmaceutical industries. Therefore, it is crucial to find products that can replace or complement the current methods. Sporocidal activity of naturally occurring compounds such as essential oils and plant-derived products is well documented (Hara-Kudo et al. 2005; Cho et al. 2008; Lawrence & Palombo 2009; Nyegue et al. 2014). Moreover, the lantibiotic nisin, an antimicrobial peptide that is widely used as food preservative, showed a great ability to prevent the outgrowth of spores of several Gram-positive bacteria, including many *Bacillus* species like *Bacillus anthracis*, *Bacillus subtilis*, *Bacillus cereus*, *Bacillus mycoides*, and *Bacillus thuringiensis* (Montville et al. 2006; Gut et al. 2008). However, to our knowledge, our results give the first demonstration of sporocidal activity of TRPs. PuroA, P1, Pina-M, Hina and indolicidin showed greatest sporocidal activity. The short analogs, W7 and WW, were less effective against the endospores, especially at

low concentration and also they did not disrupt the integrity of spore membranes, suggesting that the peptide length is an important determinant for sporicidal activity of AMPs. SEM and membrane integrity analysis indicated that exposure of spores to the relatively longer peptides, PuroA, P1, Pina-M and Hina, resulted in visible damage and loss of intracellular material, suggesting that spore death was via irreversible disruption of their integrity, similar to that observed with strong acids (Setlow et al. 2002). *B. subtilis* spores are dormant and metabolically inactive (Stragier & Losick 1996) and incubating them with TRPs in the presence of germinant did not allow the spores to establish an active metabolism. These results show that TRPs inhibit *B. subtilis* spores outgrowth; they inhibit them from becoming metabolically active and developing into vegetative bacilli, however, the detailed modes of action of the peptides need to be further elucidated.

Some bacteria attach to natural and abiotic surfaces and encase themselves in a self-secreted polysaccharide matrix, forming a slimy layer called biofilm (Costerton et al. 1987). Biofilm formation is a two-stages process; an initial reversible (weak) attachment phase is followed by an irreversible (strong) attachment phase (Stoodley et al. 2002). Biofilm cells (sessile cells) differ phenotypically and physiologically from planktonic cells (non-adhered cells) (Hall-Stoodley et al. 2004). Biofilms cause very serious problems in the health sector (Høiby et al. 2010; Römling & Balsalobre 2012) and food industry (Kumar & Anand 1998; Simões et al. 2010), as they are very tolerant to antimicrobials and extreme physiological environments. Several mechanisms are believed to be involved in biofilm tolerance and resistance, including: slow or incomplete penetration of the antimicrobial agent into the biofilm; change of the chemical microenvironment within the biofilm (Stewart & Costerton 2001; Van Acker et al. 2014), and presence of a subpopulation of extremely tolerant slowly growing cells, called ‘persister cells’, that neither grow nor die by microbicidal antibiotics (Keren et al. 2004). Since most AMPs work on bacterial cell membranes, they might be more effective against these persister cells than antibiotics; however, the extracellular matrix could block their diffusion into biofilms (Lewis 2001; Otto 2006). Therefore, it is crucial to find AMPs that can penetrate preformed biofilms and kill the cells and/or condition the surfaces to make them unsuitable for bacterial cell attachment. Other TRPs such as lactoferrin (Singh et al. 2002) and indolicidin

(Overhage et al. 2008; Pompilio et al. 2011) showed a preventive effect on biofilm formation and development. In the current study, the anti-biofilm action of the TRPs peptides was tested on both the initial cell attachment of planktonic cells and on preformed biofilms (6 h) of clinically or commercially important pathogens, *P. aeruginosa*, *L. monocytogenes*, *L. innocua* and MRSA. *L. innocua* is a nonpathogenic strain usually used as a surrogate for studies on *L. monocytogenes* (Vaz-Velho et al. 2001; Oulahal et al. 2008). Two methods were used to evaluate the anti-biofilm activity of the peptides, MTT assay and CV assay. Both methods showed notable anti-biofilm activity exhibited by tested TRPs on inhibition of biofilms formation or the reduction of preformed biofilms. However, in most cases, the percentage of inhibition was substantially higher when evaluated by MTT assay compared to CV. The CV assay gives indication of attached biomass but does not reveal the metabolic status of cells, as it stains both viable and non-viable cells. In contrast, MTT works as a respiratory indicator of live cells only, and it stains live adherent cells (Krom et al. 2007; Schillaci et al. 2008). These observations suggest that the peptides efficiently penetrated the biofilms and killed the biofilm-forming bacteria. Although the short peptides, W7 and WW, had higher antibacterial activity against the planktonic cell of tested pathogens and also significantly inhibited the initial cell attachment these planktonic cells and form biofilms, they were less effective in eradication the preformed biofilms of *P. aeruginosa* and *L. monocytogenes*. Similar to sporicidal activity, the peptide length appears to play an important role in biofilms penetration. The current study highlighted the ability of PIN-based peptides to significantly inhibit the initial cell attachment of *P. aeruginosa* and *L. monocytogenes* biofilm to abiotic surfaces (HDPE) commonly found in food processing environments (Dourou et al. 2011).

Overall, the results reveal that the tested peptides are effective antimicrobial agents against *B. subtilis* endospores and sessile and planktonic cells of *P. aeruginosa*, *L. monocytogenes*, *L. innocua* and the tested MRSA strains. Those activities, together with their specificity against microbial membranes (Phillips et al. 2011) and high stability in a broad range of temperature and pH (Alfred et al. 2013a), make them hold great promise to control persistent microbes in the food industry and health sector.

Chapter 5

Mechanism of action of PuroA peptide

5.1 Abstract

Antimicrobial peptides (AMPs) are excellent candidates as a novel and sustainable anti-infection strategy. In this chapter, we present assays for studying the mechanisms of action of AMPs that provide details of the interaction kinetics with cellular, sub-cellular and molecular targets and the sequence of these interactions that are necessary for their antimicrobial activity. The synthetic peptide, PuroA, based on the unique tryptophan-rich domain of the wheat endosperm protein, puroindoline A, displays potent antibacterial and antifungal activities which have been attributed to peptide-induced membrane destabilization, or intracellular mechanisms of action (DNA-binding) or both. Time-lapse fluorescence lifetime imaging microscopy (FLIM) and time-lapse fluorescence microscopy were used to directly observe the localization and interaction kinetics of a fluorescently-tagged PuroA peptide on single *Candida albicans* and *Escherichia coli* cells in real time. Our results revealed the sequence of events leading to cell death. Surprisingly, membrane integrity disruption was not the initial step in the yeast killing mechanism. Within 1 minute, PuroA was observed to translocate across the cell wall, cytoplasmic membrane and nuclear membrane, and bind to SYTO-labelled nucleic acids of *C. albicans*, resulting in a noticeable quenching in the fluorescence lifetime of the peptide label at the yeast cell nucleus, and cell-cycle arrest. A propidium iodide (PI) influx assay confirmed that peptide translocation itself did not disrupt the cell membrane integrity; however, PI entry occurred 25-45 minutes later, which correlated with an increase in fractional fluorescence of pores from 7% to 25-30% as assessed by peptide label lifetime self-quenching and an overall loss of cell size. The detailed sequence of events could not be recorded in case of *E. coli*, however, PuroA induced pronounced filamentation on bacterial cells treated for 3 h. This observation suggested that the peptide might translocate across the cell membranes in non-disrupting manner and bind to nucleic acids, resulted in the filamentation effect. From fluorescence lifetime measurements, the calculated fractional fluorescence of pores in bacteria was only 3% and did not noticeably change over 2 min-2 h. However, there was substantial quenching in fluorescence lifetime of the FITC-PuroA inside the bacterial cells when PI influx took place, giving clear evidence of interactions between FITC-PuroA and PI-nucleic acids. Together, these observations suggest that loss of membrane integrity and/or pore formation at bacterial or yeast membranes occur after intracellular interactions.

5.2 Introduction

Antimicrobial peptides (AMPs) are natural defence molecules produced by most living organisms, from microorganisms to humans. AMPs are excellent candidates to fight antimicrobial drug resistance. Compared to commercial antibiotics, it is a mystery how AMPs have been used successfully by nature for millions of years and remained so efficient during evolution (Yeaman & Yount 2003). AMPs often exert microbicidal effects, resulting from irreversible disruption of vital cellular structures and/or functions (detailed in Chapter 1, Section 1.7). The mechanism by which antimicrobial peptides act is a complex issue. It is essential to understand how these peptides act to entirely exploit them as antimicrobial agents.

Many studies aimed to understand their mode of action have shown that AMPs attach to and insert into membrane bilayers to form stable transmembrane pores such as barrel-stave pores (Yang et al. 2001) or toroidal pores (Matsuzaki et al. 1996) or micellization in a detergent-like way (carpet mechanism) (Gazit et al. 1995). At the cell membrane, a critical threshold concentration needs to be reached to trigger significant membrane disturbance. It was proposed that the membrane-bound peptides with minimum inhibitory concentration (MIC) values in the micromolar range can reach millimolar local concentrations and trigger disruptive effects on membranes (Melo et al. 2009). However, recent studies suggested that their membrane-compromising activity is not the only mechanism of microbial killing and their mechanism of action is much more complex and diverse (Nguyen et al. 2011b). It has been shown that the killing mechanism of AMPs depends on the membrane composition, the peptide concentration, and the final peptide: lipid ratio. Alternatively, at low peptide: lipid ratios, AMPs can translocate across cell membranes, disturbing their structure in a transient, non-lethal manner, and then reach their intracellular target (Nicolas 2009). Many AMPs have intracellular targets as their main mechanism of action or complementary to membrane perturbation (detailed in Chapter 1, Section 1.7).

It has become apparent that some AMPs apply simultaneous and multiple, independent or cooperative actions that probably result in their generally quick and potent antimicrobial activities. Some AMPs have a single mode of action which is concentration-independent, like apidaecin which showed no lytic activity at any concentration tested (Casteels et al. 1989). In contrast, some AMPs, like Arasin 1,

used a dual mechanism of action which was concentration-dependent; at concentrations above the MIC, Arasin 1 lysed membranes in a detergent-like manner, while at concentrations below MIC, Arasin 1 penetrated membranes and bound to intracellular targets (Cudic & Otvos Jr 2002; Paulsen et al. 2013). However, despite numerous studies, there are still unanswered significant questions pertaining to AMPs mechanism of action (Wimley & Hristova 2011). Previous biophysical studies gave only partial explanation of the actual microbe killing mechanism(s). Knowledge of the sequence of the molecular interactions that are necessary for antimicrobial activity of AMPs is lacking. When AMPs have transmembrane pore-forming mechanisms combined with intracellular targets, it is believed that the AMPs form those pores to reach their intracellular targets (Yang et al. 2006; Alfred et al. 2013b; Hong et al. 2015; Li et al. 2016a).

The synthetic peptide PuroA (FPVTWRWWKWWKG-NH₂) showed antimicrobial activity against a number of bacteria, fungi and/or yeasts (Jing et al. 2003; Phillips et al. 2011) (discussed in more detail in Chapter 1, Section 1.6.6). Vogel's group suggested that PuroA acts on bacterial membranes and uses a lytic mechanism of action to exert its antimicrobial activity (Jing et al. 2003). Recently, the same group suggested that the antibacterial mechanism of PuroA is more complex than originally assumed as the peptide bound to DNA *in vitro* and inhibited macromolecular synthesis at sub-inhibitory concentrations in *E. coli* and did not disrupt cytoplasmic membrane integrity in *E. coli* cells. Therefore, they proposed that the interaction of puroindoline peptides with bacterial membranes is only an initial step, followed by translocation into the cell, where they mainly exert their antibacterial effect (Haney et al. 2013). Parallel, studies of our group (Alfred et al. 2013b) showed that *Saccharomyces cerevisiae* cells treated with PuroA appeared intact with pore-like structures in the membranes and leakage of extracellular material (scanning electron micrographs of *S. cerevisiae* cells treated with PuroA are shown in Chapter 1, Figure 1.11). Furthermore, and in agreement with Vogel's findings, the peptide was found to bind to DNA *in vitro* and selectively permeabilised negatively charged vesicles. Therefore, they suggested that PuroA exerts its antimicrobial effects by disrupting the integrity of the cell membrane, followed by intracellular mechanisms of activity (Alfred et al. 2013b).

It has been believed that AMPs (~20 residues) are unlikely to form stable pores, as they require membrane-spanning α -helices, however, they might form transient pores (Glukhov et al. 2005). There are two leading models for membranes disruption by short AMPs; the carpet model and the aggregate model (described in Chapter 1, Section 1.7). The carpet model does not depend upon a particular length or sequence conformation. The alternative aggregate model proposes formation of lipid/peptide aggregates that form unstable bilayer spanning channels which that allow ion diffusion (Hancock & Chapple 1999). It was suggested that PuroA resides at the solvent-lipid interface rather than deep in the hydrophobic region of the membranes (Jing et al. 2003). This observation is shared by the full-length PINA protein, which appears to locate just below the negatively charged DPPG lipid monolayer in the lipid headgroup region but not deeper into the acyl chain region of the lipid layer (Clifton et al. 2011). As PuroA is a short peptide (13 residue) that appears to prefer to reside at the solvent-lipid interface of the membrane and therefore not span the length of the lipid bilayer, it is unlikely to form stable membrane-spanning pores, as required by the aggregate model. Alfred et al. (2013b) thus suggested that PuroA forms pores at the membranes using carpet model, in which the peptides are only required to be on or just below the surface to exert their effect.

These previous studies raise the following questions: what are the temporal dynamics of interaction between the peptide and its dual targets? Does pore formation precede DNA interaction, or vice-versa? Is cell death triggered by one or the other interaction, or are both involved? Finding the precise mechanism of action of PuroA is very significant for considering its applications in food, health and agriculture contexts. Therefore, in this study, a combination of biophysical techniques and biological assays were used to try to answer these questions. Two biophysical techniques were used, time-lapse fluorescence lifetime imaging microscopy (FLIM) and time-lapse fluorescence microscopy, to directly observe the localization and interaction kinetics of a fluorescently-tagged PuroA peptide on single *C. albicans* and *E. coli* cells in real time. Two biological assays were performed, time-kill assay to measure the timescale for inducing biocidal effects by PuroA, and cell cycle analysis for the *C. albicans* cells to clarify what happens after the peptide binds to its intracellular target. The methods and principles applied in this work are detailed in Sections 2.15 to 2.20. The results are presented below. A major part of this study has been published in (Shagaghi et al. 2017).

5.3 Results

5.3.1 The effect of PuroA peptide on *C. albicans* and *E. coli* morphology

Under SEM, control *C. albicans* cells exposed only to PBS showed a regular cell shape with intact cell membrane (Fig. 5.1 A and Fig. 5.1 B). After 1 h incubation with PuroA, at $0.5 \times \text{MIC}$ and $1 \times \text{MIC}$ (64 $\mu\text{g}/\text{mL}$ and 125 $\mu\text{g}/\text{mL}$, respectively), pores were observed on the surface of some peptide-treated cells. Additionally, in some cells, extracellular material was observed leaking from the cells (Fig. 5.1 C & D).

In case of *E. coli*, similar to *C. albicans*, the cells treated for 1 h with PuroA at $0.5 \times \text{MIC}$ and $1 \times \text{MIC}$ (8 $\mu\text{g}/\text{mL}$ and 16 $\mu\text{g}/\text{mL}$, respectively) appeared regular in size with pores on the cell surface. Whereas the untreated control *E. coli* cells which were exposed only to PBS, showed a regular cell shape with intact cell wall (Fig. 5.2 B). However, as mentioned in Chapter 3, after 3 h of exposure to PuroA over a range of concentrations (final peptide concentration 0 – 250 $\mu\text{g}/\text{mL}$), a profound effect on the morphology of *E. coli* cells was observed at MIC (16 $\mu\text{g}/\text{mL}$). The peptide induced filamentous growth in the cells (Fig. 5.2 C). The mean length of normal *E. coli* cells at log-phase was about 1-2 μm . Addition of PuroA peptide resulted in 7-fold to 14-fold increase in the average cell length within 3 h. The appearance of pores was observed on the surface of some filamentous cells.

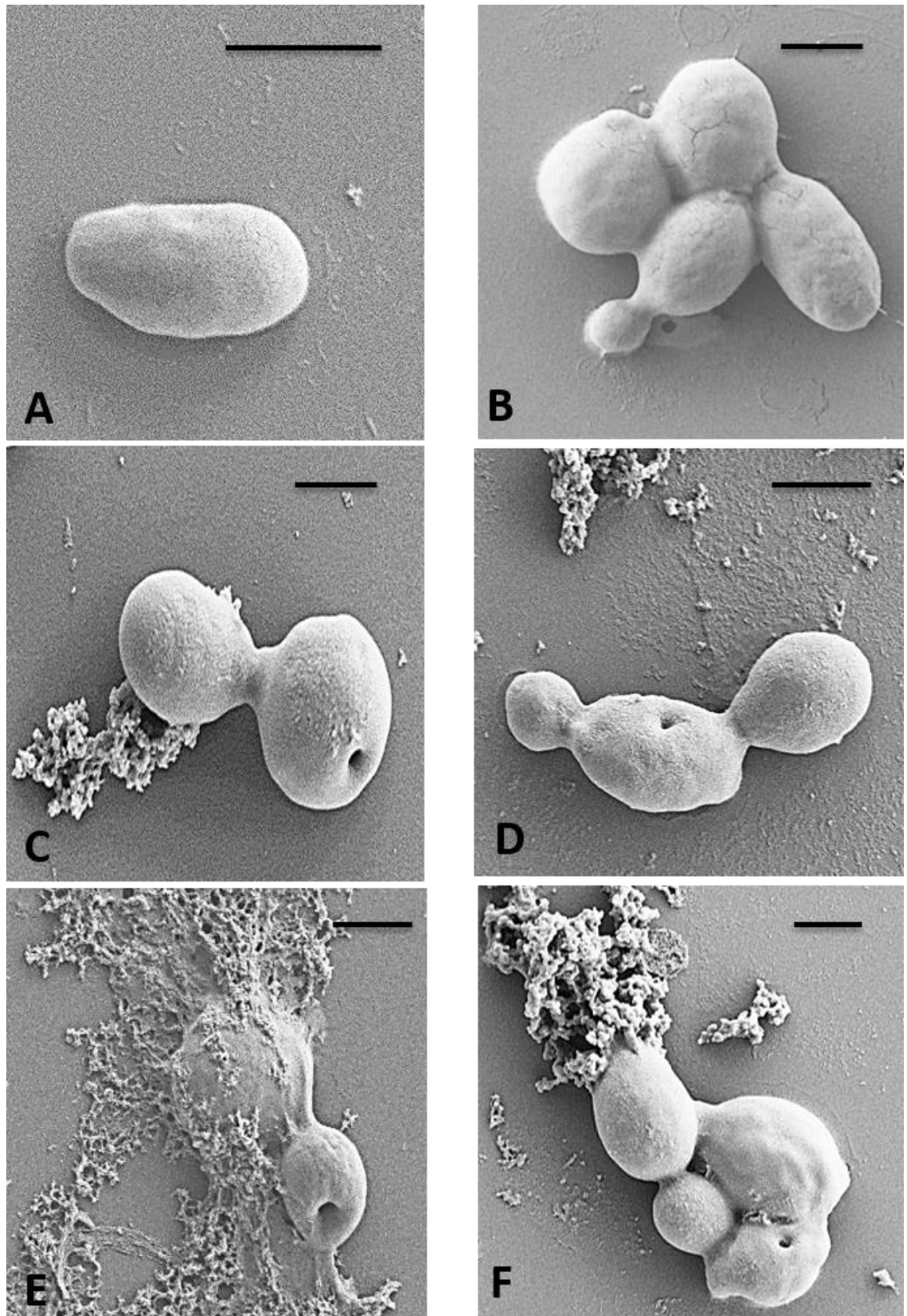


Figure 5.1 Scanning electronmicrographs of *C. albicans* treated with PuroA. A & B. No-peptide control; C & D. Puro A at 64 $\mu\text{g}/\text{mL}$; E & F. PuroA at 125 $\mu\text{g}/\text{mL}$. Magnifications 20,000 \times , scale bar = 2 μm . Pore size is 0.25-0.40 μm .

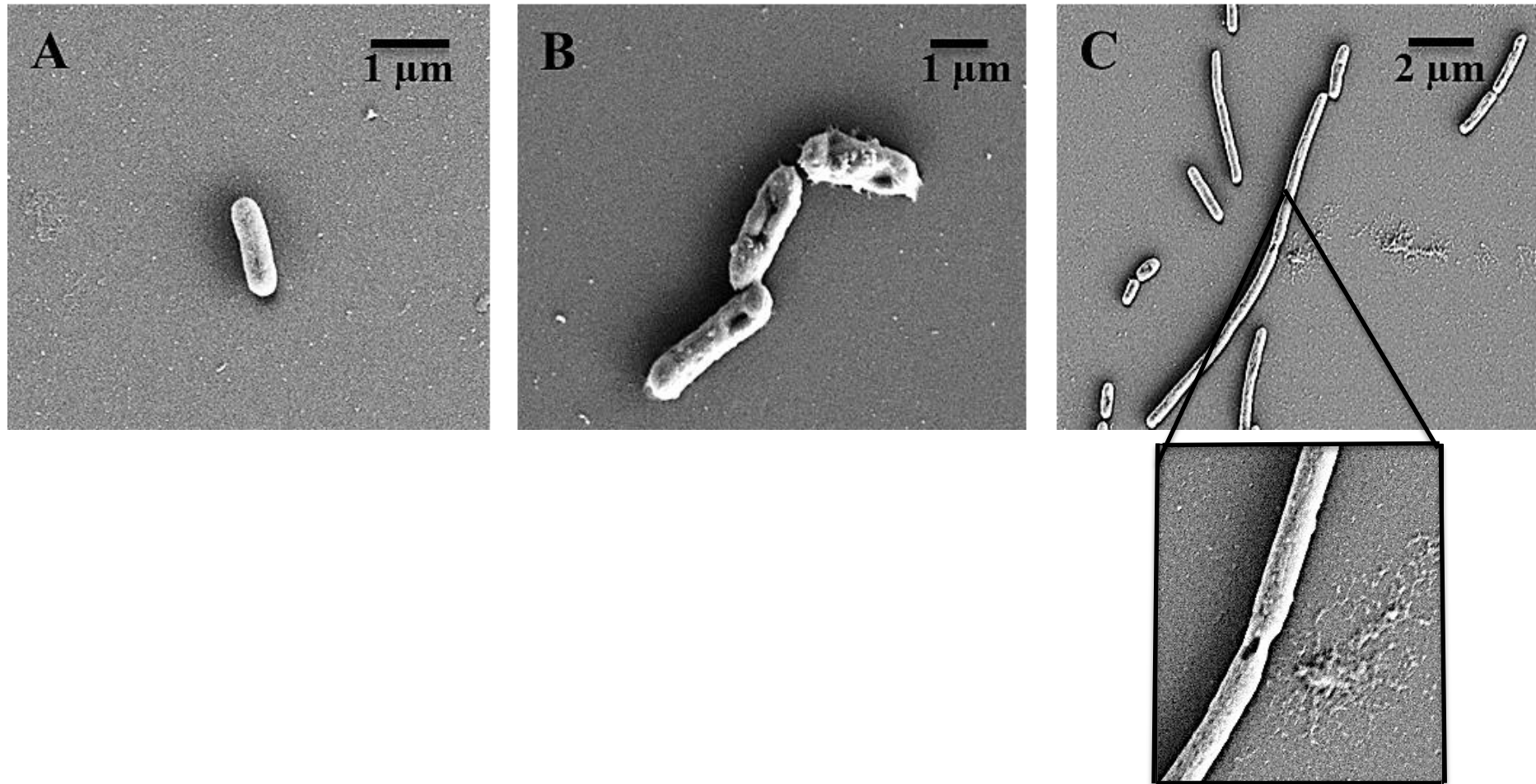


Figure 5.2 Scanning electronmicrographs of *E. coli* treated with PuroA.

A. No-peptide control; B. Puro A at 16 µg/mL, 1 h treatment; C.PuroA at 16 µg/mL, 3 h treatment. Pore size is 0.20-0.35 µm.

The filamentation effect of PuroA was also observed using light microscopy after staining the cells with crystal violet (CV) (Fig. 5.3) and confocal microscopy after using SYTO 9, a green fluorescent cell-permeant nucleic acid stain (Fig. 5.4). The observation of filaments using light microscope is consistent with the results of Alfred et al. (2013b), however, the filamentation-inducing concentration is different, the previously published concentration being 32 $\mu\text{g/mL}$, or $2 \times \text{MIC}$.

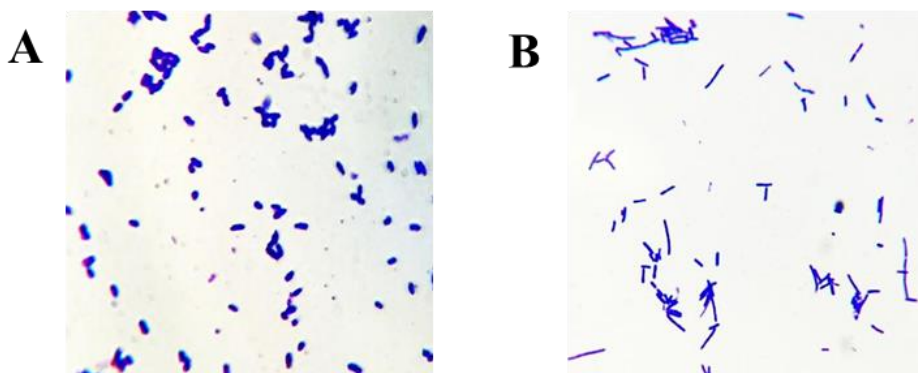


Figure 5.3 Morphological changes induced in *E. coli* cells by PuroA observed by light microscopy.

The cells were observed using light microscopy at $\times 1000$ magnification under oil immersion after incubation with peptide for 3 h at 37 °C. Panels are: **A.** no peptide control; **B.** PuroA 16 $\mu\text{g/mL}$.

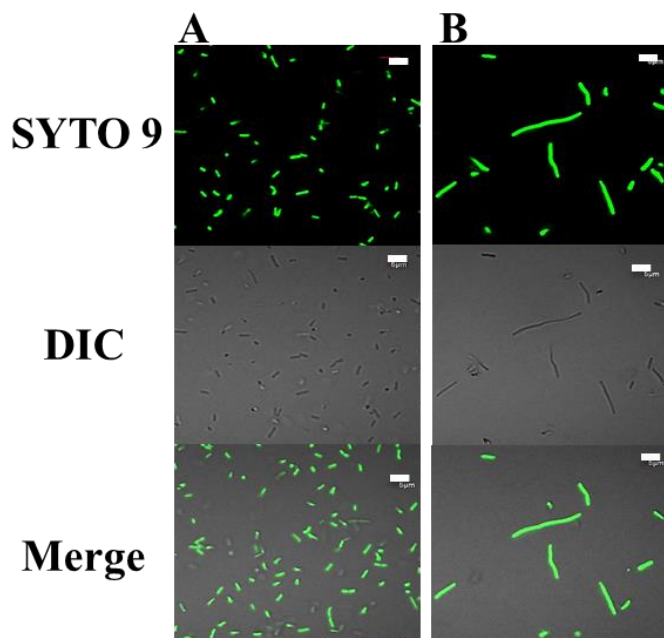


Figure 5.4 Morphological changes induced in *E. coli* cells by PuroA using confocal microscopy.

The cells were observed using confocal microscopy at $\times 1000$ magnification under oil immersion after incubation with peptide for 3 h at 37 °C. Panels are: **A.** no peptide control; **B.** PuroA 16 $\mu\text{g/mL}$. Scale bar?

5.3.2 Time-kill assay

The timescale to induce biocidal effects on *C. albicans* cells by FITC-PuroA was determined by a time-kill assay. The peptide caused an 85% reduction in viable yeast cells at 30 min and complete killing (>99%) of all *C. albicans* cells at 60 min. The time-kill kinetics were the same as with the unlabeled peptide (Fig. 5.5).

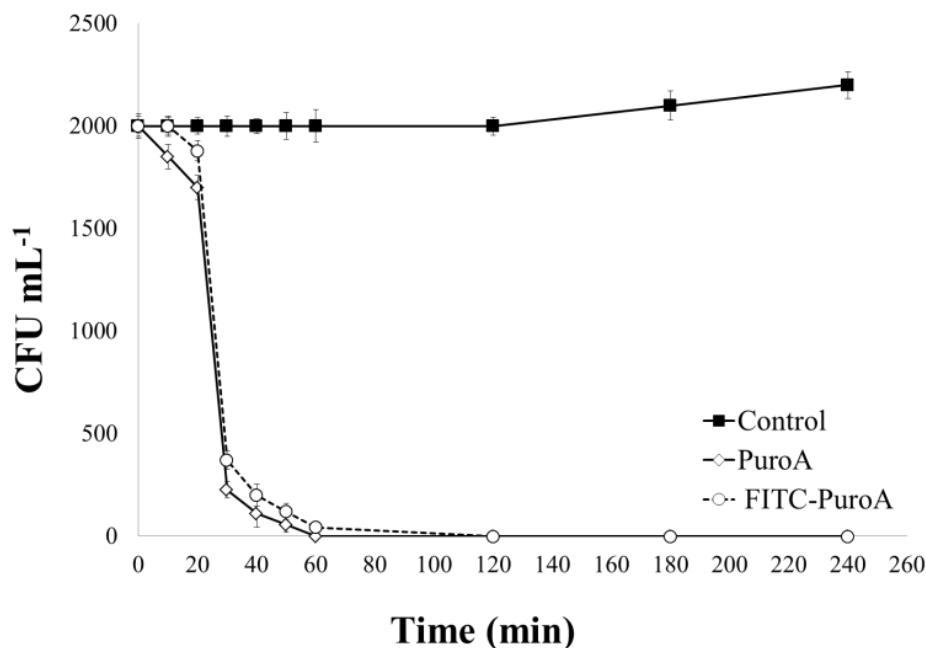


Figure 5.5 *C. albicans* killing kinetics by PuroA and FITC-PuroA peptides.

C. albicans cells were treated with peptides at MIC, and yeast survival was determined by viable cell counting at different times. Significant reduction of cell numbers was observed at 30 min. Data are presented as mean values \pm standard deviations of three independent experiments.

The kinetics of the bactericidal effect of FITC-PuroA were different from fungicidal kinetics. The peptide started to induce killing in *E. coli* cells after 1 h and caused a 65% reduction in viable yeast cells at 3 h, although complete killing (>99%) of *E. coli* cells was not achieved even after 24 h (Fig. 5.6).

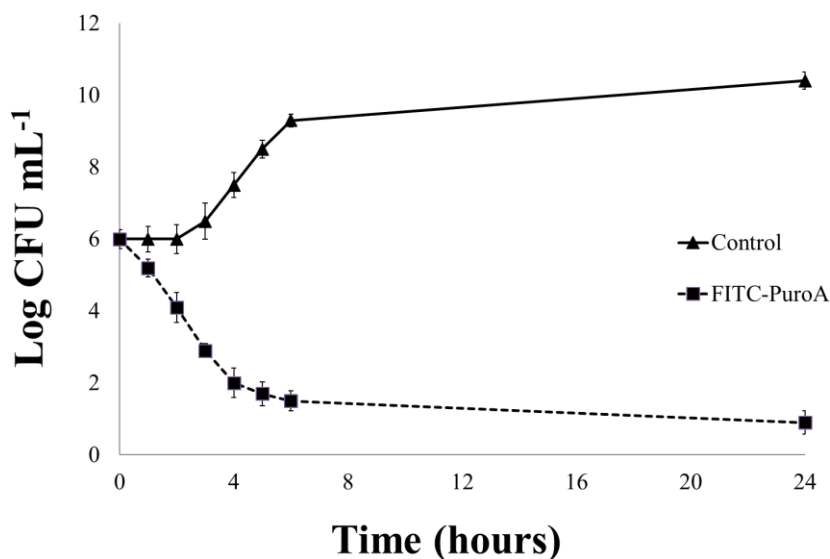


Figure 5.6 *E. coli* killing kinetics by FITC-PuroA peptide.

E. coli cells were treated with PuroA at MIC, and bacteria survival was determined by viable cell counting at different times. Significant reduction of cell numbers was observed at 3 h. Data are presented as mean values \pm standard deviations of three independent experiments.

5.3.3 Effect of PuroA on *C. Albicans* cell cycle

In order to investigate the effects of PuroA peptide on the intracellular physiology of *C. albicans* cells, particularly on DNA and/or protein synthesis *in vivo*, cell cycle analyses were performed for the yeast cells. The DNA content of untreated *C. albicans* cells and cells treated with 125 μ g/mL of PuroA for 25 min was determined by flow cytometry after staining with PI (known as DNA-intercalating agent). As shown in Fig. 5.7, in absence of PuroA, the percentages of cells in G1-phase, S-phases and G2-M phase were 56.73 %, 18.58 %, and 24.69 %, respectively. After PuroA treatment, the proportion of *C. albicans* cells in S-phase increased to 37.28 %, while that in G1-phase and G2-M phase decreased to 44.67 % and 18.05 %, respectively. Fig. 5.8 shows the fluorescence intensity histogram profiles corresponding to Fig. 5.7. The results suggest that PuroA arrested cell proliferation at the S-phase in *C. albicans*, resulting in inhibition of normal cellular processes.

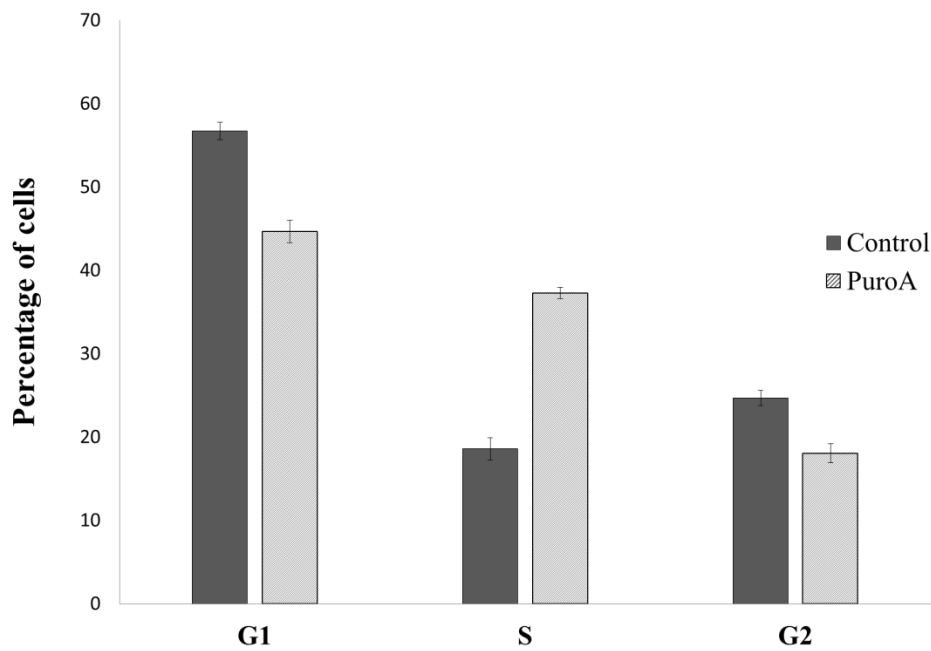


Figure 5.7 The effects of PuroA on the cell cycle progression of *C. albicans* cells. The cells were treated with PBS or 125 $\mu\text{g}/\text{mL}$ of PuroA and their DNA contents was labelled with PI and analysed by flow cytometer. Histogram indicates the percentage of *C. albicans* cells in each phase of the cell cycle. Data are presented as mean values \pm standard deviations of two independent experiments.

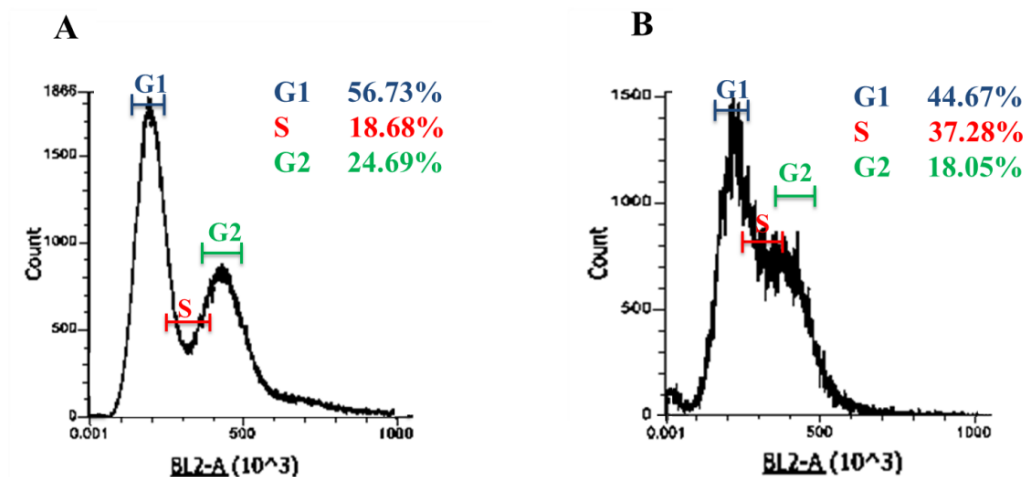


Figure 5.8 Fluorescence intensity histogram profiles of *C. albicans* cells after treatment with 125 $\mu\text{g}/\text{mL}$ of PuroA using flow cytometer. (A) The cell cycle progression of untreated cells; (B) The cell cycle progression of treated cells with PuroA for 25 min.

5.3.4 Time-lapse confocal microscopy

We monitored the dynamic sequence of events in the antimicrobial action of PuroA peptide at 8 $\mu\text{g/mL}$ using time-lapse confocal microscopy (Fig. 5.9). PuroA labelled with a green-fluorescent FITC probe was used in single and/or two-colour experiments to monitor the peptide localization in time. The green channel monitored emission from the labelled peptide and the red channel monitored emission from the DNA stain SYTO 85 Orange and PI. SYTO 85 Orange is a cell-permeant nucleic acid stain whereas PI is a cell-impermeant nucleic acid stain that enters the cell only when the membrane is compromised, binds to nucleic acids, and fluoresces strongly. Interleaved phase contrast microscopy observations allowed monitoring of changes in cell morphology with time.

To our surprise, we found that within 30 seconds of exposing the yeast cells to the peptide, FITC-PuroA appeared to be located at the cell nucleus. This was confirmed via the strong co-localisation of the FITC-PuroA fluorescence with the red fluorescence from the nucleic acid stain SYTO 85 Orange (Fig. 5.9 A). The localization of the peptide in the nucleus persisted for about 20 minutes. After 20-40 minutes (Fig 5.9 A and Fig 5.9 B), the peptide accumulated at the cell membrane, as evidenced by the increased cell surface fluorescence and, in some cells, enlargement of the cell's vacuole was observed via phase contrast microscopy (Fig. 5.9 B).

Forty minutes after peptide addition, peptide-induced disruption of membranes was observed by PI influx into the cell cytosol. The PI distribution was not uniform throughout the cell suggesting PI entry was localised (Fig. 5.9 B). In parallel to the cytosolic influx of PI, a decrease in cell size was observed (by 35%) but complete dissolution of the cell was not apparent at this time point. These dynamic changes are summarized in Figure 5.10 whereupon the average signals from peptide, PI and phase contrast from a single cell are plotted as a function of time.

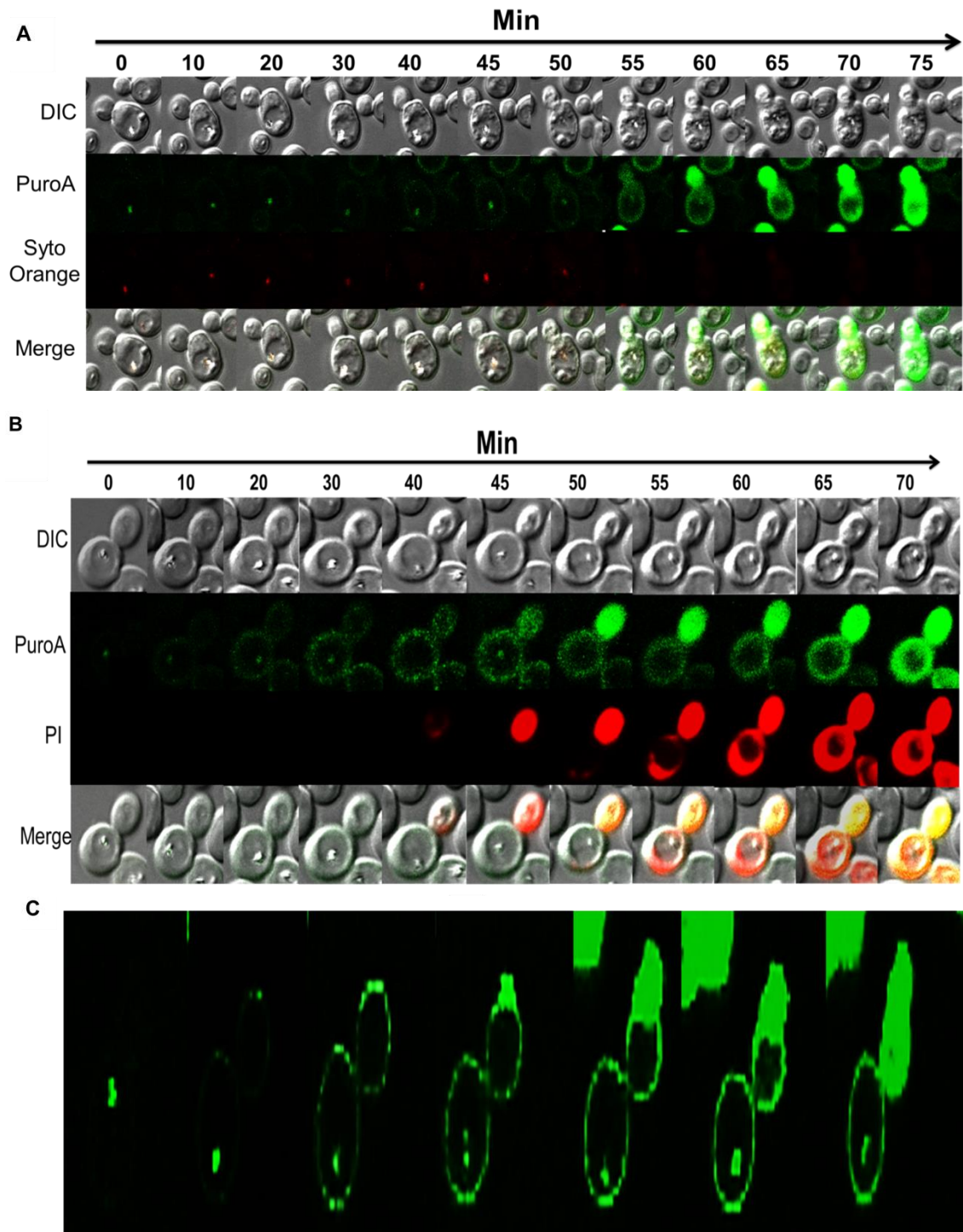


Figure 5.9 Sequence of events during attack of a single *C. albicans* cell by FITC-PuroA at $8 \mu\text{g/mL}$, time-lapse confocal microscopy images taken in real time.

(A) Cell nucleus stained with SYTO 85 Orange before addition of FITC-PuroA; the snapshots were taken from a single [Movie](#) at the times shown at top. (B) PI was added simultaneously with the peptide, the snapshots were taken from a single [Movie](#) at the times shown at top, right scale shows total intensity of green and red fluorescence associated with the cell vs. time over 70 min. (C) Single colour experiments using only FITC-PuroA. DIC: Differential interference contrast.

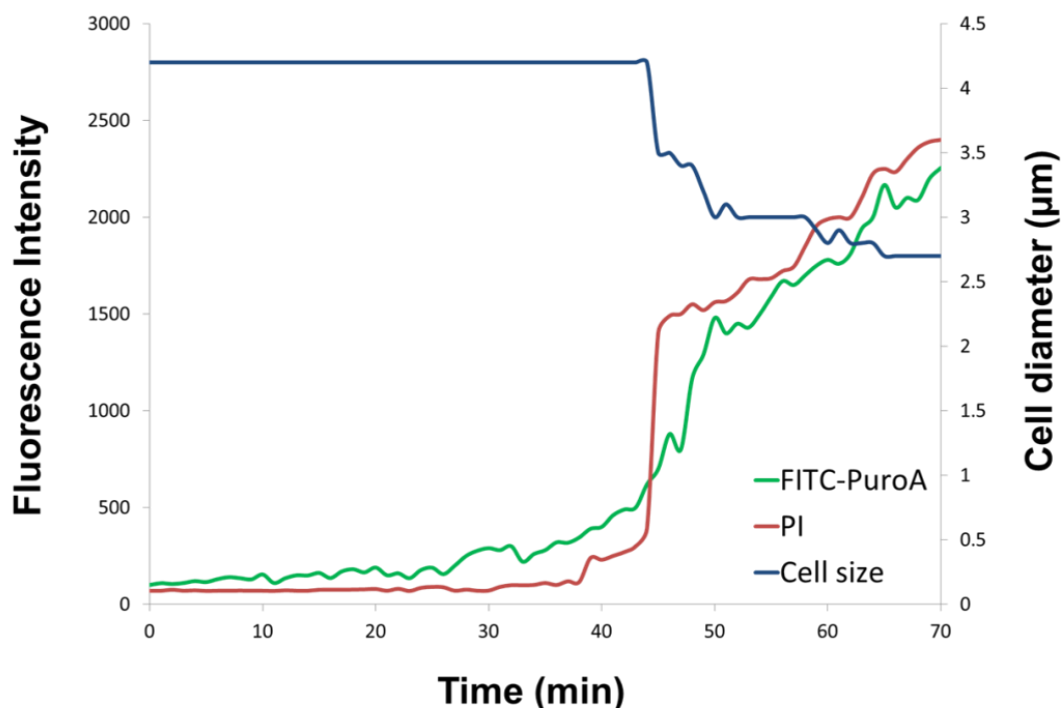


Figure 5.10 Plot of total FITC intensity (green line) and total PI intensity (red line) (right scale) and relative cell size (blue line) (left scale) vs time over 70 min. Only a single cell was amenable to quantitative analysis.

The detailed dynamic sequence of events of PuroA peptide (at 8 μg/ml) attacking *E. coli* cells was difficult to monitor. This was due to the rapid internalization of FITC-PuroA inside the bacterial cell. Within a few seconds (≤ 30 sec) after peptide addition, FITC-PuroA was uniformly distributed within the cytosol of the *E. coli* cell as shown in Figure 5.11. Compared to the yeast cells, the interaction and internalization kinetics were much faster and occurred on a timescale of seconds.

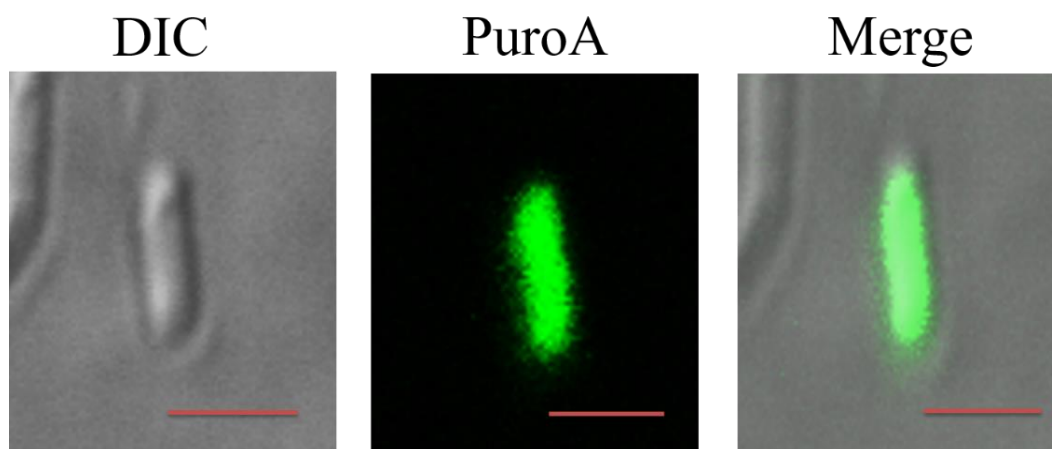


Figure 5.11 shows *E. coli* cell exposed to FITC-PuroA peptide at 8 μg/ml. Scale bar = 2 μm. DIC: Differential interference contrast.

5.3.5 Time-lapse FLIM

To determine the kinetics of peptide-peptide, peptide-membrane and peptide-nucleic acids interactions at the nanometer scale (i.e. <10nm), we recorded fluorescence lifetime images as a function of time after adding FITC-PuroA peptide. The fluorescence lifetime of peptide changes when its state changes, i.e. peptide free in solution, peptide participating in pore formation, and bound peptide (Ningsih et al. 2012; Gee et al. 2013).

FITC-PuroA peptide bound to its intracellular target immediately after addition to the yeast cell, as evidenced by the quenching in the FITC-PuroA fluorescence lifetime from 2.5 ns to 2 ns. In the experiments where the cells' nuclei were stained with SYTO 85 Orange (Fig. 5.12 A), a further reduction in the fluorescence lifetime of the FITC-PuroA peptide was observed (from 2 ns to 1.8 ns) indicating nanoscale proximity to the SYTO dye. After a lag time of about 35 to 45 min, the pore formation stage started as detected from the decrease in the fluorescence lifetime of the FITC-PuroA at the cell membrane (lifetime dropped from 2 ns to 1.6-1.3ns). This observation is supported by the finding that the aggregated form is substantially quenched, compared to the monomer form (Stella et al. 2004) and also the fluorescence lifetime of fluorescent labelled AMPs was quenched upon pore formation (Rapson et al. 2011). In the context of a simple two-state pore/non-pore model, the calculated fractional fluorescence of pores increased from 7% during the lag phase, to 25-30% at 50 minutes and plateaued at 75% pore fraction at 60 minutes and beyond (Fig. 5.12 C).

Addition of PI to the cell after pore formation and subsequent PI influx confirmed that the cell membrane was compromised. There was further quenching in fluorescence lifetime of the FITC-PuroA inside the cell when PI influx took place, again giving clear evidence of nanoscale interactions between FITC-PuroA and PI-nucleic acids in the cytosol.

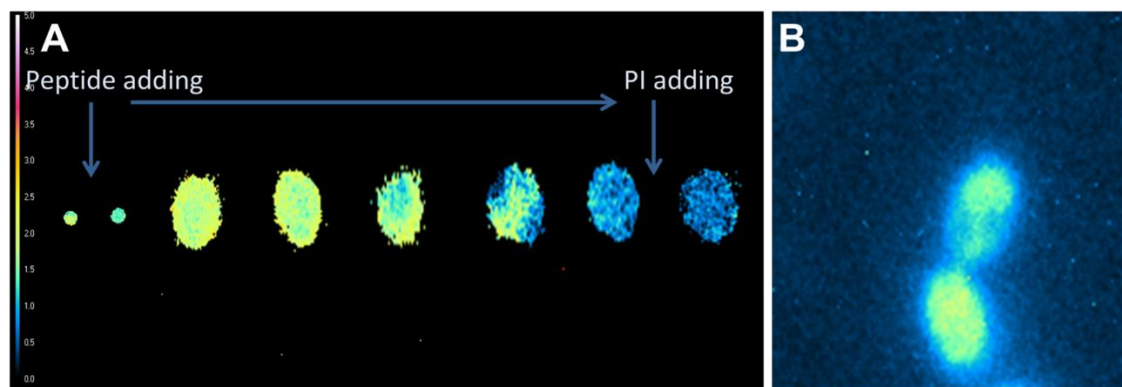


Figure 5.12 Time-lapse fluorescence lifetime images of FITC-PuroA interacting with a single *C. albicans* cell. (A) Fluorescence lifetime images of a single *C. albicans* cell before and after adding the peptide. Note the quenching in lifetime of the SYTO 85 Orange-stained nucleus after addition of the peptide. **(B)** Fluorescence intensity image of *C. albicans* cell during pore formation stage.

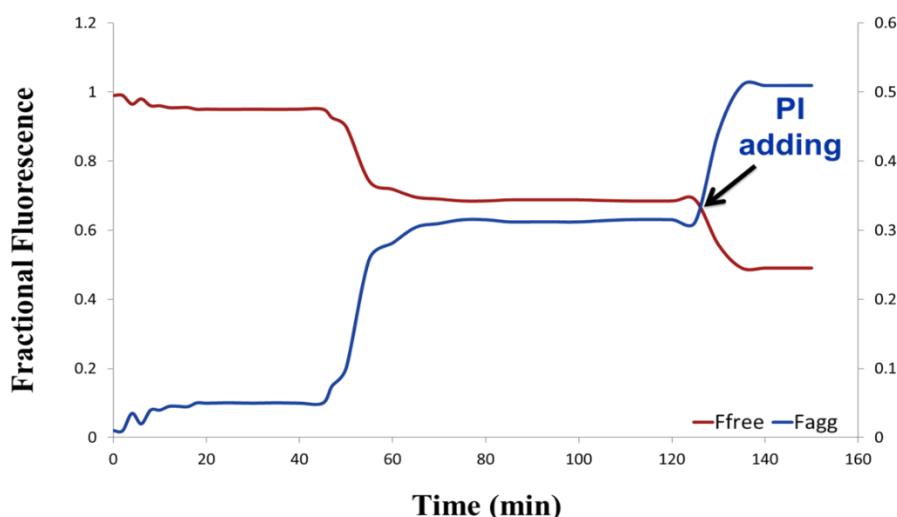


Figure 5.13 Fractional fluorescence from free PuroA, pore forming PuroA and nucleic acids bound PuroA, as a function of time during attack of a single *C. albicans* cell.

In case of *E. coli* cells, fractional fluorescence of pores was only 3%, fractional fluorescence of free peptide was 97% and the fractional fluorescence of pores did not noticeably change over the time of 2 h. It was also found that a small percent of the peptide was involved in pore formation (12.5%) and most of the peptide was in a free state (87.5%). Both peptide and peptide in bacterial cells had the same fluorescence lifetime (2.5 ns). However, after adding the PI, influx took place in some bacteria

cells (after 2h) and a noticeable quenching in the fluorescence lifetime of peptide inside the bacterial cells was observed (from 2.5 to 1.7 ns). This observation could suggest that most of the free peptide was bound to nucleic acids inside the cells, and when PI entered the membrane-comprised cells and bound to the nucleic acids as well, subsequent energy transfer from the FITC-PuroA to PI occurred and the quenching in fluorescence lifetime was seen. The notion that most of the peptide inside the cell is bound to nucleic acids could also explain the unnoticeable change in fractional fluorescence of pores over the time of the experiment, as almost 87 % of the peptide was inside the cell and much less outside participating in pore formation. Thus, the kinetics of loss of membrane integrity in *E. coli* were more difficult to define compared to those of *C. albicans*.

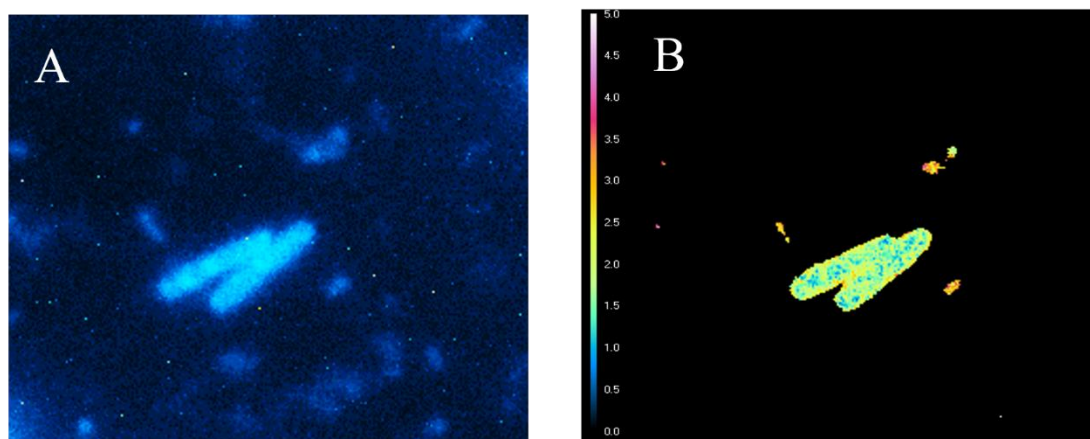


Figure 5.14 Fluorescence lifetime images of FITC-PuroA interacting with *E. coli* cells.

(A) Fluorescence intensity image of *E. coli* cells after adding FITC-PuroA. (B) Fluorescence lifetime image of *E. coli* cells after adding the peptide and PI influx took place. The lifetime of the peptide in bacteria was 1.7 ns.

5.4 Discussion

5.4.1 Anti-*Candida* mechanism of PuroA

The major findings of this work helped to understand how PuroA attacks *C. albicans* cells in real time and determine the main target that causes cell death. The cell membrane appears to be the primary target of most membranolytic AMPs and the intracellular targets are generally considered secondary targets subsequent to membrane damage. Somewhat surprisingly, we showed that PuroA-FITC can translocate the cell membranes and reach its intracellular targets well before forming pores into membrane bilayers and disrupting the membrane integrity. FITC-PuroA showed three distinct phases of attack. The first phase involved translocation of FITC-PuroA across the cell membranes. In the second phase, peptide in the cytosol bound to nucleic acids. The third phase involved FITC-PuroA accumulation at the cell membrane and pore formation causing membrane disruption, PI and peptide influx, and a decrease in cell size (Fig. 5.15). These findings highlight the importance of assessing the interactions between AMPs and target cells using a range of exposure times to enable complete elucidation of the AMP's mechanisms of action. These real time imaging experiments revealed three distinct events which occurred at different times at the same peptide concentration.

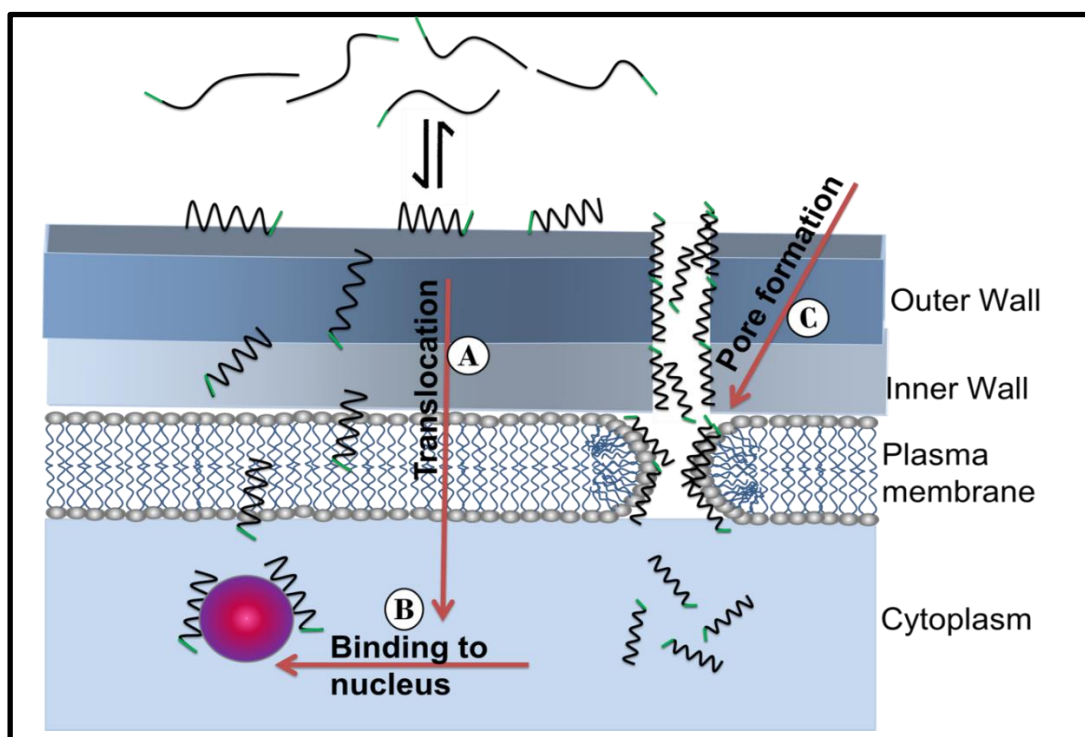


Figure 5.15 Schematic showing the sequence of the three events (A, B and C) occurring upon interaction of PuroA peptides with *C. albicans* cell.

Clear pores were observed on the surface of the *C. albicans* cells incubated with PuroA for 1h. Previously, PuroA showed *in vivo* and *in vitro* DNA binding ability (Alfred et al. 2013b; Haney et al. 2013). Thus, the expected anti-*Candida* mechanism of this peptide was formation of pores in the cell membrane, followed by intracellular mechanisms of activity. However, surprisingly, live cell imaging revealed that the peptide appeared inside the cell before the pore formation stage. Thus, pore formation is secondary to rather than concurrent with PuroA entry to cells. This emphasises the importance of live cell imaging in real time in understanding the mechanism of action of PuroA in this instance.

The distinct temporal dynamics of the peptide location and interaction may provide clues as to the precise mechanism of cell killing in this case. From the time-kill assay on a population of cells, it is clear that cell killing is not immediate but requires a lag phase of tens of minutes before a discernible drop in CFU is observed. Moreover, the significant reduction in the number of PuroA-treated cells after 45 min is consistent with the timescale of pore formation and loss in membrane integrity observed in our single cell assay. This would suggest that pore formation and disruption of the cellular integrity is the main mechanism of cell killing, and membrane permeabilization and cell shrinkage are effects from which the cells cannot recover. The loss in cell volume (cell shrinkage) in parallel to the permeabilization effect during attack by AMPs was also observed previously in *C. albicans* when treated with chicken cathelicidin-2 (CATH-2) peptide (Ordonez et al. 2014) and in the Gram-positive bacterium *Bacillus subtilis* when treated with LL-37 and alamethicin (Barns & Weisshaar 2013, 2016). At the intracellular level and before forming pores, this cationic peptide seemed to interact with the cell's nucleic acids and inhibited some functions in the nucleus. From the flow cytometric analysis of the cell cycle and DNA distribution, it was determined that PuroA prevented cells from entering the G2 phase of the cell cycle, resulting in the accumulation of cells in S phase where DNA replication occurs. We stress that these observations apply only to *C. albicans*, and the relative importance of membrane disruption versus peptide-nucleic acid interactions on cell impairment may depend on the exact microorganism under examination.

C. albicans is an opportunistic pathogen that causes oral candidiasis and other conditions in immune-compromised individuals (Cannon et al. 1995). The *C. albicans* cell wall is mainly (80–90%) composed of carbohydrate to protect the cells from osmotic stress and maintain structural integrity (Martínez et al. 1998). In less than one minute, PuroA translocated the outer and inner cell-walls that are composed of polymers of mannose (mannan), mannoproteins (Kapteyn et al. 2000), polymers of glucose and polymers of N-acetyl-D-glucosamine (GlcNAc) containing β -1,4 bonds (chitin) (Chaffin et al. 1998), as well as translocating the cytoplasmic membrane and binding to the nucleus. This rapid translocation through cell wall and cytoplasmic membrane and binding to nucleus could be due its unique tryptophan-rich domain (the role of Trp residue in insertion of AMPs into membranes and binding with intracellular targets discussed in details in Chapter 1, Section 1.8).

Other AMPs, like the histidine-rich histatin 5 (Hst 5) peptide, bound to laminarin (β -1,3-glucan) at the cell wall of *C. albicans* then translocated through cell wall and cytoplasmic membrane in a non-disturbing manner. After translocation, uniform PI entrance occurred due to vacuolar expansion; PI uptake was a consequence of ionic efflux and vacuole expansion caused by cytosolic translocation of Hst 5 (Jang et al. 2010). However, it was previously proposed that the uptake of Hst-5 is a dichotomous event; at low concentrations, the peptide is internalized to the vacuole via receptor-mediated endocytosis, whereas at high conditions, Hst-5 cytoplasmic uptake occurs through a single break site on the plasma membrane (Mochon & Liu 2008). On the other hand, our data clearly show that PI entry occurs well after translocation of PuroA through a single point in the cell membranes and is due to a substantial accumulation of PuroA at that point and forming pores with all these events happening at the same peptide concentration.

5.4.2 Proposed bactericidal mechanism of PuroA

PuroA was shown to have rapid interaction, penetration and internalization kinetics when it attacked *E. coli* cells. However, its bacterial killing kinetics were much slower than yeast killing kinetics; bactericidal activity involved a lag phase of hours before a noticeable drop in CFU was observed. These observations suggested that the immediate internalization of PuroA into the bacterial cells is not associated with cell death; PuroA probably translocates the membranes of *E. coli* cells without causing permanent membrane perturbation, binds to DNA and induces filamentous growth in the bacterial cells.

Filamentation is a defect in cell division with the cell continuing to grow without septum formation (Donachie & Robinson 1987). It could be due to the inhibition of membrane proteins that are involved in septum formation (Botta & Park 1981) or the blocking of DNA synthesis (Lutkenhaus 1990) (described in Chapter 1, Section 1.7.3). This seems to be a common mechanism among Trp-rich peptides (TRPs), as indolicidin induced filamentation of *E. coli* cells and this morphological change was proposed to be a result of DNA synthesis inhibition (Subbalakshmi & Sitaram 1998). Another TRP, lactoferricin B, also induced profound filamentation of *E. coli*, this effect was correlated to the induction of an SOS-like response in the bacterial cells (Ulvatne et al. 2004). Moreover, the Trp- and Arg-rich synthetic hexapeptides, WRWYCR and KWWCRW, induced filamentation in *E. coli* cells by interfering with DNA damage repair through trapping Holliday junctions (HJ), which are branched DNA intermediates that arise in several central DNA repair pathways and replication fork restarts. This eventually leads to the accumulation of DNA damage, DNA loss, chromosome missegregation and filamentation (Gunderson & Segall 2006).

In this study, PuroA appeared to somehow disrupt cell division of *E. coli* as cells treated with the peptide for 3 h continued to elongate, failed to septate and thus formed filaments. These results suggest a non-membranolytic intracellular mechanism of action, and as PuroA showed strong affinity for plasmid DNA in gel retardation assays (Alfred et al. 2013b; Haney et al. 2013) and as it is shown in Chapter 3, Section 3.3.7, it is possible that its intracellular mechanism is binding to nucleic acids and/or inhibiting nucleic acids synthesis. However, further work is needed to accurately identify the intracellular target(s) of PuroA. On the other hand, and in disagreement

with observations that PuroA does not seem to disrupt cytoplasmic membrane integrity in *E. coli* cells (Haney et al. 2013), clear pore-like structures on the surface of PuroA-treated bacterial cells were observed under SEM, suggesting a membranolytic mechanism of action. Clearly PuroA has a dual bactericidal mechanism of action, thus the next important questions are, which mechanism occurs first, and what is the main cause of bacterial cell death? Although the detailed sequence of events and the interaction kinetics of the bactericidal mechanism could not be recorded using time-lapse confocal microscopy and FLIM, and *E. coli* is a prokaryotic organism whereas *C. albicans* is eukaryotic, PuroA might be exerting its bactericidal effect using similar phases of attack that are used for yeast cells. These could involve, firstly, translocation across the cell membrane without disruption of it, then binding to nucleic acids and inducing filamentation, and thirdly, slow accumulation at the cell membrane and, upon reaching a specific threshold, forming pores and disrupting the membrane. This theory is supported by: (i) the induction of filamentation, which is the result of a different intracellular mechanism; (ii) the slow killing kinetics and the good correlation of these kinetics with the low unchanged fractional fluorescence of pores over the same timescale and; (iii) the clear pore-like structures on the surface of some peptide-treated *E. coli* cells. However, further investigation is required to determine the validity of this theory and to understand the precise sequence of events during bacterial cell attack and the main cause of cell death.

In summary, our results reveal that live cell imaging can be a useful adjunct to other approaches for investigating the mechanisms of action of AMPs. First, FLIM provides a measure of the nanoscale interactions of peptides with other labelled molecules or cellular constituents in real time. Second, imaging provides a measurement of the localization of the peptide relative to membranes, cytosol, nucleus or other organelles. By combining these biophysical methods with biological assays (e.g. time-kill assay and cell cycle analysis), the kinetics of peptide interactions and cell death can be compared, leading to mechanistic insights. It is important to stress that the results gleaned in the present study are specific to the peptide and the cells being investigated. Indeed, we might expect the balance of intracellular and membrane disruption interactions to be cell-type specific and to also depend on other variables. The methods utilized here will be useful in investigating these issues in future work.

Chapter 6

Experimental evolution of resistance to TRPs

6.1 Abstract

A new class of antimicrobial agents based on the immune peptides of many living organisms is attracting increasing interest as effective and potent therapeutics against multi-resistant microbes. It has been claimed that AMPs exert fundamental change(s) on the microbial cell that minimise the possible evolution of resistance compared to conventional antibiotics. However, precise information about the rate of resistance development to AMPs and the subsequent impact on the microbial fitness and cross-resistance is limited. Using experimental evolution of resistance, the development of resistance to selected Tryptophan (Trp)-rich peptides (TRPs) including PuroA and its analogues, P1 and W7, as well as indolicidin, in *Staphylococcus aureus*, *Escherichia coli*, *Staphylococcus epidermidis* and *Candida albicans* was tested. In these selection experiments, 5/6 independent lineages of *S. aureus* and 2/6 independent lineages of *E. coli* developed resistance to PuroA and 2/6 and 4/6 independent lineages of *S. aureus* developed resistance to P1 and indolicidin, respectively, when independently propagated in media supplemented with progressively increasing concentrations of peptides for 300–350 generations. *S. epidermidis* and *C. albicans* did not develop resistance toward any of the tested peptides, and all the four microbes did not develop resistance to the short analogue of PuroA, W7. Experimentally developed resistance to PuroA and indolicidin was physiologically costly, in terms of decreasing the growth rate of *S. aureus* and *E. coli*; however, the resistance and the cost were completely ameliorated when resistant strains propagated in the absence of the selection pressure of peptide exposure. Importantly, resistance to PuroA or indolicidin did not provide the bacteria cross-resistance to other tested TRPs. Although a combination of any two of the tested peptides did not display synergistic effects in *S. aureus* and *E. coli*, combining W7 with PuroA or indolicidin was a useful approach to prevent development of resistance against the latter two peptides. Our data suggest that development of resistance to TRPs is possible, but is transient and probably develops through mechanisms that do not confer cross-resistance to other peptides from the same class.

6.2 Introduction

The failure of some of the most powerful antibiotics to treat life-threatening infections associated with drug-resistant pathogens has created a global health crisis (Arias & Murray 2009). The continuing emergence of resistant strains at an alarming rate spurs researchers to find new therapeutics. Since their discovery, AMPs have been seen as new antimicrobial agents, due to their broad-spectrum and potent activity and long evolutionary history. In addition, it has been proposed that resistance development to AMPs is less likely, as they often act non-specifically on one or multiple conserved target(s), such as the entire bacterial cellular membrane; therefore, bacteria will only develop resistance to AMPs with high cost (Zasloff 2002).

A number of studies have described the molecular mechanisms of resistance in bacteria (reviewed in Yeaman & Yount 2003; Brogden 2005; Anaya-López et al. 2013; Bechinger & Gorr 2017) (detailed in Chapter 1, Section 1.11). In most of these studies, resistance to AMPs has been artificially induced in the laboratory (Guo et al. 1998; Guina et al. 2000; Tamayo et al. 2005; Lewis et al. 2009; Weatherspoon-Griffin et al. 2014), and recognized as a required component of virulence of some bacteria (Groisman et al. 1992; Peschel & Vincent Collins 2001; Poyart et al. 2003; Yang et al. 2012). However, there are limited experimental studies of microbial responses to prolonged exposure to AMPs and the consequences of using molecules from our own innate immune system to treat microbial infections. A few studies have experimentally tested the evolution of resistance to AMPs in bacteria *in vitro*, and demonstrated that this is possible. Such AMPs include pexiganan (GIGKFLKK AKKFGKAFVKILKKR) (Perron et al. 2006; Habets & Brockhurst 2012), LL-37 (LLGDFFRKSKEKIGKEFKRIVQRIKDFLRNLPRTES), CNY-100HL (CKYIL LLRRQLARAWRRGLR) and wheat germ histones (WGH, is a mixture of different histones and shorter histone peptides) (Lofton et al. 2013) and colistin (polymyxin E, is a mixture of cyclic polypeptides) (Jochumsen et al. 2016). Only in the last two studies were the resistance mutations identified and characterized in detail. Mutations in *waaY*, a component of the lipopolysaccharide (LPS) core biosynthesis pathway, decreased susceptibility of *Salmonella typhimurium* to LL-37, CNY100HL and wheat germ histones (Lofton et al. 2013). Recently, Jochumsen et al. (2016) showed that colistin resistance in *Pseudomonas aeruginosa* is a very complex and multistep

process which involves mutations in at least five independent loci, including *lpxC*, *phoQ* and *pmrB38*, that act synergistically to form the resistant phenotype.

Study of AMP resistance helps in gaining insight into the physiological effects on microbes and the resistant mechanisms, which could facilitate the developing of efficient new antimicrobials. The previous chapters have extensively reviewed TRPs, presenting data on design of several TRPs based on the tryptophan-rich domain (TRD) of puroindoline-a (PINA), the potential applications of these against biofilms and endospores, and the mechanism of action of the PuroA peptide. In this Chapter, an ‘evolution’ experiment was performed in which *S. aureus*, *E. coli*, *S. epidermidis* and *C. albicans* were subjected to successively increasing concentrations of four TRPs: PuroA, P1 and W7 (design detailed in chapter 3), as well as indolicidin. In addition, resistant isolates were further characterized in terms of resistance stability, cost of resistance and cross-resistance. The methods and strategies applied in this work are comprehensively explained in Sections 2.21 to 2.26 and the results are presented below.

6.3 Results

6.3.1 Resistance to TRPs after selection

Six lineages of each bacterium (*S. aureus*, *E. coli*, *S. epidermidis*) and yeast (*C. albicans*) were independently serially passaged for 45 days in the presence of increasing concentrations of peptides, called the ‘positive selection lines’. The serial passage was started at a peptide concentration of $0.5 \times \text{MIC}$ (to the respective organism) to reduce the growth of, but not kill, the bacteria or yeast. Two control lines were grown in absence of peptides for the entire duration of the experiment. After about 150 generations of growth, some of positive selection bacterial lines showed growth in the presence of peptide concentrations that were much higher than at the start of the experiment. Changes in peptides susceptibility between positive selection and control lineages were confirmed by minimal inhibitory concentrations (MIC) assays.

Within 28 transfers, five of six populations of *S. aureus* and two of six of populations of *E. coli* were capable of growth in $1000 \mu\text{g mL}^{-1}$ PuroA. Evolved bacteria showed an increase in MICs of peptides by approximately $8\text{--}16 \times$ that of ancestral bacteria. Increased resistance occurred at relatively faster rates in *S. aureus* than in *E. coli*. The positive selection and control lineages had the same MICs at the end of the experiment in *S. epidermidis* and *C. albicans* (Table 6.1).

Only two of six lines of *S. aureus* developed resistance to P1 and grew in its presence at the highest test concentration ($1000 \mu\text{g mL}^{-1}$), while the control lines failed to grow in the presence of P1 at $16 \mu\text{g mL}^{-1}$. No resistance was observed within the positive selection lines of *E. coli*, *S. epidermidis* and *C. albicans* toward P1 (Table 6.1). In comparison, all tested bacteria and yeast positive selection lineages showed no growth at a high concentration of W7 peptide, $250 \mu\text{g mL}^{-1}$. The selection lineages that showed last growth had no observable changes in MICs compared to control lines (Table 6.1).

In case of indolicidin, after selection, four of the six populations of *S. aureus* evolved tolerance and were able to grow in $1000 \mu\text{g mL}^{-1}$ of peptide. Evolved *S. aureus* lines had increased MICs, approximately $16 \times$ higher than ancestral clones. In contrast, after transfer 44, MICs of indolicidin against *E. coli*, *S. epidermidis* and *C. albicans* remained the same (Table 6.1).

Table 6.1 Selection response for resistance to selected TRPs.

Organism	Peptide used in selection treatments	No. of selection lines	No. of resistant populations	MIC ($\mu\text{g mL}^{-1}$) of resistant populations	
				Before selection	After selection
<i>S. aureus</i>	PuroA	6	5	16	125-250
	P1	6	2	16	125
	W7	6	0	8	N/A*
	Indolicidin	6	4	32	250
<i>E. coli</i>	PuroA	6	2	16	125
	P1	6	0	16	N/A
	W7	6	0	4	N/A
	Indolicidin	6	0	32	N/A
<i>S. epidermidis</i>	PuroA	6	0	8	N/A
	P1	6	0	8	N/A
	W7	6	0	4	N/A
	Indolicidin	6	0	8	N/A
<i>C. albicans</i>	PuroA	6	0	125	N/A
	P1	6	0	64	N/A
	W7	6	0	64	N/A
	Indolicidin	6	0	125	N/A

Selection lines were cultured in medium supplemented with successively increasing concentrations of the peptides.

*N/A – not applicable (no development of resistant populations).

6.3.2 Time-kill assay

The evolution of resistance to peptides was confirmed by examining time-kill kinetics of the resistant isolates at peptide MICs before selection (Figure 6.1). The *S. aureus* and *E. coli* isolates resistant to PuroA were not affected by $16 \mu\text{g mL}^{-1}$ of peptide (MIC for both species before selection), whereas the controls were completely killed (Figure 6.1 A). The survival of resistant lineages was about 3–4 logs greater at 3 h and 8–10 logs greater at 6 h relative to controls. The indolicidin-resistant *S. aureus* could also survive in $32 \mu\text{g/mL}$ of peptide whereas the ancestral bacteria were killed at this concentration.

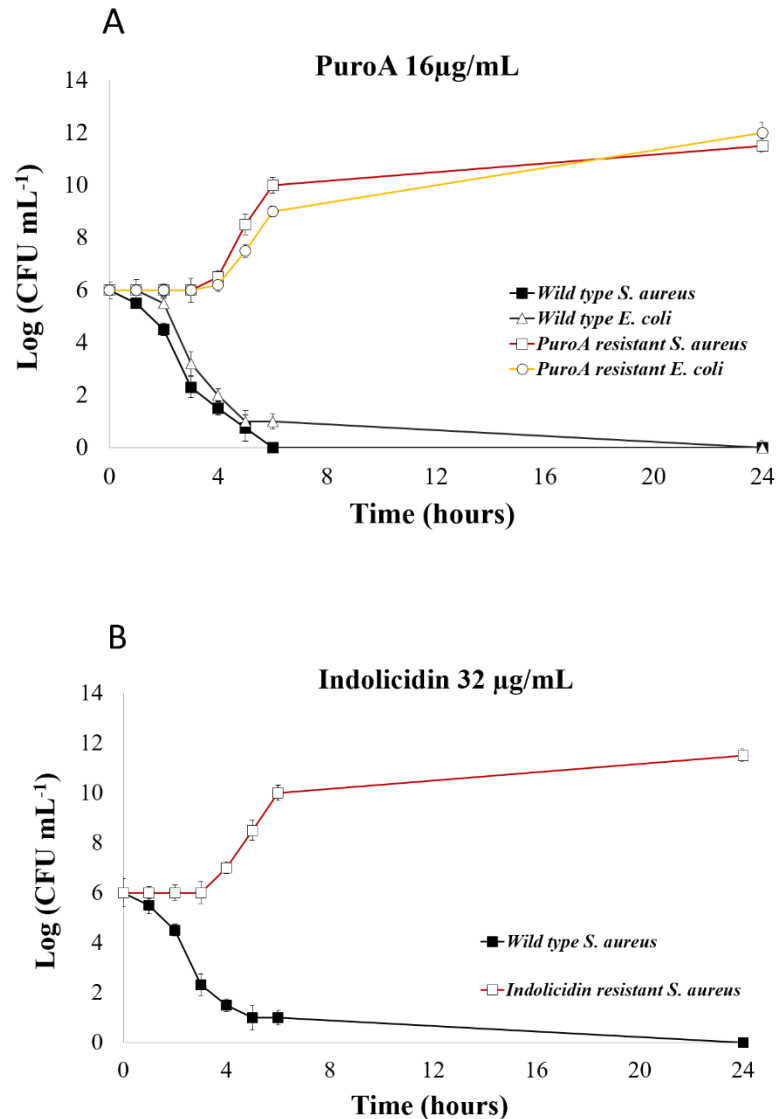


Figure 6.1 Time killing kinetics of resistant isolates.

(A) PuroA-resistant and untreated controls of *S. aureus* and *E. coli* were incubated at 37 °C in MHB containing 16 µg/mL of PuroA. (B) Indolicidin-resistant and untreated controls of *S. aureus* were incubated at 37 °C in MHB containing 32 µg/mL of indolicidin. Data are presented as mean values ± standard deviations of three independent experiments.

6.3.3 Cost of resistance

Conditional beneficial mutations in bacteria, e.g., antimicrobial resistance mutations, are usually associated with a cost under non-selective conditions. Resistance is often associated with a fitness cost that is typically seen as a reduction in bacterial growth rate (Andersson & Hughes 2010). The growth behaviour of lines that developed resistance to PuroA and indolicidin in *S. aureus* and *E. coli* were compared with the growth behaviour of controls. The acquisition of resistance appeared to change the

growth rate, as all the resistant bacterial populations showed a reduction in fitness. The PuroA-resistant *S. aureus* lines suffered from the greatest fitness reduction of 25% compared to 15% in indolicidin-resistant *S. aureus* lines and about 10-12% in PuroA-resistant *E. coli*.

Table 6.2 Growth behaviours of control and positive selection lines in unsupplemented medium

Organism	Strain	Relative Growth rate	Lag phase (h)
<i>S. aureus</i>	Untreated controls	1	3.5
	PuroA-resistant isolate	0.75	4
	Indolicidin-resistant isolate	0.85	3.9
<i>E. coli</i>	Untreated controls	1	2.3
	PuroA-resistant isolate	0.89	4.6

Maximal growth rate (V_{MAX}) during exponential growth of evolved and ancestral bacteria was also quantified and all evolved populations showed reduced V_{MAX} (Figure 6.2).

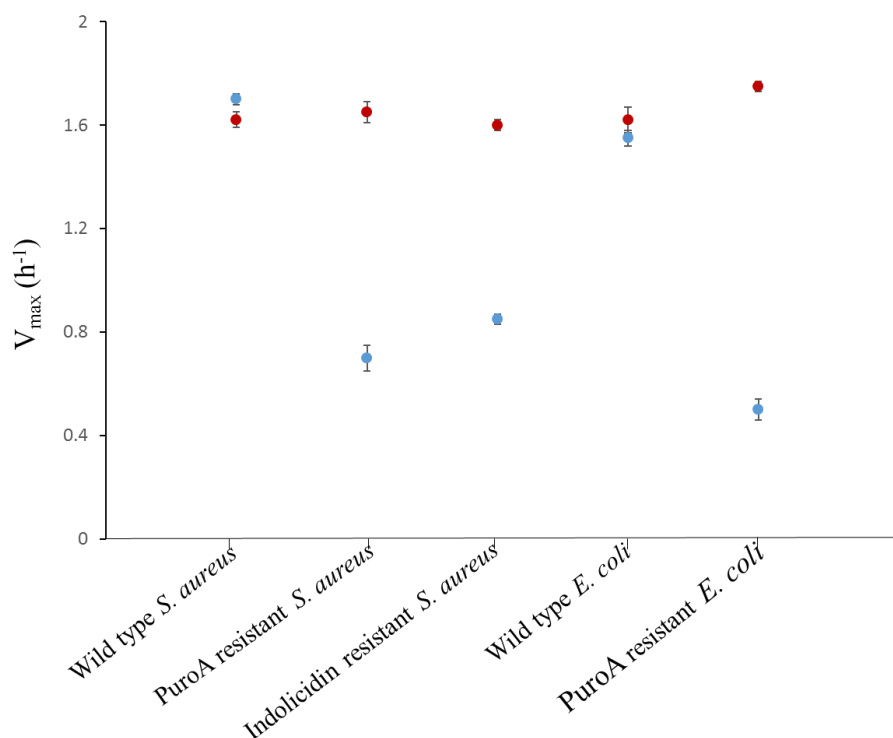


Figure 6.2 Effect of resistance development on maximum growth rate (V_{MAX}) of bacteria.

V_{MAX} of bacteria before selection is showed in blue and V_{MAX} after selection is showed in red.

6.3.4 Stability of resistance

In order to test the heritable nature of the developed resistance, the control and positive selection lines were subsequently transferred to medium containing no peptides for about 60-70 generations (10 days) and the MICs and growth rates were subsequently measured. All positive selection lines of both species, *S. aureus* and *E. coli* failed to grow at the original MIC again, similar to controls (Table 6.3). These results show that resistance to PuroA, P1 and indolicidin is not stable or heritable. The cost of resistance was also completely ameliorated as the bacterial populations with highest cost-of-resistance reached growth rates similar to those of the ancestral bacteria.

Table 6.3 Response to compensatory adaptation selection for PuroA and indolicidin

Organism	Peptide ID	No. of resistant populations	MIC ($\mu\text{g mL}^{-1}$)		
			Before selection	After selection	After selection in absence of peptide
<i>S. aureus</i>	PuroA	5	16	125-250	16
	P1	2	16	125	16
	Indolicidin	4	32	250	32
<i>E. coli</i>	PuroA	2	16	125	16
	P1	0	16	16	16
	Indolicidin	0	32	32	32

6.3.5 Cross-resistance studies

Cross-resistance is the development of resistance to a substance (such as an antimicrobial agent) as a result of previous exposure and evolve resistance to a similar acting or related substance (Inoue et al. 1978). The resistant bacteria were examined for cross-resistance to other TRPs as compared to the founding ancestor. The differences in susceptibility of the control and resistant strains was determined using MIC assays. Overall, no observable cross-resistance or decrease in susceptibility was found in resistant lines. PuroA-resistant *S. aureus* and *E. coli* showed the same susceptibility to W7, indolicidin, P1 and Pina-M peptides compared to their founding ancestor. Likewise, PuroA, W7, P1 and Pina-M had the same MIC for indolicidin-resistant *S. aureus* and its susceptible parental strain. It seems that evolved resistance to PuroA or indolicidin does not confer cross-resistance to other TRPs.

Table 6.4 Cross-resistance between peptides

Organism	Strain	MIC ($\mu\text{g mL}^{-1}$)				
		PuroA	P1	W7	Pina-M	Indolicidin
<i>S. aureus</i>	Wild type controls	16	16	8	8	32
	PuroA resistant isolate	250	16	8	8	32
	Indolicidin resistant isolate	16	16	8	8	250
<i>E. coli</i>	Wild type controls	16	16	4	8	32
	PuroA resistant isolate	125	16	4	8	32

6.3.6 Determining the effects of peptide combinations on MIC and resistance development

The activity of PuroA in combination with W7, P1, Pina-M and indolicidin was determined using the broth microdilution checkerboard assay against the same *S. aureus* and *E. coli* strains, and the fractional inhibitory concentration index (FICI) for these combinations was calculated (Table 6.5). All peptides combinations were found to be non-synergistic and there was no interaction between PuroA and any of the tested peptides.

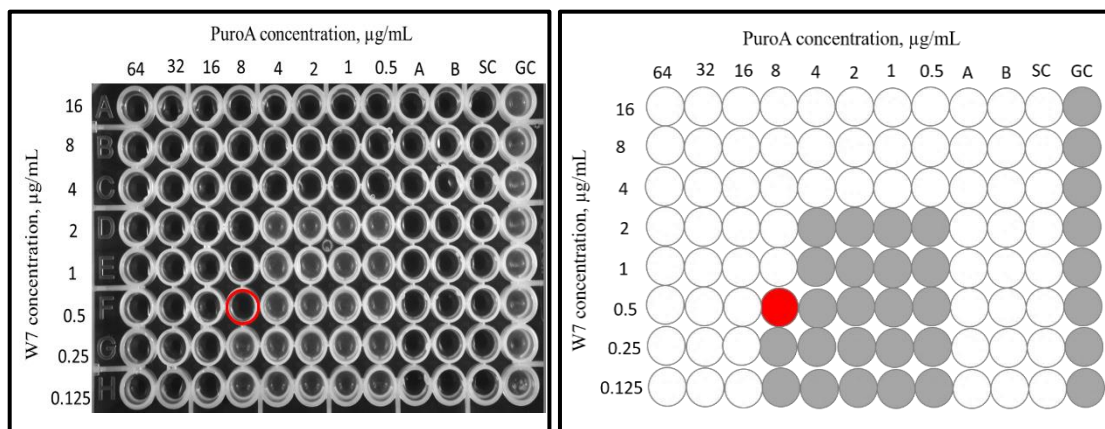


Figure 6.3 Checkerboard assay in the 96-well microtiter plate of PuroA and W7 combination against *S. aureus*.

The two rightmost columns contain the growth control without peptides (GC), and medium-sterility control (SC). Column A contains PuroA only at MIC against *S. aureus* and B contains W7 only at MIC against *S. aureus*. The red circle indicates the peptides combination that resulted in no interaction effect, for which the FICI calculation should be $[8/16+0.5/4] = 0.625$. (See Chapter 2, Section for more detailed calculation.

Table 6.5 Combination activities of PuroA with other TRPs

Strains	FICI*			
	W7	P1	Pina-M	Indolicidin
<i>S. aureus</i>	0.75	1	0.625	0.625
<i>E. coli</i>	0.625	0.75	1	0.625

* Results shown are the mean of triplicate assays. FICI of ≤ 0.5 means synergistic combination, FICI of 0.56-1 means no interaction and FICI of >4 means antagonistic combination.

In order to test the development of resistance in the presence of two peptides, six lines of *S. aureus* were serially passaged in the presence of increasing concentrations of W7 together with PuroA or indolicidin. No growth was observed at $32 \mu\text{g mL}^{-1}$ of W7 mixed with $125 \mu\text{g mL}^{-1}$ of PuroA or $250 \mu\text{g mL}^{-1}$ of indolicidin. The selection lineages also had no observable changes in MICs compared to control lines.

5.4 Discussion

It has been surmised that development of resistance by sensitive microbes towards AMPs is improbable, because the common target of most AMPs is the bacterial membrane. Microbes would, therefore, have to change greatly and reorganize their membranes, which is energetically impracticable (Zasloff 2002). In this study, it was found that resistance to TRPs can experimentally evolve in *S. aureus* and *E. coli* when they are consistently exposed to increased levels of AMPs. These results agree with previous prediction that continued selection in bacterial populations can lead to resistance evolution against AMPs (Bell & Gouyon 2003). As the selection experiments continued for about 300-350 generations only, it is concerning that AMP resistance seemed to have developed readily. When *Pseudomonas fluorescens* and *E. coli* evolved resistance to pexiganan, Perron et al. (2006) hypothesized that AMPs are highly dynamic systems that have evolved in response to continual host pathogen coevolution and the high diversity of AMPs is consistent with this theory. It was assumed that the range of AMPs produced by the host matches the range of pathogens that attack it, meaning every peptide is very specific and it is able to change if the microbial community changes or if the pathogen adapts and evolves resistance to that peptide (Vanhoye et al. 2003; Perron et al. 2006).

Resistance mechanisms often cause a reduction in biological fitness. The fitness level of resistant bacteria measured as growth rate gives an indication of their survival probability in an environment wherein susceptible bacteria which are more fit are present and can outcompete them when antimicrobials pressure is absent (Andersson & Hughes 2010). However, it was found that resistant bacteria can overcome the fitness costs by acquiring fitness-compensatory mutations in addition to the resistance mutations (Schrag & Perrot 1996; Nilsson et al. 2006; Marcusson et al. 2009). Further, resistant mutants can have a growth advantage over susceptible strains at low antibiotic concentrations which are present in many natural environments (e.g. soil or aquatic or soil) (Gullberg et al. 2011). In this study, the fitness of PuroA and indolicidin resistant mutants was measured in absence of AMP pressure, and showed between 10-25% fitness reductions. These results indicate that in the absence of the selection pressure, resistant populations could be outcompeted by the fitter susceptible bacteria over time. In terms of fitness level, PuroA-resistant *S. aureus* isolates had the

greatest cost of resistance, with 25% reduction in fitness, suggesting that the resistant isolates carried more mutations than others.

Another potential problem with using AMPs as therapeutics is cross-resistance. It has been argued that the therapeutic use of certain AMPs might change natural environments and create a source of continual selection which would lead to resistance evolution (Bell & Gouyon 2003). This potential problem is of main concern due to the possibility of cross resistance with human defence peptides. Surprisingly, despite similarities in the structure and mechanism of action, there was no observable cross-resistance between the tested TRPs. This observation indicating that the evolved resistance mechanism is peptide-specific and could not even be conferred to other peptides from the same class. Testing cross-resistance further against different classes of AMPs, including human defence peptides and conventional antibiotics, would be useful in investigating the potential problems associated with the therapeutic use of AMPs. The first evidence that developed resistance to therapeutic AMPs can confer cross-resistance to a human defence peptides was seen when evolved resistance to pexiganan peptide could confer cross-resistance to human-neutrophil-defensin-1 (HNP-1) (Habets & Brockhurst 2012), even though pexiganan and HNP-1 belong to structurally different classes of AMPs with distinct mechanisms of action (Brogden 2005). Therefore, it was suggested that bacteria can develop generalized protection mechanisms against multiple AMPs, however, this theory is not consistent with our results. We also showed that the evolved resistance to PuroA and indolicidin is not stable and heritable as resistant bacteria failed to grow at MIC and showed the same growth rate as the ancestral bacteria after growing for a few generations without TRP selection pressure. The resistant bacteria, therefore, seem to not acquire additional fitness-compensatory mutations over the course of experiment, which can counterbalance the fitness reduction and stabilize the populations in the absence of AMPs. Further study using whole genome sequencing would be useful to understand in depth the genetic basis and the mechanism of resistance to PuroA, P1 and indolicidin.

Drug combinations can result in synergism, additivity, or antagonism interactions, meaning that combined medicines can have stronger, equal or weaker effect, respectively, than that of equivalent concentrations of single medicines (Greco et al.

1995; Chou 2006; Cokol et al. 2011; Imamovic & Sommer 2013). The strategy of combination therapies is supposed to potentially treat multi-resistant pathogens, delay the development of drug resistance, and/or reduce the dose of individual drugs, and thus, reduce the side effects of high doses (Tamma et al. 2012; Worthington & Melander 2013). However, the success of the combination approach is context dependent, mainly when using it against a mix of sensitive and resistant populations (Chait et al. 2007; Yeh et al. 2009; Pena-Miller et al. 2013). Synergistic antibiotics can efficiently treat bacterial infections, but can also increase the rate of resistance selection, whereas antagonistic combinations show the opposite effects (Yu et al. 2016). In health applications, AMPs would ideally interact positively with human defence peptides. Some studies, thus, tested the effect of AMPs interactions with each other, particularly with mammalian immune peptides. Interactions of AMPs were mostly synergetic against bacteria (Yan & Hancock 2001), multi-resistant strains and biofilms (Berditsch et al. 2015; Yu et al. 2016) and even tumour cells (Westerhoff et al. 1995; Kelly et al. 2016). Therefore, it was suggested that synergism is a common phenomenon in AMPs interactions (Yu et al. 2016). PuroA does not seem a promising synergistic agent as, in this study, it showed no *in vitro* interaction activities with other TRPs. Structure and mechanism of action similarities between the tested TRPs could explain these non-synergistic interactions. Indolicidin, from bovine neutrophils, also did not show synergistic effects with AMPs from different classes, including the human peptide LL-37 and the bovine neutrophil peptide bactenecin (Yan & Hancock 2001). Whereas lactoferricin (Lfcin) acted synergistically with its parent protein, lactoferrin (LF), against *E. coli* and *S. epidermidis* and acted antagonistically with nisin (López-Expósito et al. 2008). Therefore, combinations of AMPs may offer the advantage of synergistic actions, however, predicting the behaviour of these combination is challenging.

In addition, the evolutionary consequences of AMPs interactions is still unclear. In this study, the development of resistance in the presence of two TRPs was tested. Over the experiment, no evolved resistance was detected in both *E. coli* and *S. aureus* toward a combination of W7 and PuroA or indolicidin, although no synergetic interactions were found between those peptides. This confirmed the cross-resistant results; evolving resistance to PuroA does not confer resistance to other tested TRPs and may explain the failure of growth in presence of two peptides. AMPs

combinations, therefore, could be a useful approaches to decrease the rate of selection of resistance.

In conclusion, although the development of resistance observed in our study was against few of the tested TRPs only and was not stable, heritable or induced cross-resistance, it seems that there is a possibility of developing resistance against AMPs, similar to conventional antimicrobial agents. Consequently the therapeutic use of AMPs may change the interaction with our commensal microbiome and increase opportunities for opportunistic infections. Although the precise correlation between the use of antibiotics and the emergence of resistance is unclear, the overuse of broad-spectrum and potent antibiotics is generally accepted as a main reason behind the high rate of emergence of drug-resistant microorganisms (superbugs) (Cruz et al. 2014). Therefore, to avoid repeating the same mistake, AMPs should be used carefully and appropriately to minimize the development of resistance. In addition, to date, there is no study on developing resistance to AMPs *in vivo*, e.g. would the commensal microbiome of an animal develop resistance with long-term exposure to natural or synthetic AMPs? Studying the potential for resistance development against these new antimicrobial molecules before their large-scale application and not assuming that microbial resistance is unlikely will help maximize their ultimate benefit to society.

Chapter 7

Preliminary investigations of cell selectivity and anticancer potential of rationally designed TRPs

7.1 Abstract

Most antimicrobial peptides (AMPs) are toxic to pathogens but not to normal mammalian cells. However, in some cases, these peptides also display cytotoxicity to a variety of cancer cells including those that are multidrug resistant. Selective cytotoxicity is a highly desirable attribute in AMPs for their potential as clinical therapeutics. In this study, the cationic Trp-rich peptides (TRPs) that were designed based on PuroA peptide with different charge, length and numbers of Trp residues, were further tested against normal and cancer mammalian cells. The well-established *in vitro* MTT assay was used to test the cytotoxicity of the peptides against two different types of mammalian cells, mouse fibroblast NIH-3T3 cells and the human cervical carcinoma HeLa cells. The haemolytic activities of the TRPs against sheep RBCs were also determined. The peptide concentrations that caused 50% growth inhibition in each cell line (IC₅₀) and lysed 50% of the RBCs (HD₅₀) were determined. All tested peptides were not significantly cytotoxic toward NIH-3T3 cells nor RBCs. R8 (RRRRWRWWRWRR-NH₂), W7 (WRWWKWW-NH₂), W8 (WRWWKWWK-NH₂) and WW (WWRWWKWW-NH₂) peptides showed cytotoxicity against HeLa cells with IC₅₀ between 125-250 µg/mL. Dimeric PuroA ((FPVTWRWWKWWKG)₂k-NH₂) and P1 (RKRWWRWWKWWKR-NH₂) peptides displayed relatively strong cytotoxicity and specificity toward HeLa cells with IC₅₀ of 32 µg/mL and therapeutic index (TI) of 7.8. Upon peptide treatment, SEM imaging revealed that HeLa cells were significantly disrupted and damaged. Our preliminary results establish the potential of these peptides as selective antitumor therapeutics that could reduce the detrimental side effects of conventional chemotherapeutics.

7.2 Introduction

Cancer remains a leading cause of mortality affecting millions of people worldwide (Thun et al. 2010; Gaspar et al. 2013). Current anticancer therapies display a worrying number of problems, such as their deleterious side-effects on healthy cells (Riedl et al. 2011), reoccurrence and/or metastasis (Harris et al. 2013) and the development of resistance by cancer cells towards them (Gatti & Zunino 2005; Pérez-Tomás 2006). Thus, the development of new, efficient and selective classes of anticancer drugs is an urgent need. An increasing number of studies have shown that some cationic AMPs also exhibit cytotoxicity against cancer cells. These studies indicate that further studies on such AMPs with both activities (antimicrobial and anticancer) are essential, as new treatment strategies and to extend our understanding of our immune system.

Although some of these anticancer peptides (ACPs) are toxic to cancer cells but not to normal mammalian cells (Papo & Shai 2005; Schweizer 2009; Slaninová et al. 2012; Harris et al. 2013), the development of selective ACPs has been a challenge. It is not yet possible to predict potency and selectivity of peptides toward cancer cells based on their structures. The progression of cancer has been correlated with changes in the cell membrane and these changes are thus believed to play a role in the selective killing of cancer cells by ACPs. The main difference is that cancer cell membranes are typically negatively charged, similar to bacterial membranes and unlike the zwitterionic membranes of normal cells (Mader & Hoskin 2006; Hoskin & Ramamoorthy 2008a). Therefore, it has been hypothesized that the molecular basis of the activity and the selectivity of AMPs and ACPs are similar (Van Zoggel et al. 2012; Gaspar et al. 2013; Liu et al. 2015), as detailed in Chapter 1, Section 1.10.1.1.

The therapeutic index (TI) is a widely used parameter to represent cell selectivity and specificity of peptides. It is commonly calculated by the ratio of HD_{50} (peptide concentration that lyses 50% of the RBCs) and GM (geometric mean of MICs against tested microorganisms) or the ratio of $IC_{50 \text{ normal}}$ (peptide concentration that causes 50% growth inhibition in normal mammalian cell line) and $IC_{50 \text{ cancer}}$ for cancerous cells (Lee et al. 2004; Chen et al. 2005; Park et al. 2009; Solanas et al. 2009; Nan et al. 2012; Jacob et al. 2014). Therefore, a larger value of TI indicates greater antimicrobial and/or anticancer specificity and cell selectivity.

Not all AMPs are ACPs, hence identifying all factors that affect the efficacy and selectivity of AMPs as ACPs is of crucial important for their therapeutic applications. In Chapter 3, the effects of some structural parameters on the antimicrobial activity, protease sensitivity and salt tolerance of 13 tryptophan (Trp)-rich peptides (TRPs) designed based on PuroA peptide were studied (see Chapter 3, Table 3.1, 3.2, 3.3 and 3.4). In this Chapter, the selectivity and cytotoxicity of these 13 peptides were investigated against two mammalian cell lines – one normal and one cancerous. The methods used in this chapter are described in detail in Sections 2.27 to 2.29. The preliminary results are presented below.

7.3 Results

7.3.1. Haemolytic activity and cytotoxicity against mammalian cells

As a primary characterization of the cytotoxic properties of the designed TRPs, their haemolytic activities against sheep RBCs were measured. The haemolytic activities of the peptides were determined by measuring the amount of haemoglobin released from sheep RBCs suspension after exposure to various peptide concentrations for 1 h (Fig. 7.1). 1% Triton X-100 (positive control) and PBS pH 7.4 (negative control) caused 100% and 0 % haemolysis, respectively. Sample absorbance was measured at 570 nm using a microplate reader (data not shown). Positive haemolytic activity was defined as the peptide concentration that lysed 50% of the RBCs (HD_{50}). Within the range of peptide concentrations tested (16-500 $\mu\text{g/mL}$), all peptides were non-toxic to erythrocytes as none of them caused 50% lysis to RBCs (Table 7.1).

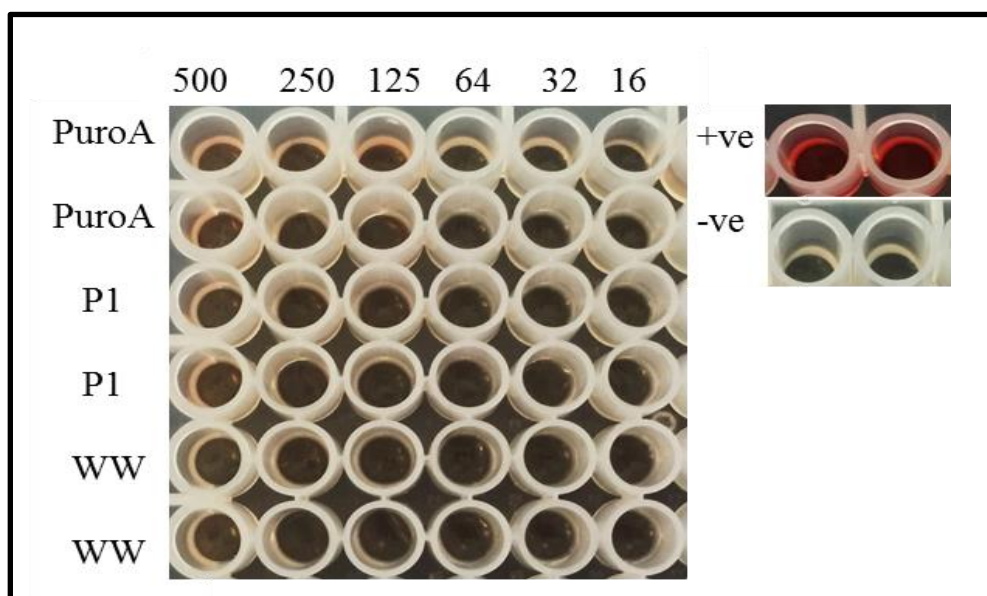


Figure 7.1 Example of haemolytic activity of peptides against sheep red blood cells (RBCs).

Peptides concentrations from column 1 to 6; 500 $\mu\text{g/mL}$, 250 $\mu\text{g/mL}$, 125 $\mu\text{g/mL}$, 64 $\mu\text{g/mL}$, 32 $\mu\text{g/mL}$ and 16 $\mu\text{g/mL}$. 100% RBC lysis (1% Triton X-100, positive control) and 0% RBC lysis (PBS pH7.4, negative control).

To assess the peptides selectivity towards microbial cells, therapeutic index (TI) was calculated. The TI of each peptide was calculated as the ratio of HD_{50} of the peptide to GM (geometric mean of the peptide MIC values against the three bacterial strains that were tested in Chapter 3; *E. coli*, *S. aureus*, *P. aeruginosa*). A larger therapeutic index value corresponds to greater cell selectivity (Table 7.2).

Table 7.1 Haemolytic activity of the designed TRPs

Peptide ID	Sequence	Percentage of haemolysis of sheep RBCs by peptides						Haemolysis* (HD ₅₀)
		500 µg/mL	250 µg/mL	125 µg/mL	64 µg/mL	32 µg/mL	16 µg/mL	
PuroA	FPVTWRWWKWWKG-NH ₂	16	9	4	0	0	0	>500
Cyclic PuroA	FPVTWRWWKWWKG	16	8	2	0	0	0	>500
Di-PuroA	(FPVTWRWWKWWKG) ₂ k-NH ₂	30	22	10	4	1	0	>500
PuroA-OH	FPVTWRWWKWWKG	18	3	2	0	0	0	>500
R8	RRRRWRWWRWRR-NH ₂	18	10	4	0	0	0	>500
P1	RKRWWRWWKWWKR-NH ₂	18	9	1	0	0	0	>500
dP1	<u>R</u> <u>K</u> <u>R</u> W <u>W</u> <u>R</u> W <u>W</u> <u>K</u> W <u>W</u> <u>K</u> R-NH ₂	17	7	1	0	0	0	>500
R6	RWWKWW-NH ₂	28	7	4	3	1	0	>500
R7	RWWKWWK-NH ₂	25	15	6	2	0	0	>500
W7	WRWWKWW-NH ₂	47	20	4	0	0	0	>500
dW7	<u>W</u> <u>R</u> W <u>W</u> <u>K</u> W <u>W</u> -NH ₂	10	8	3	1	0	0	>500
W8	WRWWKWWK-NH ₂	48	22	9	3	0	0	>500
WW	WWRWWKWW-NH ₂	10	4	0	0	0	0	>500
dWW	W <u>W</u> <u>R</u> W <u>W</u> <u>K</u> W <u>W</u> -NH ₂	12	5	0	0	0	0	>500

Underlined and bold amino acids are D-enantiomers.

HC₅₀: concentration to induce 50% lysis of erythrocytes.

Results shown are the average of two independent experiments conducted in triplicates.

Table 7.2 Antibacterial activity, haemolytic activity and cell selectivity (therapeutic index) of the designed TRPs

Peptide ID	Sequences	MIC ($\mu\text{g mL}^{-1}$)*			GM ($\mu\text{g mL}^{-1}$)	HD ₅₀ ($\mu\text{g mL}^{-1}$)	TI (HD ₅₀ /GM)
		<i>E. coli</i>	<i>S. aureus</i>	<i>P. aeruginosa</i>			
PuroA	FPVTWRWWKWWKG-NH ₂	16	16	64	32	>500	>15.6
Cyclic PuroA	FPVTWRWWKWWKG	250	125	>250	>208	>500	ND
Di-PuroA	(FPVTWRWWKWWKG) ₂ k-NH ₂	250	250	>250	>250	>500	ND
PuroA-OH	FPVTWRWWKWWKG	32	64	125	73.6	>500	>6.8
R8	RRRRWRWRRWRR-NH ₂	64	64	64	64	>500	>7.8
P1	RKRWRRWWKWWKR-NH ₂	16	16	16	16	>500	>31.2
dP1	RKR <u>W</u> WR <u>W</u> W <u>K</u> WW <u>K</u> R-NH ₂	16	16	16	16	>500	>31.2
R6	RWWKWW-NH ₂	32	16	32	26.6	>500	>18.7
R7	RWWKWWK-NH ₂	8	16	32	18.6	>500	>26.8
W7	WRWWKWW-NH ₂	4	8	32	14.6	>500	>34.2
dW7	WR <u>W</u> W <u>K</u> WW-NH ₂	8	8	16	10.6	>500	>47.1
W8	WRWWKWWK-NH ₂	4	8	32	14.6	>500	>34.2
WW	WWRWWKWW-NH ₂	8	8	32	16	>500	>31.2
dWW	WWR <u>W</u> W <u>K</u> WW-NH ₂	8	8	32	16	>500	>31.2

*MIC: the lowest peptide concentration to completely inhibit growth of the tested bacteria (values taken from Chapter 3, Table 3.2). GM: The geometric mean of MICs from three bacterial strains. Therapeutic index (TI): Ratio of HD₅₀ ($\mu\text{g mL}^{-1}$) to GM ($\mu\text{g mL}^{-1}$). ND: not determined. The “>” in TI means that there were no exact HD₅₀ values to calculate the TI within the tested concentration range of peptides, i.e., the stated values in the table are minimum TI calculated with 500 $\mu\text{g mL}^{-1}$.

Some TRPs have shown antitumor activity (see Chapter 1, Section 1.10.1.2), hence the selectivity as well as the toxicity of our peptides were tested further against mammalian cells. The well-established *in vitro* MTT assay was used to test the cytotoxicity of the peptides against two different types of mammalian cells, mouse fibroblast NIH-3T3 cells and the human cervical carcinoma HeLa cells. The cells were treated with increasing concentrations of peptides (4-250 $\mu\text{g/mL}$) for 24 h and, then, the cell viability was quantified colourimetrically to determine the ability of their mitochondrial dehydrogenase to reduce the tetrazolium salt MTT to the purple formazan. Untreated cells were used as controls and cell viability was determined relatively to the untreated control, as detailed in Chapter 2, Section 2.28.4. Results are shown in Fig. 7.3 and 7.4. Positive cytotoxic activity was defined as the peptide concentration that caused 50% growth inhibition in each cell line (IC_{50}) (Table 7.3). To measure the cell specificity of the peptides to cancerous cells, the TI was calculated. The TI of each peptide was calculated as the ratio IC_{50} T3T ($\mu\text{g mL}^{-1}$) to IC_{50} HeLa ($\mu\text{g mL}^{-1}$).

Table 7.3 Cytotoxicity activity of Trp-rich peptides against NIH 3T3 and HeLa

Peptide ID	IC_{50} ($\mu\text{g/mL}$)*		TI (IC_{50} T3T/HeLa)
	NIH-3T3	HeLa	
PuroA	250	>250	<1
Cyclic PuroA	>250	>250	ND
Di-PuroA	250	32	7.8
PuroA-OH	>250	>250	ND
R8	>250	250	>1
P1	250	32	7.8
dP1	250	125	2
R6	250	>250	<1
R7	250	>250	<1
W7	250	250	2
dW7	>250	125	>3
W8	>250	250	>2
WW	>250	250	>2
dWW	250	125	2

* IC_{50} : concentration causing 50% cell growth inhibition. Therapeutic index = Ratio of IC_{50} T3T ($\mu\text{g mL}^{-1}$) to IC_{50} HeLa ($\mu\text{g mL}^{-1}$). ND = not determined. The “<” indicates the maximum TI calculated with 250 $\mu\text{g mL}^{-1}$. The “>” indicates the minimum TI calculated with 250 $\mu\text{g mL}^{-1}$.

As can be seen in Table 7.3 and Fig 7.3, PuroA, dimeric PuroA, P1, dP1, R6, R7, W7 and dWW peptides showed toxicity to NIH-3T3 mouse fibroblasts (representing non-cancer mammalian cells) at concentration of 250 $\mu\text{g}/\text{mL}$. In contrast, no toxicity was detected for Cyclic PuroA, non-amidated PuroA, R8, dW7, W8 and WW peptides against fibroblasts up to 250 $\mu\text{g}/\text{mL}$.

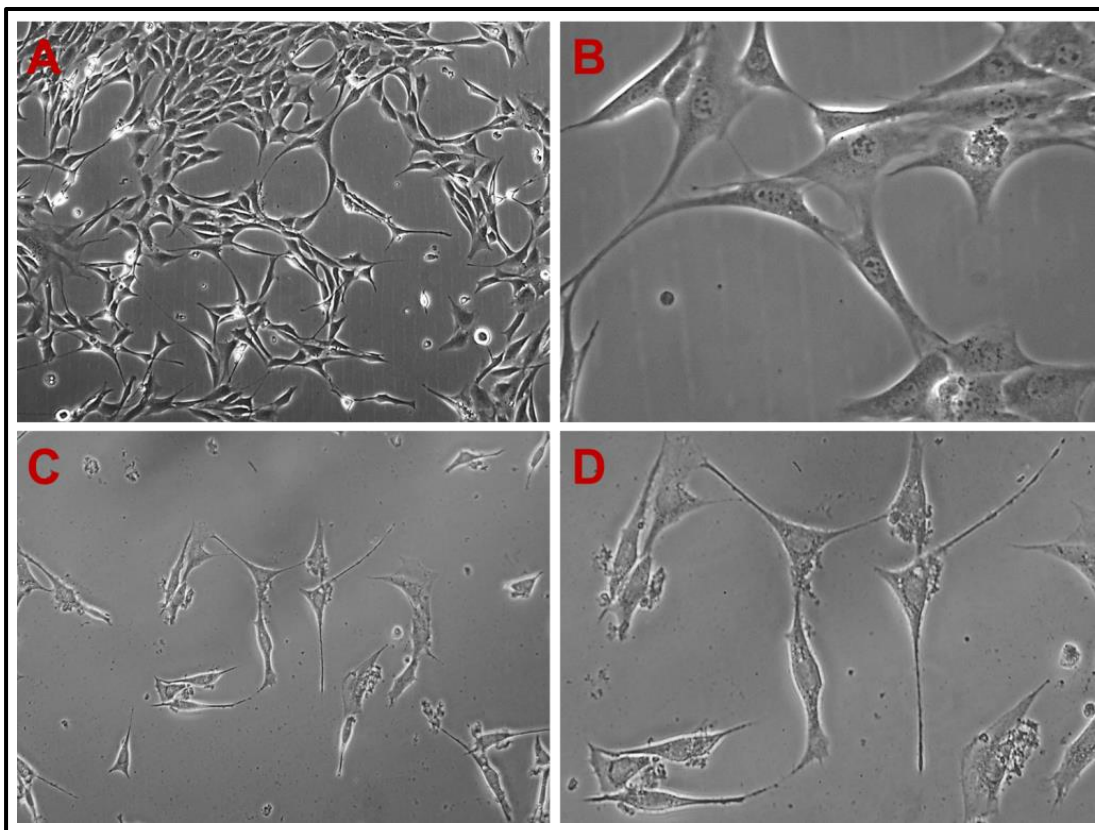


Figure 7.2 Light microscopy images of NIH-3T3 fibroblasts. Magnifications are 100 \times in A, 200 \times in C, and 400 \times in B & D.

The TRPs were less effective against cancer cells than prokaryotic cells. R8, dP1, W7, dW7, W8, WW and dWW showed cytotoxicity activity against HeLa cells with IC_{50} between 125-250 $\mu\text{g}/\text{mL}$ (Fig. 7.4). Dimeric PuroA and P1 peptides displayed relatively strong cytotoxicity and specificity toward cancer cells; both have IC_{50} of 32 $\mu\text{g}/\text{mL}$ and therapeutic index of 7.8 (Table 7.3).

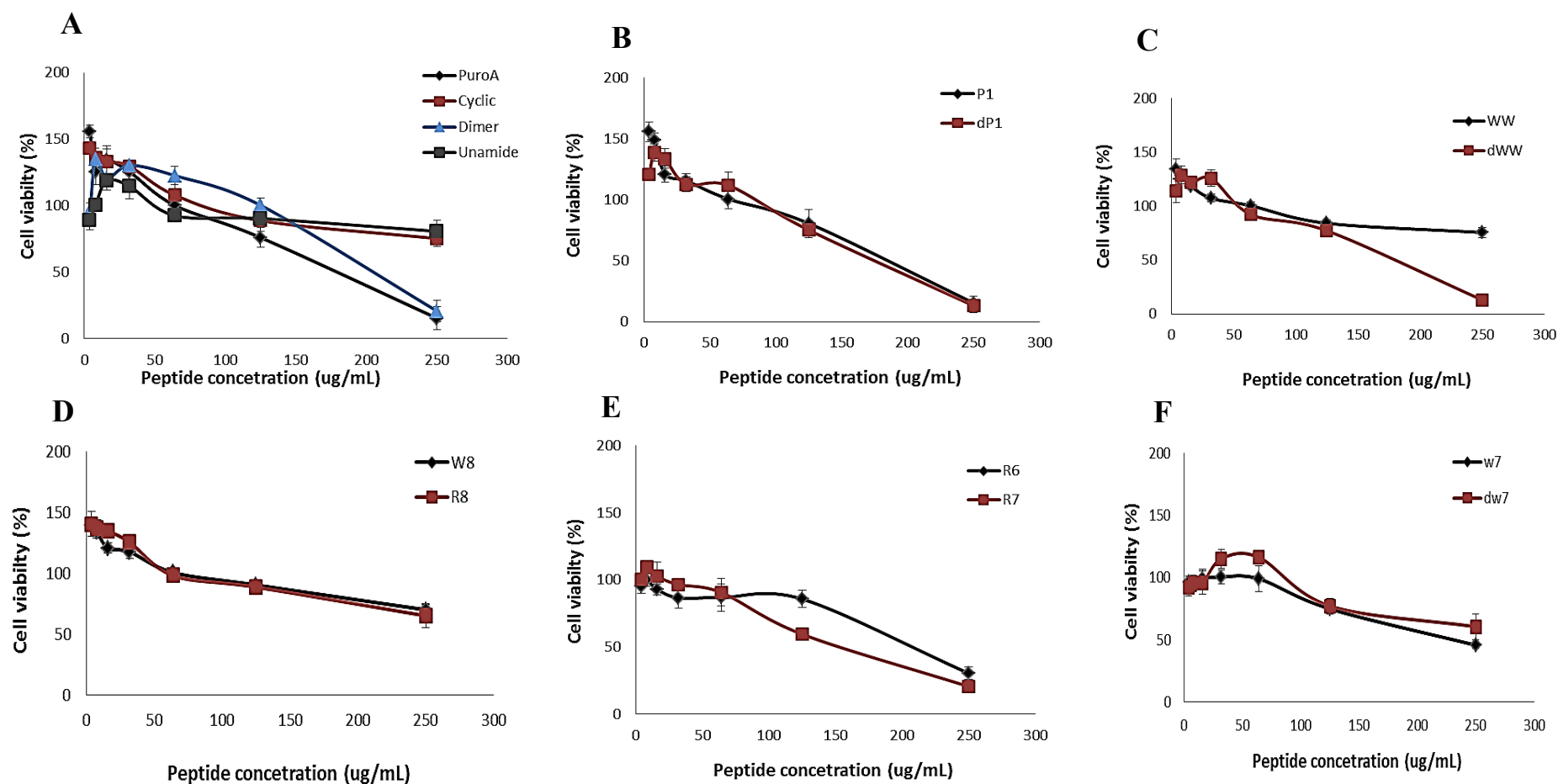


Figure 7.3 Cell viability of mouse NIH-3T3 fibroblasts after peptide treatment.

Cell viability was measured by the MTT assay after 24 h incubation with indicated amount of the peptides. Results shown are the average of three independent experiments conducted in triplicates. **A.** PuroA, Cyclic PuroA, Di-PuroA and PuroA-OH; **B.** P1 and dP1; **C.** WW and dWW; **D.** W8 and R8. **E.** R6 and R7; **F.** W7 and dW7.

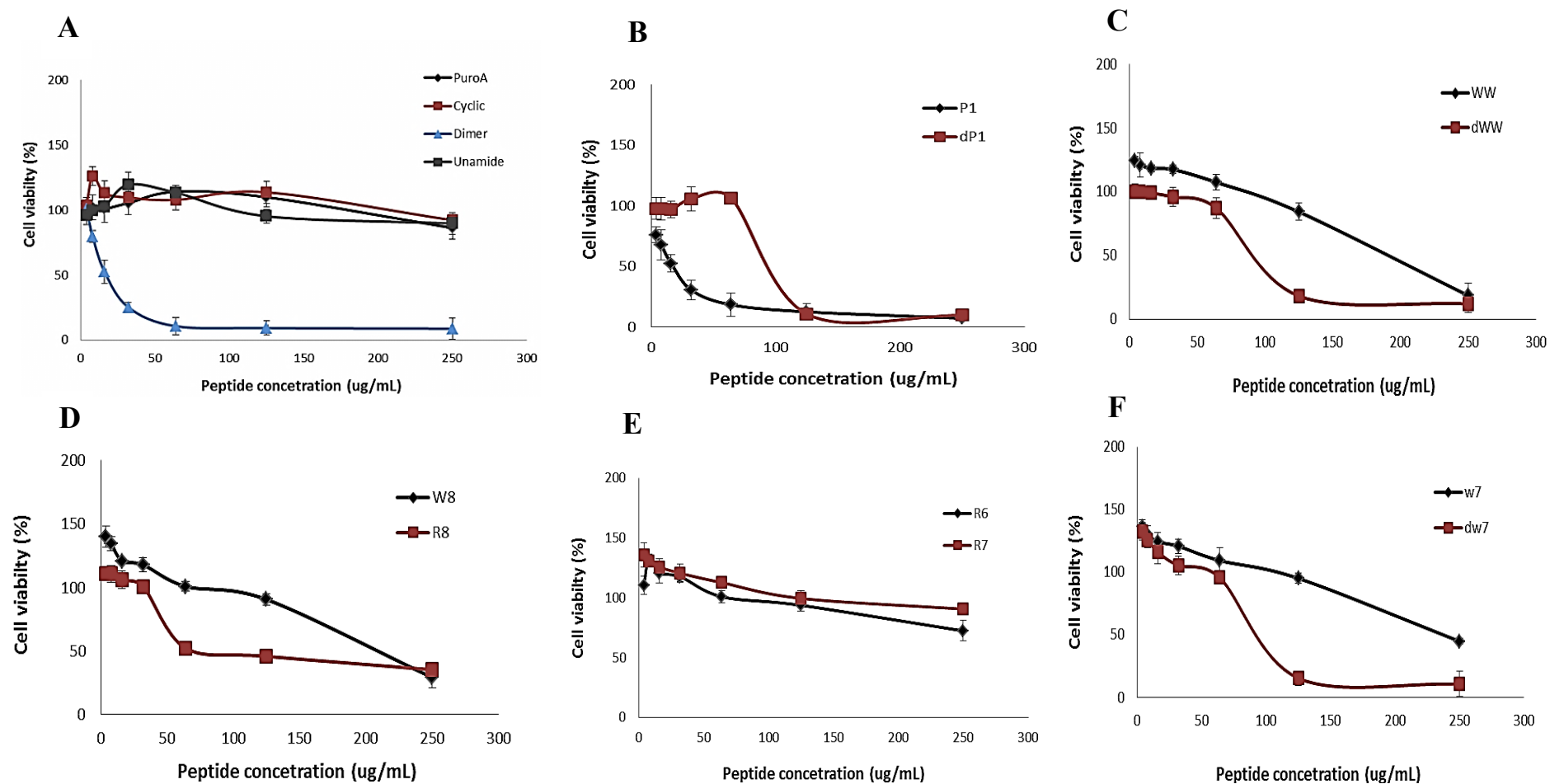


Figure 7.4 Cell viability of human cervical carcinoma HeLa cells after peptide treatment.

Cell viability was measured by the MTT assay after 24 h incubation with indicated amount of the peptides. Results shown are the average of three independent experiments conducted in triplicates. **A.** PuroA, Cyclic PuroA, Di-PuroA and PuroA-OH; **B.** P1 and dP1; **C.** WW and dWW; **D.** W8 and R8. **E.** R6 and R7; **F.** W7 and dW7.

The anticancer activity of P1 and Di-PuroA peptides against HeLa cells was further examined using light microscopy and SEM. These two microscopy techniques were used to visualize the subtle morphologic changes of HeLa cells after exposure to peptides for 24 h. In the absence of any peptide, untreated (control) cells showed normal morphology; flattened or rounded in shape with several microvilli on the surface and extending lamellipodia (a flattened “veil-like” projection) (Fig. 7.6). In contrast, upon peptide treatment, almost all cells were heavily disrupted and significantly damaged (Fig. 7.5 and 7.6). In SEM images, treated cells were characterized by pronounced shrinkage, leakage of cytoplasmic contents, and loss of microvilli. These results confirm the inhibitory effect of the TRPs on the growth of HeLa cells and could suggest a membranolytic mechanism of action.

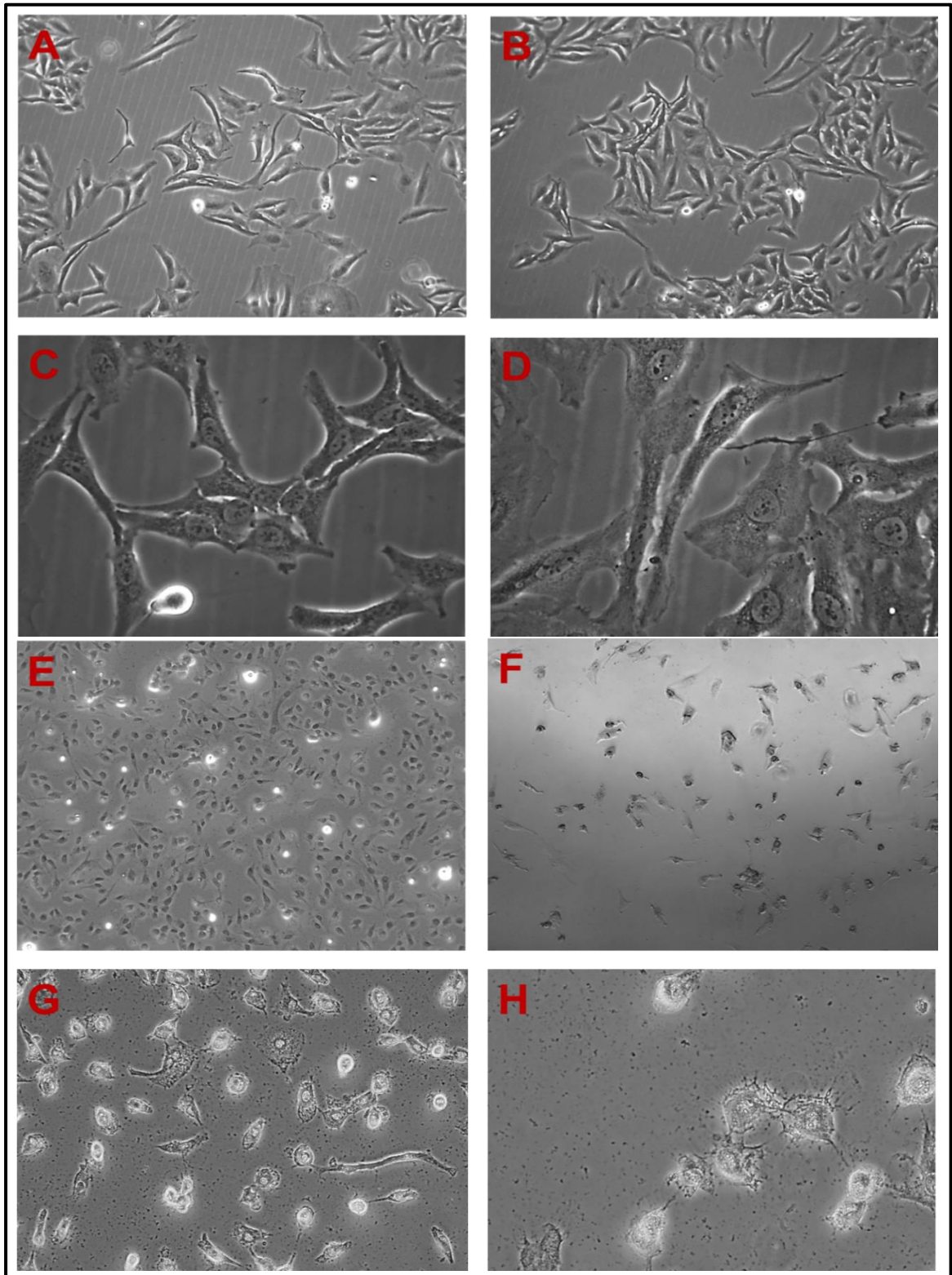


Figure 7.5 Light microscopy images of HeLa cells.

A, B, C and D: untreated cells control; E and G are treated cells with peptide P1 64 µg/mL; F and H: treated cells with peptide Di-PuroA 64 µg/mL. Magnifications are 100 × in A, B, E and F; 200 × in G; 400 × in C, D and H.

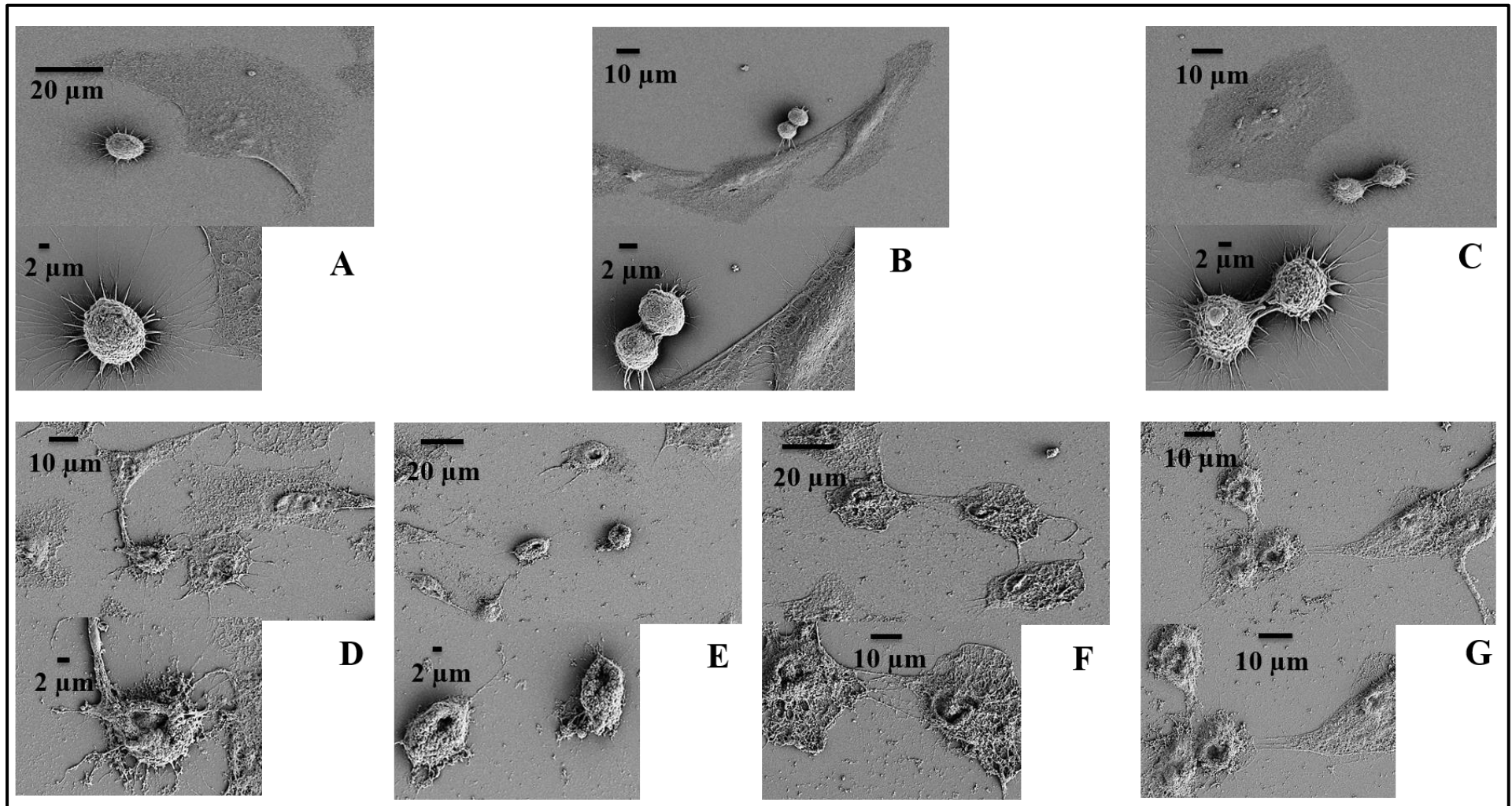


Figure 7.6 Scanning electronmicrographs of HeLa cells after P1 and Di-PuroA treatment.

Panels are: **A, B** and **C**. no peptide control; **D**. P1 32 μg/mL; **E**. P1 64 μg/mL; **F**. P1 125 μg/mL; **G**. Di-PuroA 64 μg/mL.

7.4 Discussion

The therapeutic potential of AMPs mainly depends on their cell selectivity. The peptide selectivity is a measure of its capability to differentiate between pathogen or cancer cells and normal host cells. AMPs generally show selectivity to microbial and/or cancer cells because of their negatively charged membranes, compared to zwitterionic membranes of normal mammalian cells (Dennison et al. 2006; Riedl et al. 2011). However, development of AMPs with high selectivity is one of the most difficult challenges, particularly if these peptides target and act on the cellular membranes (Jacob et al. 2014).

Cancer remains a primary cause of mortality throughout the world and AMPs could provide new, efficient and less harmful alternatives to the currently used cancer therapies (detailed in Chapter 1, Section 1.10.1.1). The TRP lactoferricin (Lfcin) has shown cytotoxic activity towards several cancer cell lines, such as THP-1 human monocytic leukemia cells (Yoo et al. 1997a; Mader et al. 2005), breast carcinoma cells (Furlong et al. 2006), neuroblastoma (Eliassen et al. 2006) and B-lymphoma cells (Furlong et al. 2010). In addition, the LfcinB derivative, LTX-315, showed activity against a wide range of cancer cell lines, including drug-resistant ones, and lower toxicity toward normal cells (Camilio et al. 2014; Haug et al. 2016). This peptide is currently being tested in clinical phase I/IIa studies as a potential first-in-class oncolytic peptide-based local immunotherapy (www.clinicaltrials.gov; identifier NCT01986426), as detailed in Chapter 1, Section 1.10.1.2. Therefore, this present study conducted some preliminary investigations into the selectivity and cytotoxicity of the designed TRPs toward the human cervical carcinoma HeLa cells over the normal mammalian cells, mouse fibroblast NIH-3T3 cells and sheep RBCs. As mentioned in Chapter 3, several strategies have been used in designing those peptides, including cyclization, dimerization, as well as changing the length, net positive charge, Trp content and hydrophobicity. Studying the effects of these parameters on the selective cytotoxicity of AMPs helps in understanding of peptide structure–selectivity correlation and subsequent design of AMPs towards therapeutic applications.

The TRPs indolicidin (Ahmad et al. 1995) and tritrypticin (Yang et al. 2002) were found to be cytotoxic and lyse human RBCs, which somewhat limits their therapeutic use. Yang et al. (2002) suggested that the multiple Trp residues in tritrypticin may play a

role in its strong haemolytic activity. However, lactoferricin (Kang et al. 1996), PuroA (Jing et al. 2003) and many PIN-based TRPs that were designed by our group (Phillips et al. 2011) showed extremely low haemolytic activity. Therefore, the Trp content in AMPs cannot be associated with high haemolytic activity, especially since all TRPs in this study showed very low cytotoxicity to sheep RBCs, even for those with six Trp residues (P1, dP1, WW, dWW)(Table 7.1). In fact, the peptides showed great antimicrobial specificity as the MIC values against tested bacteria were much less compared to the concentrations that caused significant haemolysis in RBC (Tables 7.1 and 7.2) or growth inhibition in the mammalian fibroblast NIH-3T3 cells (Table 7.3). In terms of anticancer specificity, only two peptides, Di-PuroA and P1, displayed relatively strong cytotoxicity and specificity toward HeLa cells with IC_{50} of 32 $\mu\text{g}/\text{mL}$ and therapeutic index (TI) of 7.8 (Table 7.3). Although the SEM imaging of HeLa cells treated with P1 and Di-PuroA suggest a membranolytic mechanism of action (cells were shrunken and/or lysed with significant membrane disruption), the mechanism of anticancer activity of these peptides needs to be investigated further.

Dimeric AMPs have shown selective anticancer activity, such as CopA3 which is a disulfide dimer of the coprisin (LLCIALRKK) (Kang et al. 2012; Lee et al. 2015). In the present cytotoxicity study, dimeric PuroA also showed relatively potent cytotoxicity toward cancer cells compared to fibroblast NIH-3T3 cells and RBCs. Dimerization, thus, seems to be useful strategy to design peptides with potent and selective anticancer activity. In addition, increasing the net positive charge to +7 in P1 and +8 in R8 did not increase the haemolytic activity or cytotoxicity toward NIH-3T3 cells. These results disagree with previous studies which state that increasing the cationicity of AMPs beyond +5 can result in dramatic increase in haemolytic activity and loss of cell selectivity (Dathe et al. 2001; Taniguchi et al. 2016b). It was also found that increasing the charge by substituting the uncharged amino acids of PuroA with Arg and Lys residues in P1, not only Arg as in R8, and increasing the Trp content to six residues, resulted in potent anticancer and selective analogue. In addition, Dennison et al. (2009) state that the presence of C-terminal amide moiety has a variable effect on the toxicity of AMPs on both microbial and cancer cells and there is no clear effect on their selectivity.

The present results showed that C-terminal amidification increased the cell selectivity (Table 7.2) but in terms of haemolytic and anticancer activities, it has a negligible effect. The short linear analogues of PuroA, R6, R7, W7, W8 and the short variant of P1, WW, showed higher antimicrobial activity compared to the longer analogues and insignificant cytotoxicity toward RBCs and NIH-3T3 cells. However, unlike the antimicrobial activity, the length of the peptides seems to play a role in their anticancer activity. For example, WW peptide (a shorter analogue of P1) showed less anticancer activity. Previous studies have stated that there is no clear or strong correlation between the sequence length and the toxicity or selectivity of anticancer peptides (Dennison et al. 2006; Harris et al. 2013). Hence, the effect of this factor on the anticancer activity needs to be investigated further.

High hydrophobicity has been correlated with increased cytotoxicity and reduced cell selectivity as it strongly controls the partition of the peptide into the membrane hydrophobic core (Kondejewski et al. 2002; Chen et al. 2005; Yount et al. 2006; Pasupuleti et al. 2009a; Strandberg et al. 2015). In this study, the most hydrophobic peptides, PuroA, Cyclic PuroA, PuroA-OH, WW and dWW, with $H = -0.08$ (Chapter 3, Table 3.1), did not show higher cytotoxicity against sheep RBCs or mammalian fibroblast cells compared to less hydrophobic peptides, such as R8 and P1 with $H = -0.94$ and -0.58 , respectively. These results are in agreement with Jeong et al. (2016) who found that increased hydrophobicity is not always associated with high haemolytic activity. It is also hard to establish a relationship between the hydrophobicity and anticancer activity as the two peptides that showed relatively strong anticancer activity, P1 and dimeric PuroA, have completely different hydrophobicity degrees; H of P1 is -0.58 and -0.11 for Di-PuroA. In terms of introducing D-amino acids into specific sites of the peptides sequences, diastereomeric peptides did not exhibit much better selectivity toward mammalian RBCs and fibroblast compared to L-isomers; this contrasts with previous studies (Shai & Oren 1996; Avrahami et al. 2001; Wang et al. 2010b). In fact, dP1 peptide showed similar selectivity and dWW peptide showed less selectivity than their L-counterpart.

In conclusion, P1 and Di-PuroA showed interesting anticancer activity with high selectivity. These results highlight the relevance of TRPs as a potential source of new anticancer therapies. In addition, examining the correlation between peptide structures and their cell selectivity toward microbial or cancer cells will enable fast progress in the rational design of peptide as antimicrobial and anticancer therapeutics.

Chapter 8

General discussion and conclusion

8.1 General discussion and conclusion

Antimicrobial peptides (AMPs) are evolutionarily conserved main effector molecules of the innate immune system of many organisms. AMPs have many advantages over conventional antibiotics, including broad-spectrum of activities, the ability to rapidly kill pathogen cells by acting on non-specific targets and low potential of developing resistance against them. There is an urgent need for developing a new effective strategies to fight against multi-drug-resistant microbes “superbugs”. The wide use of broad-spectrum and potent antibiotics has driven the emergence of superbugs at an unprecedented rate. The antibiotic resistance has also been identified as a serious growing threat to public health by the World Health Organization (WHO) (<http://www.who.int/drugresistance/documents/surveillancereport/en/>; last accessed June 2016) and it is also listed in the Global Risks 2017 report as one of six global risks related to social stability (http://www3.weforum.org/docs/GRR17_Report_web.pdf; last accessed May 2017). Thus, AMPs offer ideal alternatives as novel antimicrobial therapeutics.

The first chapter was devoted to an extensive review of literature on AMPs, highlighting the research and developments in this field. The Chapter discusses the interdependent biochemical determinants that significantly affect the efficiency, spectrum of activity and cytotoxic selectivity of AMPs, including length, sequence, charge, secondary structure, hydrophobicity, amphipathicity and membrane composition. In AMP design, all these intrinsic physicochemical properties and environmental properties need to be considered, and predicting the results of modifying one or more of these properties beforehand is still an unmet challenge. Chapter 1 focused on Trp-rich antimicrobial peptides (TRPs) as they display broad and potent activity bacteria, fungi and/or viruses, and some are also active against protozoan pathogens and/or cancer cells. These activities have been credited to the unique biochemical properties of Trp as it has a strong tendency to insert deeply and partition into membranes. This part of the literature review Chapter has been published (Shagghi et al. 2016b).

The wheat grain puroindoline (PIN) proteins, puroindoline-a (PINA) and puroindoline-b (PINB) are small, basic proteins with a conserved 10 Cys-backbone and a tryptophan rich domain (TRD). Both PINs exhibit numerous natural mutations

of diverse type, and the effect of these mutations on grain texture is well-established. While the primary *in vivo* role of PINs is believed to be to protect the wheat seed from phytopathogens, the effect of mutations in the TRD on the antimicrobial activity of PINs has not been widely studied, as detailed in Chapter 1. The synthetic peptide, PuroA (FPVTWRWWKWWKG-NH₂), based on the TRD of PINA showed antimicrobial activity against Gram-positive and Gram-negative bacteria, phytopathogenic fungi and fungi spores. The antimicrobial activities of PuroA have been attributed to peptide-induced membrane destabilization, or intracellular mechanisms of action (DNA-binding) or both. These results indicated that PuroA offers a template to design TRPs with potential significance in food, health and agriculture applications. Thus, the major aim of the current study was to design antimicrobial peptides based on the TRD of PINA that have effective, wide spectrum and selective antimicrobial activities. This objective was addressed through the specific aims outlined below:

5. To design a number of PINA-based peptides with varying biochemical properties, and assess the effects of these variations on the antimicrobial activity, salt tolerance and protease stability of the peptides.
2. To investigate the antimicrobial applications of selected PIN-based peptides, including effect on persistent pathogens and drug-resistant isolates.
3. To investigate the mechanisms of action of PuroA peptide at cellular and intracellular levels.
4. To test the possibility of development of bacterial and fungal resistance to selected PIN-based peptides.
5. To determine the anticancer potential of some of the designed PIN-based AMPs by studying the effect on selected mammalian cell lines.

These aims were addressed by applications of a number of experimental approaches as outlined in **Chapter 2**. The methods used included microbiological and cell culture methodologies (e.g., culturing and aseptic techniques applied to bacterial cells, unicellular fungi, bacterial spores and mammalian cells), biochemical and molecular methodologies (e.g., synthetic peptide design, DNA extraction, electrophoresis, MTT

assays and flow cytometry), biophysical techniques (e.g., light-microscopy confocal scanning laser microscopy, fluorescence-lifetime imaging microscopy and scanning electron microscopy) and analytical chemistry techniques (e.g., spectrophotometry and circular dichroism spectroscopy).

The first aim was addressed in **Chapter 3** (results chapter 1). This chapter investigated the antimicrobial activities of 13 TRPs peptides which were designed based PuroA peptide, with different length, Trp contents, net charge, hydrophobicity and amphipathicity. In addition, the antibacterial activities of the designed peptides were tested in the presence of salt and proteases. The results showed that: (1) not all the 13 amino acids in PuroA are required for its antimicrobial activity; the shorter variants based on its Trp-, Arg, and Lys-rich center were all more active against the tested bacteria and yeast than the parent 13-mer peptide; (2) increasing the charge improved the antimicrobial activity of PuroA, however, increasing it beyond +7 reduced the activity; (3) increasing the peptide charge seems to improve its salt resistance and overcome the charge-shielding effect of salt; (4) the short TRPs with a net positive charge of +2 or +3 show excellent salt-tolerance behaviour, suggesting that the amphipathic structure of these peptides and the cluster of the Trp-residues could protect them from the salt inactivation effect; (5) the C-terminal amide group in PuroA is important for its antimicrobial activity; (6) there is no correlation between the hydrophobicity and antimicrobial activity of the peptides; (7) many of the designed TRPs do not need to conform to a recognized secondary structure to exert their antimicrobial activities; adapting amphipathic configuration seems to be more important; (8) once a potent variant is designed, D-amino acids can be introduced into certain positions in this peptide to produce a new peptide with same potency and less to enzymatic susceptibility; (9) head-to-tail cyclization of PuroA is not an effective strategy to improve the peptide antimicrobial activity or to reduce/eliminate the proteolytic degradation; (10) dimerization of PuroA is not a useful strategy to improve its antimicrobial activity, or its salt or proteases resistance; (11) the designed peptides showed different affinity for the plasmid DNA *in vitro*, however, this had no correlation to their antimicrobial activities; (12) all designed TRPs, except dimeric PuroA, induced filamentation in *E. coli* cells, regardless their physicochemical characteristic, suggesting a role of Trp(s) in inducing this morphological change by some intracellular activity.

The second aim were addressed in **Chapter 4** (results chapter 2). The potential applications of PIN-based peptides in controlling selected persistent pathogens in food and health contexts were explored in this Chapter. The persistent pathogens included biofilms of *P. aeruginosa*, *Listeria monocytogenes* and Methicillin-resistant *S. aureus* isolates and endospores of *Bacillus subtilis*. The results revealed that: (1) the peptide Pina-M that represent the natural mutation at the TRD of PINA (Pro-35 to Ser), had better inhibitory effect on the planktonic cells of all tested bacteria than the wild-type PINA; (2) substitution of the basic residue Lys (Lys42 of PINA) with an uncharged Thr in Hina peptide resulted in completely abolish the antibacterial against *P. aeruginosa*; (3) the membrane disrupting property of PuroA on *L. monocytogenes*, *P. aeruginosa* and MRSA cells depends on the concentrations and exposure time; (4) TRPs are effective anti-biofilm agents; they capable of preventing biofilm formation and the initial cell attachment by planktonic cells, as well as they can reduce the biomass of 6 h preformed biofilms and kill the biofilm-forming bacteria; (5) peptide length is an important determinant for anti-biofilm activity, as the short PuroA variants were less effective in eradication preformed biofilms; (6) some of the tested TRPs are potent sporicidal agents, reducing the number of viable spores by at least 4 log units and causing visible damage to treated spores; (7) peptide length is important factor for sporicidal activity of TRPs. This work has been published (Shagaghi et al. 2016a).

The third aim was addressed in **Chapter 5** (results Chapter 2). AMPs often exert microbicidal effects due to disruption of vital cellular structures and/or functions. The mechanisms by which antimicrobial peptides act are diverse and complex. As many AMPs use multiple killing mechanisms, it is difficult to identify all the molecular interactions that occur during AMP attack. Since it is essential to understand how peptides act on cells to properly exploit their use as antimicrobial agents, Chapter 5 sought to investigate the mechanism of action of PuroA. This work was done using time-lapse fluorescence lifetime imaging microscopy (FLIM) to measure the nanoscale interactions of the fluorescently-tagged PuroA peptide with other labelled molecules or cellular constituents, and time-lapse fluorescence microscopy to directly observe the localization FITC-PuroA peptide on single *Candida albicans* and *Escherichia coli* cells in real time. The results showed that: (1) PuroA may have dual targets in *C. albicans* cells, membranolytic mechanism as showed in SEM data and non-membranolytic mechanism (binding to nucleic acids), interestingly, the

disruption of the membrane integrity is not the initial step in the yeast killing mechanism; (2) the real time imaging experiments revealed three distinct events which occurred at different times at the same peptide concentration when FITC-PuroA attacks *C. albicans* cell; (3) the first phase involves translocation of FITC-PuroA across the cell membranes of *C. albicans* without permanent disruption of membranes, secondly, peptide in the cytosol binds to nucleic acids and thirdly, FITC-PuroA accumulates at the cell membrane and forms pores causing membrane disruption, PI and peptide influx; (4) membrane disruption appears to be the mechanism by which the *C. albicans* cells are killed; (5) cell cycle analysis data showed that PuroA can also arrest cell proliferation at the S-phase in *C. albicans*, resulting in inhibition of normal cellular processes; (6) PuroA disrupts the cell division and induces filamentation in *E. coli* cells, suggestion that the peptide probably translocates the membranes of *E. coli* cells without causing permanent membrane perturbation, binds to intracellular target(s) and induces filamentous growth in the bacterial cells; (7) SEM data shows membranolytic mechanism of action in *E. coli* cells as clear pore-like structures in the membranes of treated bacterial cells, suggesting PuroA has a dual bactericidal mechanism of action; (7) live cell imaging approaches is a useful adjunct to other approaches for precisely investigating the mechanisms of action of AMPs. This work has been published (Shagaghi et al. 2017)

Aim four was addressed in **Chapter 6** (results chapter 4). In brief, in this chapter the potential of bacteria and yeast to develop resistance to PIN-based peptides was investigated using ‘evolution’ experiments. In these, *S. aureus*, *E. coli*, *S. epidermidis* and *C. albicans* were exposed to successively increasing concentrations of four TRPs, PuroA, P1, W7 and indolicidin. The resistant isolates were further characterized in terms of resistance stability, cost of resistance and cross-resistance. The results revealed that: (1) resistance to TRPs can experimentally evolve in *S. aureus* and *E. coli* when they are consistently exposed to increasing levels of peptides, thus AMPs should be used appropriately to minimize the development of resistance; (2) resistance mechanisms often cause a reduction in biological fitness which is measured as growth rate; PuroA-resistant *S. aureus* isolates showed the highest cost of resistance (with 25% reduction in fitness), suggesting that these isolates carried more mutations than others; (3) the evolved resistance to PuroA and indolicidin in *S. aureus* and *E. coli* is not stable or heritable and is peptide-specific as there was no observable cross-

resistance between the tested TRPs, despite similarities in the structure and mechanism of action; (4) combinations of AMPs may offer the advantage of synergistic antimicrobial actions, however, PuroA, in particular, does not seem a promising synergistic agent as it did not show *in vitro* interaction activities with other TRPs; (5) resistance did not develop in *E. coli* and *S. aureus* toward a combination of W7 with PuroA or indolicidin, suggesting that AMPs combinations could be a useful approaches to decrease the rate of selection of resistance.

Finally, aim five was addressed in **Chapter 7** (results chapter 5). Chapter 7 undertook a preliminary investigation into the selectivity and cytotoxicity profiles of the designed peptides toward the human cervical carcinoma HeLa cells, and the normal mammalian cells, mouse fibroblast NIH-3T3 cells and sheep RBCs. The results showed that: (1) Trp content in AMPs does not associate with high haemolytic activity, as all TRPs in this study showed very low cytotoxicity to sheep RBCs, even for those with six Trp residues; (2) among the 13 TRPs, only Di-PuroA and P1 show relatively strong cytotoxicity and specificity toward HeLa cells, thus dimerization could be a useful strategy to design peptides with potent and selective anticancer activity; (4) increasing the peptide charge to +7 or +8 did not increase the haemolytic activity or cytotoxicity toward RBCs or NIH-3T3 cells, respectively; (4) the length of the peptides and C-terminal amide moiety have no clear effects on the selectivity of the TRPs to microbial cells; (5) increased hydrophobicity is not always associated with high haemolytic activity, and it is also difficult to establish a relationship between the hydrophobicity and anticancer activity, as Di-PuroA and P1 greatly differ in hydrophobicity; (6) introducing D-amino acids into the peptides sequences does not improve the peptides selectivity toward mammalian RBCs and fibroblasts compared to their L-counterparts.

In conclusion, the findings from the current study demonstrated that: (1) some of the designed TRPs have excellent antimicrobial activity and hence, they have the potential to be used for biocidal applications against organisms of interest in health, food and agriculture, as well as persistent pathogens such as bacterial biofilms and endospores; (2) PuroA has a dual mechanism of action, membranolytic and intracellular mechanism, of which the disruption of the membrane integrity and pore formation could be the main cause of cell death, but not the initial step; (3) there is a possibility of developing bacterial resistance against AMPs; (4) the designed TRPs have high

selectivity toward microbes and some of them also have the potential as antitumor therapeutics.

8.2 Future directions

Short AMPs with potent and broad spectrum antimicrobial activity, metabolic stability and low cytotoxicity on normal mammalian cells are highly desired (Hilpert et al. 2005; Nguyen et al. 2010). The designed peptides in this study may use as a template for future novel design and engineering of short TRPs for improved antimicrobial activity, salt tolerance, and biocompatibility properties. For example, the principles revealed here regarding salt-tolerance of short TRPs bedside their potent antimicrobial activities could may accelerate the development of improved anti-infective agents towards systemic applications.

As antimicrobial peptides, the designed PIN-based peptides appear amenable to a range of applications. Their potency, efficacy and specificity to microbial cells and lack of haemolytic and cytotoxicity activities toward tested normal mammalian cells indicates these peptides, which are originally coming from a most common edible source (wheat), could be highly valuable in pharmaceutical, food and/or agriculture industries. Further, the high salt stability of some of the peptides could make them excellent candidates as food preservatives. For this purpose, it will be useful testing their pH and thermal stability as well. The peptides tested in this study showed potential to control persistent pathogens which are of significant concern in healthcare sector and food industry, such as bacterial biofilms including methicillin-resistant *S. aureus* (MRSA) biofilm and *Bacillus* species endospores. Therefore, they might able to control other persistent pathogens, such as fungal biofilms and *Clostridium* species endospores. Additionally, many of the well-studied TRPs, such as indolicidin and lactoferricin, are also effective against several virus and protozoa (reviewed in Chapter 1, Section 1.4.2 and 1.4.3). Due to their similarities that PINs share with these well-studied TRPs, it would be interesting to explore these potential applications for the PIN-based peptides.

Beyond these direct applications, investigating the mechanisms of action of AMPs may reveal favourable pharmacologic properties that can lead to further pharmaceutical development. For example, some AMPs have cell penetrating

properties. Cell-penetrating peptides (CPPs) are a new class of vectors with high pharmaceutical potential to deliver bioactive cargos, such as DNAs, oligonucleotides, proteins and liposomes into cells (Schmidt et al. 2010). These peptides are often rich in Arg, Trp and/or Lys, such as bLFcin6 CPP, RRWQWR, was derived from bovine lactoferricin (Fang et al. 2013). In addition, indolicidin has the potential to be used as a carrier for anionic materials, such as plasmid DNA for gene delivery (Hu et al. 2013). As PuroA were found in this study to rapidly translocate the cell wall and cytoplasmic membrane and binding to nucleus of *C. albicans*, it will be interesting to test the potential application of PuroA as a carrier to deliver anionic molecules into cells.

The combination of diverse biophysical methods and biological assays applied in this study were useful approach for investigating the mechanisms of action of PuroA, particularly on *C. albicans* cells and revealing of detailed mechanistic insights. As the mechanisms of action of AMPs are peptide specific and cell-type specific, such approach can be applied to study the mechanism of action of other AMPs and other cell types, particularly AMPs with multiple mechanism of action to determine the sequence of events during that ultimately cause cell death. It is also important to investigate how PuroA disrupts the cell division of *E. coli* and induces cell filamentation; is it by DNA synthesis inhibition and/or by inhibition of membrane proteins that are involved in septum formation?

A more detailed study of the potential of resistance development against AMPs is required before their large-scale applications. From the present study, developing resistance against AMPs seems to be possible, although it was not stable or heritable. The mechanism(s) that the bacteria use to develop this resistance is unclear, thus a study using whole genome sequencing could be useful to understand the genetic basis of the resistance mechanisms. It will be also interesting to study the developing resistance to AMPs *in vivo*.

The strategy of drug combinations could offer the advantage of synergistic actions, and has been proposed to potentially treat multi-resistant pathogens, delay the development of drug resistance, and/or reduce the dose of individual drugs. It would be useful to further explore the effect of combining PuroA and other TRPs with mammalian immune peptides and conventional antibiotics.

Certain AMPs, such as the TRP lactoferricin and LTX-315 peptide have showed potential as anticancer agents. In the current work, preliminary attempts were made to investigate the cytotoxicity of the designed TRPs against cancerous mammalian cells. Two of the peptides, P1 and Di-PuroA showed interesting anticancer activity with high selectivity against human cervical carcinoma HeLa cells. These peptides may have the potential to be used as anticancer therapeutics that may help in reducing the detrimental side effects of conventional chemotherapeutics. Thus, investigating the anticancer activity of these peptides against other cancerous cell lines and study their anticancer mechanisms is important.

Since their discovery, AMPs have been seen as novel antimicrobial agents and the quest to gain deeper understanding into their functions, structures, and mechanisms has resulted in substantial discoveries. Yet, it seems that the emergence of new knowledge is unearthing further questions about these interesting defence effector molecules will be worth investigating in the future.

References

- Aarbiou J, Tjabringa GS, Verhoosel RM, Ninaber DK, White SR, Peltenburg LTC, Rabe KF, Hiemstra PS. 2006. Mechanisms of cell death induced by the neutrophil antimicrobial peptides α -defensins and LL-37. *Inflammation Research* 55:119-127.
- Abachin E, Poyart C, Pellegrini E, Milohanic E, Fiedler F, Berche P, Trieu-Cuot P. 2002. Formation of D-alanyl-lipoteichoic acid is required for adhesion and virulence of *Listeria monocytogenes*. *Molecular Microbiology* 43:1-14.
- Abi Khattar Z, Rejasse A, Destoumieux-Garzón D, Escoubas JM, Sanchis V, Lereclus D, Givaudan A, Kallassy M, Nielsen-Leroux C, Gaudriault S. 2009. The dlt operon of *Bacillus cereus* is required for resistance to cationic antimicrobial peptides and for virulence in insects. *Journal of Bacteriology* 191:7063-7073.
- Afacan NJ, Yeung ATY, Pena OM, Hancock REW. 2012. Therapeutic potential of host defense peptides in antibiotic-resistant infections. *Current Pharmaceutical Design* 18:807-819.
- Agerberth B, Lee JY, Bergman T, Carlquist M, Boman HG, Mutt V, Jornvall H. 1991. Amino acid sequence of PR-39. Isolation from pig intestine of a new member of the family of proline-arginine-rich antibacterial peptides. *European Journal of Biochemistry* 202:849-854.
- Ahmad I, Perkins WR, Lupan DM, Selsted ME, Janoff AS. 1995. Liposomal entrapment of the neutrophil-derived peptide indolicidin endows it with *in vivo* antifungal activity. *Biochimica et Biophysica Acta - Biomembranes* 1237:109-114.
- Aley SB, Zimmerman M, Hetsko M, Selsted ME, Gillin FD. 1994. Killing of *Giardia lamblia* by cryptidins and cationic neutrophil peptides. *Infection and Immunity* 62:5397-5403.
- Alfred RL, Palombo EA, Panozzo JF, Bariana H, Bhave M. 2013a. Stability of puroindoline peptides and effects on wheat rust. *World Journal of Microbiology and Biotechnology* 29: 1409-1419.
- Alfred RL, Palombo EA, Panozzo JF, Bhave M. 2013b. The antimicrobial domains of wheat puroindolines are cell-penetrating peptides with possible intracellular mechanisms of action. *PLoS ONE* 8:e75488.
- Alfred RL, Palombo EA, Panozzo JF, Bhave M. 2014. The co-operative interaction of puroindolines in wheat grain texture may involve the hydrophobic domain. *Journal of Cereal Science* 60:323-330.
- Aliste MP, MacCallum JL, Tieleman DP. 2003. Molecular dynamics simulations of pentapeptides at interfaces: salt bridge and cation- π interactions. *Biochemistry* 42:8976-8987.

- Amos SBTA, Vermeer LS, Ferguson PM, Kozłowska J, Davy M, Bui TT, Drake AF, Lorenz CD, Mason AJ. 2016. Antimicrobial peptide potency is facilitated by greater conformational flexibility when binding to Gram-negative bacterial inner membranes. *Scientific Reports* 6:37639.
- Anaya-López JL, López-Meza JE, Ochoa-Zarzosa A. 2013. Bacterial resistance to cationic antimicrobial peptides. *Critical Reviews in Microbiology* 39:180-195.
- Andersen JH, Osbakk SA, Vorland LH, Traavik T, Gutteberg TJ. 2001. Lactoferrin and cyclic lactoferricin inhibit the entry of human cytomegalovirus into human fibroblasts. *Antiviral Research* 51:141-149.
- Andersson DI, Hughes D. 2010. Antibiotic resistance and its cost: Is it possible to reverse resistance? *Nature Reviews Microbiology* 8:260-271.
- Andrä J, Goldmann T, Ernst CM, Peschel A, Gutschmann T. 2011. Multiple peptide resistance factor (MprF)-mediated resistance of *Staphylococcus aureus* against antimicrobial peptides coincides with a modulated peptide interaction with artificial membranes comprising lysyl-phosphatidylglycerol. *Journal of Biological Chemistry* 286:18692-18700.
- Andreu D, Rivas L. 1998. Animal antimicrobial peptides: An overview. *Biopolymers - Peptide Science Section* 47:415-433.
- Anghel R, Jitaru D, Bădescu L, Bădescu M, Ciocoiu M. 2013. The cytotoxic effect of magainin II on the MDA-MB-231 and M14K tumour cell lines. *BioMed Research International* 2013:831709.
- Anunthawan T, De La Fuente-Núñez C, Hancock REW, Klaynongsruang S. 2015. Cationic amphipathic peptides KT2 and RT2 are taken up into bacterial cells and kill planktonic and biofilm bacteria. *Biochimica et Biophysica Acta - Biomembranes* 1848:1352-1358.
- Arias CA, Murray BE. 2009. Antibiotic-resistant bugs in the 21st century - A clinical super-challenge. *New England Journal of Medicine* 360:439-443.
- Arias M. 2015. Hydroxy-tryptophan containing derivatives of tritrypticin: modification of antimicrobial activity and membrane interactions. *Biochimica et biophysica acta* 1848:277-288.
- Arias M, Hoffarth ER, Ishida H, Aramini JM, Vogel HJ. 2016. Recombinant expression, antimicrobial activity and mechanism of action of tritrypticin analogs containing fluoro-tryptophan residues. *Biochimica et Biophysica Acta - Biomembranes* 1858:1012-1023.
- Arias M, McDonald LJ, Haney EF, Nazmi K, Bolscher JGM, Vogel HJ. 2014. Bovine and human lactoferricin peptides: chimeras and new cyclic analogs. *BioMetals* 27:935-948.

- Avitabile C, D'Andrea LD, Romanelli A. 2014. Circular dichroism studies on the interactions of antimicrobial peptides with bacterial cells. *Scientific Reports* 4:04293.
- Avrahami D, Oren Z, Shai Y. 2001. Effect of multiple aliphatic amino acids substitutions on the structure, function, and mode of action of diastereomeric membrane active peptides. *Biochemistry* 40:12591-12603.
- Ayala M, Guzmán C, Peña RJ, Alvarez JB. 2016. Genetic diversity and molecular characterization of puroindoline genes (*Pina-D1* and *Pinb-D1*) in bread wheat landraces from Andalusia (Southern Spain). *Journal of Cereal Science* 71:61-65.
- Bahar AA, Ren D. 2013. Antimicrobial peptides. *Pharmaceuticals* 6:1543-1575.
- Baker MA, Maloy WL, Zasloff M, Jacob LS. 1993. Anticancer efficacy of magainin2 and analogue peptides. *Cancer Research* 53:3052-3057.
- Barns KJ, Weisshaar JC. 2013. Real-time attack of LL-37 on single *Bacillus subtilis* cells. *Biochimica et Biophysica Acta - Biomembranes* 1828:1511-1520.
- Barns KJ, Weisshaar JC. 2016. Single-cell, time-resolved study of the effects of the antimicrobial peptide alamethicin on *Bacillus subtilis*. *Biochimica et Biophysica Acta - Biomembranes* 1858:725-732.
- Bastos M, Bai G, Gomes P, Andreu D, Goormaghtigh E, Prieto M. 2008. Energetics and partition of two cecropin-melittin hybrid peptides to model membranes of different composition. *Biophysical Journal* 94:2128-2141.
- Bechinger B. 1999. The structure, dynamics and orientation of antimicrobial peptides in membranes by multidimensional solid-state NMR spectroscopy. *Biochimica et Biophysica Acta - Biomembranes* 1462:157-183.
- Bechinger B, Gorr SU. 2017. Antimicrobial Peptides: mechanisms of Action and Resistance. *Journal of Dental Research* 96:254-260.
- Beecher B, Bowman J, Martin JM, Bettge AD, Morris CF, Blake TK, Giroux MJ. 2002. Hordoindolines are associated with a major endosperm-texture QTL in Barley (*Hordeum vulgare*). *Genome* 45:584-591.
- Bell G, Gouyon PH. 2003. Arming the enemy: the evolution of resistance to self-proteins. *Microbiology* 149:1367-1375.
- Bellamy W, Takase M, Wakabayashi H, Kawase K, Tomita M. 1992. Antibacterial spectrum of lactoferricin B, a potent bactericidal peptide derived from the N-terminal region of bovine lactoferrin. *Journal of Applied Bacteriology* 73:472-479.
- Bellamy W, Yamauchi K, Wakabayashi H, Takase M, Takakura N, Shimamura S, Tomita M. 1994. Antifungal properties of lactoferricin B, a peptide derived from the N-terminal region of bovine lactoferrin. *Letters in Applied Microbiology* 18:230-233.

References

- Berditsch M, Jäger T, Stempel N, Schwartz T, Overhage J, Ulrich AS. 2015. Synergistic effect of membrane-active peptides polymyxin B and gramicidins on multidrug-resistant strains and biofilms of *Pseudomonas aeruginosa*. *Antimicrobial Agents and Chemotherapy* 59:5288-5296.
- Beresford MR, Andrew PW, Shama G. 2001. *Listeria monocytogenes* adheres to many materials found in food-processing environments. *Journal of Applied Microbiology* 90:1000-1005.
- Bhargava A, Osusky M, Hancock RE, Forward BS, Kay WW, Misra S. 2007. Antiviral indolicidin variant peptides: evaluation for broad-spectrum disease resistance in transgenic *Nicotiana tabacum*. *Plant Science* 172:515-523.
- Bhave M, Morris CF. 2008a. Molecular genetics of *puroindolines* and related genes: allelic diversity in wheat and other grasses. *Plant Molecular Biology* 66:205-219.
- Bhave M, Morris CF. 2008b. Molecular genetics of *puroindolines* and related genes: regulation of expression, membrane binding properties and applications. *Plant Molecular Biology* 66:221-231.
- Bhutia SK, Maiti TK. 2008. Targeting tumors with peptides from natural sources. *Trends in Biotechnology* 26:210-217.
- Bierbaum G, Sahl HG. 1987. Autolytic system of *Staphylococcus simulans* 22: influence of cationic peptides on activity of N-acetylmuramoyl-L-alanine amidase. *Journal of Bacteriology* 169:5452-5458.
- Bjellqvist B, Hughes GJ, Pasquali C, Paquet N, Ravier F, Sanchez JC, Frutiger S, Hochstrasser D. 1993. The focusing positions of polypeptides in immobilized pH gradients can be predicted from their amino acid sequences. *Electrophoresis* 14:1023-1031.
- Blochet J-E, Chevalier C, Forest E, Pebay-Peyroula E, Gautier M-F, Jourdris P, Pézolet M, Marion D. 1993. Complete amino acid sequence of puroindoline, a new basic and cysteine-rich protein with a unique tryptophan-rich domain, isolated from wheat endosperm by Triton X-114 phase partitioning *FEBS Journal* 329:336-340.
- Blondelle SE, Houghten RA. 1996. Novel antimicrobial compounds identified using synthetic combinatorial library technology. *Trends in Biotechnology* 14:60-65.
- Boman HG, Agerberth B, Boman A. 1993. Mechanisms of action on *Escherichia coli* of cecropin P1 and PR-39, two antibacterial peptides from pig intestine. *Infection and Immunity* 61:2978-2984.
- Botta GA, Park JT. 1981. Evidence for involvement of penicillin-binding protein 3 in murein synthesis during septation but not during cell elongation. *Journal of Bacteriology* 145:333-340.

References

- Bottone EJ. 2010. *Bacillus cereus*, a volatile human pathogen. *Clinical Microbiology Reviews* 23:382-398.
- Bozelli Jr JC, Sasahara ET, Pinto MRS, Nakaie CR, Schreier S. 2012. Effect of head Group and curvature on binding of the antimicrobial peptide tritrypticin to lipid membranes. *Chemistry and Physics of Lipids* 165:365-373.
- Branda SS, Vik Å, Friedman L, Kolter R. 2005. Biofilms: The matrix revisited. *Trends in Microbiology* 13:20-26.
- Brennan CS, Harris N, Smith D, Shewry PR. 1996. Structural differences in the mature endosperms of good and poor malting barley cultivars. *Journal of Cereal Science* 24:171-177.
- Breukink E, Wiedemann I, Van Kraaij C, Kuipers OP, Sahl HG, De Kruijff B. 1999. Use of the cell wall precursor lipid II by a pore-forming peptide antibiotic. *Science* 286:2361-2364.
- Brewer D, Lajoie G. 2002. Structure-based design of potent histatin analogues. *Biochemistry* 41:5526-5536.
- Brogden K. 2005. Antimicrobial peptides: pore formers or metabolic inhibitors in bacteria? *Nature Reviews Microbiology* 3:238-250.
- Brogden KA, De Lucca AJ, Bland J, Elliott S. 1996. Isolation of an ovine pulmonary surfactant-associated anionic peptide bactericidal for *Pasteurella haemolytica*. *Proceedings of the National Academy of Sciences of the United States of America* 93:412-416.
- Brötz H, Bierbaum G, Leopold K, Reynolds PE, Sahl HG. 1998. The lantibiotic mersacidin inhibits peptidoglycan synthesis by targeting lipid II. *Antimicrobial Agents and Chemotherapy* 42:154-160.
- Bucki R, Janmey PA. 2006. Interaction of the gelsolin-derived antibacterial PBP 10 peptide with lipid bilayers and cell membranes. *Antimicrobial Agents and Chemotherapy* 50:2932-2940.
- Bulet P, Hetru C, Dimarcq JL, Hoffmann D. 1999. Antimicrobial peptides in insects; structure and function. *Developmental and Comparative Immunology* 23:329-344.
- Cahill K. 2010. Molecular electroporation and the transduction of oligoarginines. *Physical Biology* 7:16001.
- Caldwell KS, Langridge P, Powell W. 2004. Comparative sequence analysis of the region harboring the hardness locus in barley and its colinear region in rice. *Plant Physiology* 136:3177-3190.
- Camilio KA, Berge G, Ravuri CS, Rekdal O, Sveinbjörnsson B. 2014. Complete regression and systemic protective immune responses obtained in B16 melanomas after treatment with LTX-315. *Cancer Immunology, Immunotherapy* 63:601-613.

- Cannon RD, Holmes AR, Mason AB, Monk BC. 1995. Oral *Candida*: clearance, colonization, or candidiasis? *Journal of Dental Research* 74:1152-1161.
- Capparelli R, Amoroso MG, Palumbo D, Iannaccone M, Faleri C, Cresti M. 2005. Two plant puroindolines colocalize in wheat seed and *in vitro* synergistically fight against pathogens. *Plant Molecular Biology* 58:857-867.
- Capparelli R, Palumbo D, Iannaccone M, Ventimiglia I, Di Salle E, Capuano F, Salvarore P, Amoroso MG. 2006. Cloning and expression of two plant proteins: similar antimicrobial activity of native and recombinant form. *Biotechnology Letters* 28:943-949.
- Capparelli R, Ventimiglia I, Palumbo D, Nicodemo D, Salvatore P, Amoroso MG, Iannaccone M. 2007. Expression of recombinant *puroindolines* for the treatment of *staphylococcal* skin infections (*acne vulgaris*). *Journal of Biotechnology* 128:606-614.
- Carmona G, Rodriguez A, Juarez D, Corzo G, Villegas E. 2013. Improved protease stability of the antimicrobial peptide pin2 substituted with d-Amino acids. *Protein Journal* 32:456-466.
- Casteels P, Ampe C, Jacobs F, Vaeck M, Tempst P. 1989. Apidaecins: Antibacterial peptides from honeybees. *EMBO Journal* 8:2387-2391.
- Chaffin WL, López-Ribot JL, Casanova M, Gozalbo D, Martínez JP. 1998. Cell wall and secreted proteins of *Candida albicans*: identification, function, and expression. *Microbiology and Molecular Biology Reviews* 62:130-180.
- Chait R, Craney A, Kishony R. 2007. Antibiotic interactions that select against resistance. *Nature* 446:668-671.
- Chakrabarti A, Ganapathi TR, Mukherjee PK, Bapat VA. 2003. MSI-99, a magainin analogue, imparts enhanced disease resistance in transgenic tobacco and banana. *Planta* 216:587-596.
- Chan DI, Prenner EJ, Vogel HJ. 2006. Tryptophan- and arginine-rich antimicrobial peptides: structures and mechanisms of action. *Biochimica et Biophysica Acta* 1758:1184-1202.
- Chang CY, Lin CW, Chiang SK, Chen PL, Huang CY, Liu SJ, Chong P, Huang MH. 2013. Enzymatic stability and immunoregulatory efficacy of a synthetic indolicidin analogue with regular enantiomeric sequence. *ACS Medicinal Chemistry Letters* 4:522-526.
- Chantret N, Cenci A, Sabot F, Anderson O, Dubcovsky J. 2004. Sequencing of the *Triticum monococcum* Hardness locus reveals good microlinearity with rice. *Molecular Genetics and Genomics* 271:377-386.
- Chen F, He ZH, Xia XC, Xia LQ, Zhang XY, Lillemo M, Morris CF. 2006. Molecular and biochemical characterisation of *puroindoline a* and *b* alleles in Chinese landraces and historical cultivars. *Theoretical and Applied Genetics* 112:400-409.

References

- Chen F, Li H, Shang X, Li X, Cui D. 2013. A novel *Puroindoline b-2* variant present in Chinese winter wheat cultivar Yunong 202. *Journal of Cereal Science* 57:249-252.
- Chen F, Xu HX, Zhang FY, Xia XC, He ZH, Wang DW, Dong ZD, Zhan KH, Cheng XY, Cui DQ. 2011. Physical mapping of *puroindoline b-2* genes and molecular characterization of a novel variant in durum wheat (*Triticum turgidum* L.). *Molecular Breeding* 28:153-161.
- Chen P, Liu HH, Cui R, Zhang ZL, Pang DW, Xie ZX, Zheng HZ, Lu ZX, Tong H. 2008. Visualized investigation of yeast transformation induced with Li⁺ and polyethylene glycol. *Talanta* 77:262-268.
- Chen Y, Guarneri MT, Vasil AI, Vasil ML, Mant CT, Hodges RS. 2007. Role of peptide hydrophobicity in the mechanism of action of α -helical antimicrobial peptides. *Antimicrobial Agents and Chemotherapy* 51:1398-1406.
- Chen Y, Mant CT, Farmer SW, Hancock REW, Vasil ML, Hodges RS. 2005. Rational design of α -helical antimicrobial peptides with enhanced activities and specificity/therapeutic index. *Journal of Biological Chemistry* 280:12316-12329.
- Chen Y, Xu X, Hong S, Chen J, Liu N, Underhill CB, Creswell K, Zhang L. 2001. RGD-tachyplesin inhibits tumor growth. *Cancer Research* 61:2434-2438.
- Chernysh S, Irina K, Irina A. 2012. Anti-tumor activity of immunomodulatory peptide alloferon-1 in mouse tumor transplantation model. *International Immunopharmacology* 12:312-314.
- Chernysh S, Kim SI, Bekker G, Pleskach VA, Filatova NA, Anikin VB, Platonov VG, Bulet P. 2002. Antiviral and antitumor peptides from insects. *Proceedings of the National Academy of Sciences of the United States of America* 99:12628-12632.
- Chevreau E, Dupuis F, Ortolan C, Parisi L. 2001. Transformation of apple for durable scab resistance: expression of a *puroindoline* gene in susceptible and resistant (Vf) genotypes. *Acta Horticulturae* 560:323-326.
- Cho WI, Choi JB, Lee K, Chung MS, Pyun YR. 2008. Antimicrobial activity of torilin isolated from *Torilis japonica* fruit against *Bacillus subtilis*. *Journal of Food Science* 73:M37-M46.
- Chou S, Shao C, Wang J, Shan A, Xu L, Dong N, Li Z. 2016. Short, multiple-stranded β -hairpin peptides have antimicrobial potency with high selectivity and salt resistance. *Acta Biomaterialia* 30:78-93.
- Chou TC. 2006. Theoretical basis, experimental design, and computerized simulation of synergism and antagonism in drug combination studies. *Pharmacological Reviews* 58:621-681.
- Chu ST, Cheng HH, Huang CJ, Chang HC, Chi CC, Su HH, Hsu SS, Wang JL, Chen IS, Liu SI, Lu YC, Huang JK, Ho CM, Jan CR. 2007. Phospholipase A2-

- independent Ca²⁺ entry and subsequent apoptosis induced by melittin in human MG63 osteosarcoma cells. *Life Sciences* 80:364-369.
- Cirac AD, Moiset G, Mika JT, Koçer A, Salvador P, Poolman B, Marrink SJ, Sengupta D. 2011. The molecular basis for antimicrobial activity of pore-forming cyclic peptides. *Biophysical Journal* 100:2422-2431.
- Clayton AHA, Hanley QS, Verveer PJ. 2004. Graphical representation and multicomponent analysis of single-frequency fluorescence lifetime imaging microscopy data. *Journal of Microscopy* 213:1-5.
- Clements A, Tull D, Jenney AW, Farn JL, Kim SH, Bishop RE, McPhee JB, Hancock REW, Hartland EL, Pearse MJ, Wijburg OLC, Jackson DC, McConville MJ, Strugnell RA. 2007. Secondary acylation of *Klebsiella pneumoniae* lipopolysaccharide contributes to sensitivity to antibacterial peptides. *Journal of Biological Chemistry* 282:15569-15577.
- Clifton LA, Green RJ, Frazier RA. 2007a. *Puroindoline-b* mutations control the lipid binding interactions in mixed puroindoline-a:puroindoline-b systems. *Biochemistry* 46:13929-13937.
- Clifton LA, Lad MD, Green RJ, Frazier RA. 2007b. Single amino acid substitutions in *puroindoline-b* mutants influence lipid binding properties. *Biochemistry* 46:2260-2266.
- Clifton LA, Sanders MR, Hughes AV, Neylon C, Frazier RA, Green RJ. 2011. Lipid binding interactions of antimicrobial plant seed defence proteins: *puroindoline-a* and β -purothionin. *Physical Chemistry Chemical Physics* 13:17153-17162.
- Cokol M, Chua HN, Tasan M, Mutlu B, Weinstein ZB, Suzuki Y, Nergiz ME, Costanzo M, Baryshnikova A, Giaever G, Nislow C, Myers CL, Andrews BJ, Boone C, Roth FP. 2011. Systematic exploration of synergistic drug pairs. *Molecular Systems Biology* 7:71.
- Costerton JW, Cheng KJ, Geesey GG, Ladd TI, Nickel JC, Dasgupta M, Marrie TJ. 1987. Bacterial biofilms in nature and disease. *Annual Review of Microbiology* 41:435-464.
- Cruciani RA, Barker JL, Zasloff M, Chen HC, Colamonici O. 1991. Antibiotic magainins exert cytolytic activity against transformed cell lines through channel formation. *Proceedings of the National Academy of Sciences of the United States of America* 88:3792-3796.
- Cruz J, Ortiz C, Guzmán F, Fernández-Lafuente R, Torres R. 2014. Antimicrobial peptides: promising compounds against pathogenic microorganisms. *Current Medicinal Chemistry* 21:2299-2321.
- Cudic M, Otvos Jr L. 2002. Intracellular targets of antibacterial peptides. *Current Drug Targets* 3:101-106.

References

- Cullen TW, Schofield WB, Barry NA, Putnam EE, Rundell EA, Trent MS, Degnan PH, Booth CJ, Yu H, Goodman AL. 2015. Antimicrobial peptide resistance mediates resilience of prominent gut commensals during inflammation. *Science* 347:170-175.
- Czihal P, Knappe D, Fritsche S, Zahn M, Berthold N, Piantavigna S, Müller U, Van Dorpe S, Herth N, Binas A, Köhler G, De Spiegeleer B, Martin LL, Nolte O, Sträter N, Alber G, Hoffmann R. 2012. Api88 is a novel antibacterial designer peptide to treat systemic infections with multidrug-resistant gram-negative pathogens. *ACS Chemical Biology* 7:1281-1291.
- da Silva A, Kawazoe U, Freitas FFT, Gatti MSV, Dolder H, Schumacher RI, Juliano MA, da Silva MJ, Leite A. 2002. Avian anticoccidial activity of a novel membrane-interactive peptide selected from phage display libraries. *Molecular and Biochemical Parasitology* 120:53-60.
- Darouiche RO. 2004. Treatment of infections associated with surgical implants. *New England Journal of Medicine* 350:1422-1429.
- Dathe M, Nikolenko H, Klose J, Bienert M. 2004. Cyclization increases the antimicrobial activity and selectivity of arginine- and tryptophan-containing hexapeptides. *Biochemistry* 43:9140-9150.
- Dathe M, Nikolenko H, Meyer J, Beyermann M, Bienert M. 2001. Optimization of the antimicrobial activity of magainin peptides by modification of charge. *FEBS Letters* 501:146-150.
- Dathe M, Schumann M, Wieprecht T, Winkler A, Beyermann M, Krause E, Matsuzaki K, Murase O, Bienert M. 1996. Peptide helicity and membrane surface charge modulate the balance of electrostatic and hydrophobic interactions with lipid bilayers and biological membranes. *Biochemistry* 35:12612-12622.
- De Clercq E. 2004. Antiviral drugs in current clinical use. *Journal of Clinical Virology* 30:115-133.
- Delves-Broughton J. 2005. Nisin as a food preservative. *Food Australia* 57:525-527.
- Dempsey CE, Ueno S, Avison MB. 2003. Enhanced membrane permeabilization and antibacterial activity of a disulfide-dimerized magainin analogue. *Biochemistry* 42:402-409.
- Den Hertog AL, Van Marle J, Van Veen HA, Van't Hof W, Bolscher JGM, Veerman ECI, Nieuw Amerongen AV. 2005. Candidacidal effects of two antimicrobial peptides: histatin 5 causes small membrane defects, but LL-37 causes massive disruption of the cell membrane. *Biochemical Journal* 388:689-695.
- Dennison SR, Harris F, Bhatt T, Singh J, Phoenix DA. 2009. The effect of c-terminal amidation on the efficacy and selectivity of antimicrobial and anticancer peptides. *Molecular and Cellular Biochemistry* 332:43-50.

References

- Dennison SR, Harris F, Phoenix DA. 2005a. Are oblique orientated α -helices used by antimicrobial peptides for membrane invasion? *Protein and Peptide Letters* 12:27-29.
- Dennison SR, Harris F, Phoenix DA. 2007. The interactions of aurein 1.2 with cancer cell membranes. *Biophysical Chemistry* 127:78-83.
- Dennison SR, Wallace J, Harris F, Phoenix DA. 2005b. Amphiphilic α -helical antimicrobial peptides and their structure/function relationships. *Protein and Peptide Letters* 12:31-39.
- Dennison SR, Whittaker M, Harris F, Phoenix DA. 2006. Anticancer α -helical peptides and structure/function relationships underpinning their interactions with tumour cell membranes. *Current Protein and Peptide Science* 7:487-499.
- Deslouches B, Islam K, Craigo JK, Paranjape SM, Montelaro RC, Mietzner TA. 2005a. Activity of the de novo engineered antimicrobial peptide WLBU2 against *Pseudomonas aeruginosa* in human serum and whole blood: implications for systemic applications. *Antimicrobial Agents and Chemotherapy* 49:3208-3216.
- Deslouches B, Phadke SM, Lazarevic V, Cascio M, Islam K, Montelaro RC, Mietzner TA. 2005b. De novo generation of cationic antimicrobial peptides: influence of length and tryptophan substitution on antimicrobial activity. *Antimicrobial Agents and Chemotherapy* 49:316-322.
- Deslouches B, Steckbeck JD, Craigo JK, Doi Y, Mietzner TA, Montelaro RC. 2013. Rational design of engineered cationic antimicrobial peptides consisting exclusively of arginine and tryptophan, and their activity against multidrug-resistant pathogens. *Antimicrobial Agents and Chemotherapy* 57:2511-2521.
- Destoumieux-Garzón D, Duquesne S, Peduzzi J, Goulard C, Desmadril M, Letellier L, Rebuffat S, Boulanger P. 2005. The iron-siderophore transporter FhuA is the receptor for the antimicrobial peptide microcin J25: role of the microcin Val11-Pro16 β -hairpin region in the recognition mechanism. *Biochemical Journal* 389:869-876.
- Destoumieux-Garzón D, Saulnier D, Garnier J, Jouffrey C, Bulet P, Bachère E. 2001. Crustacean immunity: antifungal peptides are generated from the C terminus of shrimp hemocyanin in response to microbial challenge. *Journal of Biological Chemistry* 276:47070-47077.
- Devaux MF, Le Deschault De Monredon F, Guibert D, Novales B, Abecassis J. 1998. Particle size distribution of break, sizing and middling wheat flours by laser diffraction. *Journal of the Science of Food and Agriculture* 78:237-244.
- Dewan PC, Anantharaman A, Chauhan VS, Sahal D. 2009. Antimicrobial action of prototypic amphipathic cationic decapeptides and their branched dimers. *Biochemistry* 48:5642-5657.

References

- Digman MA, Caiolfa VR, Zamai M, Gratton E. 2008. The phasor approach to fluorescence lifetime imaging analysis. *Biophysical Journal* 94:L14-L16.
- Ding H, Jin G, Zhang L, Dai J, Dang J, Han Y. 2015. Effects of tachyplesin I on human U251 glioma stem cells. *Molecular Medicine Reports* 11:2953-2958.
- Djordjevic D, Wiedmann M, McLandsborough LA. 2002. Microtiter plate assay for assessment of *Listeria monocytogenes* biofilm formation. *Applied and Environmental Microbiology* 68:2950-2958.
- Donachie WD, Robinson AC 1987. Cell division: parameter values and the process. In: FC Neidhardt (ed.). *Escherichia coli* and *Salmonella typhimurium* – cellular and molecular biology. American Society of Microbiology: Washington, DC. p. 1578-1593.
- Dong W, Dong Z, Mao X, Sun Y, Li F, Shang D. 2016. Structure-activity analysis and biological studies of chensinin-1b analogues. *Acta Biomaterialia* 37:59-68.
- Dosler S, Mataraci E. 2013. *In vitro* pharmacokinetics of antimicrobial cationic peptides alone and in combination with antibiotics against methicillin resistant *Staphylococcus aureus* biofilms. *Peptides* 49:53-58.
- Douliez J-P, Michon T, Elmorjani K, Marion D. 2000. Structure, biological and technological functions of lipid transfer proteins and indolines, the major lipid binding proteins from cereal kernels. *Journal of Cereal Science* 32:1-20.
- Dourou D, Beauchamp CS, Yoon Y, Geornaras I, Belk KE, Smith GC, Nychas GJE, Sofos JN. 2011. Attachment and biofilm formation by *Escherichia coli* O157:H7 at different temperatures, on various food-contact surfaces encountered in beef processing. *International Journal of Food Microbiology* 149:262-268.
- Doyle J, Brinkworth CS, Wegener KL, Carver JA, Llewellyn LE, Olver IN, Bowie JH, Wabnitz PA, Tyler MJ. 2003. nNOS inhibition, antimicrobial and anticancer activity of the amphibian skin peptide, citropin 1.1 and synthetic modifications: The solution structure of a modified citropin 1.1. *European Journal of Biochemistry* 270:1141-1153.
- Drechsler S, Andrä J. 2011. Online monitoring of metabolism and morphology of peptide-treated neuroblastoma cancer cells and keratinocytes. *Journal of Bioenergetics and Biomembranes* 43:275-285.
- Drenkard E, Ausubel FM. 2002. *Pseudomonas* biofilm formation and antibiotic resistance are linked to phenotypic variation. *Nature* 416:740-743.
- Dubreil L, Compoin J-P, Marion D. 1997. Interaction of puroindolines with wheat flour polar lipids determines their foaming properties. *Journal of Agricultural and Food Chemistry* 45:108-116.
- Dubreil L, Gaborit T, Bouchet B, Gallant DJ, Broekaert WF, Quillien L, Marion D. 1998. Spatial and temporal distribution of the major isoforms of

- puroindolines (puroindoline-a and puroindoline-b) and non specific lipid transfer protein (ns-LTP1e1) of *Triticum aestivum* seeds. Relationships with their *in vitro* antifungal properties. *Plant Science* 138:121-135.
- Ebbensgaard A, Mordhorst H, Overgaard MT, Nielsen CG, Aarestrup FM, Hansen EB. 2015. Comparative evaluation of the antimicrobial activity of different antimicrobial peptides against a range of pathogenic Bacteria. *PLoS ONE* 10:e0144611.
- Eisenberg D, Schwarz E, Komaromy M, Wall R. 1984. Analysis of membrane and surface protein sequences with the hydrophobic moment plot. *Journal of Molecular Biology* 179:125-142.
- Eisenberg D, Weiss RM, Terwilliger TC. 1982. The helical hydrophobic moment: a measure of the amphiphilicity of a helix. *Nature* 299:371-374.
- Eliassen L, Berge G, Sveinbjørnsson B, Svendsen JS, Vorland LH, Rekdal Ø. 2002. Evidence for a direct antitumor mechanism of action of bovine lactoferricin. *Anticancer Research* 22:2703-2710.
- Eliassen LT, Berge G, Leknessund A, Wikman M, Lindin I, Løkke C, Ponthan F, Johnsen JI, Sveinbjørnsson B, Kogner P, Flægstad T, Rekdal Ø. 2006. The antimicrobial peptide, Lactoferricin B, is cytotoxic to neuroblastoma cells *in vitro* and inhibits xenograft growth *in vivo*. *International Journal of Cancer* 119:493-500.
- Epand RM, Epand RF. 2011. Bacterial membrane lipids in the action of antimicrobial agents. *Journal of Peptide Science* 17:298-305.
- Esbjörner EK, Caesar CEB, Albinsson B, Lincoln P, Nordén B. 2007. Tryptophan orientation in model lipid membranes. *Biochemical and Biophysical Research Communications* 361:645-650.
- Espinel-Ingroff A, Cantón E 2007. Antifungal susceptibility testing of yeasts. In: R Schwalbe (ed.). *Antimicrobial susceptibility testing protocols* CRC: Hoboken. p. 173-207.
- Essig A, Hofmann D, Münch D, Gayathri S, Künzler M, Kallio PT, Sahl HG, Wider G, Schneider T, Aebi M. 2014. Copsin, a novel peptide-based fungal antibiotic interfering with the peptidoglycan synthesis. *Journal of Biological Chemistry* 289:34953-34964.
- Evrard A, Lagarde V, Joudrier P, Gautier M-F. 2008. Puroindoline-a and puroindoline-b interact with the *Saccharomyces cerevisiae* plasma membrane through different amino acids present in their tryptophan-rich domain. *Journal of Cereal Science* 48:379-386.
- Fabretti F, Theilacker C, Baldassarri L, Kaczynski Z, Kropec A, Holst O, Huebner J. 2006. Alanine esters of enterococcal lipoteichoic acid play a role in biofilm formation and resistance to antimicrobial peptides. *Infection and Immunity* 74:4164-4171.

- Faize M, Sourice S, Dupuis F, Parisi L, Gautier M-F, Chevreua E. 2004. Expression of wheat *puroindoline-b* reduces scab susceptibility in transgenic apple (*Malus x domestica* Borkh.). *Plant Science* 167:347-354.
- Falla TJ, Hancock REW. 1997. Improved activity of a synthetic indolicidin analog. *Antimicrobial Agents and Chemotherapy* 41:771-775.
- Falla TJ, Karunaratne DN, Hancock REW. 1996. Mode of action of the antimicrobial peptide indolicidin. *The Journal of Biological Chemistry* 271:19298-19303.
- Falord M, Karimova G, Hiron A, Msadeka T. 2012. GraXSR proteins interact with the VraFG ABC transporter to form a five-component system required for cationic antimicrobial peptide sensing and resistance in *Staphylococcus aureus*. *Antimicrobial Agents and Chemotherapy* 56:1047-1058.
- Fang B, Guo HY, Zhang M, Jiang L, Ren FZ. 2013. The six amino acid antimicrobial peptide bLFcin6 penetrates cells and delivers siRNA. *FEBS Journal* 280:1007-1017.
- Fantner GE, Barbero RJ, Gray DS, Belcher AM. 2010. Kinetics of antimicrobial peptide activity measured on individual bacterial cells using high-speed atomic force microscopy. *Nature Nanotechnology* 5:280-285.
- Fernández-Musoles R, Castelló-Ruiz M, Arce C, Manzanares P, Ivorra MD, Salom JB. 2014. Antihypertensive mechanism of lactoferrin-derived peptides: angiotensin receptor blocking effect. *Journal of Agricultural and Food Chemistry* 62:173-181.
- Fernández-Vidal M, Jayasinghe S, Ladokhin AS, White SH. 2007. Folding amphipathic helices into membranes: amphiphilicity trumps hydrophobicity. *Journal of Molecular Biology* 370:459-470.
- Fernandez DI, Le Brun AP, Whitwell TC, Sani MA, James M, Separovic F. 2012. The antimicrobial peptide aurein 1.2 disrupts model membranes via the carpet mechanism. *Physical Chemistry Chemical Physics* 14:15739-15751.
- Fimland G, Eijsink VGH, Nissen-Meyer J. 2002. Mutational analysis of the role of tryptophan residues in an antimicrobial peptide. *Biochemistry* 41:9508-9515.
- Fittipaldi N, Sekizaki T, Takamatsu D, De La Cruz Domínguez-Punaro M, Harel J, Bui NK, Vollmer W, Gottschalk M. 2008. Significant contribution of the *pgdA* gene to the virulence of *Streptococcus suis*. *Molecular Microbiology* 70:1120-1135.
- Fjell CD, Hiss JA, Hancock REW, Schneider G. 2012. Designing antimicrobial peptides: Form follows function. *Nature Reviews Drug Discovery* 11:37-51.
- Freire JM, Gaspar D, De La Torre BG, Veiga AS, Andreu D, Castanho MARB. 2014. Monitoring antibacterial permeabilization in real time using time-resolved flow cytometry. *Biochimica et Biophysica Acta - Biomembranes* 1848:554-560.

- Friedrich CL, Moyles D, Beveridge TJ, Hancock REW. 2000. Antibacterial action of structurally diverse cationic peptides on gram-positive bacteria. *Antimicrobial Agents and Chemotherapy* 44:2086-2092.
- Friedrich CL, Rozek A, Patrzykat A, Hancock REW. 2001. Structure and mechanism of action of an indolicidin peptide derivative with improved activity against Gram-positive bacteria. *Journal of Biological Chemistry* 276:24015-24022.
- Furlong SJ, Mader JS, Hoskin DW. 2006. Lactoferricin-induced apoptosis in estrogen-nonresponsive MDA-MB-435 breast cancer cells is enhanced by C6 ceramide or tamoxifen. *Oncology Reports* 15:1385-1390.
- Furlong SJ, Mader JS, Hoskin DW. 2010. Bovine lactoferricin induces caspase-independent apoptosis in human B-lymphoma cells and extends the survival of immune-deficient mice bearing B-lymphoma xenografts. *Experimental and Molecular Pathology* 88:371-375.
- Gaspar D, Freire JM, Pacheco TR, Barata JT, Castanho MARB. 2015. Apoptotic human neutrophil peptide-1 anti-tumor activity revealed by cellular biomechanics. *Biochimica et Biophysica Acta - Molecular Cell Research* 1853:308-316.
- Gaspar D, Salomé Veiga A, Castanho MARB. 2013. From antimicrobial to anticancer peptides. A review. *Frontiers in Microbiology* 4:294.
- Gatti L, Zunino F. 2005. Overview of tumor cell chemoresistance mechanisms. *Methods in molecular medicine* 111:127-148.
- Gautier M-F, Aleman M-E, Guirao A, Marion D, Joudrier P. 1994. *Triticum aestivum* puroindolines, two basic cysteine-rich seed proteins: cDNA sequence analysis and developmental gene expression. *Plant Molecular Biology* 25:43-57.
- Gautier M-F, Cosson P, Guirao A, Alary R, Joudrier P. 2000. *Puroindoline* genes are highly conserved in diploid ancestor wheats and related species but absent in tetraploid *Triticum* species. *Plant Science* 153:81-91.
- Gazit E, Boman A, Boman HG, Shai Y. 1995. Interaction of the mammalian antibacterial peptide cecropin P1 with phospholipid vesicles. *Biochemistry* 34:11479-11488.
- Gazza L, Sgrulletta D, Cammerata A, Gazzelloni G, Perenzin M, Pogna NE. 2011. Pastamaking and breadmaking quality of soft-textured durum wheat lines. *Journal of Cereal Science* 54:481-487.
- Gee ML, Burton M, Grevis-James A, Hossain MA, McArthur S, Palombo EA, Wade JD, Clayton AHA. 2013. Imaging the action of antimicrobial peptides on living bacterial cells. *Scientific Reports* 3:01557.
- Gennaro R, Zanetti M. 2000. Structural features and biological activities of the cathelicidin-derived antimicrobial peptides. *Peptide Science* 55:31-49.

- Gentilucci L, de Marco R, Cerisoli L. 2010. Chemical modifications designed to improve peptide stability: incorporation of non-natural amino acids, pseudo-peptide bonds, and cyclization. *Current Pharmaceutical Design* 16:3185-3203.
- Ghosh A, Kar RK, Jana J, Saha A, Jana B, Krishnamoorthy J, Kumar D, Ghosh S, Chatterjee S, Bhunia A. 2014. Indolicidin targets duplex DNA: structural and mechanistic insight through a combination of spectroscopy and microscopy. *ChemMedChem* 9:2052-2058.
- Ghraiiri T, Chaftar N, Hani K 2012. Bacteriocins: recent advances and opportunities. In. *Progress in Food Preservation*. p. 485-511.
- Giangaspero A, Sandri L, Tossi A. 2001. Amphipathic α helical antimicrobial peptides: a systematic study of the effects of structural and physical properties on biological activity. *European Journal of Biochemistry* 268:5589-5600.
- Gifford JL, Hunter HN, Vogel HJ. 2005. Lactoferricin: a lactoferrin-derived peptide with antimicrobial, antiviral, antitumor and immunological properties. *Cellular and Molecular Life Sciences* 62:2588-2598.
- Giroux MJ, Morris CF. 1997. A glycine to serine change in puroindoline b is associated with wheat grain hardness and low levels of starch-surface friabilin. *Theoretical and Applied Genetics* 95:857-864.
- Giroux MJ, Morris CF. 1998. Wheat grain hardness results from highly conserved mutations in the friabilin components *puroindoline a* and *b*. *Proceedings in the National Academy of Sciences of the United States of America* 95:6262-6266.
- Glukhov E, Stark M, Burrows LL, Deber CM. 2005. Basis for selectivity of cationic antimicrobial peptides for bacterial *versus* mammalian membranes. *Journal of Biological Science* 280:33960-33967.
- Goldman MJ, Anderson GM, Stolzenberg ED, Kari UP, Zasloff M, Wilson JM. 1997. Human beta-defensin-1 is a salt-sensitive antibiotic in lung that is inactivated in cystic fibrosis. *Cell* 88:553.
- Goodrich JS, Sutton-Shields TN, Kerr A, Wedd JP, Miller MB, Gilligan PH. 2009. Prevalence of community-associated methicillin-resistant *Staphylococcus aureus* in patients with cystic fibrosis. *Journal of Clinical Microbiology* 47:1231-1233.
- Gopal R, Na H, Seo CH, Park Y. 2012. Antifungal activity of (KW)_n or (RW)_n peptide against *Fusarium solani* and *Fusarium oxysporum*. *International Journal of Molecular Sciences* 13:15042-15053.
- Gopal R, Seo CH, Song PI, Park Y. 2013. Effect of repetitive lysine-tryptophan motifs on the bactericidal activity of antimicrobial peptides. *Amino Acids* 44:645-660.

- Greco WR, Bravo G, Parsons JC. 1995. The search for synergy: a critical review from a response surface perspective. *Pharmacological Reviews* 47:331-385.
- Greenwell P, Schofield JD. 1986. A starch Granule protein associated with endosperm softness in wheat. *Cereal Chemistry* 63:379-380.
- Groisman EA, Parra-Lopez C, Salcedo M, Lipps CJ, Heffron F. 1992. Resistance to host antimicrobial peptides is necessary for *Salmonella* virulence. *Proceedings of the National Academy of Sciences of the United States of America* 89:11939-11943.
- Guilhelmelli F, Vilela N, Albuquerque P, Derengowski LS, Silva-Pereira I, Kyaw CM. 2013. Antibiotic development challenges: the various mechanisms of action of antimicrobial peptides and of bacterial resistance. *Frontiers in Microbiology* 4:353.
- Guina T, Yi EC, Wang H, Hackett M, Miller SI. 2000. A PhoP-regulated outer membrane protease of *Salmonella enterica* serovar typhimurium promotes resistance to alpha-helical antimicrobial peptides. *Journal of Bacteriology* 182:4077-4086.
- Gullberg E, Cao S, Berg OG, Ilbäck C, Sandegren L, Hughes D, Andersson DI. 2011. Selection of resistant bacteria at very low antibiotic concentrations. *PLoS Pathogens* 7:e1002158.
- Gunderson CW, Segall AM. 2006. DNA repair, a novel antibacterial target: holliday junction-trapping peptides induce DNA damage and chromosome segregation defects. *Molecular Microbiology* 59:1129-1148.
- Gunn JS, Lim KB, Krueger J, Kim K, Guo L, Hackett M, Miller SI. 1998. PmrA-PmrB-regulated genes necessary for 4-aminoarabinose lipid A modification and polymyxin resistance. *Molecular Microbiology* 27:1171-1182.
- Gunn JS, Miller SI. 1996. PhoP-PhoQ activates transcription of pmrAB, encoding a two-component regulatory system involved in *Salmonella typhimurium* antimicrobial peptide resistance. *Journal of Bacteriology* 178:6857-6864.
- Guo L, Lim KB, Poduje CM, Daniel M, Gunn JS, Hackett M, Miller SI. 1998. Lipid A acylation and bacterial resistance against vertebrate antimicrobial peptides. *Cell* 95:189-198.
- Gut IM, Prouty AM, Ballard JD, Van Der Donk WA, Blanke SR. 2008. Inhibition of *Bacillus anthracis* spore outgrowth by nisin. *Antimicrobial Agents and Chemotherapy* 52:4281-4288.
- Guzmán F, Marshall S, Ojeda C, Albericio F, Carvajal-Rondanelli P. 2013. Inhibitory effect of short cationic homopeptides against Gram-positive bacteria. *Journal of Peptide Science* 19:792-800.
- Haaber J, Cohn MT, Frees D, Andersen TJ, Ingmer H. 2012. Planktonic aggregates of *Staphylococcus aureus* protect against common antibiotics. *PLoS ONE* 7:e41075.

References

- Habets MGJL, Brockhurst MA. 2012. Therapeutic antimicrobial peptides may compromise natural immunity. *Biology Letters* 8:416-418.
- Hale JDF, Hancock REW. 2007. Alternative mechanisms of action of cationic antimicrobial peptides on bacteria. *Expert Review of Anti-Infective Therapy* 5:951-959.
- Hall-Stoodley L, Costerton JW, Stoodley P. 2004. Bacterial biofilms: from the natural environment to infectious diseases. *Nature Reviews Microbiology* 2:95-108.
- Hall K, Lee TH, Mechler AI, Swann MJ, Aguilar MI. 2014. Real-time measurement of membrane conformational states induced by antimicrobial peptides: balance between recovery and lysis. *Scientific Reports* 4:05479.
- Hallock KJ, Lee DK, Omnaas J, Mosberg HI, Ramamoorthy A. 2002. Membrane composition determines Pardaxin's mechanism of lipid bilayer disruption. *Biophysical Journal* 83:1004-1013.
- Han FF, Gao YH, Luan C, Xie YG, Liu YF, Wang YZ. 2013a. Comparing bacterial membrane interactions and antimicrobial activity of porcine lactoferricin-derived peptides. *Journal of Dairy Science* 96:3471-3487.
- Han Y, Cui Z, Li YH, Hsu WH, Lee BH. 2016. *In vitro* and *in vivo* anticancer activity of pardaxin against proliferation and growth of oral squamous cell carcinoma. *Marine Drugs* 14:2.
- Han YY, Liu HY, Han DJ, Zong XC, Zhang SQ, Chen YQ. 2013b. Role of glycosylation in the anticancer activity of antibacterial peptides against breast cancer cells. *Biochemical Pharmacology* 86:1254-1262.
- Hancock REW, Chapple DS. 1999. Peptide antibiotics. *Antimicrobial Agents and Chemotherapy* 43:1317-1323.
- Hancock REW, Sahl HG. 2006. Antimicrobial and host-defense peptides as new anti-infective therapeutic strategies. *Nature Biotechnology* 24:1551-1557.
- Hancock REW, Speert DP. 2000. Antibiotic resistance in *Pseudomonas aeruginosa*: Mechanisms and impact on treatment. *Drug Resistance Updates* 3:247-255.
- Haney EF, Hancock REW. 2013. Peptide design for antimicrobial and immunomodulatory applications. *Biopolymers* 100:572-583.
- Haney EF, Nathoo S, Vogel HJ, Prenner EJ. 2010. Induction of non-lamellar lipid phases by antimicrobial peptides: a potential link to mode of action. *Chemistry and Physics of Lipids* 163:82-93.
- Haney EF, Petersen AP, Lau CK, Jing W, Storey DG, Vogel HJ. 2013. Mechanism of action of puoroindoline derived tryptophan-rich antimicrobial peptides. *Biochimica et Biophysica Acta - Biomembranes* 1828:1802-1813.

- Hara-Kudo Y, Yamasaki A, Sasaki M, Okubo T, Minai Y, Haga M, Kondo K, Sugita-Konishi Y. 2005. Antibacterial action on pathogenic bacterial spore by green tea catechins. *Journal of the Science of Food and Agriculture* 85:2354-2361.
- Harris F, Dennison SR, Phoenix DA. 2009. Anionic antimicrobial peptides from eukaryotic organisms. *Current Protein and Peptide Science* 10:585-606.
- Harris F, Dennison SR, Phoenix DA. 2011. Anionic antimicrobial peptides from eukaryotic organisms and their mechanisms of action. *Current Chemical Biology* 5:142-153.
- Harris F, Dennison SR, Singh J, Phoenix DA. 2013. On the selectivity and efficacy of defense peptides with respect to cancer cells. *Medicinal Research Reviews* 33:190-234.
- Haug BE, Camilio KA, Eliassen LT, Stensen W, Svendsen JS, Berg K, Mortensen B, Serin G, Mirjolet JF, Bichat F, Rekdal O. 2016. Discovery of a 9-mer cationic peptide (LTX-315) as a potential first in class oncolytic peptide. *Journal of Medicinal Chemistry* 59:2918-2927.
- Haug BE, Stensen W, Kalaaji M, Rekdal Ø, Svendsen JS. 2008. Synthetic antimicrobial peptidomimetics with therapeutic potential. *Journal of Medicinal Chemistry* 51:4306-4314.
- Haug BE, Svendsen JS. 2001. The role of tryptophan in the antibacterial activity of a 15-residue bovine lactoferricin peptide. *Journal of Peptide Science* 7:190-196.
- He J, Furmanski P. 1995. Sequence specificity and transcriptional activation in the binding of lactoferrin to DNA. *Nature* 373:721-724.
- Heinze K, Kiszonas AM, Murray JC, Morris CF, Lullien-Pellerin V. 2016. *Puroindoline* genes introduced into durum wheat reduce milling energy and change milling behavior similar to soft common wheats. *Journal of Cereal Science* 71:183-189.
- Henzler Wildman KA, Lee DK, Ramamoorthy A. 2003. Mechanism of lipid bilayer disruption by the human antimicrobial peptide, LL-37. *Biochemistry* 42:6545-6558.
- Hetian L, Ping A, Shumei S, Xiaoying L, Luowen H, Jian W, Lin M, Meisheng L, Junshan Y, Chengchao S. 2002. A novel peptide isolated from a phage display library inhibits tumor growth and metastasis by blocking the binding of vascular endothelial growth factor to its kinase domain receptor. *Journal of Biological Chemistry* 277:43137-43142.
- Hilpert K, Volkmer-Engert R, Walter T, Hancock REW. 2005. High-throughput generation of small antibacterial peptides with improved activity. *Nature Biotechnology* 23:1008-1012.

References

- Ho YH, Sung TC, Chen CS. 2012. Lactoferricin B inhibits the phosphorylation of the two-component system response regulators BasR and CreB. *Molecular and Cellular Proteomics* 11:M111.014720
- Hogg AC, Sripo T, Beecher B, Martin JM, Giroux MJ. 2004. Wheat puroindolines interact to form friabilin and control wheat grain hardness. *Theoretical and Applied Genetics* 108:1089-1097.
- Høiby N, Bjarnsholt T, Givskov M, Molin S, Ciofu O. 2010. Antibiotic resistance of bacterial biofilms. *International Journal of Antimicrobial Agents* 35:322-332.
- Hollmann A, Martínez M, Noguera ME, Augusto MT, Disalvo A, Santos NC, Semorile L, Maffia PC. 2016. Role of amphipathicity and hydrophobicity in the balance between hemolysis and peptide-membrane interactions of three related antimicrobial peptides. *Colloids and Surfaces B: Biointerfaces* 141:528-536.
- Hong J, Guan W, Jin G, Zhao H, Jiang X, Dai J. 2015. Mechanism of tachyplesin I injury to bacterial membranes and intracellular enzymes, determined by laser confocal scanning microscopy and flow cytometry. *Microbiological Research* 170:69-77.
- Hoskin DW, Ramamoorthy A. 2008a. Studies on anticancer activities of antimicrobial peptides. *Biochimica et Biophysica Acta* 1778:357-375.
- Hoskin DW, Ramamoorthy A. 2008b. Studies on anticancer activities of antimicrobial peptides. *Biochimica et Biophysica Acta - Biomembranes* 1778:357-375.
- Hsu CH, Chen C, Jou ML, Yueh-Luen Lee A, Lin YC, Yu YP, Huang WT, Wu SH. 2005. Structural and DNA-binding studies on the bovine antimicrobial peptide, indolicidin: evidence for multiple conformations involved in binding to membranes and DNA. *Nucleic Acids Research* 33:4053-4064.
- Hsu STD, Breukink E, Tischenko E, Lutters MAG, De Kruijff B, Kaptein R, Bonvin AMJJ, Van Nuland NAJ. 2004. The nisin-lipid II complex reveals a pyrophosphate cage that provides a blueprint for novel antibiotics. *Nature Structural and Molecular Biology* 11:963-967.
- Hu WW, Lin ZW, Ruaan RC, Chen WY, Jin SLC, Chang Y. 2013. A novel application of indolicidin for gene delivery. *International Journal of Pharmaceutics* 456:293-300.
- Hu Y, Liu A, Vaudrey J, Vaiciunaite B, Moigboi C, McTavish SM, Kearns A, Coates A. 2015. Combinations of β -lactam or aminoglycoside antibiotics with plectasin are synergistic against methicillin-sensitive and methicillin-resistant *Staphylococcus aureus*. *PLoS ONE* 10:e0117664.
- Huang HN, Rajanbabu V, Pan CY, Chan YL, Wu CJ, Chen JY. 2013. A cancer vaccine based on the marine antimicrobial peptide pardaxin (GE33) for control of bladder-associated tumors. *Biomaterials* 34:10151-10159.

- Huang HW. 2000. Action of antimicrobial peptides: Two-state model. *Biochemistry* 39:8347-8352.
- Huang TC, Chen JY. 2013. Proteomic analysis reveals that pardaxin triggers apoptotic signaling pathways in human cervical carcinoma HeLa cells: cross talk among the UPR, c-Jun and ROS. *Carcinogenesis* 34:1833-1842.
- Huang TC, Lee JF, Chen JY. 2011. Pardaxin, an antimicrobial peptide, triggers caspase-dependent and ROS-mediated apoptosis in HT-1080 cells. *Marine Drugs* 9:1995-2009.
- Huang Y, He L, Li G, Zhai N, Jiang H, Chen Y. 2014a. Role of helicity of α -helical antimicrobial peptides to improve specificity. *Protein & Cell* 5: 631-642.
- Huang Y, He L, Li G, Zhai N, Jiang H, Chen Y. 2014b. Role of helicity of α -helical antimicrobial peptides to improve specificity. *Protein and Cell* 5:631-642.
- Hui L, Leung K, Chen HM. 2002. The combined effects of antibacterial peptide cecropin A and anti-cancer agents on leukemia cells. *Anticancer Research* 22:2811-2816.
- Hwang PM, Zhou N, Shan X, Arrowsmith CH, Vogel HJ. 1998. Three-dimensional solution structure of lactoferricin B, an antimicrobial peptide derived from bovine lactoferrin. *Biochemistry* 37:4288-4298.
- Ikeda TM, Cong H, Suzuki T, Takata K. 2010. Identification of new *Pina* null mutations among Asian common wheat cultivars. *Journal of Cereal Science* 51:235-237.
- Imamovic L, Sommer MOA. 2013. Use of collateral sensitivity networks to design drug cycling protocols that avoid resistance development. *Science Translational Medicine* 5:204ra132.
- Inácio ÂS, Domingues NS, Nunes A, Martins PT, Moreno MJ, Estronca LM, Fernandes R, Moreno AJM, Borrego MJ, Gomes JP, Vaz WLC, Vieira OV. 2016. Quaternary ammonium surfactant structure determines selective toxicity towards bacteria: mechanisms of action and clinical implications in antibacterial prophylaxis. *Journal of Antimicrobial Chemotherapy* 71:641-654.
- Infante VV, Miranda-Olvera AD, De Leon-Rodriguez LM, Anaya-Velazquez F, Rodriguez MC, Avila EE. 2011. Effect of the antimicrobial peptide tritripticin on the *in vitro* viability and growth of trichomonas vaginalis. *Current Microbiology* 62:301-306.
- Inoue S, Ohue T, Yamagishi J, Nakamura S, Shimizu M. 1978. Mode of incomplete cross-resistance among pipemidic, piromidic, and nalidixic acids. *Antimicrobial Agents and Chemotherapy* 14:240-245.
- Ishida H, Ishida Y, Kurosaka Y, Otani T, Sato K, Kobayashi H. 1998. *In vitro* and *in vivo* activities of levofloxacin against biofilm-producing *Pseudomonas aeruginosa*. *Antimicrobial Agents and Chemotherapy* 42:1641-1645.

- Islam D, Bandholtz L, Nilsson J, Wigzell H, Christensson B, Agerberth B, Gudmundsson GH. 2001. Downregulation of bactericidal peptides in enteric infections: a novel immune escape mechanism with bacterial DNA as a potential regulator. *Nature Medicine* 7:180-185.
- Jacob B, Kim Y, Hyun JK, Park IS, Bang JK, Shin SY. 2014. Bacterial killing mechanism of sheep myeloid antimicrobial peptide-18 (SMAP-18) and its Trp-substituted analog with improved cell selectivity and reduced mammalian cell toxicity. *Amino Acids* 46:187-198.
- Jadhav S, Bhavne M, Palombo EA. 2012. Methods used for the detection and subtyping of *Listeria monocytogenes*. *Journal of Microbiological Methods* 88:327-341.
- Jadhav S, Shah R, Bhavne M, Palombo EA. 2013. Inhibitory activity of yarrow essential oil on *Listeria* planktonic cells and biofilms. *Food Control* 29:125-130.
- Jang JH, Kim YJ, Kim H, Kim SC, Cho JH. 2015. Buforin IIb induces endoplasmic reticulum stress-mediated apoptosis in HeLa cells. *Peptides* 69:144-149.
- Jang WS, Bajwa JS, Sun JN, Edgerton M. 2010. Salivary histatin 5 internalization by translocation, but not endocytosis, is required for fungicidal activity in *Candida albicans*. *Molecular Microbiology* 77:354-370.
- Jenssen H, Andersen JH, Uhlin-Hansen L, Gutteberg TJ, Rekdal Ø. 2004. Anti-HSV activity of lactoferricin analogues is only partly related to their affinity for heparan sulfate. *Antiviral Research* 61:101-109.
- Jenssen H, Hamill P, Hancock REW. 2006. Peptide antimicrobial agents. *Clinical Microbiology Reviews* 19:491-511.
- Jeong MC, Jeon D, Shin A, Jin S, Shin SY, Park YS, Kim Y. 2016. Effects of hydrophobic peptoid substitutions on the bacterial cell selectivity and antimicrobial activity of Piscidin 1. *Bulletin of the Korean Chemical Society* 37:1545-1551.
- Jiang Z, Vasil AI, Hale JD, Hancock REW, Vasil ML, Hodges RS. 2008. Effects of net charge and the number of positively charged residues on the biological activity of amphipathic α -helical cationic antimicrobial peptides. *Biopolymers - Peptide Science Section* 90:369-383.
- Jing W, Demcoe AR, Vogel HJ. 2003. Conformation of a bactericidal domain of puoindoline a: structure and mechanism of action of a 13-residue antimicrobial peptide. *Journal of Bacteriology* 185:4938-4947.
- Jochumsen N, Marvig RL, Damkiær S, Jensen RL, Paulander W, Molin S, Jelsbak L, Folkesson A. 2016. The evolution of antimicrobial peptide resistance in *Pseudomonas aeruginosa* is shaped by strong epistatic interactions. *Nature Communications* 7:13002.
- Johansson J, Gudmundsson GH, Rottenberg ME, Berndt KD, Agerberth B. 1998. Conformation-dependent antibacterial activity of the naturally occurring human peptide LL-37. *Journal of Biological Chemistry* 273:3718-3724.

- Johansson L, Thulin P, Sendi P, Hertzén E, Linder A, Åkesson P, Low DE, Agerberth B, Norrby-Teglund A. 2008. Cathelicidin LL-37 in severe *Streptococcus pyogenes* soft tissue infections in humans. *Infection and Immunity* 76:3399-3404.
- Jones A, Geörg M, Maudsdotter L, Jonsson AB. 2009. Endotoxin, capsule, and bacterial attachment contribute to *Neisseria meningitidis* resistance to the human antimicrobial peptide LL-37. *Journal of Bacteriology* 191:3861-3868.
- Joshi S, Dewangan RP, Yar MS, Rawat DS, Pasha S. 2015. N-terminal aromatic tag induced self assembly of tryptophan-arginine rich ultra short sequences and their potent antibacterial activity. *RSC Advances* 5:68610-68620.
- Kaiser ET, Kezdy FJ. 1983. Secondary structures of proteins and peptides in amphiphilic environments (A review). *Proceedings of the National Academy of Sciences of the United States of America* 80:1137-1143.
- Kang BR, Kim H, Nam SH, Yun EY, Kim SR, Ahn MY, Chang JS, Hwang JS. 2012. CopA3 peptide from *Copris tripartitus* induces apoptosis in human leukemia cells via a caspase-independent pathway. *BMB Reports* 45:85-90.
- Kang JH, Lee MK, Kim KL, Hahm KS. 1996. Structure-biological activity relationships of 11-residue highly basic peptide segment of bovine lactoferrin. *International Journal of Peptide and Protein Research* 48:357-363.
- Kapteyn JC, Hoyer LL, Hecht JE, Müller WH, Andel A, Verkleij AJ, Makarow M, Van Den Ende H, Klis FM. 2000. The cell wall architecture of *Candida albicans* wild-type cells and cell wall-defective mutants. *Molecular Microbiology* 35:601-611.
- Karshikov A, Berendes R, Burger A, Cavalié A, Lux HD, Huber R. 1992. Annexin V membrane interaction: an electrostatic potential study. *European Biophysics Journal* 20:337-344.
- Kathariou S. 2002. *Listeria monocytogenes* virulence and pathogenicity, a food safety perspective. *Journal of Food Protection* 65:1811-1829.
- Keil B. 1992. Specificity of Proteolysis. Springer-Verlag, 1992.
- Kelly GJ, Kia AFA, Hassan F, O'Grady S, Morgan MP, Creaven BS, McClean S, Harmey JH, Devocelle M. 2016. Polymeric prodrug combination to exploit the therapeutic potential of antimicrobial peptides against cancer cells. *Organic and Biomolecular Chemistry* 14:9278-9286.
- Keo T, Collins J, Kunwar P, Blaser MJ, Iovine NM. 2011. Campylobacter capsule and lipooligosaccharide confer resistance to serum and cationic antimicrobials. *Virulence* 2:30-40.
- Keren I, Kaldalu N, Spoering A, Wang Y, Lewis K. 2004. Persister cells and tolerance to antimicrobials. *FEMS Microbiology Letters* 230:13-18.

- Keymanesh K, Soltani S, Sardari S. 2009. Application of antimicrobial peptides in agriculture and food industry. *World Journal of Microbiology and Biotechnology* 25:933-944.
- Khan AR, Sadiq IZ, Abdullahi LI, Danlami D, Taneja P. 2016. Chemoprotective role of bovine lactoferricin against 7, 12 dimethylbenz (A) anthracene induced skin cancer in female swiss albino mice. *International Journal of Pharmacy and Pharmaceutical Sciences* 8:215-222.
- Kiba A, Saitoh H, Nishihara M, Omiya K, Yamamura S. 2003. C-terminal domain of a hevein-like protein from *Wasabia japonica* has potent antimicrobial activity. *Plant and Cell Physiology* 44:296-303.
- Kim JY, Park SC, Yoon MY, Hahm KS, Park Y. 2011. C-terminal amidation of PMAP-23: translocation to the inner membrane of Gram-negative bacteria. *Amino Acids* 40:183-195.
- Kim KH, Feiz L, Dyer AT, Grey W, Hogg AC, Martin JM, Giroux MJ. 2012. Increased resistance to *Penicillium* seed rot in transgenic wheat over-expressing puroindolines. *Journal of Phytopathology* 160:243-247.
- Kim YS, Cha HJ. 2006. High-throughput and facile assay of antimicrobial peptides using pH-controlled fluorescence resonance energy transfer. *Antimicrobial Agents and Chemotherapy* 50:3330-3335.
- Klein S, Lorenzo C, Hoffmann S, Walther JM, Storbeck S, Piekarski T, Tindall BJ, Wray V, Nimtz M, Moser J. 2009. Adaptation of *Pseudomonas aeruginosa* to various conditions includes tRNA-dependent formation of alanyl-phosphatidylglycerol. *Molecular Microbiology* 71:551-565.
- Knappe D, Zahn M, Sauer U, Schiffer G, Sträter N, Hoffmann R. 2011. Rational design of oncocin derivatives with superior protease stabilities and antibacterial activities based on the high-resolution structure of the oncocin-DnaK complex. *ChemBioChem* 12:874-876.
- Kobayashi S, Chikushi A, Tougu S, Imura Y, Nishida M, Yano Y, Matsuzaki K. 2004. Membrane translocation mechanism of the antimicrobial peptide buforin 2. *Biochemistry* 43:15610-15616.
- Kocourková L, Novotná P, Čujová S, Čerovský V, Urbanová M, Setnička V. 2017. Conformational study of melectin and antapin antimicrobial peptides in model membrane environments. *Spectrochimica Acta - Part A: Molecular and Biomolecular Spectroscopy* 170:247-255.
- Kolossova OA, Usachev KS, Aganov AV, Klochkov VV. 2016. Antimicrobial peptide protegrins interact with DPC micelles by apolar hydrophobic cluster: structural studies by high-resolution NMR spectroscopy. *BioNanoScience* 6:317-319.
- Kondejewski LH, Lee DL, Jelokhani-Niaraki M, Farmer SW, Hancock REW, Hodges RS. 2002. Optimization of microbial specificity in cyclic peptides by

- modulation of hydrophobicity within a defined structural framework. *Journal of Biological Chemistry* 277:67-74.
- Kooijman M, Orsel R, Hessing M, Hamer RJ, Bekkers ACAPA. 1997. Spectroscopic characterisation of the lipid-binding properties of wheat puroindolines. *Journal of Cereal Science* 26:145-159.
- Koszalka P, Kamysz E, Wejda M, Kamysz W, Bigda J. 2011. Antitumor activity of antimicrobial peptides against U937 histiocytic cell line. *Acta Biochimica Polonica* 58:111-117.
- Kouidhi B, Zmantar T, Bakhrouf A. 2010. Anti-cariogenic and anti-biofilms activity of Tunisian propolis extract and its potential protective effect against cancer cells proliferation. *Anaerobe* 16:566-571.
- Kovács M, Halfmann A, Fedtke I, Heintz M, Peschel A, Vollmer W, Hakenbeck R, Brückner R. 2006. A functional *dlt* operon, encoding proteins required for incorporation of D-alanine in teichoic acids in gram-positive bacteria, confers resistance to cationic antimicrobial peptides in *Streptococcus pneumoniae*. *Journal of Bacteriology* 188:5797-5805.
- Kragol G, Lovas S, Varadi G, Condie BA, Hoffmann R, Otvos Jr L. 2001. The antibacterial peptide pyrrolicin inhibits the ATPase actions of DnaK and prevents chaperone-assisted protein folding. *Biochemistry* 40:3016-3026.
- Krajewski K, Marchand C, Long Y-Q, Pommier Y, Roller PP. 2004. Synthesis and HIV-1 integrase inhibitory activity of dimeric and tetrameric analogs of indolicidin. *Bioorganic & Medicinal Chemistry Letters* 14:5595-5598.
- Kraus D, Peschel A 2006, in *Current Topics in Microbiology and Immunology*, Vol. 306, pp. 231-250.
- Krishnamurthy K, Balconi C, Sherwood JE, Giroux MJ. 2001. Wheat puroindolines enhance fungal disease resistance in transgenic rice. *Molecular Plant - Microbe Interactions* 14:1255-1260.
- Kristensen K, Henriksen JR, Andresen TL. 2014. Quantification of leakage from large unilamellar lipid vesicles by fluorescence correlation spectroscopy. *Biochimica et Biophysica Acta - Biomembranes* 1838:2994-3002.
- Krom BP, Cohen JB, McElhaney Feser GE, Cihlar RL. 2007. Optimized candidal biofilm microtiter assay. *Journal of Microbiological Methods* 68:421-423.
- Kruzel ML, Bacsı A, Choudhury B, Sur S, Boldogh I. 2006. Lactoferrin decreases pollen antigen-induced allergic airway inflammation in a murine model of asthma. *Immunology* 119:159-166.
- Kumar CG, Anand SK. 1998. Significance of microbial biofilms in food industry: a review. *International Journal of Food Microbiology* 42:9-27.
- Kuroda K, Fukuda T, Yoneyama H, Katayama M, Isogai H, Okumura K, Isogai E. 2012. Anti-proliferative effect of an analogue of the LL-37 peptide in the

- colon cancer derived cell line HCT116 p53 ^{+/+}and p53. *Oncology Reports* 28:829-834.
- Laaberki MH, Pfeffer J, Clarke AJ, Dworkin J. 2011. O-acetylation of peptidoglycan is required for proper cell separation and S-layer anchoring in *Bacillus anthracis*. *Journal of Biological Chemistry* 286:5278-5288.
- Laadhari M, Arnold AA, Gravel AE, Separovic F, Marcotte I. 2016. Interaction of the antimicrobial peptides caerin 1.1 and aurein 1.2 with intact bacteria by 2H solid-state NMR. *Biochimica et Biophysica Acta - Biomembranes* 1858:2959-2964.
- Lai Y, Gallo RL. 2009. AMPed up immunity: how antimicrobial peptides have multiple roles in immune defense. *Trends in Immunology* 30:131-141.
- Lai Y, Villaruz AE, Li M, Cha DJ, Sturdevant DE, Otto M. 2007. The human anionic antimicrobial peptide dermcidin induces proteolytic defence mechanisms in *staphylococci*. *Molecular Microbiology* 63:497-506.
- Lakshman DK, Natarajan S, Mandal S, Mitra A. 2013. Lactoferrin-derived resistance against plant pathogens in transgenic plants. *Journal of Agricultural and Food Chemistry* 61:11730-11735.
- Lauth X, Von Kœckritz-Blickwede M, McNamara CW, Myskowski S, Zinkernagel AS, Beall B, Ghosh P, Gallo RL, Nizet V. 2009. M1 protein allows group a *streptococcal* survival in phagocyte extracellular traps through cathelicidin inhibition. *Journal of Innate Immunity* 1:202-214.
- Lawrence HA, Palombo EA. 2009. Activity of essential oils against *Bacillus subtilis* spores. *Journal of Microbiology and Biotechnology* 19:1590-1595.
- Lawyer C, Pai S, Watabe M, Borgia P, Mashimo T, Eagleton L, Watabe K. 1996. Antimicrobial activity of a 13 amino acid tryptophan-rich peptide derived from a putative porcine precursor protein of a novel family of antibacterial peptides. *FEBS Letters* 390:95-98.
- Le Bihan T, Blochet J-E, Désormeaux A, Marion D, Pézolet M. 1996. Determination of the secondary structure and conformation of puroidolines by infrared and ramen spectroscopy. *Biochemistry* 35:12712-12722.
- Le CF, Fang CM, Sekaran SD. 2017. Intracellular targeting mechanisms by antimicrobial peptides. *Antimicrobial Agents and Chemotherapy* 61:e02340-16.
- Le CF, Yusof MYM, Hassan H, Sekaran SD. 2015. *In vitro* properties of designed antimicrobial peptides that exhibit potent antipneumococcal activity and produces synergism in combination with penicillin. *Scientific Reports* 5:09761.
- Le Guernevé C, Seigneuret M, Marion D. 1998. Interaction of the wheat endosperm lipid-binding protein puroidoline-a with phospholipids. *Archives of Biochemistry and Biophysics* 360:179-186.

- Lee CC, Sun Y, Qian S, Huang HW. 2011. Transmembrane pores formed by human antimicrobial peptide LL-37. *Biophysical Journal* 100:1688-1696.
- Lee DL, Powers JPS, Pfliegerl K, Vasil ML, Hancock REW, Hodges RS. 2004. Effects of single D-amino acid substitutions on disruption of β -sheet structure and hydrophobicity in cyclic 14-residue antimicrobial peptide analogs related to gramicidin S. *Journal of Peptide Research* 63:69-84.
- Lee HS, Park CB, Kim JM, Jang SA, Park IY, Kim MS, Cho JH, Kim SC. 2008a. Mechanism of anticancer activity of buforin IIb, a histone H2A-derived peptide. *Cancer Letters* 271:47-55.
- Lee JH, Kim IW, Kim SH, Yun EY, Nam SH, Ahn MY, Kang DC, Hwang JS. 2015. Anticancer activity of CopA3 dimer peptide in human gastric cancer cells. *BMB Reports* 48:324-329.
- Lee JK, Seo CH, Luchian T, Park Y. 2016a. Antimicrobial peptide CMA3 derived from the CA-MA hybrid peptide: antibacterial and anti-inflammatory activities with low cytotoxicity and mechanism of action in *Escherichia coli*. *Antimicrobial Agents and Chemotherapy* 60:495-506.
- Lee JY, Yang ST, Lee SK, Jung HH, Shin SY, Hahm KS, Kim JI. 2008b. Salt-resistant homodimeric bactenecin, a cathelicidin-derived antimicrobial peptide. *FEBS Journal* 275:3911-3920.
- Lee TH, Hall KN, Aguilar MI. 2016b. Antimicrobial peptide structure and mechanism of action: a focus on the role of membrane structure. *Current Topics in Medicinal Chemistry* 16:25-39.
- Leggett MJ, McDonnell G, Denyer SP, Setlow P, Maillard JY. 2012. Bacterial spore structures and their protective role in biocide resistance. *Journal of Applied Microbiology* 113:485-498.
- Lehmann J, Retz M, Sidhu SS, Suttmann H, Sell M, Paulsen F, Harder J, Unteregger G, Stöckle M. 2006. Antitumor activity of the antimicrobial peptide magainin II against bladder cancer cell lines. *European Urology* 50:141-147.
- Leitgeb B, Szekeres A, Manczinger L, Vágvölgyi C, Kredics L. 2007. The history of Alamethicin: a review of the most extensively studied peptaibol. *Chemistry and Biodiversity* 4:1027-1051.
- Leptihn S, Har JY, Chen J, Ho B, Wohland T, Ding JL. 2009. Single molecule resolution of the antimicrobial action of quantum dot-labeled sushi peptide on live bacteria. *BMC Biology* 7:
- Lesage VS, Bouchet B, Rhazi L, Elmorjani K, Branlard G, Marion D. 2011. New insight into puroindoline function inferred from their subcellular localization in developing hard and soft near-isogenic endosperm and their relationship with polymer size of storage proteins. *Journal of Cereal Science* 53:231-238.
- Lewis K. 2001. Riddle of biofilm resistance. *Antimicrobial Agents and Chemotherapy* 45:999-1007.

- Lewis LA, Choudhury B, Balthazar JT, Martin LE, Ram S, Rice PA, Stephens DS, Carlson R, Shafer WM. 2009. Phosphoethanolamine substitution of lipid A and resistance of *Neisseria gonorrhoeae* to cationic antimicrobial peptides and complement-mediated killing by normal human serum. *Infection and Immunity* 77:1112-1120.
- Li B, Gu W, Zhang C, Huang XQ, Han KQ, Ling CQ. 2006. Growth arrest and apoptosis of the human hepatocellular carcinoma cell line Bel-7402 induced by melittin. *Onkologie* 29:367-371.
- Li L, Shi Y, Cheng X, Xia S, Cheserek MJ, Le G. 2015. A cell-penetrating peptide analogue, P7, exerts antimicrobial activity against *Escherichia coli* ATCC25922 via penetrating cell membrane and targeting intracellular DNA. *Food Chemistry* 166:231-239.
- Li L, Song F, Sun J, Tian X, Xia S, Le G. 2016a. Membrane damage as first and DNA as the secondary target for anti-*candidal* activity of antimicrobial peptide P7 derived from cell-penetrating peptide ppTG20 against *Candida albicans*. *Journal of Peptide Science* 22:427-433.
- Li L, Sun J, Xia S, Tian X, Cheserek MJ, Le G. 2016b. Mechanism of antifungal activity of antimicrobial peptide APP, a cell-penetrating peptide derivative, against *Candida albicans*: intracellular DNA binding and cell cycle arrest. *Applied Microbiology and Biotechnology* 100:3245-3253.
- Li QF, Ouyang GL, Peng XX, Hong SG. 2003. Effects of tachyplesin on the regulation of cell cycle in human hepatocarcinoma SMMC-7721 cells. *World Journal of Gastroenterology* 9:454-458.
- Li W, Tailhades J, O'Brien-Simpson NM, Separovic F, Otvos L, Jr., Hossain MA, Wade JD. 2014. Proline-rich antimicrobial peptides: potential therapeutics against antibiotic-resistant bacteria. *Amino Acids* 46:2287-2294.
- Li WT, Jiang QT, Chen GY, Pu ZE, Liu YX, Wang JR, Zheng YL, Wei YM. 2011. Comparative analysis of *hina* gene sequences in wild (*Hordeum spontaneum*) and cultivated (*H. vulgare*) barleys. *Agricultural Sciences in China* 10:1313-1322.
- Li X, Saravanan R, Kwak SK, Leong SSJ. 2013. Biomolecular engineering of a human beta defensin model for increased salt resistance. *Chemical Engineering Science* 95:128-137.
- Li X, Shen B, Chen Q, Zhang X, Ye Y, Wang F, Zhang X. 2016c. Antitumor effects of cecropin B-LHRH' on drug-resistant ovarian and endometrial cancer cells. *BMC Cancer* 16:251.
- Lillemo M, Morris CF. 2000. A leucine to proline mutation in *puroindoline b* is frequently present in hard wheats from Northern Europe. *Theoretical and Applied Genetics* 100:1100-1107.
- Lim K, Chua RRY, Saravanan R, Basu A, Mishra B, Tambyah PA, Ho B, Leong SSJ. 2013. Immobilization studies of an engineered arginine-tryptophan-rich

- peptide on a silicone surface with antimicrobial and antibiofilm activity. *ACS Applied Materials and Interfaces* 5:6412-6422.
- Lin J, Motylinski J, Krauson AJ, Wimley WC, Searson PC, Hristova K. 2012. Interactions of membrane active peptides with planar supported bilayers: an impedance spectroscopy study. *Langmuir* 28:6088-6096.
- Liu B, Huang H, Yang Z, Liu B, Gou S, Zhong C, Han X, Zhang Y, Ni J, Wang R. 2017. Design of novel antimicrobial peptide dimer analogues with enhanced antimicrobial activity *in vitro* and *in vivo* by intermolecular triazole bridge strategy. *Peptides* 88:115-125.
- Liu BR, Huang YW, Aronstam RS, Lee HJ. 2016. Identification of a short cell-penetrating peptide from bovine lactoferricin for intracellular delivery of DNA in human A549 cells. *PLoS ONE* 11:e0150439.
- Liu X, Li Y, Li Z, Lan X, Leung PHM, Li J, Yang M, Ko F, Qin L. 2015. Mechanism of anticancer effects of antimicrobial peptides. *Journal of Fiber Bioengineering and Informatics* 8:25-36.
- Liu YF, Han FF, Xie YG, Wang YZ. 2011. Comparative antimicrobial activity and mechanism of action of bovine lactoferricin-derived synthetic peptides. *BioMetals* 24:1069-1078.
- Liu Z, Brady A, Young A, Rasimick B, Chen K, Zhou C, Kallenbach NR. 2007. Length effects in antimicrobial peptides of the (RW)_n series. *Antimicrobial Agents and Chemotherapy* 51:597-603.
- Loewe S. 1953. The problem of synergism and antagonism of combined drugs. *Arzneimittel-Forschung* 3:285-290.
- Lofton H, Pr anting M, Thulin E, Andersson DI. 2013. Mechanisms and fitness costs of resistance to antimicrobial peptides LL-37, CNY100HL and wheat germ histones. *PLoS ONE* 8:e68875.
- Lohner K. 2009. New strategies for novel antibiotics: Peptides targeting bacterial cell membranes. *General Physiology and Biophysics* 28:105-116.
- Long Zhu WL, Shin SY. 2009. Effects of dimerization of the cell-penetrating peptide Tat analog on antimicrobial activity and mechanism of bactericidal action. *Journal of Peptide Science* 15:345-352.
- L pez-Exp sito I, Pellegrini A, Amigo L, Recio I. 2008. Synergistic effect between different milk-derived peptides and proteins. *Journal of Dairy Science* 91:2184-2189.
- L pez-Garc a B, P rez-Pay  E, Marcos JF. 2002. Identification of novel hexapeptides bioactive against phytopathogenic fungi through screening of a synthetic peptide combinatorial library. *Applied and Environmental Microbiology* 68:2453-2460.

References

- Lorenzón EN, Cespedes GF, Vicente EF, Nogueira LG, Bauab TM, Castro MS, Cilli EM. 2012. Effects of dimerization on the structure and biological activity of antimicrobial peptide Ctx-Ha. *Antimicrobial Agents and Chemotherapy* 56:3004-3010.
- Lorenzón EN, Sanches PRS, Nogueira LG, Bauab TM, Cilli EM. 2013. Dimerization of aurein 1.2: effects in structure, antimicrobial activity and aggregation of *Cândida albicans* cells. *Amino Acids* 44:1521-1528.
- Lu Y, Zhang TF, Shi Y, Zhou HW, Chen Q, Wei BY, Wang X, Yang TX, Chinn YE, Kang J, Fu CY. 2016. PFR peptide, one of the antimicrobial peptides identified from the derivatives of lactoferrin, induces necrosis in leukemia cells. *Scientific Reports* 6:20823.
- Ludtke SJ, He K, Heller WT, Harroun TA, Yang L, Huang HW. 1996. Membrane pores induced by magainin. *Biochemistry* 35:13723-13728.
- Luo L, Zhang J, Yang G, Li Y, Li K, He G. 2008. Expression of *puroindoline a* enhances leaf rust resistance in transgenic tetraploid wheat. *Molecular Biology Reports* 35:195-200.
- Lutkenhaus J. 1990. Regulation of cell division in *E. coli*. *Trends in Genetics* 6:22-25.
- Ma JC, Dougherty DA. 1997. The cation- π interaction. *Chemical Reviews* 97:1303-1324.
- Macfarlene ELA, Kwasnicka A, Hancock REW. 2000. Role of *Pseudomonas aeruginosa* Phop-PhoQ in resistance to antimicrobial cationic peptides and aminoglycosides. *Microbiology* 146:2543-2554.
- Mader JS, Hoskin DW. 2006. Cationic antimicrobial peptides as novel cytotoxic agents for cancer treatment. *Expert Opinion on Investigational Drugs* 15:933-946.
- Mader JS, Mookherjee N, Hancock REW, Bleackley RC. 2009. The human host defense peptide LL-37 induces apoptosis in a calpain- and apoptosis-inducing factor-dependent manner involving Bax activity. *Molecular Cancer Research* 7:689-702.
- Mader JS, Salsman J, Conrad DM, Hoskin DW. 2005. Bovine lactoferricin selectively induces apoptosis in human leukemia and carcinoma cell lines. *Molecular Cancer Therapeutics* 4:612-624.
- Mah TFC, O'Toole GA. 2001. Mechanisms of biofilm resistance to antimicrobial agents. *Trends in Microbiology* 9:34-39.
- Mai JC, Mi Z, Kim SH, Ng B, Robbins PD. 2001. A proapoptotic peptide for the treatment of solid tumors. *Cancer Research* 61:7709-7712.
- Maloney E, Stankowska D, Zhang J, Fol M, Cheng QJ, Lun S, Bishai WR, Rajagopalan M, Chatterjee D, Madiraju MV. 2009. The two-domain LysX protein of *Mycobacterium tuberculosis* is required for production of

- lysinylated phosphatidylglycerol and resistance to cationic antimicrobial peptides. *PLoS Pathogens* 5:e1000534.
- Manzini MC, Perez KR, Riske KA, Bozelli Jr JC, Santos TL, Da Silva MA, Saraiva GKV, Politi MJ, Valente AP, Almeida FCL, Chaimovich H, Rodrigues MA, Bemquerer MP, Schreier S, Cuccovia IM. 2014. Peptide:Lipid ratio and membrane surface charge determine the mechanism of action of the antimicrobial peptide BP100. Conformational and functional studies. *Biochimica et Biophysica Acta - Biomembranes* 1838:1985-1999.
- Marchand C, Krajewski K, Lee H-F, Antony S, Johnson AA, Amin R, Roller P, Kvaratskhelia M, Pommier Y. 2006. Covalent binding of the natural antimicrobial peptide indolicidin to DNA abasic sites. *Nucleic Acids Research* 34:5157-5165.
- Marcusson LL, Frimodt-Møller N, Hughes D. 2009. Interplay in the selection of fluoroquinolone resistance and bacterial fitness. *PLoS Pathogens* 5:e1000541.
- Mardirossian M, Grzela R, Giglione C, Meinnel T, Gennaro R, Mergaert P, Scocchi M. 2014. The host antimicrobial peptide Bac71-35 binds to bacterial ribosomal proteins and inhibits protein synthesis. *Chemistry and Biology* 21:1639-1647.
- Martin JM, Froberg RC, Morris CF, Talbert LE, Giroux MJ. 2001. Milling and bread baking traits associated with puroindoline sequence type in hard red spring wheat. *Crop Science* 41:228-234.
- Martínez JP, Gil ML, López-Ribot JL, Chaffin WL. 1998. Serologic response to cell wall mannoproteins and proteins of *Candida albicans*. *Clinical Microbiology Reviews* 11:121-141.
- Martínez Viedma P, Abriouel H, Ben Omar N, López RL, Gálvez A. 2011. Inhibition of spoilage and toxigenic *Bacillus* species in dough from wheat flour by the cyclic peptide enterocin AS-48. *Food Control* 22:756-761.
- Mason KM, Munson Jr RS, Bakaletz LO. 2005. A mutation in the sap operon attenuates survival of nontypeable *Haemophilus influenzae* in a chinchilla model of otitis media. *Infection and Immunity* 73:599-608.
- Masson PL, Heremans JF, Dive CH. 1966. An iron-binding protein common to many external secretions. *Clinica Chimica Acta* 14:735-739.
- Mathew MK, Balaram P. 1983. A helix dipole model for alamethicin and related transmembrane channels. *FEBS Letters* 157:1-5.
- Matson JS, Yoo HJ, Hakansson K, Dirita VJ. 2010. Polymyxin B resistance in el tor *vibrio cholerae* requires lipid acylation catalyzed by MsbB. *Journal of Bacteriology* 192:2044-2052.

- Matsuzaki K. 1998. Magainins as paradigm for the mode of action of pore forming polypeptides. *Biochimica et Biophysica Acta - Reviews on Biomembranes* 1376:391-400.
- Matsuzaki K. 2009. Control of cell selectivity of antimicrobial peptides. *Biochimica et Biophysica Acta - Biomembranes* 1788:1687-1692.
- Matsuzaki K, Mitani Y, Akada KY, Murase O, Yoneyama S, Zasloff M, Miyajima K. 1998. Mechanism of synergism between antimicrobial peptides magainin 2 and PGLa. *Biochemistry* 37:15144-15153.
- Matsuzaki K, Murase O, Fujii N, Miyajima K. 1996. An antimicrobial peptide, magainin 2, induced rapid flip-flop of phospholipids coupled with pore formation and peptide translocation. *Biochemistry* 35:11361-11368.
- McCann KB, Lee A, Wan J, Roginski H, Coventry MJ. 2003. The effect of bovine lactoferrin and lactoferricin B on the ability of feline calicivirus (a norovirus surrogate) and poliovirus to infect cell cultures. *Journal of Applied Microbiology* 95:1026-1033.
- McCubbin GA, Praporski S, Piantavigna S, Knappe D, Hoffmann R, Bowie JH, Separovic F, Martin LL. 2011. QCM-D fingerprinting of membrane-active peptides. *European Biophysics Journal* 40:437-446.
- McPhee JB, Lewenza S, Hancock REW. 2003. Cationic antimicrobial peptides activate a two-component regulatory system, PmrA-PmrB, that regulates resistance to polymyxin B and cationic antimicrobial peptides in *Pseudomonas aeruginosa*. *Molecular Microbiology* 50:205-217.
- Melo MN, Ferre R, Castanho MARB. 2009. Antimicrobial peptides: linking partition, activity and high membrane-bound concentrations. *Nature Reviews Microbiology* 7:245-250.
- Miao Y, Chen L, Wang C, Wang Y, Zheng Q, Gao C, Yang G, He G. 2012. Expression, purification and antimicrobial activity of puroindoline A protein and its mutants. *Amino Acids* 43:1689-1696.
- Michael Henderson J, Lee KYC. 2013. Promising antimicrobial agents designed from natural peptide templates. *Current Opinion in Solid State and Materials Science* 17:175-192.
- Mihajlovic M, Lazaridis T. 2012. Charge distribution and imperfect amphipathicity affect pore formation by antimicrobial peptides. *Biochimica et Biophysica Acta - Biomembranes* 1818:1274-1283.
- Minoux H, Chipot C. 1999. Cation- π interactions in proteins: can simple models provide an accurate description? *Journal of the American Chemical Society* 121:10366-10372.
- Mitchell JBO, Nandi CL, McDonald IK, Thornton JM, Price SL. 1994. Amino/aromatic interactions in proteins: is the evidence stacked against hydrogen bonding? *Journal of Molecular Biology* 239:315-331.

- Miteva M, Andersson M, Karshikoff A, Otting G. 1999. Molecular electroporation: a unifying concept for the description of membrane pore formation by antibacterial peptides, exemplified with NK-lysin. *FEBS Letters* 462:155-158.
- Mochon AB, Liu H. 2008. The antimicrobial peptide histatin-5 causes a spatially restricted disruption on the *Candida albicans* surface, allowing rapid entry of the peptide into the cytoplasm. *PLoS Pathogens* 4:e1000190.
- Montville TJ, De Siano T, Nock A, Padhi S, Wade D. 2006. Inhibition of *Bacillus anthracis* and potential surrogate bacilli growth from spore inocula by nisin and other antimicrobial peptides. *Journal of Food Protection* 69:2529-2533.
- Moon DO, Park SY, Choi YH, Kim ND, Lee C, Kim GY. 2008. Melittin induces Bcl-2 and caspase-3-dependent apoptosis through downregulation of Akt phosphorylation in human leukemic U937 cells. *Toxicol* 51:112-120.
- Moore AJ, Devine DA, Bibby MC. 1994. Preliminary experimental anticancer activity of cecropins. *Peptide Research* 7:265-269.
- Morell EA, Balkin DM. 2010. Methicillin-resistant *Staphylococcus aureus*: A pervasive pathogen highlights the need for new antimicrobial development. *Yale Journal of Biology and Medicine* 83:223-233.
- Morris CF, Casper J, Kiszonas AM, Fuerst EP, Murray J, Simeone MC, Lafiandra D. 2015. Soft kernel durum wheat - A new bakery ingredient? *Cereal Foods World* 60:76-83.
- Morris CF, Simeone MC, King GE, Lafiandra D. 2011. Transfer of soft kernel texture from *Triticum aestivum* to durum wheat, *Triticum turgidum* ssp. durum. *Crop Science* 51:114-122.
- Mularski A, Wilksch JJ, Hanssen E, Strugnell RA, Separovic F. 2016. Atomic force microscopy of bacteria reveals the mechanobiology of pore forming peptide action. *Biochimica et Biophysica Acta - Biomembranes* 1858:1091-1098.
- Müller CA, Markovic-Lipkovski J, Klatt T, Gamper J, Schwarz G, Beck H, Deeg M, Kalbacher H, Widmann S, Wessels JT, Becker V, Müller GA, Flad T. 2002. Human α -defensins HNPs-1, -2, and -3 in renal cell carcinoma: Influences on tumor cell proliferation. *American Journal of Pathology* 160:1311-1324.
- Muñoz A, López-García B, Marcos JF. 2007. Comparative study of antimicrobial peptides to control citrus postharvest decay caused by *Penicillium digitatum*. *Journal of Agricultural and Food Chemistry* 55:8170-8176.
- Muñoz A, Marcos JF. 2006. Activity and mode of action against fungal phytopathogens of bovine lactoferricin-derived peptides. *Journal of Applied Microbiology* 101:1199-1207.
- Muñoz A, Marcos JF, Read ND. 2012. Concentration-dependent mechanisms of cell penetration and killing by the *de novo* designed antifungal hexapeptide PAF26. *Molecular Microbiology* 85:89-106.

References

- Murray JC, Kiszonas AM, Morris CF. 2017. Influence of soft kernel texture on the flour, water absorption, rheology, and baking quality of durum wheat. *Cereal Chemistry* 94:215-222.
- Murray JC, Kiszonas AM, Wilson J, Morris CF. 2016. Effect of soft kernel texture on the milling properties of soft durum wheat. *Cereal Chemistry* 93:513-517.
- Musrati AA, Tervahartiala T, Gürsoy M, Könönen E, Fteita D, Sorsa T, Uitto VJ, Gürsoy UK. 2016. Human neutrophil peptide-1 affects matrix metalloproteinase-2, -8 and -9 secretions of oral squamous cell carcinoma cell lines *in vitro*. *Archives of Oral Biology* 66:1-7.
- Nagpal S, Gupta V, Kaur KJ, Salunke DM. 1999. Structure-function analysis of tritrypticin, an antibacterial peptide of innate immune origin. *Journal of Biological Chemistry* 274:23296-23304.
- Naito M, Fridrich E, Fields JA, Pryjma M, Li J, Cameron A, Gilbert M, Thompson SA, Gaynor EC. 2010. Effects of sequential *Campylobacter jejuni* 81-176 lipooligosaccharide core truncations on biofilm formation, stress survival, and pathogenesis. *Journal of Bacteriology* 192:2182-2192.
- Nan YH, Bang JK, Jacob B, Park IS, Shin SY. 2012. Prokaryotic selectivity and LPS-neutralizing activity of short antimicrobial peptides designed from the human antimicrobial peptide LL-37. *Peptides* 35:239-247.
- Nan YH, Park KH, Park Y, Jeon YJ, Kim Y, Park IS, Hahm KS, Shin SY. 2009. Investigating the effects of positive charge and hydrophobicity on the cell selectivity, mechanism of action and anti-inflammatory activity of a Trp-rich antimicrobial peptide indolicidin. *FEMS Microbiology Letters* 292:134-140.
- Nan YH, Shin SY. 2011. Effect of disulphide bond position on salt resistance and LPS-neutralizing activity of α -helical homo-dimeric model antimicrobial peptides. *BMB Reports* 44:747-752.
- Neale C, Hsu JCY, Yip CM, Pomès R. 2014. Indolicidin binding induces thinning of a lipid bilayer. *Biophysical Journal* 106:L29-L31.
- Nelson DL, Cox MM. 2008. Lehninger principles of biochemistry. 5th edn., New York: W.H. Freeman.
- Neville F, Gidalevitz D, Kale G, Nelson A. 2007. Electrochemical screening of antimicrobial peptide LL-37 interaction with phospholipids. *Bioelectrochemistry* 70:205-213.
- Nguyen LT, Chau JK, Perry NA, de Boer L, Zaat SAJ, Vogel HJ. 2010. Serum stabilities of short tryptophan- and arginine-rich antimicrobial peptide analogs. *PLoS ONE* 5:1-8.
- Nguyen LT, Chau JK, Zaat SAJ, Vogel HJ. 2011a. Cyclic tritrypticin analogs with distinct biological activities. *Probiotics and Antimicrobial Proteins* 3:132-143.

References

- Nguyen LT, Haney EF, Vogel HJ. 2011b. The expanding scope of antimicrobial peptide structures and their modes of action. *Trends in Biotechnology* 29:464-472.
- Nguyen LT, Schibli DJ, Vogel HJ. 2005. Structural studies and model membrane interactions of two peptides derived from bovine lactoferricin. *Journal of Peptide Science* 11:379-389.
- Nicolas P. 2009. Multifunctional host defense peptides: Intracellular-targeting antimicrobial peptides. *FEBS Journal* 276:6483-6496.
- Nijnik A, Hancock REW. 2009. The roles of cathelicidin LL-37 in immune defences and novel clinical applications. *Current Opinion in Hematology* 16:41-47.
- Niknejad A, Webster D, Bhave M. 2016. Production of bioactive wheat puroindoline proteins in *Nicotiana benthamiana* using a virus-based transient expression system. *Protein Expression and Purification* 125:43-52.
- Nilsson AI, Zorzet A, Kanth A, Dahlström S, Berg OG, Andersson DI. 2006. Reducing the fitness cost of antibiotic resistance by amplification of initiator tRNA genes. *Proceedings of the National Academy of Sciences of the United States of America* 103:6976-6981.
- Nilsson MR, Dobson CM. 2003. *In vitro* characterization of lactoferrin aggregation and amyloid formation. *Biochemistry* 42:375-382.
- Ningsih Z, Hossain MA, Wade JD, Clayton AHA, Gee ML. 2012. Slow insertion kinetics during interaction of a model antimicrobial peptide with unilamellar phospholipid vesicles. *Langmuir* 28:2217-2224.
- Nishi H, Komatsuzawa H, Fujiwara T, McCallum N, Sugai M. 2004. Reduced content of lysyl-phosphatidylglycerol in the cytoplasmic membrane affects susceptibility to moenomycin, as well as vancomycin, gentamicin, and antimicrobial peptides, in *Staphylococcus aureus*. *Antimicrobial Agents and Chemotherapy* 48:4800-4807.
- Noto PB, Abbadessa G, Cassone M, Mateo GD, Agelan A, Wade JD, Szabo D, Kocsis B, Nagy K, Rozgonyi F, Otvos Jr L. 2008. Alternative stabilities of a proline-rich antibacterial peptide *in vitro* and *in vivo*. *Protein Science* 17:1249-1255.
- Nyegue MA, Ndoye-Foe F, Etoa FX, Zollo et PHA, Menut C. 2014. Study of chemical composition, growth inhibition and antigerminative effect of three essential oils from Cameroon on Four *Bacillus* strains. *Journal of Essential Oil-Bearing Plants* 17:1335-1342.
- Odds FC. 2003. Synergy, antagonism, and what the chequerboard puts between them. *Journal of Antimicrobial Chemotherapy* 52:1.
- Ogawa C, Liu YJ, Kobayashi KS. 2011. Muramyl dipeptide and its derivatives: peptide adjuvant in immunological disorders and cancer therapy. *Current Bioactive Compounds* 7:180-197.

- Okesola AO. 2011. Community-acquired methicillin-resistant *Staphylococcus aureus*--a review of literature. *African journal of medicine and medical sciences* 40:97-107.
- Okumura K, Itoh A, Isogai E, Hirose K, Hosokawa Y, Abiko Y, Shibata T, Hirata M, Isogai H. 2004. C-terminal domain of human CAP18 antimicrobial peptide induces apoptosis in oral squamous cell carcinoma SAS-H1 cells. *Cancer Letters* 212:185-194.
- Olsen I. 2015. Biofilm-specific antibiotic tolerance and resistance. *European Journal of Clinical Microbiology and Infectious Diseases* 34:877-886.
- Omata Y, Satake M, Maeda R, Saito A, Shimazaki K, Yamauchi K, Uzuka Y, Tanabe S, Sarashina T, Mikami T. 2001. Reduction of the infectivity of *Toxoplasma gondii* and *Eimeria stiedai* sporozoites by treatment with bovine lactoferricin. *Journal of Veterinary Medical Science* 63:187-190.
- Orädd G, Schmidtchen A, Malmsten M. 2011. Effects of peptide hydrophobicity on its incorporation in phospholipid membranes - An NMR and ellipsometry study. *Biochimica et Biophysica Acta - Biomembranes* 1808:244-252.
- Ordonez SR, Amarullah IH, Wubbolts RW, Veldhuizen EJA, Haagsman HP. 2014. Fungicidal mechanisms of cathelicidins LL-37 and CATH-2 revealed by live-cell imaging. *Antimicrobial Agents and Chemotherapy* 58:2240-2248.
- Orioni B, Bocchinfuso G, Kim JY, Palleschi A, Grande G, Bobone S, Park Y, Kim JI, Hahn Ks, Stella L. 2009. Membrane perturbation by the antimicrobial peptide PMAP-23: A fluorescence and molecular dynamics study. *Biochimica et Biophysica Acta - Biomembranes* 1788:1523-1533.
- Otto M. 2006. Bacterial evasion of antimicrobial peptides by biofilm formation. *Current Topics in Microbiology and Immunology* 306:251-258.
- Otto M 2008, in *Current Topics in Microbiology and Immunology*, Vol. 322, pp. 207-228.
- Otvos Jr L. 2002. The short proline-rich antibacterial peptide family. *Cellular and Molecular Life Sciences* 59:1138-1150.
- Otvos Jr L, Insug O, Rogers ME, Consolvo PJ, Condie BA, Lovas S, Bulet P, Blaszczyk-Thurin M. 2000. Interaction between heat shock proteins and antimicrobial peptides. *Biochemistry* 39:14150-14159.
- Oulahal N, Brice W, Martial A, Degraeve P. 2008. Quantitative analysis of survival of *Staphylococcus aureus* or *Listeria innocua* on two types of surfaces: polypropylene and stainless steel in contact with three different dairy products. *Food Control* 19:178-185.
- Ourth DD. 2011. Antitumor cell activity *in vitro* by myristoylated-peptide. *Biomedicine and Pharmacotherapy* 65:271-274.

References

- Overhage J, Campisano A, Bains M, Torfs ECW, Rehm BHA, Hancock REW. 2008. Human host defense peptide LL-37 prevents bacterial biofilm formation. *Infection and Immunity* 76:4176-4182.
- Pace CN, Scholtz JM. 1998. A helix propensity scale based on experimental studies of peptides and proteins. *Biophysical Journal* 75:422-427.
- Palumbo D, Iannaccone M, Porta A, Capparelli R. 2010. Experimental antibacterial therapy with puroindolines, lactoferrin and lysozyme in *Listeria monocytogenes*-infected mice. *Microbes and Infection* 12:538-545.
- Pan CY, Lin CN, Chiou MT, Yu CY, Chen JY, Chien CH. 2015. The antimicrobial peptide pardaxin exerts potent anti-tumor activity against canine perianal gland adenoma. *Oncotarget* 6:2290-2301.
- Pan WR, Chen PW, Chen YLS, Hsu HC, Lin CC, Chen WJ. 2013. Bovine lactoferricin B induces apoptosis of human gastric cancer cell line AGS by inhibition of autophagy at a late stage. *Journal of Dairy Science* 96:7511-7520.
- Papo N, Oren Z, Pag U, Sahl HG, Shai Y. 2002. The consequence of sequence alteration of an amphipathic α -helical antimicrobial peptide and its diastereomers. *Journal of Biological Chemistry* 277:33913-33921.
- Papo N, Shai Y. 2003. Exploring peptide membrane interaction using surface plasmon resonance: differentiation between pore formation versus membrane disruption by lytic peptides. *Biochemistry* 42:458-466.
- Papo N, Shai Y. 2005. Host defence peptides as new weapons in cancer treatment. *Cellular and Molecular Life Sciences* 62:784-790.
- Park CB, Kim HS, Kim SC. 1998. Mechanism of action of the antimicrobial peptide buforin II: buforin II kills microorganisms by penetrating the cell membrane and inhibiting cellular functions. *Biochemical and Biophysical Research Communications* 244:253-257.
- Park CJ, Park CB, Hong SS, Lee HS, Lee SY, Kim SC. 2000. Characterization and cDNA cloning of two glycine- and histidine-rich antimicrobial peptides from the roots of shepherd's purse, *Capsella bursa-pastoris*. *Plant Molecular Biology* 44:187-197.
- Park KH, Nan YH, Park Y, Kim JI, Park I-S, Hahm K-S, Shin SY. 2009. Cell specificity, anti-inflammatory activity, and plausible bactericidal mechanism of designed Trp-rich model antimicrobial peptides. *Biochimica et Biophysica Acta (BBA) - Biomembranes* 1788:1193-1203.
- Parra-Lopez C, Baer MT, Groisman EA. 1993. Molecular genetic analysis of a locus required for resistance to antimicrobial peptides in *Salmonella typhimurium*. *EMBO Journal* 12:4053-4062.
- Pasupuleti M, Chalupka A, Mörgelin M, Schmidtchen A, Malmsten M. 2009a. Tryptophan end-tagging of antimicrobial peptides for increased potency

- against *Pseudomonas aeruginosa*. *Biochimica et Biophysica Acta - General Subjects* 1790:800-808.
- Pasupuleti M, Schmidtchen A, Chalupka A, Ringstad L, Malmsten M. 2009b. End-tagging of ultra-short antimicrobial peptides by W/F stretches to facilitate bacterial killing. *PLoS ONE* 4:
- Pasupuleti M, Schmidtchen A, Malmsten M. 2012. Antimicrobial peptides: Key components of the innate immune system. *Critical Reviews in Biotechnology* 32:143-171.
- Pasupuleti M, Walse B, Svensson B, Malmsten M, Schmidtchen A. 2008. Rational design of antimicrobial C3a analogues with enhanced effects against *staphylococci* using an integrated structure and function-based approach. *Biochemistry* 47:9057-9070.
- Patrzykat A, Friedrich CL, Zhang L, Mendoza V, Hancock REW. 2002. Sublethal concentrations of pleurocidin-derived antimicrobial peptides inhibit macromolecular synthesis in *Escherichia coli*. *Antimicrobial Agents and Chemotherapy* 46:605-614.
- Paul M, Somkuti GA. 2010. Hydrolytic breakdown of lactoferricin by lactic acid bacteria. *Journal of Industrial Microbiology and Biotechnology* 37:173-178.
- Paulsen VS, Blencke HM, Benincasa M, Haug T, Eksteen JJ, Styrvold OB, Scocchi M, Stensvåg K. 2013. Structure-activity relationships of the antimicrobial peptide Arasin 1 - and mode of action studies of the N-terminal, proline-rich region. *PLoS ONE* 8:e53326.
- Pauly A, Pareyt B, Fierens E, Delcour JA. 2013. Wheat (*Triticum aestivum* L. and *T. turgidum* L. ssp. durum) kernel hardness: I. current view on the role of *Puroindolines* and polar Lipids. *Comprehensive Reviews in Food Science and Food Safety* 12:413-426.
- Pena-Miller R, Laehnemann D, Jansen G, Fuentes-Hernandez A, Rosenstiel P, Schulenburg H, Beardmore R. 2013. When the most potent combination of antibiotics selects for the greatest bacterial load: the smile-frown transition. *PLoS Biology* 11: e1001540.
- Pence MA, Rooijackers SHM, Cogen AL, Cole JN, Hollands A, Gallo RL, Nizet V. 2010. *Streptococcal* inhibitor of complement promotes innate immune resistance phenotypes of invasive M1T1 group A *Streptococcus*. *Journal of Innate Immunity* 2:587-595.
- Perczel A, Hollosi M 1996. Turns, Circular Dichroism and the Conformational Analysis of Biomolecules. In. Plenum Press New York. p. 285-380.
- Perczel A, Hollósi M, Foxman BM, Fasman GD. 1991. Conformational analysis of pseudocyclic hexapeptides based on quantitative circular dichroism (CD), NOE, and X-ray data. The pure CD spectra of type I and type II β -turns. *Journal of the American Chemical Society* 113:9772-9784.

- Pérez-Tomás R. 2006. Multidrug resistance: Retrospect and prospects in anti-cancer drug treatment. *Current Medicinal Chemistry* 13:1859-1876.
- Perrin BS, Tian Y, Fu R, Grant CV, Chekmenev EY, Wieczorek WE, Dao AE, Hayden RM, Burzynski CM, Venable RM, Sharma M, Opella SJ, Pastor RW, Cotten ML. 2014. High-resolution structures and orientations of antimicrobial peptides piscidin 1 and piscidin 3 in fluid bilayers reveal tilting, kinking, and bilayer immersion. *Journal of the American Chemical Society* 136:3491-3504.
- Perron GG, Zasloff M, Bell G. 2006. Experimental evolution of resistance to an antimicrobial peptide. *Proceedings of the Royal Society B: Biological Sciences* 273:251-256.
- Peschel A, Jack RW, Otto M, Collins LV, Staubitz P, Nicholson G, Kalbacher H, Nieuwenhuizen WF, Jung G, Tarkowski A, Van Kessel KPM, Van Strijp JAG. 2001. *Staphylococcus aureus* resistance to human defensins and evasion of neutrophil killing via the novel virulence factor MprF is based on modification of membrane lipids with L-lysine. *Journal of Experimental Medicine* 193:1067-1076.
- Peschel A, Otto M, Jack RW, Kalbacher H, Jung G, Götz F. 1999. Inactivation of the *dlt* operon in *Staphylococcus aureus* confers sensitivity to defensins, protegrins, and other antimicrobial peptides. *Journal of Biological Chemistry* 274:8405-8410.
- Peschel A, Sahl HG. 2006. The co-evolution of host cationic antimicrobial peptides and microbial resistance. *Nature Reviews Microbiology* 4:529-536.
- Peschel A, Vincent Collins L. 2001. *Staphylococcal* resistance to antimicrobial peptides of mammalian and bacterial origin. *Peptides* 22:1651-1659.
- Phillips RL, Palombo EA, Panozzo JF, Bhave M. 2011. Puroindolines, Pin alleles, hordoinolines and grain softness proteins are sources of bactericidal and fungicidal peptides. *Journal of Cereal Science* 53:112-117.
- Phoenix DA, Dennison SR, Harris F 2013. Cationic Antimicrobial Peptides. In. Antimicrobial Peptides. Wiley-VCH Verlag GmbH & Co: KGaA, Weinheim, Germany.
- Pieta P, Majewska M, Su Z, Grossutti M, Wladyka B, Piejko M, Lipkowski J, Mak P. 2016. Physicochemical studies on orientation and conformation of a new bacteriocin BacSp222 in a planar phospholipid bilayer. *Langmuir* 32:5653-5662.
- Pietiäinen M, François P, Hyyryläinen H, Tangomo M, Sass V, Sahl H, Schrenzel J, Kontinen VP. 2009. Transcriptome analysis of the responses of *Staphylococcus aureus* to antimicrobial peptides and characterization of the roles of *vraDE* and *vraSR* in antimicrobial resistance. *BMC Genomics* 10:429.

- Pokorny A, Almeida PFF. 2004. Kinetics of dye efflux and lipid flip-flop induced by δ -lysine in phosphatidylcholine vesicles and the mechanism of graded release by amphipathic, α -helical peptides. *Biochemistry* 43:8846-8857.
- Pokorny A, Almeida PFF. 2005. Permeabilization of raft-containing lipid vesicles by δ -lysine: a mechanism for cell sensitivity to cytotoxic peptides. *Biochemistry* 44:9538-9544.
- Pompilio A, Pomponio S, Di Vincenzo V, Crocetta V, Nicoletti M, Piovano M, Garbarino JA, Di Bonaventura G. 2013. Antimicrobial and antibiofilm activity of secondary metabolites of lichens against methicillin-resistant *Staphylococcus aureus* strains from cystic fibrosis patients. *Future Microbiology* 8:281-292.
- Pompilio A, Scocchi M, Pomponio S, Guida F, Di Primio A, Fiscarelli E, Gennaro R, Di Bonaventura G. 2011. Antibacterial and anti-biofilm effects of cathelicidin peptides against pathogens isolated from cystic fibrosis patients. *Peptides* 32:1807-1814.
- Pouny Y, Rapaport D, Mor A, Nicolas P, Shai Y. 1992. Interaction of antimicrobial dermaseptin and its fluorescently labeled analogues with phospholipid membranes. *Biochemistry* 31:12416-12423.
- Poyart C, Pellegrini E, Marceau M, Baptista M, Jaubert F, Lamy MC, Trieu-Cuot P. 2003. Attenuated virulence of *Streptococcus agalactiae* deficient in D-alanyl-lipoteichoic acid is due to an increased susceptibility to defensins and phagocytic cells. *Molecular Microbiology* 49:1615-1625.
- Praporski S, Mechler A, Separovic F, Martin LL. 2015. Subtle differences in initial membrane interactions underpin the selectivity of small antimicrobial peptides. *ChemPlusChem* 80:91-96.
- Prenner EJ, Kiricsi M, Jelokhani-Niaraki M, Lewis RNAH, Hodges RS, McElhaney RN. 2005. Structure-activity relationships of diastereomeric lysine ring size analogs of the antimicrobial peptide gramicidin S: mechanism of action and discrimination between bacterial and animal cell membranes. *Journal of Biological Chemistry* 280:2002-2011.
- Pushpanathan M, Gunasekaran P, Rajendhran J. 2013. Antimicrobial peptides: Versatile biological properties. *International Journal of Peptides* 2013:675391.
- Qin G, Chen Y, Li H, Xu S, Li Y, Sun J, Rao W, Chen C, Du M, He K, Ye Y. 2016. Melittin inhibits tumor angiogenesis modulated by endothelial progenitor cells associated with the SDF-1 α /CXCR4 signaling pathway in a UMR-106 osteosarcoma xenograft mouse model. *Molecular Medicine Reports* 14:57-68.
- Quintieri L, Pistillo BR, Caputo L, Favia P, Baruzzi F. 2013. Bovine lactoferrin and lactoferricin on plasma-deposited coating against spoilage *Pseudomonas* spp. *Innovative Food Science and Emerging Technologies* 20:215-222.

References

- Raguse TL, Porter EA, Weisblum B, Gellman SH. 2002. Structure - Activity studies of 14-helical antimicrobial β -peptides: probing the relationship between conformational stability and antimicrobial potency. *Journal of the American Chemical Society* 124:12774-12785.
- Ramalingam A 2012, *Genetic variability and protein-protein interactions of puroindolines in relation to wheat grain texture and antimicrobial properties*, PhD thesis, Faculty of Life and Social Science, Swinburne University of Technology, Melbourne, Australia.
- Ramalingam A, Palombo EA, Bhave M. 2012. The *Pinb-2* genes in wheat comprise a multigene family with great sequence diversity and important variants. *Journal of Cereal Science* 56:171-180.
- Rapsch K, Bier FF, Von Nickisch-Rosenegk M. 2014. Rational design of artificial β -strand-forming antimicrobial peptides with biocompatible properties. *Molecular Pharmaceutics* 11:3492-3502.
- Rapson AC, Hossain MA, Wade JD, Nice EC, Smith TA, Clayton AHA, Gee ML. 2011. Structural dynamics of a lytic peptide interacting with a supported lipid bilayer. *Biophysical Journal* 100:1353-1361.
- Ratledge C, Wilkinson SG. 1988. Microbial lipids. London : Academic Press, London.
- Redford GI, Clegg RM. 2005. Polar plot representation for frequency-domain analysis of fluorescence lifetimes. *Journal of Fluorescence* 15:805-815.
- Rekdal Ø, Andersen J, Vorland LH, Svendsen JS. 1999. Construction and synthesis of lactoferricin derivatives with enhanced antibacterial activity. *Journal of Peptide Science* 5:32-45.
- Richardson A, de Antueno R, Duncan R, Hoskin DW. 2009. Intracellular delivery of bovine lactoferricin's antimicrobial core (RRWQWR) kills T-leukemia cells. *Biochemical and Biophysical Research Communications* 388:736-741.
- Riedl S, Leber R, Rinner B, Schaidler H, Lohner K, Zwegytick D. 2015. Human lactoferricin derived di-peptides deploying loop structures induce apoptosis specifically in cancer cells through targeting membranous phosphatidylserine. *Biochimica et Biophysica Acta - Biomembranes* 1848:2918-2931.
- Riedl S, Zwegytick D, Lohner K. 2011. Membrane-active host defense peptides - Challenges and perspectives for the development of novel anticancer drugs. *Chemistry and Physics of Lipids* 164:766-781.
- Risso A, Braidot E, Sordano MC, Vianello A, Macrì F, Skerlavaj B, Zanetti M, Gennaro R, Bernardi P. 2002. BMAP-28, an antibiotic peptide of innate immunity, induces cell death through opening of the mitochondrial permeability transition pore. *Molecular and Cellular Biology* 22:1926-1935.
- Risso A, Zanetti M, Gennaro R. 1998. Cytotoxicity and apoptosis mediated by two peptides of innate immunity. *Cellular Immunology* 189:107-115.

References

- Robinson WE, McDougall B, Tran D, Selsted ME. 1998. Anti-HIV-1 activity of indolicidin, an antimicrobial peptide from neutrophils. *Journal of Leukocyte Biology* 63:94-100.
- Rodríguez Saint-Jean S, Pérez Prieto SI, López-Expósito I, Ramos M, de las Heras AI, Recio I. 2012. Antiviral activity of dairy proteins and hydrolysates on salmonid fish viruses. *International Dairy Journal* 23:24-29.
- Rokitskaya TI, Kolodkin NI, Kotova EA, Antonenko YN. 2011. Indolicidin action on membrane permeability: carrier mechanism versus pore formation. *Biochimica et Biophysica Acta - Biomembranes* 1808:91-97.
- Römling U, Balsalobre C. 2012. Biofilm infections, their resilience to therapy and innovative treatment strategies. *Journal of Internal Medicine* 272:541-561.
- Rosenfeld Y, Barra D, Simmaco M, Shai Y, Mangoni ML. 2006. A synergism between temporins toward Gram-negative bacteria overcomes resistance imposed by the lipopolysaccharide protective layer. *Journal of Biological Chemistry* 281:28565-28574.
- Rosengren KJ, Clark RJ, Daly NL, Göransson U, Jones A, Craik DJ. 2003. Microcin J25 has a threaded sidechain-to-backbone ring structure and not a head-to-tail cyclized backbone. *Journal of the American Chemical Society* 125:12464-12474.
- Rosicka-Kaczmarek J, Stasiuk M, Nebesny E, Komisarczyk A. 2015. Fluorimetric studies of the interactions of wheat puroindolines with polar lipids on the surface starch granules. *Journal of Cereal Science* 66:53-58.
- Roy A, Kucukural A, Zhang Y. 2010. I-TASSER: a unified platform for automated protein structure and function prediction. *Nature Protocols* 5:725-738.
- Rożek A, Friedrich CL, Hancock REW. 2000a. Structure of the bovine antimicrobial peptide indolicidin bound to dodecylphosphocholine and sodium dodecyl sulfate micelles. *Biochemistry* 39:15765-15774.
- Rożek A, Powers JPS, Friedrich CL, Hancock REW. 2003. Structure-based design of an indolicidin peptide analogue with increased protease stability. *Biochemistry* 42:14130-14138.
- Rożek T, Bowie JH, Wallace JC, Tyler MJ. 2000b. The antibiotic and anticancer active aurein peptides from the Australian Bell Frogs *Litoria aurea* and *Litoria raniformis*. Part 2. Sequence determination using electrospray mass spectrometry. *Rapid Communications in Mass Spectrometry* 14:2002-2011.
- Rubinchik E, Dugourd D, Algara T, Pasetka C, Friedland HD. 2009. Antimicrobial and antifungal activities of a novel cationic antimicrobial peptide, omiganan, in experimental skin colonisation models. *International Journal of Antimicrobial Agents* 34:457-461.
- Russell AD. 1990. Bacterial spores and chemical sporicidal agents. *Clinical Microbiology Reviews* 3:99-119.

- Rydlo T, Miltz J, Mor A. 2006. Eukaryotic antimicrobial peptides: promises and premises in food safety. *Journal of Food Science* 71:R125-R135.
- Sader HS, Fedler KA, Rennie RP, Stevens S, Jones RN. 2004. Omiganan pentahydrochloride (MBI 226), a topical 12-amino-acid cationic peptide: spectrum of antimicrobial activity and measurements of bactericidal activity. *Antimicrobial Agents and Chemotherapy* 48:3112-3118.
- Salay LC, Ferreira M, Oliveira ON, Nakaie CR, Schreier S. 2012. Headgroup specificity for the interaction of the antimicrobial peptide tritrpticin with phospholipid Langmuir monolayers. *Colloids and Surfaces B: Biointerfaces* 100:95-102.
- Salay LC, Procopio J, Oliveira E, Nakaie CR, Schreier S. 2004. Ion channel-like activity of the antimicrobial peptide tritrpticin in planar lipid bilayers. *FEBS Letters* 565:171-175.
- Sanders MR, Clifton LA, Frazier RA, Green RJ. 2016. Role of lipid composition on the interaction between a Tryptophan-rich [rotein and model bacterial membranes. *Langmuir* 32:2050-2057.
- Sanders MR, Clifton LA, Frazier RA, Green RJ. 2017. Tryptophan to arginine substitution in *puroindoline-b* alters binding to model eukaryotic membrane. *Langmuir* 33:4847-4853.
- Sanders MR, Clifton LA, Neylon C, Frazier RA, Green RJ. 2013. Selected wheat seed defense proteins exhibit competitive binding to model microbial lipid interfaces. *Journal of Agricultural and Food Chemistry* 61:6890-6900.
- Sani MA, Whitwell TC, Gehman JD, Robins-Browne RM, Pantarat N, Attard TJ, Reynolds EC, O'Brien-Simpson NM, Separovic F. 2013. Maculatin 1.1 disrupts *staphylococcus aureus* lipid membranes via a pore mechanism. *Antimicrobial Agents and Chemotherapy* 57:3593-3600.
- Santos-Filho NA, Lorenzon EN, Ramos MAS, Santos CT, Piccoli JP, Bauab TM, Fusco-Almeida AM, Cilli EM. 2015. Synthesis and characterization of an antibacterial and non-toxic dimeric peptide derived from the C-terminal region of Bothropstoxin-I. *Toxicon* 103:160-168.
- Saravanan R, Li X, Lim K, Mohanram H, Peng L, Mishra B, Basu A, Lee JM, Bhattacharjya S, Leong SSJ. 2014. Design of short membrane selective antimicrobial peptides containing tryptophan and arginine residues for improved activity, salt-resistance, and biocompatibility. *Biotechnology and Bioengineering* 111:37-49.
- Schibli DJ, Epand RF, Vogel HJ, Epand RM. 2002. Tryptophan-rich antimicrobial peptides: comparative properties and membrane interactions. *Biochemistry and Cell Biology* 80:667-677.
- Schibli DJ, Hwang PM, Vogel HJ. 1999. Structure of the antimicrobial peptide tritrpticin bound to micelles: a distinct membrane-bound peptide fold. *Biochemistry* 38:16749-16755.

- Schibli DJ, Nguyen LT, Kernaghan SD, Rekdal Ø, Vogel HJ. 2006. Structure-function analysis of tritrypticin analogs: potential relationships between antimicrobial activities, model membrane interactions, and their micelle-bound NMR structures. *Biophysical Journal* 91:4413-4426.
- Schiffer M, Edmundson AB. 1967. Use of helical wheels to represent the structures of proteins and to identify segments with helical potential. *Biophysical Journal* 7:121-135.
- Schillaci D, Arizza V, Dayton T, Camarda L, Di Stefano V. 2008. *In vitro* anti-biofilm activity of *Boswellia* spp. oleogum resin essential oils. *Letters in Applied Microbiology* 47:433-438.
- Schmidt N, Mishra A, Lai GH, Wong GCL. 2010. Arginine-rich cell-penetrating peptides. *FEBS Letters* 584:1806-1813.
- Schmidtchen A, Frick IM, Andersson E, Tapper H, Björck L. 2002. Proteinases of common pathogenic bacteria degrade and inactivate the antibacterial peptide LL-37. *Molecular Microbiology* 46:157-168.
- Schmidtchen A, Pasupuleti M, Mörgelin M, Davoudi M, Alenfall J, Chalupka A, Malmsten M. 2009. Boosting antimicrobial peptides by hydrophobic oligopeptide end tags. *Journal of Biological Chemistry* 284:17584-17594.
- Schneider T, Kruse T, Wimmer R, Wiedemann I, Sass V, Pag U, Jansen A, Nielsen AK, Mygind PH, Raventós DS, Neve S, Ravn B, Bonvin AMJJ, De Maria L, Andersen AS, Gammelgaard LK, Sahl HG, Kristensen HH. 2010. Plectasin, a fungal defensin, targets the bacterial cell wall precursor lipid II. *Science* 328:1168-1172.
- Schneider VAF, Coorens M, Ordonez SR, Tjeerdsma-Van Bokhoven JLM, Posthuma G, Van Dijk A, Haagsman HP, Veldhuizen EJA. 2016. Imaging the antimicrobial mechanism(s) of cathelicidin-2. *Scientific Reports* 6:32948.
- Schrag SJ, Perrot V. 1996. Reducing antibiotic resistance [3]. *Nature* 381:120-121.
- Schweizer F. 2009. Cationic amphiphilic peptides with cancer-selective toxicity. *European Journal of Pharmacology* 625:190-194.
- Scocchi M, Lüthy C, Decarli P, Mignogna G, Christen P, Gennaro R. 2009. The Proline-rich antibacterial peptide Bac7 binds to and inhibits *in vitro* the molecular chaperone DnaK. *International Journal of Peptide Research and Therapeutics* 15:147-155.
- Scudiero DA, Shoemaker RH, Paull KD, Monks A, Tierney S, Nofziger TH, Currens MJ, Seniff D, Boyd MR. 1988. Evaluation of a soluble tetrazolium/formazan assay for cell growth and drug sensitivity in culture using human and other tumor cell lines. *Cancer Research* 48:4827-4833.
- Seelig J. 2004. Thermodynamics of lipid-peptide interactions. *Biochimica et Biophysica Acta - Biomembranes* 1666:40-50.

References

- Selsted ME. 2004. θ -Defensins: Cyclic antimicrobial peptides produced by binary ligation of truncated α -defensins. *Current Protein and Peptide Science* 5:365-371.
- Selsted ME, Brown DM, DeLange RJ, Harwig SS, Lehrer RI. 1985. Primary structures of six antimicrobial peptides of rabbit peritoneal neutrophils. *Journal of Biological Chemistry* 260:4579-4584.
- Selsted ME, Novotny MJ, Morris WJ, Tang Y-Q, Smith W, Cullor JS. 1992. Indolicidin, a novel bactericidal tridecapeptide amide from neutrophils. *The Journal of Biological Chemistry* 267:4292-4295.
- Sengupta D, Leontiadou H, Mark AE, Marrink SJ. 2008. Toroidal pores formed by antimicrobial peptides show significant disorder. *Biochimica et Biophysica Acta - Biomembranes* 1778:2308-2317.
- Sengupta J, Saha S, Khetan A, Sarkar SK, Mandal SM. 2012. Effects of lactoferricin B against keratitis-associated fungal biofilms. *Journal of Infection and Chemotherapy* 18:698-703.
- Setlow B, Loshon CA, Genest PC, Cowan AE, Setlow C, Setlow P. 2002. Mechanisms of killing spores of *Bacillus subtilis* by acid, alkali and ethanol. *Journal of Applied Microbiology* 92:362-375.
- Setlow P. 2006. Spores of *Bacillus subtilis*: Their resistance to and killing by radiation, heat and chemicals. *Journal of Applied Microbiology* 101:514-525.
- Shafer WM, Qu XD, Waring AJ, Lehrer RI. 1998. Modulation of *Neisseria gonorrhoeae* susceptibility to vertebrate antibacterial peptides due to a member of the resistance/nodulation/division efflux pump family. *Proceedings of the National Academy of Sciences of the United States of America* 95:1829-1833.
- Shagaghi N, Alfred RL, Clayton AHA, Palombo EA, Bhave M. 2016a. Anti-biofilm and sporicidal activity of peptides based on wheat puroindoline and barley hordoindoline proteins. *Journal of Peptide Science* 22:492-500.
- Shagaghi N, Bhave M, Palombo EA, Clayton AHA. 2017. Revealing the sequence of interactions of PuroA peptide with *Candida albicans* cells by live-cell imaging. *Scientific Reports* 7:43542.
- Shagaghi N, Palombo EA, Clayton AHA, Bhave M. 2016b. Archetypal tryptophan-rich antimicrobial peptides: properties and applications. *World Journal of Microbiology and Biotechnology* 32:1-10.
- Shai Y, Oren Z. 1996. Diastereomers of cytolysins, a novel class of potent antibacterial peptides. *Journal of Biological Chemistry* 271:7305-7308.
- Shang D, Zhang Q, Dong W, Liang H, Bi X. 2016. The effects of LPS on the activity of Trp-containing antimicrobial peptides against Gram-negative bacteria and endotoxin neutralization. *Acta Biomaterialia* 33:153-165.

- Sharma R, Lomash S, Salunke DM. 2013. Putative bioactive motif of tritrypticin revealed by an antibody with biological receptor-like properties. *PLoS ONE* 8:e75582.
- Sherman PJ, Jackway RJ, Gehman JD, Praporski S, McCubbin GA, Mechler A, Martin LL, Separovic F, Bowie JH. 2009. Solution structure and membrane interactions of the antimicrobial peptide fallaxidin 4.1a: An NMR and QCM study. *Biochemistry* 48:11892-11901.
- Shi J, Ross CR, Chengappa MM, Sylte MJ, McVey DS, Blecha F. 1996. Antibacterial activity of a synthetic peptide (PR-26) derived from PR-39, a proline-arginine-rich neutrophil antimicrobial peptide. *Antimicrobial Agents and Chemotherapy* 40:115-121.
- Shi SL, Wang YY, Liang Y, Li QF. 2006. Effects of tachyplesin and n-sodium butyrate on proliferation and gene expression of human gastric adenocarcinoma cell line BGC-823. *World Journal of Gastroenterology* 12:1694-1698.
- Shi X, Zhu X. 2009. Biofilm formation and food safety in food industries. *Trends in Food Science and Technology* 20:407-413.
- Shimamura M, Yamamoto Y, Ashino H, Oikawa T, Hazato T, Tsuda H, Iigo M. 2004. Bovine lactoferrin inhibits tumor-induced angiogenesis. *International Journal of Cancer* 111:111-116.
- Shin SY. 2013. Prokaryotic selectivity, bactericidal mechanism and lps-neutralizing activity of lys-linked dimeric peptide of indolicidin C-terminal hexapeptide. *Bulletin of the Korean Chemical Society* 34:2187-2190.
- Shin SY, Yang ST, Park EJ, Eom SH, Song WK, Kim JI, Kim Y, Hahm KS. 2002. Salt resistance and synergistic effect with vancomycin of α -helical antimicrobial peptide P18. *Biochemical and Biophysical Research Communications* 290:558-562.
- Sieprawska-Lupa M, Mydel P, Krawczyk K, Wójcik K, Puklo M, Lupa B, Suder P, Silberring J, Reed M, Pohl J, Shafer W, McAleese F, Foster T, Travis J, Potempa J. 2004. Degradation of human antimicrobial peptide LL-37 by *Staphylococcus aureus*-derived proteinases. *Antimicrobial Agents and Chemotherapy* 48:4673-4679.
- Simões M, Simões LC, Vieira MJ. 2010. A review of current and emergent biofilm control strategies. *LWT - Food Science and Technology* 43:573-583.
- Singh PK, Parsek MR, Greenberg EP, Welsh MJ. 2002. A component of innate immunity prevents bacterial biofilm development. *Nature* 417:552-555.
- Slaninová J, Mlsová V, Kroupová H, Alán L, Tůmová T, Monincová L, Borovičková L, Fučík V, Čerovský V. 2012. Toxicity study of antimicrobial peptides from wild bee venom and their analogs toward mammalian normal and cancer cells. *Peptides* 33:18-26.

- Sochacki KA, Barns KJ, Bucki R, Weisshaar JC. 2011. Real-time attack on single *Escherichia coli* cells by the human antimicrobial peptide LL-37. *Proceedings of the National Academy of Sciences of the United States of America* 108:E77-E81.
- Solanas C, De La Torre BG, Fernández-Reyes M, Santiveri CM, Jiménez MÁ, Rivas L, Jiménez AI, Andreu D, Cativiela C. 2009. Therapeutic index of gramicidin S is strongly modulated by D-phenylalanine analogues at the β -turn. *Journal of Medicinal Chemistry* 52:664-674.
- Sood R, Domanov Y, Pietiäinen M, Kontinen VP, Kinnunen PKJ. 2008. Binding of LL-37 to model biomembranes: insight into target vs host cell recognition. *Biochimica et Biophysica Acta - Biomembranes* 1778:983-996.
- Spelbrink RG, Dilmac N, Allen A, Smith TJ, Shah DM, Hockerman GH. 2004. Differential antifungal and calcium channel-blocking activity among structurally related plant defensins. *Plant Physiology* 135:2055-2067.
- Staniszewska M, Bondaryk M, Zielińska P, Urbańczyk-Lipkowska Z. 2014. The *in vitro* effects of new D186 dendrimer on virulence factors of *Candida albicans*. *Journal of Antibiotics* 67:425-432.
- Starner TD, Swords WE, Apicella MA, McCray Jr PB. 2002. Susceptibility of nontypeable *Haemophilus influenzae* to human β -defensins is influenced by lipooligosaccharide acylation. *Infection and Immunity* 70:5287-5289.
- Staubitz P, Peschel A, Nieuwenhuizen WF, Otto M, Götz F, Jung G, Jack RW. 2001. Structure-function relationships in the tryptophan-rich, antimicrobial peptide indolicidin. *Journal of Peptide Science* 7:552-564.
- Stella L, Mazzuca C, Venanzi M, Palleschi A, Didonè M, Formaggio F, Toniolo C, Pispisa B. 2004. Aggregation and water-membrane partition as major determinants of the activity of the antibiotic peptide trichogin GA IV. *Biophysical Journal* 86:936-945.
- Stepanović S, Vuković D, Hola V, Di Bonaventura G, Djukić S, Ćirković I, Ruzicka F. 2007. Quantification of biofilm in microtiter plates: overview of testing conditions and practical recommendations for assessment of biofilm production by staphylococci. *APMIS* 115:891-899.
- Stewart PS, Costerton JW. 2001. Antibiotic resistance of bacteria in biofilms. *Lancet* 358:135-138.
- Stoodley P, Sauer K, Davies DG, Costerton JW. 2002. Biofilms as complex differentiated communities. *Annual Review of Microbiology* 56:187-209.
- Stragier P, Losick R 1996, in *Annual Review of Genetics*, Vol. 30, pp. 297-341.
- Strandberg E, Morein S, Rijkers DTS, Liskamp RMJ, Van der Wel PCA, Antoinette Killian J. 2002. Lipid dependence of membrane anchoring properties and snorkeling behavior of aromatic and charged residues in transmembrane peptides. *Biochemistry* 41:7190-7198.

- Strandberg E, Zerweck J, Horn D, Pritz G, Berditsch M, Bürck J, Wadhvani P, Ulrich AS. 2015. Influence of hydrophobic residues on the activity of the antimicrobial peptide magainin 2 and its synergy with PGLa. *Journal of Peptide Science* 21:436-445.
- Strøm MB, Haug BE, Skar ML, Stensen W, Stiberg T, Svendsen JS. 2003. The pharmacophore of short cationic antibacterial peptides. *Journal of Medicinal Chemistry* 46:1567-1570.
- Strøm MB, Rekdal Ø, Svendsen JS. 2000. Antibacterial activity of 15-residue laccoferricin derivatives. *Journal of Peptide Research* 56:265-274.
- Strøm MB, Rekdal Ø, Svendsen JS. 2002a. Antimicrobial activity of short arginine- and tryptophan-rich peptides. *Journal of Peptide Science* 8:431-437.
- Strøm MB, Rekdal Ø, Svendsen JS. 2002b. The effects of charge and lipophilicity on the antibacterial activity of undecapeptides derived from bovine lactoferricin. *Journal of Peptide Science* 7:36-43.
- Strub JM, Goumon Y, Lugardon K, Capon C, Lopez M, Moniatte M, Van Dorsselaer A, Aunis D, Metz-Boutigue MH. 1996. Antibacterial activity of glycosylated and phosphorylated chromogranin A-derived peptide 173-194 from bovine adrenal medullary chromaffin granules. *Journal of Biological Chemistry* 271:28533-28540.
- Su LY, Willner DL, Segall AM. 2010. An antimicrobial peptide that targets DNA repair intermediates *in vitro* inhibits *Salmonella* growth within murine macrophages. *Antimicrobial Agents and Chemotherapy* 54:1888-1899.
- Subbalakshmi C, Nagaraj R, Sitaram N. 1999. Biological activities of C-terminal 15-residue synthetic fragment of melittin: design of an analog with improved antibacterial activity. *FEBS Letters* 448:62-66.
- Subbalakshmi C, Sitaram N. 1998. Mechanism of antimicrobial action of indolocidin. *FEMS Microbiology Letters* 160:91-96.
- Sun D, Forsman J, Lund M, Woodward CE. 2014. Effect of arginine-rich cell penetrating peptides on membrane pore formation and life-times: A molecular simulation study. *Physical Chemistry Chemical Physics* 16:20785-20795.
- Taggart CC, Greene CM, Smith SG, Levine RL, McCray Jr PB, O'Neill S, McElvaney NG. 2003. Inactivation of human β -defensins 2 and 3 by elastolytic cathepsins. *Journal of Immunology* 171:931-937.
- Takahashi A, Ikeda TM, Takayama T, Yanagisawa T. 2010. A barley Hordoindoline mutation resulted in an increase in grain hardness. *Theoretical and Applied Genetics* 120:519-526.
- Tamayo R, Choudhury B, Septer A, Merighi M, Carlson R, Gunn JS. 2005. Identification of *cptA*, a PmrA-regulated locus required for phosphoethanolamine modification of the *Salmonella enterica* serovar

- typhimurium lipopolysaccharide core. *Journal of Bacteriology* 187:3391-3399.
- Tamma PD, Cosgrove SE, Maragakis LL. 2012. Combination therapy for treatment of infections with gram-negative bacteria. *Clinical Microbiology Reviews* 25:450-470.
- Tanaka H, Morris CF, Haruna M, Tsujimoto H. 2008. Prevalence of puroindoline alleles in wheat varieties from eastern Asia including the discovery of a new SNP in puroindoline b. *Plant Genetic Resources* 6:142-152.
- Taniguchi M, Ochiai A, Fukuda S, Sato T, Saitoh E, Kato T, Tanaka T. 2016a. AmyI-1-18, a cationic α -helical antimicrobial octadecapeptide derived from α -amylase in rice, inhibits the translation and folding processes in a protein synthesis system. *Journal of Bioscience and Bioengineering* 122:385-392.
- Taniguchi M, Ochiai A, Takahashi K, Nakamichi SI, Nomoto T, Saitoh E, Kato T, Tanaka T. 2016b. Effect of alanine, leucine, and arginine substitution on antimicrobial activity against *candida albicans* and action mechanism of a cationic octadecapeptide derived from α -amylase of rice. *Biopolymers* 106:219-229.
- Teixeira V, Feio MJ, Bastos M. 2012. Role of lipids in the interaction of antimicrobial peptides with membranes. *Progress in Lipid Research* 51:149-177.
- Thun MJ, DeLancey JO, Center MM, Jemal A, Ward EM. 2010. The global burden of cancer: priorities for prevention. *Carcinogenesis* 31:100-110.
- Tomasinsig L, Scocchi M, Mettullo R, Zanetti M. 2004. Genome-wide transcriptional profiling of the Escherichia coli response to a proline-rich antimicrobial peptide. *Antimicrobial Agents and Chemotherapy* 48:3260-3267.
- Tomita M, Takase M, Bellamy W, Shimakura S. 1994. A review: the active peptide of lactoferrin. *Acta Paediatrica Japonica (Overseas Edition)* 36:585-591.
- Torcato IM, Huang YH, Franquelim HG, Gaspar D, Craik DJ, Castanho MARB, Troeira Henriques S. 2013. Design and characterization of novel antimicrobial peptides, R-BP100 and RW-BP100, with activity against Gram-negative and Gram-positive bacteria. *Biochimica et Biophysica Acta - Biomembranes* 1828:944-955.
- Tossi A, Sandri L, Giangaspero A. 2000. Amphipathic, α -helical antimicrobial peptides. *Biopolymers - Peptide Science Section* 55:4-30.
- Tossi A, Scocchi M, Skerlavaj B, Gennaro R. 1994. Identification and characterization of a primary antibacterial domain in CAP18, a lipopolysaccharide binding protein from rabbit leukocytes. *FEBS Letters* 339:108-112.
- Trinquier G, Sanejouand YH. 1998. Which effective property of amino acids is best preserved by the genetic code? *Protein Engineering* 11:153-169.

References

- Tu YH, Ho YH, Chuang YC, Chen PC, Chen CS. 2011. Identification of lactoferricin B intracellular targets using an *escherichia coli* proteome chip. *PLoS ONE* 6:e28197.
- Turuspekov Y, Beecher B, Darlington Y, Bowman J, Blake TK, Giroux MJ. 2008. *Hardness* locus sequence variation and endosperm texture in spring barley. *Crop Science* 48:1007-1019.
- Tzeng YL, Ambrose KD, Zughaier S, Zhou X, Miller YK, Shafer WM, Stephens DS. 2005. Cationic antimicrobial peptide resistance in *Neisseria meningitidis*. *Journal of Bacteriology* 187:5387-5396.
- Ulvatne H, Haukland HH, Olsvik O, Vorland LH. 2001. Lactoferricin B causes depolarization of the cytoplasmic membrane of *Escherichia coli* ATCC 25922 and fusion of negatively charged liposomes. *FEBS Letters* 492:62-65.
- Ulvatne H, Haukland HH, Samuelsen Ø, Krämer M, Vorland LH. 2002. Proteases in *Escherichia coli* and *Staphylococcus aureus* confer reduced susceptibility to lactoferricin B. *Journal of Antimicrobial Chemotherapy* 50:461-467.
- Ulvatne H, Samuelsen Ø, Haukland HH, Krämer M, Vorland LH. 2004. Lactoferricin B inhibits bacterial macromolecular synthesis in *Escherichia coli* and *Bacillus subtilis*. *FEMS Microbiology Letters* 237:377-384.
- Unger T, Oren Z, Shai Y. 2001. The effect of cyclization of magainin 2 and melittin analogues on structure, function, and model membrane interactions: Implication to their mode of action. *Biochemistry* 40:6388-6397.
- Utsugi T, Schroit AJ, Connor J, Bucana CD, Fidler IJ. 1991. Elevated expression of phosphatidylserine in the outer membrane leaflet of human tumor cells and recognition by activated human blood monocytes. *Cancer Research* 51:3062-3066.
- Van Acker H, Van Dijck P, Coenye T. 2014. Molecular mechanisms of antimicrobial tolerance and resistance in bacterial and fungal biofilms. *Trends in Microbiology* 22:326-333.
- Van Zoggel H, Carpentier G, Dos Santos C, Hamma-Kourbali Y, Courty J, Amiche M, Delbé J. 2012. Antitumor and angiostatic activities of the antimicrobial peptide dermaseptin B2. *PLoS ONE* 7: e44351.
- Vanhoye D, Bruston F, Nicolas P, Amiche M. 2003. Antimicrobial peptides from hylid and ranin frogs originated from a 150-million-year-old ancestral precursor with a conserved signal peptide but a hypermutable antimicrobial domain. *European Journal of Biochemistry* 270:2068-2081.
- Vaz-Velho M, Fonseca F, Silva M, Gibbs P. 2001. Is *Listeria innocua* 2030c, a tetracycline-resistant strain, a suitable marker for replacing *L. monocytogenes* in challenge studies with cold-smoked fish? *Food Control* 12:361-364.

- Végh AG, Nagy K, Bálint Z, Kerényi A, Rákhely G, Váró G, Szegletes Z. 2011. Effect of antimicrobial peptide-amide: indolicidin on biological membranes. *Journal of biomedicine & biotechnology* 2011:670589.
- Verkleij AJ, Zwaal RFA, Roelofsen B, Comfurius P, Kastelijn D, van Deenen LLM. 1973. The asymmetric distribution of phospholipids in the human red cell membrane. A combined study using phospholipases and freeze-etch electron microscopy. *BBA - Biomembranes* 323:178-193.
- Vogel HJ, Schibli DJ, Jing W, Lohmeier-Vogel EM, Epand RF, Epand RM. 2002. Towards a structure-function analysis of bovine lactoferricin and related tryptophan- and arginine-containing peptides. *Biochemistry and Cell Biology* 80:49-63.
- Wakabayashi H, Hiratani T, Uchida K, Yamaguchi H. 1996. Antifungal spectrum and fungicidal mechanism of an N-terminal peptide of bovine lactoferrin. *Journal of Infection and Chemotherapy* 1:185-189.
- Wallace BA, Lees JG, Orry AJW, Lobley A, Janes RW. 2003. Analyses of circular dichroism spectra of membrane proteins. *Protein Science* 12:875-884.
- Wang G, Li X, Zasloff M 2010a. A database view of naturally occurring antimicrobial peptides: Nomenclature, classification and amino acid sequence analysis. In. *Antimicrobial Peptides: Discovery, Design and Novel Therapeutic Strategies*. p. 1-21.
- Wang KF, Nagarajan R, Camesano TA. 2015a. Differentiating antimicrobial peptides interacting with lipid bilayer: molecular signatures derived from quartz crystal microbalance with dissipation monitoring. *Biophysical Chemistry* 196:53-57.
- Wang P, Nan YH, Yang ST, Kang SW, Kim Y, Park IS, Hahm KS, Shin SY. 2010b. Cell selectivity and anti-inflammatory activity of a Leu/Lys-rich α -helical model antimicrobial peptide and its diastereomeric peptides. *Peptides* 31:1251-1261.
- Wang S, Tu J, Zhou C, Li J, Huang L, Tao L, Zhao L. 2015b. The effect of Lfcin-B on non-small cell lung cancer H460 cells is mediated by inhibiting VEGF expression and inducing apoptosis. *Archives of pharmacal research* 38:261-271.
- Wang YS, Li D, Shi HS, Wen YJ, Yang L, Xu N, Chen XC, Chen X, Chen P, Li J, Deng HX, Wang CT, Xie G, Huang S, Mao YQ, Chen LJ, Zhao X, Wei YQ. 2009. Intratumoral expression of mature human neutrophil peptide-1 mediates antitumor immunity in mice. *Clinical Cancer Research* 15:6901-6911.
- Watkins RR, David MZ, Salata RA. 2012. Current concepts on the virulence mechanisms of methicillin-resistant *Staphylococcus aureus*. *Journal of Medical Microbiology* 61:1179-1193.

- Weatherspoon-Griffin N, Yang D, Kong W, Hua Z, Shi Y. 2014. The CpxR/CpxA Two-component regulatory system up-regulates the multidrug resistance cascade to facilitate *Escherichia coli* resistance to a model antimicrobial peptide. *Journal of Biological Chemistry* 289:32571-32582.
- Wei S-Y, Wu J-M, Kuo Y-Y, Chen H-L, Yip B-S, Tzeng S-R, Cheng J-W. 2006. Solution structure of a novel tryptophan-rich peptide with bidirectional antimicrobial activity. *Journal of Bacteriology* 188:328-334.
- Weinberg ED. 2003. The therapeutic potential of lactoferrin. *Expert Opinion on Investigational Drugs* 12:841-851.
- Weinberg ED. 2007. Antibiotic properties and applications of lactoferrin. *Current Pharmaceutical Design* 13:801-811.
- Welling MM, Brouwer CPJM, Van 'T Hof W, Veerman ECI, Nieuw Amerongen AV. 2007. Histatin-derived monomeric and dimeric synthetic peptides show strong bactericidal activity towards multidrug-resistant *Staphylococcus aureus* in vivo. *Antimicrobial Agents and Chemotherapy* 51:3416-3419.
- Westerhoff HV, Juretic D, Hendler RW, Zasloff M. 1989. Magainins and the disruption of membrane-linked free-energy transduction. *Proceedings of the National Academy of Sciences of the United States of America* 86:6597-6601.
- Westerhoff HV, Zasloff M, Rosner JL, Hendler RW, De Waal A, Gomes AV, Jongsma APM, Riethorst A, Juretić D. 1995. Functional synergism of the magainins PGLa and magainin-2 in *Escherichia coli*, tumor cells and liposomes. *European Journal of Biochemistry* 228:257-264.
- Wiedemann I, Breukink E, Van Kraaij C, Kuipers OP, Bierbaum G, De Kruijff B, Sahl HG. 2001. Specific binding of nisin to the peptidoglycan precursor lipid II combines pore formation and inhibition of cell wall biosynthesis for potent antibiotic activity. *Journal of Biological Chemistry* 276:1772-1779.
- Wiegand I, Hilpert K, Hancock REW. 2008. Agar and broth dilution methods to determine the minimal inhibitory concentration (MIC) of antimicrobial substances. *Nature Protocols* 3:163-175.
- Wieprecht T, Apostolov O, Beyermann M, Seelig J. 1999. Thermodynamics of the α -helix-coil transition of amphipathic peptides in a membrane environment: Implications for the peptide-membrane binding equilibrium. *Journal of Molecular Biology* 294:785-794.
- Wilcox MH, Fawley WN. 2000. Hospital disinfectants and spore formation by *Clostridium difficile*. *Lancet* 356:1324.
- Wilkinson M, Wan Y, Tosi P, Leverington M, Snape J, Mitchell RAC, Shewry PR. 2008. Identification and genetic mapping of variant forms of puroindoline b expressed in developing wheat grain. *Journal of Cereal Science* 48:722-728.
- Wimley WC, Hristova K. 2011. Antimicrobial peptides: successes, challenges and unanswered questions. *The Journal of membrane biology* 239:27-34.

- Wimley WC, White SH. 1996. Experimentally determined hydrophobicity scale for proteins at membrane interfaces. *Nature Structural Biology* 3:842-848.
- Woody RW. 1994. Contributions of tryptophan side chains to the far-ultraviolet circular dichroism of proteins. *European Biophysics Journal* 23:253-262.
- Woong SJ, Lee SC, Young SL, Yong PS, Kyoung HS, Boo HS, Kim BS, Soo HL, In HL. 2007. Antimicrobial effect of halocidin-derived peptide in a mouse model of *Listeria* infection. *Antimicrobial Agents and Chemotherapy* 51:4148-4156.
- Worthington RJ, Melander C. 2013. Combination approaches to combat multidrug-resistant bacteria. *Trends in Biotechnology* 31:177-184.
- Wu JM, Jan PS, Yu HC, Haung HY, Fang HJ, Chang YI, Cheng JW, Chen HM. 2009. Structure and function of a custom anticancer peptide, CB1a. *Peptides* 30:839-848.
- Wu M, Maier E, Benz R, Hancock REW. 1999. Mechanism of interaction of different classes of cationic antimicrobial peptides with planar bilayers and with the cytoplasmic membrane of *Escherichia coli*. *Biochemistry* 38:7235-7242.
- Wu SP, Huang TC, Lin CC, Hui CF, Lin CH, Chen JY. 2012. Pardaxin, a fish antimicrobial peptide, exhibits antitumor activity toward murine fibrosarcoma in Vitro and in Vivo. *Marine Drugs* 10:1852-1872.
- Wu X, Wang Z, Li X, Fan Y, He G, Wan Y, Yu C, Tang J, Li M, Zhang X, Zhang H, Xiang R, Pan Y, Liu Y, Lu L, Yang L. 2014. *In vitro* and *in vivo* activities of antimicrobial peptides developed using an amino acid-based activity prediction method. *Antimicrobial Agents and Chemotherapy* 58:5342-5349.
- Xie C, Zeng P, Ericksen B, Wu Z, Lu WY, Lu W. 2005. Effects of the terminal charges in human neutrophil α -defensin 2 on its bactericidal and membrane activity. *Peptides* 26:2377-2383.
- Xiong M, Lee MW, Mansbach RA, Song Z, Bao Y, Peek RM, Jr., Yao C, Chen LF, Ferguson AL, Wong GCL, Cheng J. 2015. Helical antimicrobial polypeptides with radial amphiphilicity. *Proceedings of the National Academy of Sciences of the United States of America* 112:13155-13160.
- Xu N, Wang YS, Pan WB, Xiao B, Wen YJ, Chen XC, Chen LJ, Deng HX, You J, Kan B, Fu AF, Li D, Zhao X, Wei YQ. 2008. Human α -defensin-1 inhibits growth of human lung adenocarcinoma xenograft in nude mice. *Molecular Cancer Therapeutics* 7:1588-1597.
- Yan H, Hancock REW. 2001. Synergistic interactions between mammalian antimicrobial defense peptides. *Antimicrobial Agents and Chemotherapy* 45:1558-1560.
- Yang L, Harroun TA, Weiss TM, Ding L, Huang HW. 2001. Barrel-stave model or toroidal model? A case study on melittin pores. *Biophysical Journal* 81:1475-1485.

- Yang SJ, Bayer AS, Mishra NN, Meehl M, Ledala N, Yeaman MR, Xiong YQ, Cheung AL. 2012. The *Staphylococcus aureus* two-component regulatory system, *grars*, senses and confers resistance to selected cationic antimicrobial peptides. *Infection and Immunity* 80:74-81.
- Yang ST, Kim JI, Shin SY. 2009. Effect of dimerization of a β -turn antimicrobial peptide, PST13-RK, on antimicrobial activity and mammalian cell toxicity. *Biotechnology Letters* 31:233-237.
- Yang ST, Shin SY, Hahm KS, Kim JI. 2006. Different modes in antibiotic action of tritrypticin analogs, cathelicidin-derived Trp-rich and Pro/Arg-rich peptides. *Biochimica et Biophysica Acta - Biomembranes* 1758:1580-1586.
- Yang ST, Yub Shin S, Kim YC, Kim Y, Hahm KS, Kim JI. 2002. Conformation-dependent antibiotic activity of tritrypticin, a cathelicidin-derived antimicrobial peptide. *Biochemical and Biophysical Research Communications* 296:1044-1050.
- Yasin B, Pang M, Turner JS, Cho Y, Dinh NN, Waring AJ, Lehrer RI, Wagar EA. 2000. Evaluation of the inactivation of infectious herpes simplex virus by host-defense peptides. *European Journal of Clinical Microbiology and Infectious Diseases* 19:187-194.
- Yau WM, Wimley WC, Gawrisch K, White SH. 1998. The preference of tryptophan for membrane interfaces. *Biochemistry* 37:14713-14718.
- Ye JS, Zheng XJ, Leung KW, Chen HM, Sheu FS. 2004. Induction of transient ion channel-like pores in a cancer cell by antibiotic peptide. *Journal of Biochemistry* 136:255-259.
- Yeaman MR, Yount NY. 2003. Mechanisms of antimicrobial peptide action and resistance. *Pharmacological Reviews* 55:27-55.
- Yeh PJ, Hegreness MJ, Aiden AP, Kishony R. 2009. Drug interactions and the evolution of antibiotic resistance. *Nature Reviews Microbiology* 7:460-466.
- Yi GS, Park CB, Kim SC, Cheong C. 1996. Solution structure of an antimicrobial peptide buforin II. *FEBS Letters* 398:87-90.
- Yin CM, Wong JH, Xia J, Ng TB. 2013. Studies on anticancer activities of lactoferrin and lactoferricin. *Current Protein and Peptide Science* 14:492-503.
- Yin LM, Edwards MA, Li J, Yip CM, Deber CM. 2012. Roles of hydrophobicity and charge distribution of cationic antimicrobial peptides in peptide-membrane interactions. *Journal of Biological Chemistry* 287:7738-7745.
- Yin ZX, He W, Chen WJ, Yan JH, Yang JN, Chan SM, He JG. 2006. Cloning, expression and antimicrobial activity of an antimicrobial peptide, epinecidin-1, from the orange-spotted grouper, *Epinephelus coioides*. *Aquaculture* 253:204-211.

- Yoneyama F, Imura Y, Ohno K, Zendo T, Nakayama J, Matsuzaki K, Sonomoto K. 2009. Peptide-lipid huge toroidal pore, a new antimicrobial mechanism mediated by a lactococcal bacteriocin, lacticin Q. *Antimicrobial Agents and Chemotherapy* 53:3211-3217.
- Yonezawa A, Kuwahara J, Fujii N, Sugiura Y. 1992. Binding of tachyplesin I to DNA revealed by footprinting analysis: significant contribution of secondary structure to DNA binding and implication for biological action. *Biochemistry* 31:2998-3004.
- Yoo YC, Watanabe R, Koike Y, Mitobe M, Shimazaki K-i, Watanabe S, Azuma I. 1997a. Apoptosis in human leukemic cells induced by lactoferricin, a bovine milk protein-derived peptide: involvement of reactive oxygen species. *Biochemical and Biophysical Research Communications* 237:624-628.
- Yoo YC, Watanabe S, Watanabe R, Hata K, Shimazaki KI, Azuma I. 1997b. Bovine lactoferrin and lactoferricin, a peptide derived from bovine lactoferrin, inhibit tumor metastasis in mice. *Japanese Journal of Cancer Research* 88:184-190.
- Yoon WH, Park HD, Lim K, Hwang BD. 1996. Effect of O-glycosylated mucin on invasion and metastasis of HM7 human colon cancer cells. *Biochemical and Biophysical Research Communications* 222:694-699.
- Young SB, Setlow P. 2003. Mechanisms of killing of *Bacillus subtilis* spores by hypochlorite and chlorine dioxide. *Journal of Applied Microbiology* 95:54-67.
- Yount NY, Bayer AS, Xiong YQ, Yeaman MR. 2006. Advances in antimicrobial peptide immunobiology. *Biopolymers - Peptide Science Section* 84:435-458.
- Yu DH, Lu Q, Xie J, Fang C, Chen HZ. 2010. Peptide-conjugated biodegradable nanoparticles as a carrier to target paclitaxel to tumor neovasculature. *Biomaterials* 31:2278-2292.
- Yu G, Baeder DY, Regoes RR, Rolff J. 2016. Combination effects of antimicrobial peptides. *Antimicrobial Agents and Chemotherapy* 60:1717-1724.
- Zahn M, Berthold N, Kieslich B, Knappe D, Hoffmann R, Sträter N. 2013. Structural studies on the forward and reverse binding modes of peptides to the chaperone DnaK. *Journal of Molecular Biology* 425:2463-2479.
- Zanetti M. 2004. Cathelicidins, multifunctional peptides of the innate immunity. *Journal of Leukocyte Biology* 75:39-48.
- Zaslhoff M. 2002. Antimicrobial peptides of multicellular organisms. *Nature* 415:389-395.
- Zhang J, Martin JM, Balint-Kurti P, Huang L, Giroux MJ. 2011. The wheat *puroindoline* genes confer fungal resistance in transgenic Corn. *Journal of Phytopathology* 159:188-190.

References

- Zhang JX, Zhang SF, Wang TD, Guo XJ, Hu RL. 2007. Mammary gland expression of antibacterial peptide genes to inhibit bacterial pathogens causing mastitis. *Journal of Dairy Science* 90:5218-5225.
- Zhang Y. 2008. I-TASSER server for protein 3D structure prediction. *BMC Bioinformatics* 9:40.
- Zhang Y, Teng D, Mao R, Wang X, Xi D, Hu X, Wang J. 2014. High expression of a plectasin-derived peptide NZ2114 in *Pichia pastoris* and its pharmacodynamics, postantibiotic and synergy against *Staphylococcus aureus*. *Applied Microbiology and Biotechnology* 98:681-694.
- Zhou Y, Peng Y. 2013. Synergistic effect of clinically used antibiotics and peptide antibiotics against Gram-positive and Gram-negative bacteria. *Experimental and Therapeutic Medicine* 6:1000-1004.
- Zhu WL, Lan H, Park Y, Yang ST, Kim JI, Park IS, You HJ, Lee JS, Park YS, Kim Y, Hahm KS, Shin SY. 2006. Effects of Pro → peptoid residue substitution on cell selectivity and mechanism of antibacterial action of tritrypticin-amide antimicrobial peptide. *Biochemistry* 45:13007-13017.
- Zhu WL, Shin SY. 2009. Antimicrobial and cytolytic activities and plausible mode of bactericidal action of the cell penetrating peptide penetratin and its Lys-linked two-stranded peptide. *Chemical Biology and Drug Design* 73:209-215.
- Zhu X, Dong N, Wang Z, Ma Z, Zhang L, Ma Q, Shan A. 2014. Design of imperfectly amphipathic α -helical antimicrobial peptides with enhanced cell selectivity. *Acta Biomaterialia* 10:244-257.
- Zielinska P, Staniszewska M, Bondaryk M, Koronkiewicz M, Urbanczyk-Lipkowska Z. 2015. Design and studies of multiple mechanism of anti-*Candida* activity of a new potent Trp-rich peptide dendrimers. *European Journal of Medicinal Chemistry* 105:106-119.
- Zucht HD, Raida M, Adermann K, Mägert HJ, Forssmann WG. 1995. Casocidin-I: a casein- α 2 derived peptide exhibits antibacterial activity. *FEBS Letters* 372:185-188.

Appendix

Below is the bio-safety clearance email from the secretary of Swinburne Biosafety Committee (SBC), Sheila Hamilton-Brown, obtained on the 12th May 2017, allowing this research project to be conducted under the regulation of Swinburne Ethics:

From: Sheila Hamilton-Brown
Sent: Friday, 12 May 2017 4:51 PM
To: Katharine Adcroft <kadcroft@swin.edu.au>; Peter Kingshott <pkingshott@swin.edu.au>; Mrinal Bhav <mbhave@swin.edu.au>
Subject: Biosafety Project 2014/SBC02 Biosafety Clearance for extension (1) and modification (3)

Dear Peter and Katharine

Biosafety Project 2014/SBC02 – Culture of Risk level 2 (AS/NZS 2243-3) Mammalian Cells in the ATC 901, 902 and 904 labs
Approved to 30/06/2021 [NEW DATE]

~~Subproject 1 - Screening for cytotoxicity of synthetic peptides~~
~~Subproject 2 - Screening for cytotoxicity of synthetic peptides~~
~~Subproject 3 - Screening for cytotoxicity of synthetic peptides~~
~~Subproject 4 - Screening for cytotoxicity of synthetic peptides~~
~~Subproject 5 - Screening for cytotoxicity of synthetic peptides~~
Subproject 6 - Screening for cytotoxicity of synthetic peptides
~~Subproject 7 - Screening for cytotoxicity of synthetic peptides~~
Subproject 8 - Screening for cytotoxicity of synthetic peptides (2) [NEW SUB-PROJECT, Prof M. Bhav]

I refer to the modification request for an extension to the above project (sub-projects 1-7) and an additional sub-project and personnel (sub-project 8).

The project has approval to proceed with standard on-going conditions here outlined.

- All teaching and research activity undertaken under Swinburne auspices must conform to Swinburne and external regulatory standards, with respect to secure data use, retention and disposal.
- The named Swinburne Chief Investigator/Supervisor remains responsible for any personnel appointed to or associated with the project being made aware of clearance conditions. Any change in chief investigator/supervisor requires timely notification and SBC endorsement.
- The above project has been approved as submitted for review by or on behalf of SBC. Amendments to approved procedures ordinarily require prior appraisal/ clearance. Separate to any Swinburne OHS reporting the SBC must be notified immediately or as soon as possible thereafter of (a) any serious or unexpected adverse events and any redress measures; (b) proposed changes in protocols.
- A duly authorised external or internal audit of the project may be undertaken at any time.
- Please also note that an annual progress report is required before the end of each fiscal year (e.g. 30 June 2017). Approval for continuation per annum is subject to annual progress reporting.

Copies of clearance emails should be retained as part of project record-keeping. Please contact the Research Ethics Office if you have any queries about the SBC process, citing the Biosafety Project number.

Kind regards,
Sheila

 **Sheila Hamilton-Brown | Biosafety Officer/Executive Officer**
Swinburne University of Technology
PO Box 218, Hawthorn, VIC 3122 | Mailbox: H68
Tel: +61 3 9214 5935 | Fax: +61 3 9214 5267